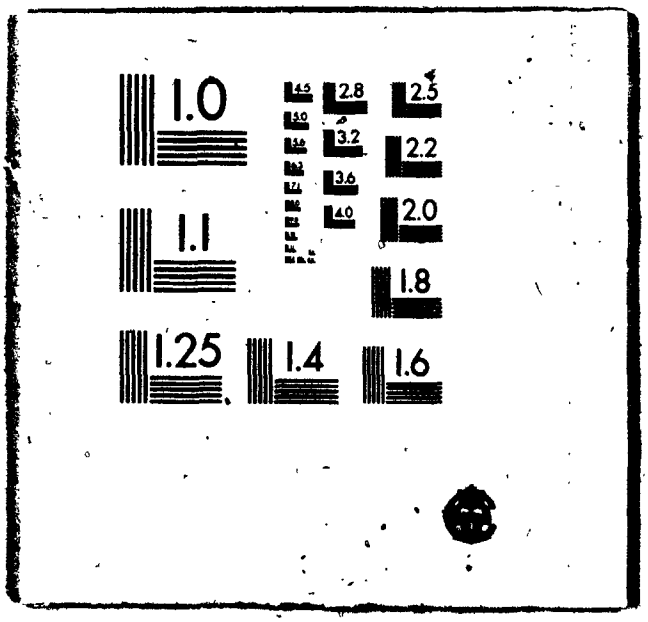
1.0
1.1
1.25
1.4
1.6
1.8
2.0
2.2
2.5
2.8
3.2
3.6
4.0
4.5
5.0

National Library of Canada | Bibliothèque nationale du Canada | CANADIAN THESES ON MICROFICHE | THÈSES CANADIENNES SUR MICROFICHE

52814

0-315-04920-0

NAME OF AUTHOR/NOM DE L'AUTEUR Leo Rothenburg

TITLE OF THESIS/TITRE DE LA THÈSE MICROMECHANICS of IDEALIZED GRANULAR SYSTEMS

UNIVERSITY/UNIVERSITÉ Carleton University, Ottawa.

DEGREE FOR WHICH THESIS WAS PRESENTED/GRADE POUR LEQUEL CETTE THÈSE FUT PRÉSENTÉE Ph. D.

YEAR THIS DEGREE CONFERRED/ANNÉE D'OBTENTION DE CE GRADE 1981

NAME OF SUPERVISOR/NOM DU DIRECTEUR DE THÈSE A.P.S. SELVADURAI

Permission is hereby granted to the NATIONAL LIBRARY OF CANADA to microfilm this thesis and to lend or sell copies of the film.

The author reserves other publication rights, and neither the thesis nor extensive extracts from it may be printed or otherwise reproduced without the author's written permission.

L'autorisation est, par la présente, accordée à la BIBLIOTHÈQUE NATIONALE DU CANADA de microfilmer cette thèse et de prêter ou de vendre des exemplaires du film.

L'auteur se réserve les autres droits de publication; ni la thèse ni de longs extraits de celle-ci ne doivent être imprimés ou autrement reproduits sans l'autorisation écrite de l'auteur.

DATED/DATÉ JAN 20, 1981 SIGNED/SIGNÉ L. Rothenburg

PERMANENT ADDRESS/RÉSIDENCE FIXÉ Dr. L. Rothenburg
c/o Mrs. N. Richmond
2601 Bathurst St. #610
TORONTO, Ont M6B 2Z5

NL-91 (3-74)

X

NOTICE

The quality of this microfiche is heavily dependent upon the quality of the original thesis submitted for microfilming. Every effort has been made to ensure the highest quality of reproduction possible.

If pages are missing, contact the university which granted the degree.

Some pages may have indistinct print especially if the original pages were typed with a poor typewriter ribbon or if the university sent us a poor photocopy.

Previously copyrighted materials (journal articles, published tests, etc.) are not filmed.

Reproduction in full or in part of this film is governed by the Canadian Copyright Act, R.S.C. 1970, c. C-30. Please read the authorization forms which accompany this thesis.

THIS DISSERTATION
HAS BEEN MICROFILMED
EXACTLY AS RECEIVED

AVIS

La qualité de cette microfiche dépend grandement de la qualité de la thèse soumise au microfilmage. Nous avons tout fait pour assurer une qualité supérieure de reproduction.

S'il manque des pages, veuillez communiquer avec l'université qui a conféré le grade.

La qualité d'impression de certaines pages peut laisser à désirer, surtout si les pages originales ont été dactylographiées à l'aide d'un ruban usé ou si l'université nous a fait parvenir une photocopie de mauvaise qualité.

Les documents qui font déjà l'objet d'un droit d'auteur (articles de revue, examens publiés, etc.) ne sont pas microfilmés.

La reproduction, même partielle, de ce microfilm est soumise à la Loi canadienne sur le droit d'auteur, SRC 1970, c. C-30. Veuillez prendre connaissance des formules d'autorisation qui accompagnent cette thèse.

LA THÈSE A ÉTÉ
MICROFILMÉE TELLE QUE
NOUS L'AVONS REÇUE

MICROMECHANICS OF IDEALIZED GRANULAR SYSTEMS

by

Leo Rothenburg,
Dipl. Phys., Moscow State University

A thesis submitted to the Faculty of Graduate Studies and Research in partial fulfillment of the requirement for the degree of Doctor of Philosophy

Faculty of Engineering
Carleton University
Ottawa, Canada

October 1980

The undersigned recommend to the Faculty of Graduate Studies and Research acceptance of the thesis, "Micromechanics of Idealized Granular Systems", submitted by Leo Rothenburg, Dipl. Phys., in partial fulfillment of the requirement for the degree of Doctor of Philosphy.

A.P.S. Selvadurai

Thesis Supervisor

John B. Dykeman

Chairman

Department of Civil Engineering

ABSTRACT

The theory studies idealized granular systems--assemblies of material discs and spheres—in conditions of static equlibrium under external loads. Particles are regarded as deformable solids interacting by means of contact forces. The objective of the study is to develop means of phenomenological description suitable for efficient analysis of stress fields in granular masses. Systems are analyzed using principles of mechanics applied at the particulate level and using developed statistical and statistico-geometrical methods.

The phenomenological stress tensor is introduced as a fluctuating function of volume through volume-additive combinations of a system's micro-parameters, contact forces and orientations of contact normals. It is shown that the introduced tensor has properties of the continuum mechanics stress tensor in the limit of an infinite homogeneous assembly under homogeneous loads on infinity.

The average of the phenomenological stress tensor over an ensemble of macroscopically similar systems under inhomogeneous loads has all the field properties of the continuum mechanics stress tensor which becomes related to average forces on contacts of the same orientation and to the contact orientation distribution. Under minimal assumptions regarding the form of directional variation of forces, the latter are expressed in terms of stress tensor invariants and the influence of anisotropy in contact orientations is investigated. It is shown that the displacement gradient considered in continuum mechanics can be introduced through conditions

of particle micro-compatibility in contacts.

Distributions of contact forces for assemblies of bonded particles are developed using principles of the information theory. Constitutive relationships for assemblies of bonded particles with linear contact interactions are derived by minimization of complementary work of internal deformations. For isotropic assemblies of spheres, the tensor of elasticity is isotropic; Poisson's ratio is given as a function of the ratio of tangential to normal stiffnesses and is automatically within thermodynamic limits. Poisson's result ($\nu = 1/4$) corresponds to zero tangential contact stiffness. Fluctuations of the phenomenological stress tensor in finite volumes are assessed.

The anisotropic case is investigated for plane assemblies only. Resulting equations of linear elasticity correspond to a non-symmetrical stress tensor, and an assumed lack of moment transfer in contacts restricts the deformational modes of anisotropic systems. Deformations are unrestricted for particles with vanishing tangential stiffnesses. The resulting relationships correspond to transversely isotropic plane materials. Deformation moduli are expressed in terms of parameters defining the shape of contact orientation distributions.

The statistico-geometrical analysis of plane systems is aimed at determining admissible shapes of contact orientation distributions compatible with the introduced condition of local stability expressed in geometrical form. The analysis results in a realtionship between the parameters of anisotropy and the system's density. The types of admissible anisotropies qualitatively differ for loose and dense assemblies.

The condition of stability also admits a relationship between the average coordination number and the system's density. The existence of maximum random and minimum stable densities is established. Comparisons with experimental data support these findings.

Assemblies of cohesionless particles are analyzed in the plane case. It is conjectured that the deformational process is of a quasi-dynamic nature due to continuous micro-cycles of "hardening" and "softening". It is suggested that the magnitudes of dissipative tangential contact forces are insignificant and can be neglected. It is also assumed that, due to low intensity of dynamic processes, a system of contact forces for any fixed structure corresponds to minimum potential energy related to deformations of grains. It is shown that the assumption enables to formally employ stress-strain characteristics of bonded particles to determine stress fields in assemblies of cohesionless particles.

Determination of stress fields from a point source on a homogeneous anisotropic granular half-plane indicates that stress distributions qualitatively differ for loose and dense assemblies. Comparison with the results of plate loading tests on granular materials shows definite qualitative similarity in the theoretical and experimental stress distributions.

The theory of earth pressure (at rest) relates K_o to parameters of structural anisotropy, so that stress fields in plane homogeneous granular assemblies are controlled by the coefficient of earth pressure (at rest) and their relative density.

ACKNOWLEDGEMENTS

The work in this dissertation was carried out under the supervision of Professor A.P.S. Selvadurai to whom the author wishes to express his sincere appreciation for stimulating guidance.

The author is greatly indebted to Professors J. Adjelian, G.E. Bauer, W.H. Bowes, and J.J. Salinas whose influence on the author's engineering education significantly contributed to the reported research.

Financial support from the Natural Science and Engineering Council of Canada (operating grant A3866) is gratefully acknowledged.

It is a pleasant opportunity to express deep gratitude to Dr. V.N. Nikolaevski of the Institute of Earth Physics of the USSR Academy of Sciences who first directed the author's attention to mechanics of granular materials and whose influence on the reported research is profound.

Heartfelt thanks to my friends and family, whose interest, support and understanding were of great encouragement, and especially to my wife, Barbara, without whom this work would not have appeared.

TABLE OF CONTENTS

LIST OF FIGURES

CHAPTER I

INTRODUCTION

1.1 Introduction

The object of studies outlined in the present work are idealized granular systems--large irregular assemblies of discs and spheres. The systems are studied in conditions of static equilibrium under external loads acting on the systems' boundaries.

The research was undertaken with the following two main objectives:

1. To re-examine principles of continuum description with regard to granular systems on the basis of fundamental principles of mechanics applied on particulate level.
2. To develop means of phenomenological description for granular systems with due recognition of their discrete nature.

The strategy for re-examination of the concept of continuum is the following:

1. To select a simple granular system and to pose a mechanical problem on a particulate level.
2. To obtain a response for assemblies of bonded granules with linear contact interactions expected as *a priori* considered in continuum mechanics.
3. To analyze principles which lead to continuum description and examine their applicability to assemblies of cohesionless granules.
4. To re-examine principles of continuum description for cohesionless assemblies.

Recognizing that micromechanics of idealized granular systems is an interdisciplinary subject of interest to several areas of science

and engineering, the present theory gives the highest priority to developing methods oriented to solution of problems originating in soil mechanics.

With regard to these problems the objectives of this research are the following:

1. To study the mechanisms of load transmission in granular assemblies.
2. To study physical parameters affecting the response of granular systems.
3. To relate physical parameters governing the response of granular systems in studied conditions to commonly used engineering parameters, thus providing their new interpretation and possibilities of new methods of determining them.
4. To investigate the modelling potential of idealized granular systems by analyzing qualitative features of load distributions in studied systems and by comparing them with performance of granular materials in similar external conditions.

Although the object of study are mainly idealized granular systems, the part of the theory related to definition of phenomenological parameters is based entirely on equations of static equilibrium and geometrical compatibility and is independent of specific shapes of particles. On the other hand, severe geometrical difficulties in analysis of irregular structures restricted the theory of anisotropic systems to analysis of plane assemblies only. Isotropic systems are analyzed in both two- and three-dimensional cases.

Of main interest from the point of view of applications are anisotropic systems. It is shown that equations governing stress distributions

in granular assemblies are of the same type for both the two- and three-dimensional cases, although coefficient magnitudes may be different, so that only qualitative comparison was possible of developed stress distributions with available experimental data.

Granular assemblies are analyzed in conditions of no pore fluid or heat transfer present. Material particles are considered as deformable solids interacting by means of contact forces. Interactions by means of moments transferred through contacts are *a priori* neglected and further assessed numerically, once contact areas become known.

The theory is restricted to analysis of mechanisms of load transfer and deformational properties are only discussed on the basis of statistico-geometrical analysis which is viewed as sufficient to account for the deformational properties of plane systems throughout all ranges of defromations up to the "ultimate state".

Section 1.2 briefly outlines the reasons for selecting the stated objectives.

1.2 Modelling of Granular Systems

It is not the objective of this section to discuss specific models of granular materials, but rather to clarify the general directions of the modelling process selected in the present research.

The majority of models of granular materials are developed in the framework of continuum description. Such a direction of modelling is understandable, since the ultimate objective is to make a model useful for predicting material behavior outside of the laboratory. Formal methods of continuum mechanics provide tools for applying models, but it is the

judgement of the applier that decides how to proceed.

To date the simplest continuum mechanics schemes have been the most successful. Problems of bearing capacity were solved within the framework of ideal plasticity, settlement of foundations in clay can be predicted by evaluating stress distributions using elastic solutions, and the theory of consolidation.

In more sophisticated applications both theories are linked together and equations must be solved to obtain a material response. The two efficient well-founded schemes of continuum mechanics lead to two meaningful design procedures. However, not only bearing capacity is of interest and not only initial and consolidation settlements must be predicted. Continuum mechanics provides formal tools for obtaining required responses, but somehow continuum models are not employed as widely in engineering practice as can be expected, judging the amount of continuum models available. There are, of course, computational difficulties and three factors responsible for the difficulties:

1. Inadequate modelling.
2. Inadequate computational procedures.
3. Inapplicable continuum mechanics schemes.

The above contains a wide range of uncertainties. Continuum mechanics cannot be blamed for not being applicable, since this is a mathematical theory. Mathematics can be blamed for not supplying adequate mathematical tools. Computers can also be blamed for attracting too much attention to their use.

Continuum models perform well in the laboratory in sophisticated test apparatus under sophisticated load paths, but one of the three

links can cause difficulties in the application of models. The most reliable way, therefore, is one which goes through the least number of steps. One such way is direct probabilistic modelling of processes of load transmission in granular materials [25 , 14]. So far it is the only method leading to simple observable solutions for stress distributions in granular materials.

Explicit features of this medium are taken into account and results are obtained that can be evaluated and corrected,empirically. The method still requires considerable ingenuity when applied in complicated conditions of load application.

General methods of continuum mechanics are still attractive and the possiblity of overcoming the mentioned obstacles is challenging. A modelling process is a starting point in a chain of developments leading to applications.

The understanding of granular materials has been greatly advanced in recent years and realistic features of granular materials are becoming recognized, such as anisotropy and fabric, contact forces [6]. Still this is only one link in the chain leading to applications and each one of the three can easily break. There is, perhaps, no perfect scheme to assure success, but an attempt is made here to select the simplest system that can reflect the features of real granular materials and analyze them from the first principle, on the basis of equations of equilibrium for individual particles.

The objective of such an investigation is to establish the most important common feature to all granular systems. The simplest system of the considered class may not explain everything, but once the pathway

to obtaining a solution for one system is found, one can hope that more complicated systems can be studied, providing the results obtained are encouraging. The main problem is to go all the way up to application stages without breaking the chain of confidence in previous steps.

Idealized granular systems provide such an opportunity, owing to the large body of experimental results available. This is of invaluable help and encouragment, since it is impossible to analyze even the simplest system without heuristic considerations based on detailed and precise experiments.

The search is still blind, however, if the method of description is unclear. The number of equations required of analysis is unmanageable even for a simple system. Should a miraculous method for solving these equations be found, the solution would be useless, since the initial conditions for any large specific system can hardly ever be available. It is therefore necessary to look for equations of mechanics that are independent, for example, of particle positions.
Such consequences of the laws of mechanics would be characteristics of a class of systems and this class can be described by so-called "phenomenological parameters".

It is a fact that large mechanical systems exhibit macroscopic regularities and two microscopically different systems can be characterized by the same, or nearly the same, phenomenological parameters [23]. A single characteristic for a class of similar systems can be defined as a certain average over a class of similar systems. Then, using statistical methods, fluctuations of these parameters between different, though

macroscopically similar, systems can be studied. This is the idea of phenomenological description: to describe a class of similar systems and establish common characteristics of the class.

Continuum description is a type of phenomenological description that does not recognize possible fluctuations of phenomenological parameters. In physical terms, continuum theories attribute characteristics of a class of systems to one single system. If the studied system consists of many particles, it can be expected that phenomenological parameters will not fluctuate significantly.

The description employed in the present theory for granular assemblies is phenomenological. The main problem is to identify phenomenological parameters and to show that a selected set of parameters is such that the introduced quantities do not indeed fluctuate significantly for large systems.

Such phenomenological parameters will be introduced in the present theory on the basis of equations of static equilibrium and geometrical compatibility between particles. The developed analysis will show that the introduced characteristics have the properties of stress and strain tensors familiar to continuum mechanics. The only difference is that here they will be introduced on the basis of mechanical analysis and the conditions under which such characteristics can be introduced will be explicitly stated.

It will be shown that the stress tensor, as understood in continuum mechanics, can be introduced for systems in static equilibrium. The situation will be entirely different with phenomenological quantities describing deformations of granular systems. It will be shown that infi-

nitesimal strain tensor is valid for systems of bonded particles (Chapters V and VII).

Substantial evidence will be presented in Chapter X that an elastic strain tensor cannot be introduced for cohesionless assemblies. Any attempt to determine a stress field, from the point of view of micromechanics, hinges on the determination of contact forces. Contact forces, in turn, are related to deformations of grains and not to slip at contacts which determines deformations referred to sometimes as "plastic deformations". If an elastic strain tensor cannot be introduced, the system is independent of boundary loads and responds accordingly to the requirements of compatibility and stability.

The developed theory introduces a concept of "continuously unstable systems" whose deformations are microscopically beyond boundary control through external loads due to inherent micro-cycles of "hardening" and "softening". Being unable to relate two states of static equilibrium by means of elastic deformations controlling contact forces, the theory proceeds without this ingredient of continuum mechanics by postulating that local deformations of particles, though independent of boundary conditions, still correspond to the state of minimum potential energy. The entire deformation process can be viewed as quasi-dynamic.

Dynamic systems are never in the state of minimum potential energy, but, according to Gibbsian mechanics [13], this state is the most probable for conditions of chaotic motion. For processes considered here, kinetic motions are not intensive. This is why as an approximation it is postulated that the system of contact forces for any fixed structure corresponds to minimum potential energy.

Minimization of potential energy results in a tensor with all the properties of the continuum mechanics elastic strain tensor, though such meaning is not attached to this quantity which acts as a useful computational tool. The reason for not interpreting it as a strain tensor is that the theory cannot indicate an experiment in which elastic strains can be separated from structural changes within the system.

The scheme for description of granular systems is therefore like that routinely employed for calculations of settlements of foundations in clays: stress fields are determined from elastic analysis and deformations are determined using plausible assumptions regarding compressibility or plastic flow.

CHAPTER II

MECHANICAL AND GEOMETRICAL ELEMENTS IN DESCRIPTION OF GRANULAR ASSEMBLIES

2.1 Introduction

The present chapter attempts to give a qualitative description of the main mechanical and geometrical elements to be employed in the following chapters. It also provides a connection between the present theory with classical statistical mechanics and the more general theories of micromechanics.

Fig. 2.1 shows an assembly of photo-elastic discs subject to boundary load. The objective of the experiment [8] was to determine a load-deformation characteristic of the assembly and visualize mechanisms of load transmission. In very rough terms this is also an objective of the present theory.

The noted illustration helps to identify the main elements which must appear in descriptions of granular systems: contact orientations and contact forces. The first characterizes assembly structure, the second is the combined result of external loads and structur[illegible] In chapter III these characteristics will be related.

2.2 Contact Orientation Distribution

Fig. 2.2 presents an assembly of discs where only segments connecting particle centers are shown. In further development of the theory only orientations of contact normals will enter formulations of all resulting

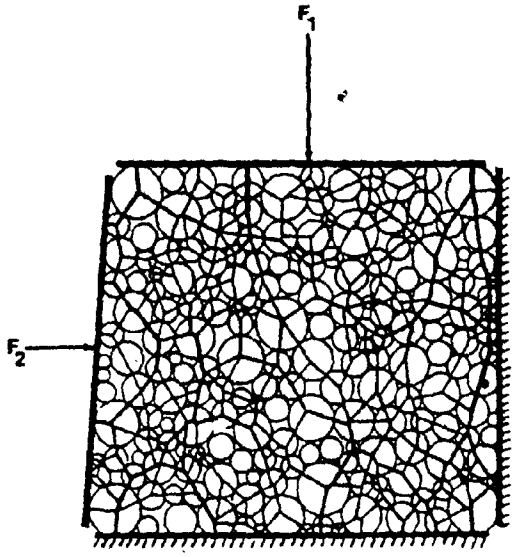

FIGURE 2.1

NETWORK OF CONTACT FORCES
(after De Jong and Verruijt [8])

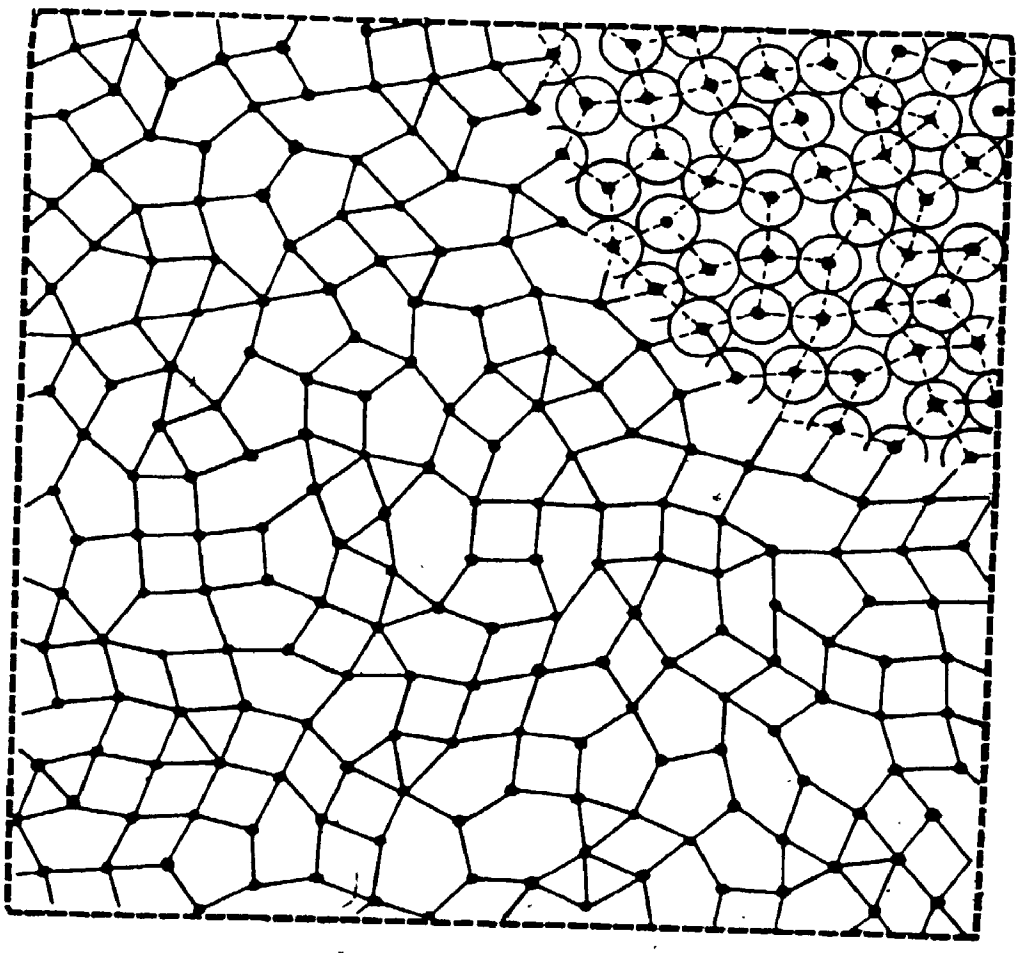

FIGURE 2.2

GEOMETRICAL REPRESENTATION OF A PLANE ASSEMBLY

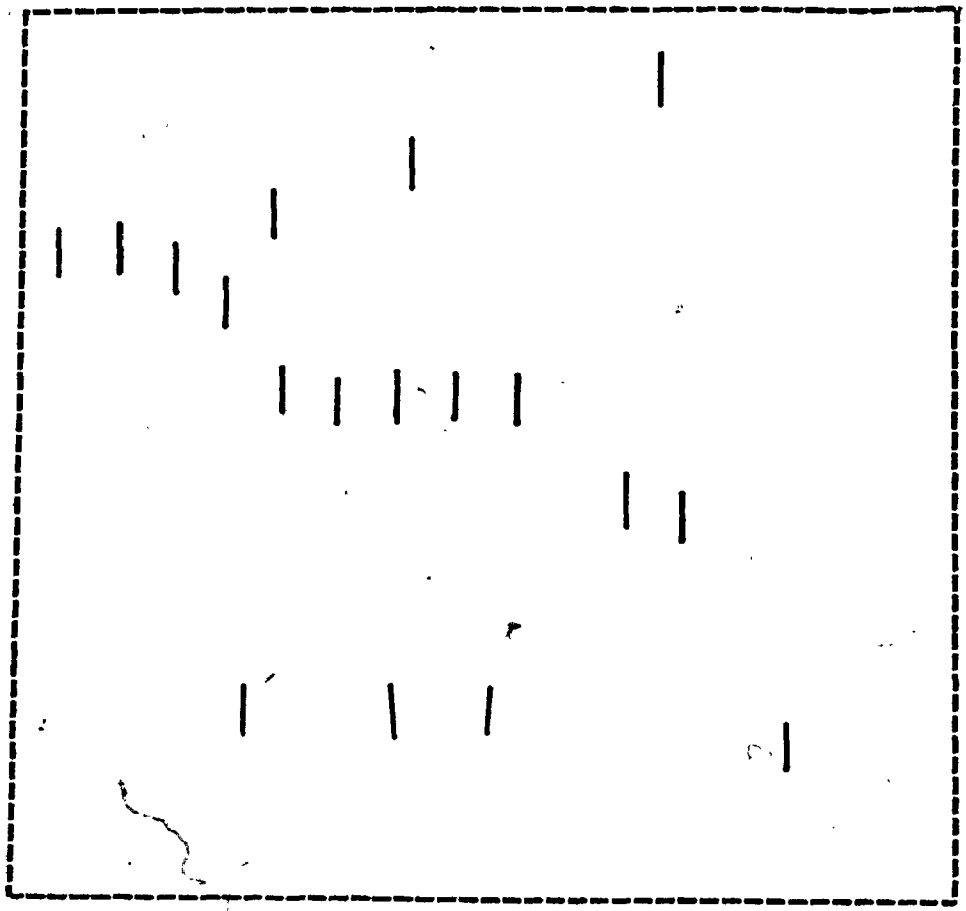

FIGURE 2.3

GROUP OF CONTACTS WITH SIMILAR ORIENTATIONS

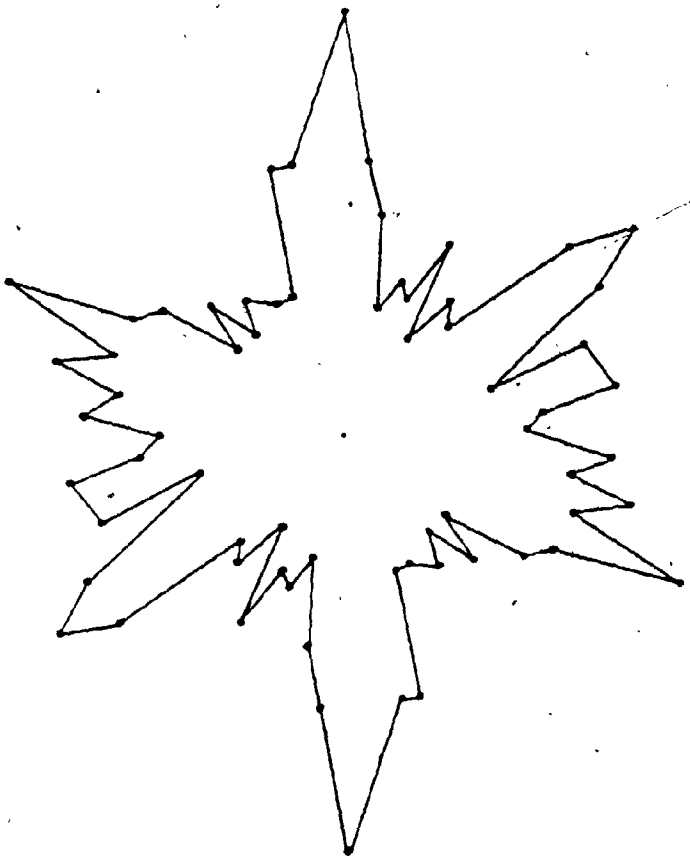

FIGURE 2.4

CONTACT ORIENTATION DISTRIBUTION

equations. Moreover, all developed relationships will depend on the number of contacts of the same orientation per unit volume (or area in plane cases). Fig. 2.3 shows one such group scatterred within the assembly.

The picture of photo-elastic discs shows that such contacts carry the highest load, since they are oriented in the direction of the load. For evaluation of gross balance of forces the number of such contacts must be specified and the same must be for all groups of contacts with similar orientations.

Let there be a total of M geometrical contacts (twice the number of physical contacts or segments connecting particle centers). All contacts can be classified into G orientation groups in such a way that contact normals of each group have similar orientations between θ_g and $\theta_g + \Delta\theta$ with respect to a reference direction. Let there be ΔM_g contacts in group g and this number be represented in the form

$$\Delta M_g = M S(\theta_g) \Delta\theta$$

where $S(\theta_g)$ is a certain generally discontinuous normalized function.

Fig. 2.4 shows $S(\theta_g)$ for 72 groups of contacts with $\Delta\theta = 5°$. It can be clearly seen that this distribution is anisotropic. The assembly in Fig. 2.2 consists of $N = 248$ particles and there are $M = 948$ contact points. The average coordination number of the assembly $\gamma = \frac{M}{N} = 3.84$ (the number of contact points in each particle averaged over all particles).

As can be seen, the histogram on Fig. 2.4 has a tendency to be symmetrical about the axis of anisotropy. Due to the small number of particles in the assembly, its shape is irregular. Suppose, however, that the size of the assembly is increased. If the assembly is truly irregular,

i.e. never exactly repeating its structure, it can be expected that the following limit will exist for an infinite assembly:

$$S(\theta) = \lim_{\Delta\theta \to 0} \lim_{V \to \infty} \frac{\Delta M_q}{M \Delta\theta} \tag{2.1}$$

and $S(\theta)$ can be expected to be a continuous function.

The above mathematical operation cannot be justified and must be accepted as a definition of an abstract entity--an infinite assembly with irregular structure characterized by $S(\theta)$. Such an infinite assembly is as abstract as a continuum. It will be shown in the next chapter that continuum mechanics relationships always appear in the limit of an infinite assembly. The significance of the introduced contact orientation distribution was first noticed by Horne[15].

There is a considerable number of experiments on plane granular assemblies that suggest that contact orientation distribution is crucial for an understanding granular systems. This function is sometimes referred to as a "probability density" with the attached meaning of giving a probability that an arbitrarily selected contact has an orientation θ. The probabilistic interpretation of $S(\theta)$ will not be used in this study for the reasons to be stated below.

Granular systems in this work are analyzed on the basis of equations of equilibrium for deterministic systems. Despite the irregular structure of studied systems, they are deterministic systems and can be analyzed using equations of equilibrium.In the proposed analysis such equations will be written for particles with precisely specified positions and equations will be analyzed as such. All final results are presented either for infinite systems or as averages over an ensemble of similar systems. The operation of taking these averages is a statistical operation over

deterministic systems for which precise description is not impossible, but difficult and unnecessary. This is why granular assemblies are called "irregular", but not "random".

Contact orientation distribution will appear in the next chapter from analysis of equations of equlibrium. Interpretation of $S(\theta)$ as probability density is legitimate as long as it refers to an arbitrarily selected contact. This is an artificial process of selecting a contact set up by the observer and the irregularities in the system are a premise for considering this process.

For isotropic systems $S(\theta) = 1/2\pi$. The question, however, is to determine the form of $S(\theta)$ for anisotropic assemblies. Considering the intention here to study granular systems in conditions of directional loads or preferred direction of deposition, it will be assumed that there will be only one direction of anisotropy, i.e. the contact orientation distribution is then of the form $S = S(\theta-\theta_o)$ which defines a frame indifference. Also, $S(\theta) = S(\theta+\pi)$, since each contact is represented by two normals of opposite orientation.

As $S(\theta)$ is periodic with period π, it can be decomposed into Fourier series of the form

$$S(\theta) = \frac{c_o}{2} + \sum_{n=1}^{\infty} [c_{2n}\cos 2n(\theta-\theta_o) + d_{2n}\sin 4(\theta-\theta_o)]$$

where c_{2n}, d_{2n} are certain coefficients.

If θ_o is the direction of anisotropy, $S(\theta-\theta_o)$ must be symmetrical under reflections, i.e. $S(\theta_o+\alpha) = S(\theta_o-\alpha)$ for any α. This means that sine terms above should not be included in $S(\theta)$. In further analysis only second and fourth Fourier components will be retained in the above series and

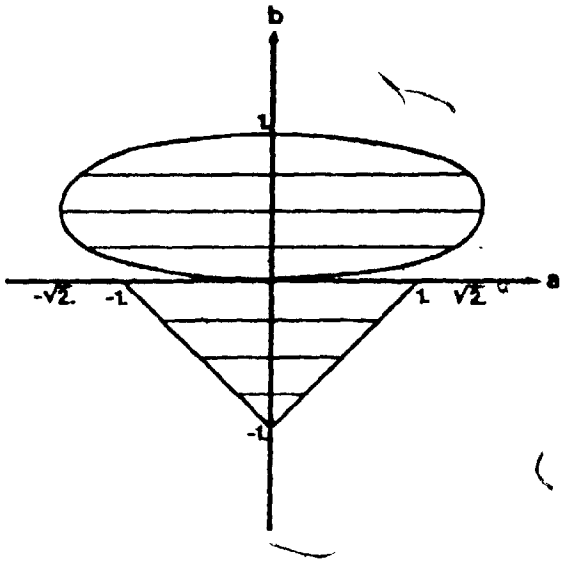

FIGURE 2.5

FEASIBILITY REGION FOR PARAMETERS OF ANISOTROPY

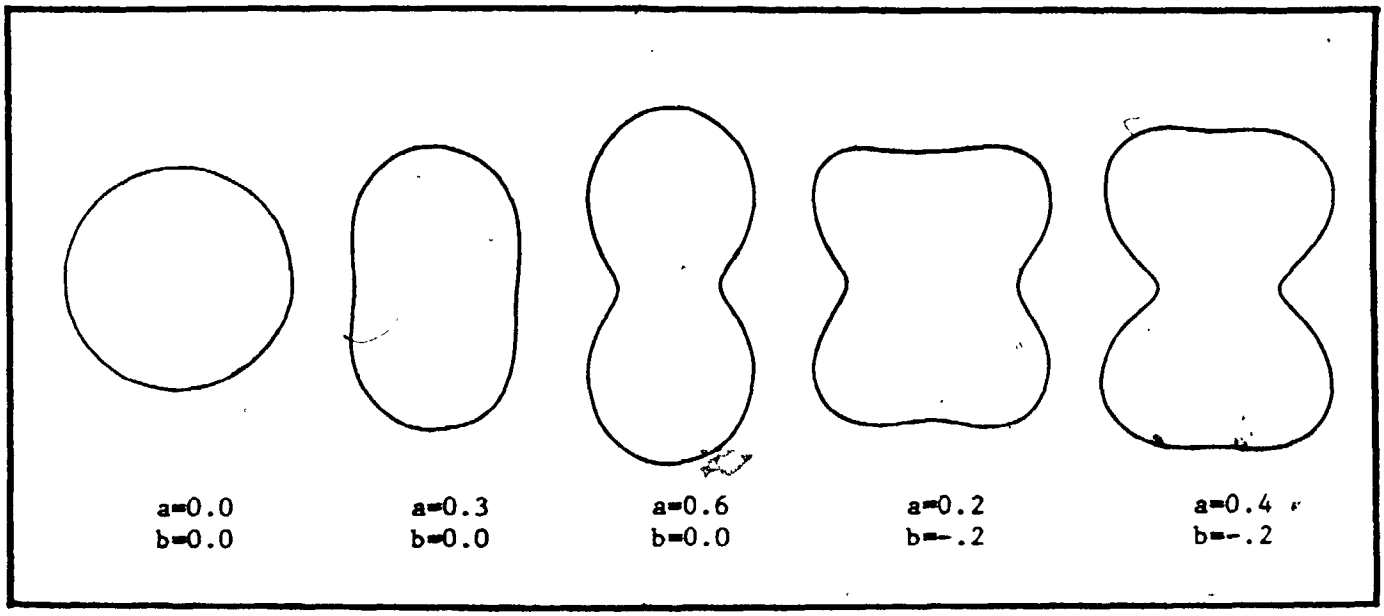

FIGURE 2.6

SHAPES OF CONTACT ORIENTATION DISTRIBUTIONS

contact orientation will be considered in the form

$$S(\theta) = \frac{1}{2\pi}[1 + a\cos 2(\theta-\theta_o) + b\cos 4(\theta-\theta_o)] \qquad (2.2)$$

where a and b will be referred to as parameters of anisotropy. Note that $S(\theta)$ is normalized.

From its physical meaning, $S(\theta)$ must be a positive quantity. The feasibility region for a, b is shown in Fig. 2.5. Several shapes of distributions are shown on Fig. 2.6. The variety of shapes controlled by a, b is significant and it can be expected that not all shapes correspond to admissible contact orientations.

Statistico-geometrical analyses distinguish between contact orientation distributions for loose and dense systems. Note that the hand-drawn assembly on Fig. 2.2 is not typical of the shapes on Fig. 2.5. This assembly is very loose ($\gamma = 3.84$) and mechanically unstable. It was drawn as such in order to check certain conclusions of statistico-geometrical analysis.

If $S(\theta)$ is taken with $b = 0$, i.e. only the second Fourier component is employed, it can be expressed in terms of a certain second rank tensor ρ_{ij}, such that

$$S(\theta) = \rho_{ij}n_i n_j = \rho_n + \rho_t\cos 2(\theta-\theta_o)$$

where $\underset{\sim}{n}\{\cos\theta, \sin\theta\}$ and

$$\rho_n = \frac{\rho_{11} + \rho_{22}}{2} = \frac{1}{2\pi}$$

$$\rho_t = \left[\left(\frac{\rho_{11} - \rho_{22}}{2}\right)^2 + \rho_{12}^2\right]^{1/2} = \frac{a}{2\pi}$$

are invariants of tensor ρ_{ij}. The direction of anisotropy is the major principal direction of ρ_{ij}. However, statistico-geometrical analysis presented in the chapter IX shows that shapes with $b = 0$ are inadmissible,

so that a second rank tensor cannot be assosiated with $S(\theta)$.

2.3 Average Forces on Contacts of the Same Orientation

Another major element in the description of granular assemblies are average forces $\overline{\underset{\sim}{f}}(\theta)$ on contacts of the same orientation group, as on Fig. 2.3. In further analysis of large systems, contributions of individual contacts will be unnoticeable in the gross behavior of the system and all properties will be expressed one way or another either through the average of forces or through the average of the square of forces $\overline{\underset{\sim}{f}^2}(\theta)$ for the same orientation group. The last average appears in all energy-related analyses.

To determine these averages or the relationships between them, another important element, distribution of forces on contacts of the same orientation, is necessary, i.e. function $P_\theta(\underset{\sim}{f})$ which gives the above averages as follows:

$$\underset{\sim}{f}(\theta) = \int \underset{\sim}{f} P_\theta(\underset{\sim}{f})\, d\underset{\sim}{f}$$

$$\overline{\underset{\sim}{f}^2}(\theta) = \int \underset{\sim}{f}^2 P_\theta(\underset{\sim}{f})\, d\underset{\sim}{f}$$

To determine this distribution for bonded and cohesionless particles is the objective of the statistics of contact forces. For a precisely specified deterministic system, determination of this function is a problem of prohibitive complexity and it was necessary to resort to probabilistic modelling. After the shape of P_θ was determined, solutions for average forces followed from the equations of mechanics.

A rough idea regarding shapes of $\overline{\underset{\sim}{f}}(\theta)$ can be obtained from continuum mechanics considerations. Gross force on a plane

with normal $n(\theta)$ can be obtained using stress tensor σ_{ij}. Normal and tangential components of gross forces are the following

$$F_n = \sigma_{ij} n_j n_i = \sigma_n + \sigma_t \cos(\theta - \theta_\sigma)$$
$$F_t = \sigma_{ij} n_j t_i = -\sigma_t \sin 2(\theta - \theta_\sigma) \qquad (2.3)$$

where σ_n, σ_t are Mohr's circle parameters (both are invariants) and θ_σ is the principal direction of σ_{ij}. Gross forces on each plane consist of contributions of all groups of contacts in different proportions and it is impossible to establish average forces for specific groups without considerable analysis.

For an isotropic system it can be expected that gross forces on the plane with orientation θ are largely due to contacts with this orientation. Still it is not known how contact forces are distributed between normal and tangential components.

The above relationships give the correct form of directional variation for forces containing only second Fourier components of a general Fourier series into which $F_n(\theta)$, $F_t(\theta)$ can be decomposed. This fact represents the very nature of continuum or phenomenological description with second rank tensors.

Expected directional variation of forces (2.3) and observations of experiments on photo-elastic discs, which show that contacts are created in the system under highly concentrated directional forces, resulted in the decision to consider $S(\theta)$ with the second Fourier components.

Creation of contacts in one direction puts the stability of other particles in jeopardy, and that is why the fourth Fourier component was added to $S(\theta)$ and stability of the system analyzed geometrically.

The above are heuristic considerations leading to the theory to be developed in the following chapters. The rest are a matter of careful analysis and adjustment of well-developed methods of classical statistical mechanics to problems of interest.

2.4 Particles in Mechanics of Granular Materials and in Classical Statistical Mechanics

Particles studied in mechanics of granular materials have a thermomechanical structure of solids and will be studied in conditions when temperature variations due to external causes and internal particle deformations are insufficient to affect deformational and frictional properties of particles. Such limitations can be viewed as being not restrictive for a variety of problems in soil mechanics and enable one to neglect an internal molecular structure of granules in order to consider them as objects with purely mechanical interactions.

A similar approach is taken in classical statistical mechanics with regard to large dynamic systems of molecules when viewed as particles with a certain mass and interacting by means of mechanical forces. Although the nature of molecular interactions is predetermined by the atomic structure of molecules and nuclear structure of atoms, these interactions can usually be described in terms of mechanical forces derivable from a certain potential function, the origin of which is irrelevant to classical statistical mechanics.

The difference between particles considered in the present theory and in statistical mechanics is the consideration of their

mass. In a variety of situations of interest to mechanics of granular materials, external actions are such that particles are in static equilibrium or near static equilibrium. In comparable external conditions, particles of statistical mechanics are in dynamic states with fast motions.

Intensity of particle motions in a system can be measured by average kinetic energy per particle $\overline{E}$ and for systems in static equilibrium $\overline{E} = 0$. Classical statistical mechanics studies motions of particles within the full range of average kinetic energies and the state of static equilibrium ($\overline{E} = 0$) is a central point of solid state physics which considers motions of molecules in solid phase as small vibrations near static equilibrium. In many cases of molecular systems, the state of static equilibrium corresponds to regular arrangements of molecules in a crystalline lattice which is formed due to specifics of intermolecular interactions.

Granular assemblies in static equilibrium generally do not form regular structures, as well as certain molecular systems which result in amorphous solids. Systems irregular in the state of static equilibrium are of specific interest to several areas of solid state physics [5, 12] with few statistical mechanical results available. Such systems are studied here in connection with problems of soil mechanics. Classical statistical mechanical formulations consider the central interparticle forces inadequate for description of frictional particles. Introduction of dissipative tangential forces into the analysis of dynamic systems results in significant complications, but dynamic formulation is not necessary here and non-central forces will be considered in static conditions. The necessity to describe states of static equilibrium in the absence of a crystalline lattice requires methods different from those traditionally employed

in statistical mechanics,which is primarily concerned with kinetic motions, and considers static equilibrium only as a reference state for dynamic perturbations. Kinetic motions and related heat properties are not considered here, but states of static equilibrium are studied under conditions of external actions usually not considered in statistical mechanics.

The theory of static equilibrium for large assemblies of particles is presented here independent of classical statistical mechanics with its specific language and interpretation of results aimed at describing thermodynamic properties of dynamic systems. Such an interpretation is necessary when particles of classical statistical mechanics are of molecular size.

Note that such an analysis is possible due to the simple nature of contact interactions in granular systems. More general theories [2] of micromechanics aimed at description of polycrystalline solids and fibrous systems must resort to additional theoretical constructions not considered in classical statistical mechanics. This is not necessary in the present theory, but its range of applicability covers systems with contact interactions, or generally irregular networks, as in Fig. 2.2.

CHAPTER III

PHENOMENOLOGICAL STRESS TENSOR

3.1 Introduction

This chapter introduces a micro-mechanical analogue of the continuum mechanics stress tensor and studies its properties. In the analysis of granular assemblies on the level of contact forces, there is no *a priori* reason for the introduction of continuum mechanics analogues. All that is necessary is the specification of forces on boundary particles or their displacements for a mechanical response to be unique.

In the present work granular assemblies are studied under conditions where only gross loads are specified on their boundaries, so that there is uniformity in both load application and material response. Such loads can be specified by viewing the boundary as a regular assembly of continuous elements subject to tractions which are functions of coordinates.

Gross loads may be taken to be redistributed between particles using a certain conveniently selected procedure to result in unique forces on boundary particles or their displacements if the latter are prescribed on the boundary.

With such an approach only certain special functions describing gross loads are permissible. There is an arbitrary element in this procedure which is reasonable only for large systems where gross response is independent of a precise pattern of boundary forces.

For finite systems in the described conditions, a response will fluctuate depending on the precise geometrical structure of a system and it is practically feasible to obtain a response in such conditions only

in probabilistic terms for a collection of macroscopically identical systems subject to identical gross loads. If similar elements of volume are selected in all these systems, physical properties related to these elements of volume will fluctuate and their response, on average, can be expected to be described in continuum mechanics terms.

Several examples in statistical mechanics, notably viscous flow of fluids [20], indicate that statistical analysis leads to continuum mechanics equations with proper definition of continuum mechanics parameters in terms of certain averages of a system's micro- parameters. In the mentioned example of viscous fluids, an expression appears for the stress tensor and constitutive relationship which relates the stress tensor to strain rates.

The following analysis of granular assemblies introduces a micromechanics analogue of the stress tensor by considering external loads on the boundaries of an assembly which corresponds to a uniform state of stress in continuum mechanics. Such loads correspond to tractions on the boundary of the form $p_i = \sigma^{\beta}_{ij} n_j$, where σ^{β}_{ij} is a certain second rank tensor and n is the normal vector at each point of a continuous boundary.

After σ^{β}_{ij} is related to contact forces within the system and the form of the relations becomes known, the phenomenological stress tensor is introduced by definition for any arbitrary volume of a system and its properties are studied. The introduced quantity is a function of volume and fluctuates for similar volumes within the assembly. In the limit of an infinite assembly the properties of the introduced tensor are similar to those of the stress tensor of continuum mechanics. Instead of considering the limit of an infinite assembly, it is possible to consider an average over infinitesimal volumes within different systems and arrive at

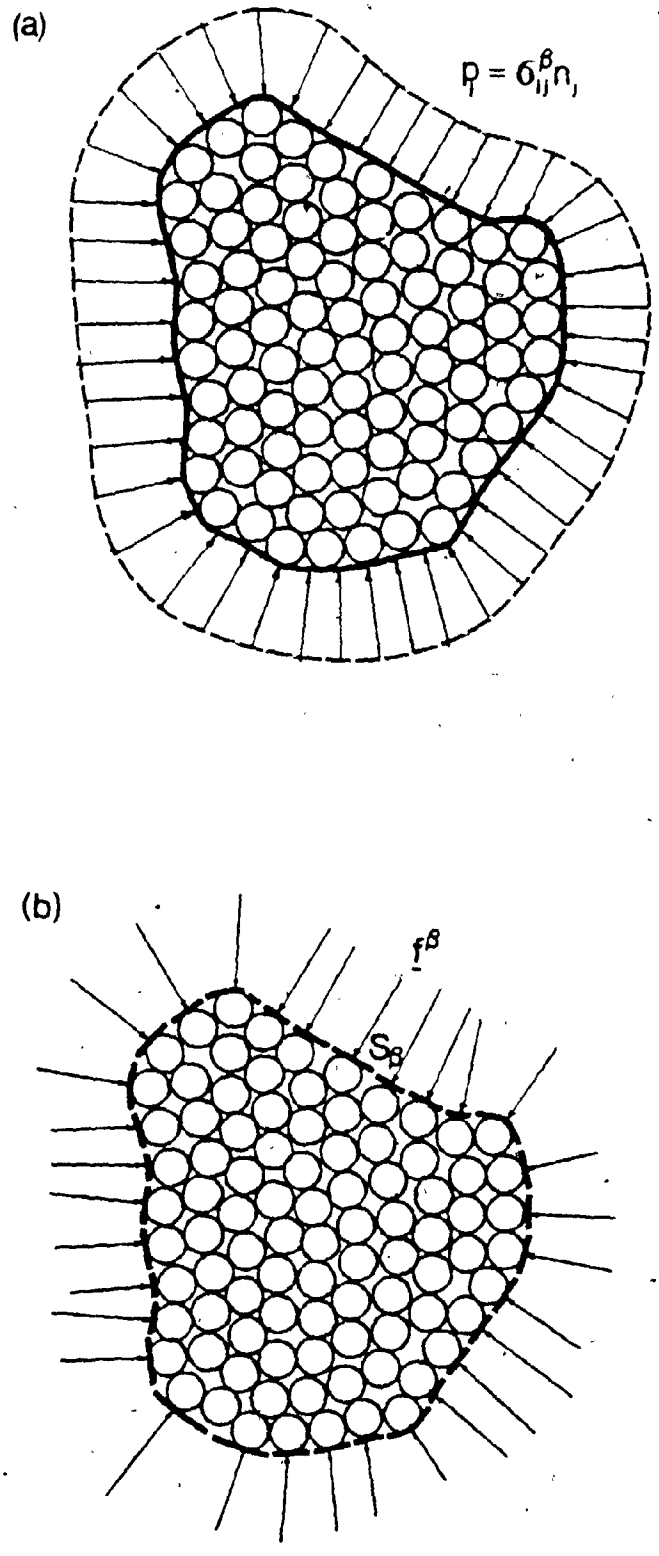

FIGURE 3.1

LOAD TRANSFER TO BOUNDARY PARTICLES

the same interpretation.

The systems analyzed are assemblies of spheres and discs of equal diameter. Generalizations are indicated for assemblies of particles varying in size and of non-regular shapes.

3.2 External Loads on an Assembly of Particles

Consider an assembly of spheres of equal size within a certain region and surround it with a continuous shell viewed as the boundary of the assembly (for conceptual simplicity Fig. 3.1[a] illustrates an assembly of discs). Let an external distributed load $\underset{\sim}{p}(\underset{\sim}{R})$ be applied at each point $\underset{\sim}{R}$ of the shell and be selected in the form

$$p_i(\underset{\sim}{R}) = \sigma^{\beta}_{ij} n_j(\underset{\sim}{R}), \tag{3.1}$$

where $n_j(\underset{\sim}{R})$ is the normal vector of the shell at point $\underset{\sim}{R}$ and σ^{β}_{ij} is a certain second rank tensor with nine position-independent components. Applied to continuum this load results in a uniform state of stress σ^{β}_{ij}.

In order to transfer the load (3.1) to boundary particles of the assembly let the complete boundary B be subdivided into regions adjacent to each particle in contact with the boundary. Let S_β be the region corresponding to particle β. The idea is to transfer the load from regions S_β to its corresponding particles.

The total force acting on area S_β is

$$f_i = \int_{S_\beta} p_i(R)\, dS \tag{3.2}$$

where $\underset{\sim}{p}$ is given by (3.1).

For further analysis it is advantageous to transfer the total force (3.2) to the particle approximately, rather than exactly, maintaining

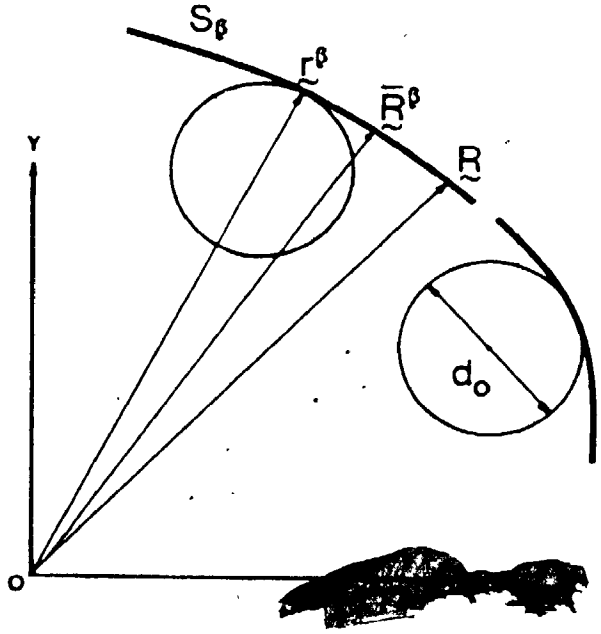

FIGURE 3.2

GEOMETRY OF BOUNDARY

a certain balance in the total transfer of forces. For the large assemblies studied here a precise pattern of external forces on boundary particles has no effect on the global response of the system.

Let r^{β} be the position of a contact on a boundary particle and be referred to a fixed Cartesian coordinate system. Let also R be an arbitrary point on boundary B. When a portion of boundary S_{β} adjacent to particle β is considered, any point R on S_{β} will deviate by no more than several particle diameters from the point r^{β} (Fig. 3.2), i.e. $|R - r^{\beta}| \sim \delta(d_o)$, where d_o is the particle diameter.

A force transferred to particle β will be of a magnitude close to (3.2), specifically:

$$f_i^{\beta} = \frac{1}{r_j^{\beta}} \int_{S_{\beta}} R_j p_i(R) dS \qquad (3.3)$$

The position vector R of an arbitrary point on S_{β} is now introduced into the integral. To compensate for this change, the integral is divided by r_j^{β}, close to R_j. The fact that (3.3) is close to (3.2) is justified using the mean-value theorem, according to which

$$f_i^{\beta} = \frac{\overline{R_j^{\beta}}}{r_j^{\beta}} \int_{S_{\beta}} p_i(R) dS$$

where $\overline{R_j^{\beta}}$ is a certain point on S_{β} (Fig.3.2). If the origin of a coordinate system is selected far from the boundary, it is quite clear that $\overline{R_j^{\beta}} \simeq r_j^{\beta}$ and

$$f_i^{\beta} \simeq \int_{S_{\beta}} p_i(R) dS,$$

so that nearly the entire force (3.2) is transferred to the particle from the part of the boundary adjacent to the particle (Fig. 3.1[b]). Note that

there is a certain freedom in transferring forces to the assembly, since the choice of regions S_β can be made within limited ranges. It is perhaps possible to select regions S_β in such a way that (3.3) will conicide with (3.2) exactly.

The main reason for transferring forces according to (3.3) is the fact that the following identity is satisfied for all boundary particles:

$$\sum_{\beta \epsilon B} f_i^\beta r_j^\beta = \int_S R_j p_i(R) dS \tag{3.4}$$

The above relationship can be obtained by adding (3.3) for all boundary particles. The integral in (3.4) is over the entire boundary and noting (3.1) it can be evaluated using the Green-Gauss theorem*. Calculations give

$$\sum_{\beta \epsilon B} f_i^\beta r_j^\beta = V \sigma_{ij}^\beta \tag{3.5}$$

In relationship (3.5) one can recognize the expression for the average stress tensor considered in continuum mechanics [22]. At this stage of analysis, boundary forces are precisely specified by (3.3) and relationship (3.5) follows readily.

---

* An integral over a closed surface can be transformed into an integral over the volume bounded by this surface through symbolic substitution [22].

$$n_k dS \rightarrow \frac{\partial}{\partial r_k} dV$$

In the present case

$$\int_S \sigma_{ik} R_j n_k dS = \int_V \sigma_{ik} \frac{\partial R_j}{\partial R_k} dV = \int_V \sigma_{ik} \delta_{jk} dV = V \sigma_{ij}$$

3.3 Volume-additive Identities for Systems in Static Equilibrium

An assembly of N particles with M contact points ($M/2$ physical contacts) can be described in terms of $3M/2$ components of contact forces which must satisfy $6N$ equations of static equilibrium for forces and moments. The number of unknown forces is usually much greater than the number of equations ($M > 4N$) and granular assemblies are usually strongly statically indeterminate. A statically determinate case corresponds to $M = 4N$, i.e. on the average four contacts per particle (average coordination number $\gamma=4$) It is not possible to determine all contact forces strictly on the basis of equations of static equilibrium and particle deformational properties must be known if all contact forces are to be determined. Even though the system may be statically indeterminate, considerable information on contact forces can be recovered on the basis of equations of static equilibrium. This is done using the proof of the "virial theorem of mechanics" [23].

An assembly of N equal size spherical particles with diameter d_o will be analyzed first. Particles are assumed to interact by means of contact forces only. In reality, particle interactions occur through a finite area and there is the possibility of resultant moment transfer at the surface of the contact. Contact area is assumed here to be small enough to neglect moment transfer through contacts. An assessment of this approximation is presented in Appendix A.

Particles in the following analysis are also assumed to be sufficiently rigid, so that no distinction is made between deformed and undeformed configurations.

Let the particles of the assembly be numbered and let r^K be the position

vector of particle k referred to a fixed Cartesian coordinate system. Also, let the contacts on each particle be numbered and let $\underset{\sim}{f}^{k,m}$ be referred to a force acting on particle k at contact m.

Equations of static equilibrium can be written in the form

$$\sum_{m=1}^{m_k} f_i^{k,m} = 0, \quad k = 1,\ldots N; \; i = 1,2,3, \tag{3.6}$$

where m_k is the number of contacts on particle k. Body forces are not considered.

To obtain the required volume-additive identities necessary to define the phenomenological stress tensor, each of equations (3.6) for a force component i of particle k must be multiplied by the component r_j^k of the position vector of the particle.

Further summation with respect to all k results in nine identities of the form

$$\sum_{k=1}^{N} \sum_{m=1}^{m_k} f_i^{k,m} r_j^k = 0; \; i,j = 1,2,3. \tag{3.7}$$

Each internal contact in the assembly contributes two terms in (3.7) with forces of the opposite sign. Let $\underset{\sim}{f}^{kl}$ be the force acting on particle k from particle l. Consider a pair of terms in (3.7) corresponding to the contact of particles k and l ($\underset{\sim}{f}^{kl} = -\underset{\sim}{f}^{lk}$) and transform them as follows:

$$f_i^{kl} r_j^k + f_i^{lk} r_j^l = -\frac{1}{2}\left[f_i^{kl}(r_j^l - r_j^k) + f_i^{lk}(r_j^k - r_j^l)\right] \tag{3.8}$$

Let $\underset{\sim}{n}^k$, $\underset{\sim}{n}^l$ be normal vectors of the same contact viewed from particles k and l, respectively. In can be seen from (3.8) that $r_j^l - r_j^k = d_o n_j^k$, so that (3.8) gives

$$f_i^{kl} r_j^k + f_i^{lk} r_j^l = -\frac{d_o}{2}\left[f_i^{kl} n_j^k + f_i^{lk} n_j^l\right] \tag{3.9}$$

(a)

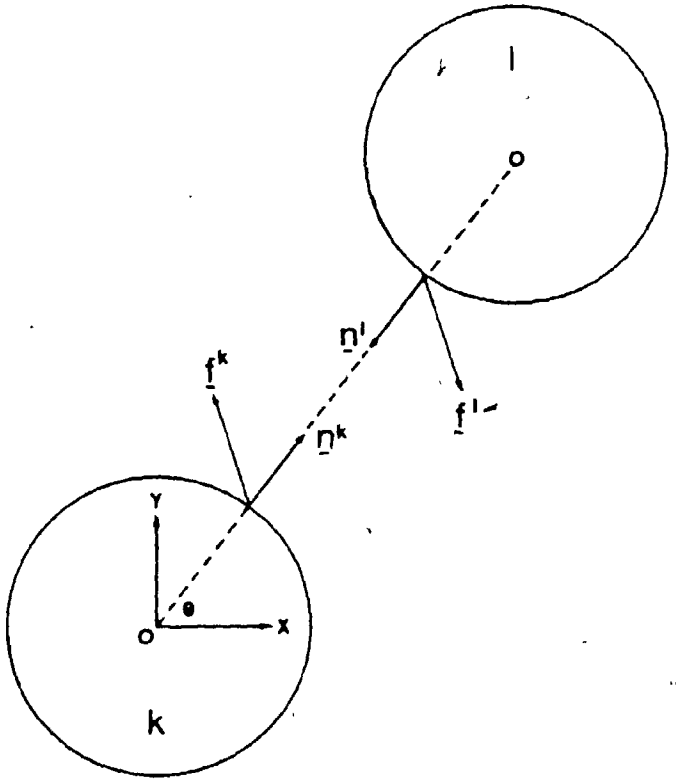

(b)

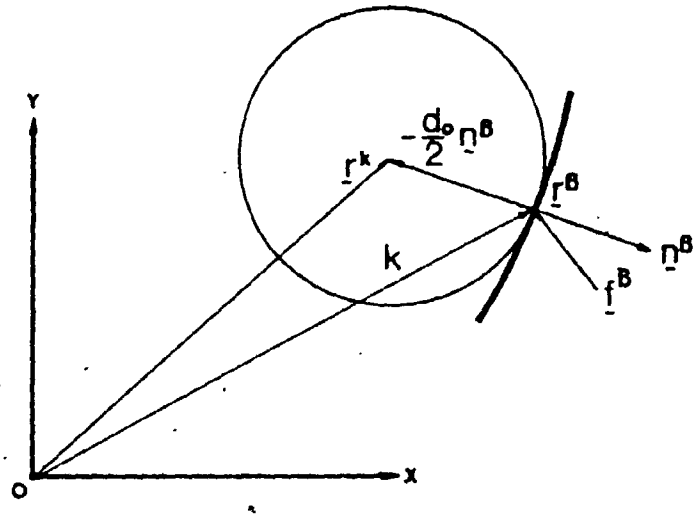

FIGURE 3.3

INTERNAL AND EXTERNAL PARTICLE CONTACTS

Note that both terms in the left-hand side of (3.9) are identical in magnitude, since forces and normal vectors related to the two particles forming a contact both change sign (Fig. 3.3[a]).

All terms in (3.7) can be classified as corresponding to either internal or external contacts of the assembly and each internal contact corresponds to two terms of the (3.9) type.

Consider now external contacts. If $\underset{\sim}{r}^{\beta}$ is the position of external contact β of particle k:

$$\underset{\sim}{r}^{k} = \underset{\sim}{r}^{\beta} - \frac{d_o}{2}\,\underset{\sim}{n}^{\beta}$$

where $\underset{\sim}{r}^{k}$ is the position of the particle and $\underset{\sim}{n}^{\beta}$ is the normal vector of the considered contact (Fig. 3.3[b]).

Terms of (3.7) corresponding to boundary contacts are of the form

$$f_i^{\beta} r_j^{k} = f_i^{\beta} r_j^{\beta} - \frac{d_o}{2} f_i^{\beta} n_j^{\beta} .$$

Taking into account the above relationship for external contacts and (3.9) for internal contacts, equations (3.7) can be rewritten in the form:

$$\sum_{\beta \in B} f_i^{\beta} r_j^{\beta} = \frac{d_o}{2} \sum_{c \in V} f_i^{c} n_j^{c} \qquad (3.10)$$

where the summation in the left-hand side is with respect to all boundary contact points and the right-hand sum corresponds to contact points on all particles in volume V.

The right-hand side of (3.10) includes contributions from all contact forces in volume V and represents a volume-additive quantity.

Equality (3.10) is valid for any system of forces that satisfies the equations of static equilibrium. Such forces are further referred to as being "statically admissible".

Generalizations for particles of arbitrary shapes will be considered below.

3.4 Phenomenological Stress Tensor and Average Stress Tensor of Continuum Mechanics

Comparison of relationship (3.10), which is valid for any arbitrary system of boundary forces, and relationship (3.5) for boundary forces specified in terms of σ^{β}_{ij} gives (for assemblies of equal size spheres)

$$\sigma^{\beta}_{ij} = \frac{1}{V} \sum_{c \in V} \frac{d_o}{2} f^c_i n^c_j \tag{3.11}$$

This expression indicates that, for any system of statically admissible forces, a volume-additive combination (3.11) is uniquely related to a tensor defining forces on boundary particles according to (3.3).

Relationship (3.11) was developed for specific force applications and has limited use. It gives no indication of the means of studying the gross actions of contact forces within an arbitrary region of the assembly.

Consider now a large assembly and select an arbitrary region of volume V within the system. The following function of the selected volume is introduced by definition

$$\hat{\sigma}_{ij}(V) = \frac{1}{V} \sum_{c \in V} \frac{d_o}{2} f^c_i n^c_j \tag{3.12}$$

where the summation is with respect to all contacts on particles of the selected volume which also can coincide with the total volume of the assembly.

There is a clear distinction between (3.11) and (3.12) in that

(3.12) is defined to have meaning for an arbitrary region within the assembly and it is not related to specifically applied boundary forces as in (3.11). The introduced quantity (3.12) will be called the "phenomenological stress tensor" and it is necessary to justify the use of the term attached to $\hat{\sigma}_{ij}(V)$ and usefulness of the introduced quantity.

Being a function of volume, $\hat{\sigma}_{ij}$ will fluctuate from volume to volume in a homogeneous assembly. It is quite clear that such fluctuations will be small for large volumes due to the volume-additive composition of (3.12).

Consider the relationship between $\hat{\sigma}_{ij}(V)$ and average stress tensor $\bar{\sigma}_{ij}(V)$ defined in continuum mechanics [22] as the volume average of the continuum stress tensor σ_{ij} as follows:

$$\bar{\sigma}_{ij} = \frac{1}{V} \int_V \sigma_{ij}(\underset{\sim}{r})\, dV \qquad (3.13)$$

Note that $\sigma_{ij}(\underset{\sim}{r})$ is defined at each point of the continuum and satisfies equations of equilibrium considered here without body forces

$$\frac{\partial \sigma_{ik}}{\partial r_k} = 0$$

An assembly of particles can be regarded as a two-phase continuum with stress tensor $\sigma_{ij}(r)$ such that $\sigma_{ij}(r) = 0$ when $\underset{\sim}{r}$ is outside of a particle's volume. This assumption makes it possible to extend integration in (3.13) over particle-filled volumes. Due to the additive property of integration, (3.13) can be rewritten in the form

$$\bar{\sigma}_{ij} = \sum_{k=1}^{N} \frac{V_k}{V} \left(\frac{1}{V_k} \int_{V_k} \sigma_{ij}(\underset{\sim}{r})\, dV \right) = \sum_{k=1}^{N} \frac{V_k}{V} \bar{\sigma}^k_{ij} \qquad (3.14)$$

where V_k is the volume of the k-th particle and σ^k_{ij} is the average stress tensor over particle k. To calculate $\bar{\sigma}^k_{ij}$, equations of equilibrium must be multiplied by r_j and integrated over volume V_k. Then

$$\frac{\partial \sigma_{ik}}{\partial r_k} r_j \, dV = \int_{V_k} \frac{\partial}{\partial r_j} (\sigma_{ik} r_j) - \int_{V_k} \sigma_{ik} \frac{\partial r_j}{\partial r_k} dV = 0 \tag{3.15}$$

Noting that $\partial r_i / \partial r_k = \delta_{ik}$ and transforming the first integral in the right-hand side of (3.15) into a surface integral using the Green-Gauss theorem (see footnote on page 35), one can obtain

$$\bar{\sigma}^k_{ij} = \frac{1}{V_k} \int_{S_k} p_i(r) \, r_j \, dS \tag{3.16}$$

where $p_i(r) = \sigma_{ij} n_j$ is the distributed force acting on the surface of particle k. Assuming that particles interact with forces applied at geometrical points, the load on the surface of the particle is of the form

$$p_i = \sum_{c \in S_k} f_i^c \, \delta(\underset{\sim}{r} - \underset{\sim}{r}^c) \tag{3.17}$$

where the delta-function is concentrated at positions of particle contacts which can be referred to particle centers when calculating the integrals of (3.16). Then $\underset{\sim}{r}^c = \frac{d_o}{2} \underset{\sim}{n}^c$ and substitution of (3.17) into (3.16) followed by integration gives

$$\bar{\sigma}^k_{ij} = \frac{1}{V_k} \sum_{c \in S_k} \frac{d_o}{2} f_i^c n_j^c \tag{3.18}$$

Substitution of the above quantity into (3.14) gives

$$\bar{\sigma}_{ij} = \frac{1}{V} \sum_{c \in V} \frac{d_o}{2} f_i^c n_j^c \tag{3.19}$$

where the summation in (3.18) is extended over all contacts on particles in volume V.

The expression for the phenomenological stress tensor (3.12) introduced on the basis of equations of static equilibrium coincides with the expression for the average stress tensor of continuum mechanics developed on the basis of the notion of a two-phase continuum. Such understanding of a continuum is legitimate within the framework of continuum mechanics, but the

analysis of such stress fields requires statistical methods foreign to continuum mechanics, the main advantage of which is efficient treatment of continuous fields and fields with "regular" discontinuities. The treatment of discontinuous fields, as in irregular assemblies is the realm of statistical micro-mechanics which requires volume-additive expressions based on the introduced phenomenological stress tensor. This, perhaps, is why volume-additive expressions, such as (3.19), are not introduced in continuum mechanics.

On the other hand, volume-additive expressions for pressure do appear in classical statistical mechanics which operates with pressure rather than stress. Tensorial pressure, however, is not usually considered, as substances in gaseous and liquid phases cannot sustain loads other than hydrostatic in equilibrium states. For viscous fluids [20], volume-additive expressions appear automatically for a non-equilibirum pressure tensor, but historically there is a tendency in physical literature to ignore the tensorial nature of pressure. Following continuum mechanics terminology, the tensorial quantity, which appears in studies of the viscous flow of fluids, was called a stress. It is sometimes mentioned in interdisciplinary studies [3 6] that pressure is a quantity of tensorial nature.

Appendix B shows how tensorial pressure appears in the statistical mechanics of dynamic systems which usually study systems with central interactions between particles. Such interactions correspond only to normal components of contact forces, therefore the conducted independent analysis of granular assemblies with arbitrary contact forces became necessary, and the phenomenological stress tensor was introduced. The terminology

used reflects a close analogy between this quantity and the average stress tensor of continuum mechanics. On the other hand, $\hat{\sigma}_{ij}(V)$ fluctuates as phenomenological pressure. The term "phenomenological stress" reflects both properties and the emphasis on stress is due to the fact that fluctuations in $\hat{\sigma}_{ij}$ disappear for infinite assemblies and the quantity has all features of the continuum mechanics stress tensor.

3.5 Contact Force Tensor

The phenomenological stress tensor was introduced above for an assembly of equal size spheres. Examination of the form of (3.12) and basic generality of the analysis suggest that given (3.12) in the form

$$\hat{\sigma}_{ij}(V) = \frac{1}{V} \sum_{c \in V} \sigma^c_{ij} , \tag{3.20}$$

where

$$\sigma^c_{ij} = \frac{d_o}{2} f^c_i n^c_j , \tag{3.21}$$

the expression will retain its form for particles of any size and shape, but with a form of tensor different from (3.21). This will be referred subsequently as the "contact force tensor". The phenomenological stress tensor (3.20) is a volume average of contact force tensors for all contacts in the volume. This quantity will be useful in the analysis below. The form of σ^c_{ij} for spheres of varying sizes is of (3.21) type with d^c, the distance between the centers of two spheres in contact, instead of d_o. To concentrate attention on the main features of granular systems, the analysis of equal size particles will be continued.

3.6 Phenomenological Stress Tensor and Simulation of Uniform State of Stress

Although volume-additive expressions for the phenomenological stress

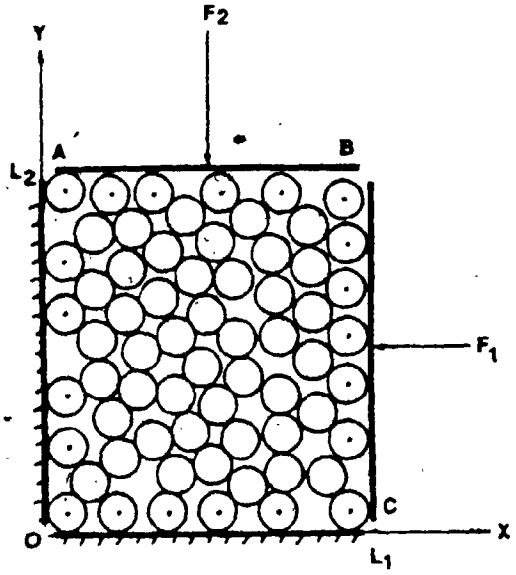

FIGURE 3.4

SIMULATION OF UNIFORM STATE OF STRESS

tensor are of chief interest, identity (3.10) makes it possible to express this quantity in the form

$$\hat{\sigma}_{ij}(V) = \frac{1}{V} \sum_{\beta \in B} f_i^\beta r_j^\beta \tag{3.22}$$

where f^β, r^β are forces and positions of contacts on boundary particles in volume V. Expression (3.22) was employed in [9] for calculating the average stress tensor in experiments with photo-elastic discs. The following example demonstrates this application.

Consider the experiment shown in Fig. 3.4 in which an assembly of discs is subject to external forces F_1 and F_2. Assume for simplicity that the boundary plates containing the assembly are frictionless. In this simple case, $\hat{\sigma}_{ij}$ given by (3.22) can be calculated explicitly. The sum corresponding to boundary forces can be evaluated separately for each of the four plates confining the assembly. Note first that V in (3.22) in the plane case is the area of the assembly $L_1 L_2$, so that

$$\hat{\sigma}_{11} = \frac{1}{L_1 L_2} \left[\sum_{\beta \in AB} f_1^\beta x_1^\beta + \sum_{\beta \in BC} f_1^\beta x_1^\beta + \sum_{\beta \in CO} f_1^\beta x_1^\beta + \sum_{\beta \in OA} f_1^\beta x_1^\beta \right] \tag{3.23}$$

As the boundaries are frictionless, f_1 components on AB and OC are zero and the corresponding sums disappear. For boundary BC all $x_1^\beta = L_1 - d_o/2$, where d_o is the disc diameter; similarly for OA, $x_1^\beta = \frac{d_o}{2}$ and (3.23) can be given in the form

$$\hat{\sigma}_{11} = \frac{1}{L_1 L_2} \left[\left(L_1 - \frac{d_o}{2} \right) \sum_{\beta \in BC} f_1 + \frac{d_o}{2} \sum_{\beta \in OA} f_1^\beta \right]$$

Due to the equilibrium of boundary forces, sums corresponding to BC and OA equal to external forces, so that

$$\hat{\sigma}_{11} = - \frac{|F_1|}{L_2} \left(1 - \frac{d_o}{L_1} \right) \simeq - \frac{|F_1|}{L_2}$$

The last expression is accurate for large assemblies ($d_o << L_1$) and corresponds to the notion of "stress" in such an experiment. Similar calculations can be performed for σ_{22} and $\sigma_{12} = \sigma_{21} = 0$ due to the lack of tangential forces on the boundary. Note that the selection of coordinate system parallel to the boundaries of the assembly resulted in σ_{11} and σ_{22} being principal stresses.

3.7 Symmetry of the Phenomenological Stress Tensor

Consider moment equilibrium of the part of the assembly within volume V. According to the assumption of no moment transfer through contacts, the equation of moment equilibrium can be written in the form

$$\sum_{\beta \in B^-} [r^\beta \times f^\beta] = 0$$

where the cross product above gives the moment of the boundary force f^β applied at point r^β.

If the above vector equation is written in terms of components

$$\sum_{\beta \in B} (r_j^\beta f_i^\beta - r_i f_j) = 0.$$

The above relationship is the condition of symmetry for the phenomenological stress tensor in the form (3.22) or in the equivalent form (3.12).

In the further presentation of the theory, the adjective "phenomenological" will occasionally be dropped for brevity, but the notation $\hat{\sigma}_{ij}$ will be retained to emphasize the meaning of the tensor as a function of volume. For infinite assemblies when fluctuations disappear; that is, when

$$\sigma_{ij} = \lim_{V \to \infty} \hat{\sigma}_{ij}(V)$$

it will be precisely the stress tensor of continuum mechanics. Such terminology will be justified by showing that σ_{ij} gives loads $p_i = \sigma_{ij} n_j$ per unit area of an infinite plane within an assembly.

3.8 Stress Tensor for an Infinite Assembly

To obtain σ_{ij} for an infinite assembly, expression (3.12) must be slightly transformed to show how the geometrical structure of the assembly enters the final result. Geometrical interpretations are presented for assemblies of discs of equal size, although the following analysis is equally applicable to assemblies of spheres of equal diameter with a symbolic change in notations for geometrical elements.

Let the orientations of all vectors be specified by the angle θ between the direction of a vector and x-axis of the fixed Cartesian coordinate system. The angle θ will be further referred to as "orientation of the vector". Contacts of the assembly can be classified into G groups such that within each group, orientations of contact normals are within θ_g and $\theta_g+\Delta\theta$ ($g = 1,\ldots,G;\ \Delta\theta = 2\pi/G$). Each physical contact results in two opposite orientations treated separately. Let M be the number of contact normals (twice the number of physical contacts) and let also $\Delta M(\theta_g)$ be the number of contacts in the group θ_g. As an example, contacts of the assembly in Fig. 2.2 were classified into 72 orientation groups. The distribution representing ΔM_g with $\Delta\theta = 5°$ was shown in Fig. 2.4. It is convenient to introduce contact distribution density $S(\theta)$ as follows:

$$\Delta M_g = M\, S(\theta_g)\, \Delta\theta \tag{3.24}$$

where $S(\theta_g)$ is a certain generally discontinuous function which also depends on the particular subdivision of contact orientations into groups. For each such subdivision

$$\sum_{g=1}^{G} S(\theta_g) = 1$$

Now let all terms in the sum (3.12) corresponding to contacts of

the same group be brought together. Assuming that $\Delta\theta$ is small and normal vectors of contacts of the same orientation group are identical (which is strictly the case of $\Delta\theta \to 0$), (3.12) can be rewritten in the form

$$V\hat{\sigma}_{ij} = \frac{d_o}{2} \sum_{g}^{G} \left\{ \left[\frac{1}{M_g} \sum_{c \in \theta_g} f_i^c \right] n_j(\theta_g) \right\} \Delta M_g(\theta_g) \tag{3.25}$$

Note that $\Delta M_g = M_g$ was introduced into the numerator and denominator to identify the quantity in brackets

$$\bar{f}_i(\theta_g) = \frac{1}{M_g} \sum_{c \in \theta_g} f_i^c \tag{3.26}$$

with the average force on contacts of the same orientation group θ_g.

Using (3.26) and (3,24), (3.25) can be rewritten in the form

$$\hat{\sigma}_{ij}(V) = \frac{1}{2} d_o \frac{M}{N} \frac{N}{V} \sum_{g=1}^{G} \bar{f}_i(\theta_g) n_j(\theta_g) S(\theta_g)] \Delta\theta \tag{3.27}$$

Consider now transition to an infinite assembly in (3.27) which is possible if the following limits exist:

$$n_v = \lim_{V\to\infty} \frac{N}{V} \qquad \gamma = \lim_{V\to\infty} \frac{M}{N}$$

$$\bar{f}(\theta) = \lim_{\Delta\theta\to 0} \lim_{V\to\infty} \frac{1}{M_g} \sum_{c \in \theta_g} f^c \tag{3.28}$$

$$S(\theta) = \lim_{\Delta\theta\to 0} \lim_{V\to\infty} S(\theta_g)$$

for any infinite part of the considered infinite assembly and $\bar{f}(\theta)$, $\bar{S}(\theta)$ are assumed continuous in the infinite limit. In this case (3.27) converges to

$$\sigma_{ij} = \frac{1}{2} \gamma n_v \int_0^{2\pi} \bar{f}_i(\theta)\, n_j(\theta)\, S(\theta)\, d\theta \tag{3.29}$$

The meaning of conditions (3.28) can be readily understood. The first two conditions indicate that infinite samples of the same assembly have the same particle density and average coordination number, i.e. the

assembly is statistically homogeneous.

The existence of a continuous contact orientation distribution $S(\theta)$ indicates that irregularity of the system is such that infinite samples of the system contain the entire spectrum of contact orientations. This property can be viewed as a reflection of hetergeneity and, perhaps, can be termed "perfect irregularity".

The existence of continuous average forces on contacts of the same orientation can be attributed to the same "perfect irregularity". The fact that average forces are identical for different parts of the assembly indicates that homogeneity with respect to forces is implicitly involved in the set of assumptions leading to (3.29).

The existence of limits for $n_v, \gamma, S(\theta)$ which define the structure of the assembly must be accepted as mathematical expressions of the introduced physical notions of "perfect irregularity" and homogeneity. They define an infinite assembly and must be accepted as primitive concepts. The proof of the existence of the above limits is only possible if the process is known in which the system was created. No attempt will be made to present such a process and the existence of systems with continuous $S(\theta)$ is simply assumed. Note that the distribution of contact orientations must be normalized, i.e.

$$\int_0^{2\pi} S(\theta)d\theta = 1$$

At this stage no insight is available into possible forms of $S(\theta)$ and such information will be obtained on the basis of geometrical analysis. It is clear, however, that $S = 1/2\pi$ corresponds to isotropic assemblies when no contact orientation has any preference. Note also that (3.29) is valid for a finite assembly with a discrete spectrum of contact

orientations. In this case

$$S(\theta) = \frac{1}{M} \sum_{c \in V} \delta(\theta - \theta^c)$$

where $\delta(\theta-\theta^c)$ is δ-function concentrated at contact orientations θ^c of all particles in volume V. Substitution of the above $S(\theta)$ into (3.29) and integration* results in (3.12).

The assumption regarding the existence of continuous $\overline{f}(\theta)$, identical for any infinite part of the assembly, can, perhaps, be proven, and it must be a consequence of equations of static equilibrium and uniform loads on the assembly.

Boundary loads on an infinite assembly can be considered as tractions on a system of surfaces which, in the limit, cover the entire assembly. Although the idea of load application $p_i = \sigma^{\beta}_{ij} n_j$ with constant σ^{β}_{ij} is a reasonable way of simulating homogeneous conditions with respect to contact forces, no proof is given here that average forces are identical for any infinite part of the assembly. This was assumed and (3.29) followed immediately.

It is now necessary to demonstrate that the phenomenological stress tensor (3.29) for an infinite assembly gives forces per unit area of an infinite plane in the form $p_i = \sigma_{ij} n_j$ for any such plane. This would indicate the analogy with the stress tensor in continuum mechanics. Note that it is impossible to establish this analogy on the basis of finite systems, since

---

*Delta functions are integrated according to the rule

$$\int_{x_o-\varepsilon}^{x_o+\varepsilon} f(x)\, \delta(x-x_o) = f(x_o)$$

where ε is an arbitrary small but finite number, and $f(x)$ is a continuous function.

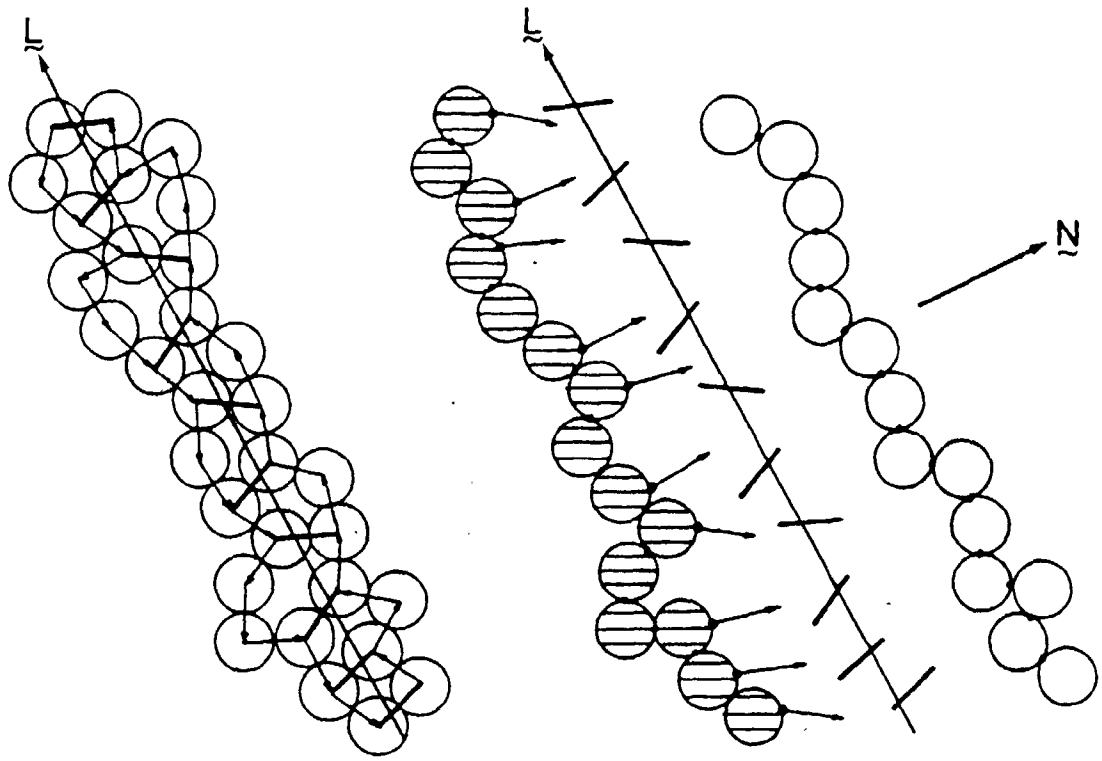

FIGURE 3.5

MICRO-ANALOGUE OF PLANE ELEMENTS

the present theory requires that the stress tensor be a function of volume.

There is also a technical difficulty even in this comparison, since plane elements in the present theory have a distinct geometrical structure, so that such elements must be identified first.

This is obviously a geometrical problem and it explains why analytical techniques employed previously resulted in an interpretation of the phenomenological stress tensor different from that which can be extracted from the continuum mechanics interpretation of the stress tensor.

Before the problem of identifying plane elements in the three-dimensional case can be approached, it is conceptually convenient to introduce line elements for plane assemblies of discs. Elements of statistical geometry are presented in the next section in connection with this problem.

3.9 Transect Analysis of Plane Assemblies of Discs

Consider a plane assembly of discs geometrically represented as a network of segments connecting disc centers (Fig. 2.1). Let L be a certain oriented line which intersects a number of polygons (Fig. 3.5[a]). Consider segments representing the sides of these polygons which are not intersected by the transect line. It may be seen from Fig. 3.5[a] that such segments connect particles which run on "average" parallel to the transect line. Fig. 3.5[b] shows these particles disconnected at contacts corresponding to the intersected segments. Forces which act at these contacts are indicated in Fig. 3.5[b]. It is reasonable to consider the chains of particles resulting from the above geometrical constructions as equivalents of line

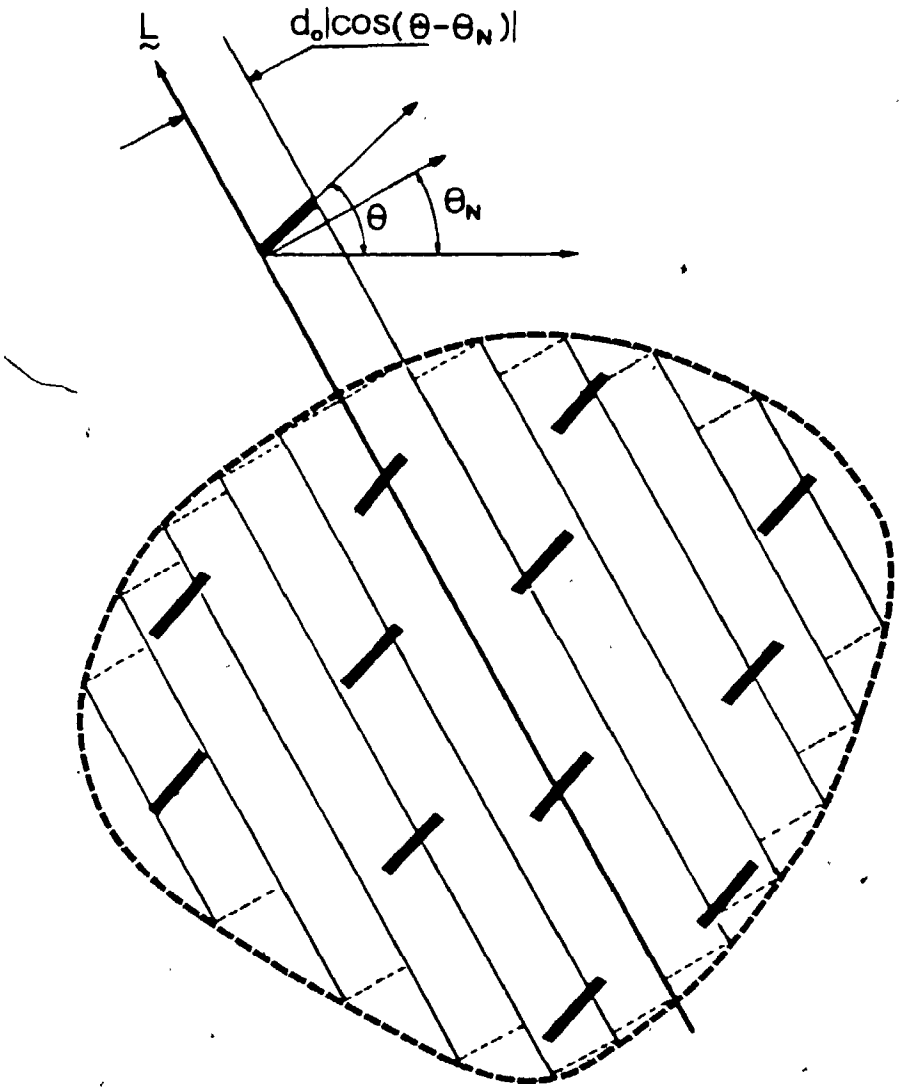

FIGURE 3.6

INTERSECTION OF SEGMENTS BY TRANSECT LINES

elements in continuum mechanics. Contact forces on these chains are associated with segments intersected by the transect line and it is necessary to determine the number of intersected segments and their orientational distribution. To calculate the number of intersections per unit length of the transect line, consider a certain area V which surrounds a transect line and has M contact points on particles in this region. The number of segments is one-half of this amount. Segments are considered non-directed and their orientational distribution can be described by $S(\theta)$ defined for any range of θ of the length π. Segments can be classified into orientation groups and let orientations of segments be between θ_g and $\theta_g + \Delta\theta$ within each group. Consider one such group g which contains

$$\Delta M(\theta_g) = \frac{1}{2} M S(\theta_g) \Delta\theta \tag{3.30}$$

segments in the considered region. One group of segments is shown in Fig.3.6 with a set of lines parallel to the transect line and spaced at distances $d = d_o|\cos(\theta_N-\theta_g)|$ where θ_N is the orientation of the vector normal to the transect line. Such spacing assures that each segment of the group will be intersected only once and no one segment will be missed.

Let ΣL be the total length of parallel lines within the considered region. It can be seen from Fig. 3.6 that

$$d_o \cos(\theta_N-\theta_g) \Sigma L \doteq V \tag{3.31}$$

and for large volumes the error associated with edge effects is negligible.

Let $\Delta M_L(\theta_g)$ be the number of intersected segments per unit length of the transect line. Since for large areas all parallel lines are equivalent due to assumed homogeneity, the product $\Delta M_L(\theta_g)\Sigma L$ is the total number of intersected segments equal to their total number in the considered

region, i.e.

$$\Delta M_L(\theta_g)\ \Sigma L \simeq \Delta M(\theta_g)$$

The equality sign can be only for an infinite region.

Using (3.30)-(3.31), the above relationship can be written in the form

$$\Delta M_L(\theta_g) \simeq \frac{1}{2}\frac{M}{V} d_o |\cos(\theta_N-\theta_g)|\ S(\theta)\ \Delta\theta \qquad (3.32)$$

If the area of the considered region is increased to infinity, edge effects in (3.31) are negligible and (3.32) also becomes an exact relationship, since all transect lines are equivalent due to homogeneity.

Taking into account that

$$\lim_{V\to\infty}\frac{M}{V} = \lim_{V\to\infty}\frac{M}{N}\cdot\lim_{V\to\infty}\frac{N}{V} = \gamma n_v,$$

(3.32) can be written in the form

$$\Delta M_L(\theta_g) = \frac{1}{2}\gamma d_o n_v |\cos(\theta_N-\theta_g)|S(\theta_g)\Delta\theta \qquad (3.33)$$

This relationship is exact if the transect lines are infinite. Derivation (3.33) is not rigorous, but physically intuitive; a rigorous analysis can be found in [31].

3.10 Forces on Line and Plane Elements

The results of the transect analysis can be used to calculate forces on plane elements directly. Let $\bar{f}(\theta_g)$ be the average force on contacts with orientation of the normal vector θ_g. To calculate the number of contacts with this orientation of the normal, note that these contacts are associated with non-directed segments and each such segment corresponds to the orientation of the normal either θ_g or $\theta_g + \pi$. Note also that contacts on one side of the chain element on Fig. 3.5[b] have normal vector orienta-

tions such that $\cos(\theta_N-\theta_g)>0$. The number of contacts with orientation θ_g per unit length of the chain element is given by (3.33), but the modulus sign can be dropped due to the above comment. The contribution to the total force per unit length from this group of contacts is $\bar{f}(\theta_g)\ \Delta M_L$ Summation for all orientation groups gives

$$\underset{\sim}{F} = \frac{1}{2}\gamma d_o n_v \sum_g \bar{f}(\theta_g)\cos(\theta_N-\theta_g)S(\theta_g)\Delta\theta \qquad (3.34)$$

The above expression is correct for $\theta_N - \frac{\pi}{2} \leq \theta_g \leq \theta_g + \frac{\pi}{2}$, so that $S(\theta_g)$ must be defined for this interval. Note, however, that for each θ_g the opposite direction of the normal corresponds to the opposite direction of the force and negative sign for $\cos(\theta_N-\theta_g)$. This enables one to consider $S(\theta_g)$ in (3.34) periodically continued with the period π and defined for the range of orientations $0 \div 2\pi$, thus coinciding with the contact orientation distribution introduced previously. The above relationship can then be rewritten in integral form if $\Delta\theta\to 0$, i.e.

$$\underset{\sim}{F} = \frac{1}{2}\gamma d_o n_v \int_0^{2\pi} \bar{f}(\theta_g)\cos(\theta_N-\theta_g)S(\theta_g)d\theta \qquad (3.35)$$

If $\underset{\sim}{N}$ is the normal vector of the line element, calculation of $F_i = \sigma_{ij}N_j$ using (3.29) gives

$$F_i = \frac{1}{2}\gamma d_o n_v \int_0^{2\pi} \bar{f}_i(\theta_g)n_j(\theta_g)N_j S(\theta)d\theta \qquad (3.36)$$

Since $n_j(\theta_g)N_j = \cos(\theta_N-\theta_g)$, (3.35) coincides with (3.36), i.e. (3.29) can be used in the limit of an infinite assembly to calculate force per unit length of an infinite line element using relationships developed in continuum mechanics.

Although the transect analysis was performed for plane assemblies, all results are applicable for spheres. In this case a transect plane must be used instead of a line, and this plane will intersect a cer-

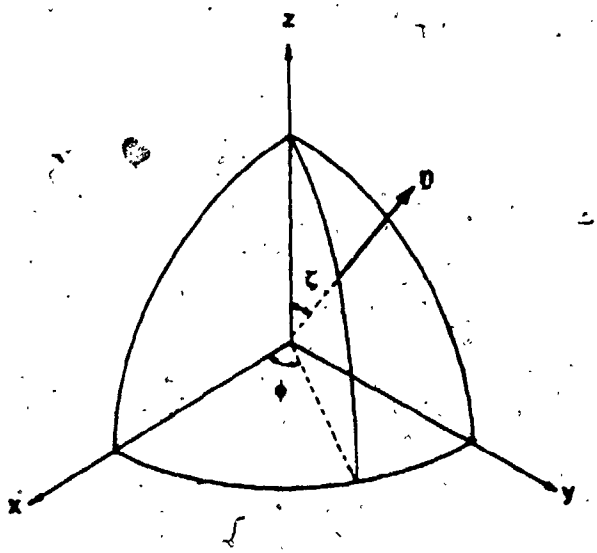

FIGURE 3.7

SPHERICAL COORDINATE SYSTEM

tain number of segments connecting sphere centers. If the two parts of the assembly separated by the plane are disengaged at contacts associated with intersected segments, two solid elements will appear, as for the plane case illustrated in Fig. 3.5. The only difference is in that orientation of each segment must be specified by two angles ζ,ϕ in the spherical coordinate system associated with the center of each sphere (Fig. 3.7) and contact orientation distribution will be a function of two angles $S = S(\zeta,\phi)$ Segments, again, must be classified according to their orientation, but groups must be selected for ranges $\sin\zeta\, d\zeta d\phi$ corresponding to an element of surface of a unit sphere $d\theta = \sin\zeta\, d\zeta d\phi$. In the case an isotropic assembly corresponds to a uniform distribution on the surface of a unit sphere $S(\zeta,\phi) = 1/4\pi$. To maintain uniformity in notation, the pair of angles ζ,ϕ can correspond to "generalized orientation" $\theta = \{\zeta,\phi\}$. All the previous relationships are applicable when the range $0\leq\zeta\leq\pi$, $0\leq\phi\leq 2\pi$ is symbolically accepted as corresponding to the interval $0\div 2\pi$ which appears in all formulas containing integration with respect to θ. The [illegible]ect analysis for one group of segments proceeds similarly by subdividing the considered volumes by planes in such a way that every segment is intersected once and not one missed. The spacing between planes must be $d_o|(n \cdot N)|$, where $n(\zeta,\phi)$ is the vector giving orientation of segments in the group. Then all resulting relationships are similar to the plane case with similar conclusions with respect to the tensor (3.29).

3.11 Statistical Ensemble of Systems in Static Equilibrium

In the preceding analysis it became possible to introduce σ_{ij} , a unique tensorial characterstic of contact forces for infinite systems:

$$\tilde{\sigma}_{ij} = \lim_{V\to\infty} \hat{\sigma}_{ij}(V)$$

where $\hat{\sigma}_{ij}$ is the phenomenological stress tensor (3.12). It was also shown that $\tilde{\sigma}_{ij}$ had some features of the continuum mechanics stress tensor in that $\tilde{\sigma}_{ij}N_j$ is the average force per unit area of an infinite micro-plane with normal vector N.

This section considers finite systems and attempts to introduce a micro-mechanical characteristic with all the properties of the continuum mechanics stress tensor. Such a characteristic cannot be introduced for one system only, but is introduced as a characeristic of a collection of macroscopically similar systems under identical gross loads. Such systems from a continuum mechanics point of view are completely identical; however, it can only be expected that a collection of similar systems can be described as being "continuum on average", as the present theory recognizes microscopic differences in such systems.

Consider an infinite, statistically homogeneous, perfectly irregular system with particle density n_v, average coordination number γ and a contact orientation distribution $S(\theta)$. This function is normalized and

$$dM = S(\theta)d\theta \tag{3.37}$$

can be regarded as the probability that an arbitrarily selected contact has orientation between θ and $\theta + d\theta$.

A collection of similar systems which will be studied here can be viewed as selected from different parts of the mentioned infinite assembly. Such construction ensures macroscopic similarity of considered systems occupying identical volumes.

Each system of the constructed ensemble has a discrete spectrum of contact orientations. Due to the specific selection of systems from

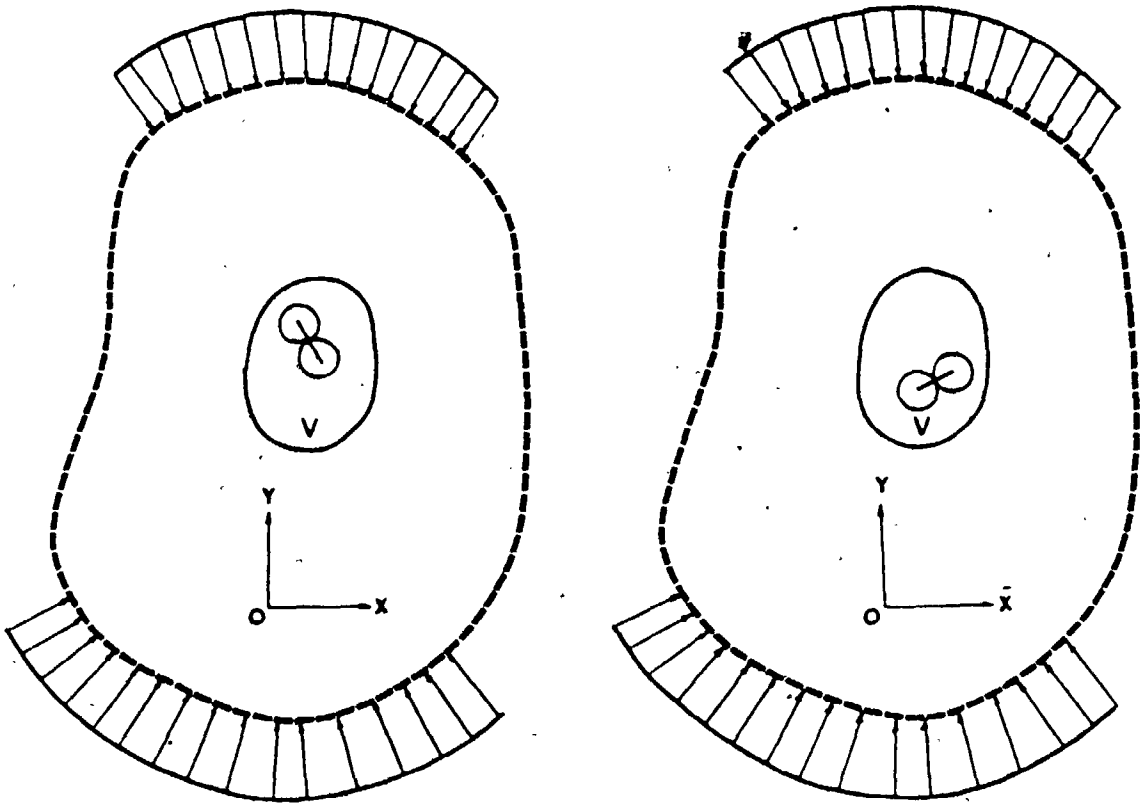

FIGURE 3.8

"STATISTICAL ENSEMBLE"

various localities in an infinite assembly, the probability that an arbitrarily selected contact within any system of the ensemble has orientation θ is given by (3.37), as for an infinite assembly actually containing all contact orientations. This property defines the structure of the ensemble systems. It is, of course, not necessary to select considered systems from an infinite system, and the feature of principal importance is the probabilistic structure of contact orientations ensured by the above construction.

Let all systems of the considered ensemble be referred to identical coordinate systems and be in static equilibrium under identical gross loads. Suppose similiar volumes are selected in identical locations within each system (Fig. 3.8). With identical sizes of selected volumes the number of contacts, their orientations and forces on these contacts may be regarded as random when one volume is examined after another. On the other hand, there exists a statistical regularity in the properties of selected volumes due to the macroscopic similarity of the considered systems.

Let the phenomenological stress tensor $\hat{\sigma}_{ij}(V)$ be defined for identical volumes in each system. The objective is to calculate its average over all systems of the ensemble. Such averages are called "ensemble averages" [13].

Systems of the ensemble are generally subject to external loads which, in continuum mechanics terms, result in a inhomogeneous state of stress. In such conditions no two contacts within an assembly are in *a priori* equivalent conditions, as is taken to be the case for contacts with similar orientations in assemblies subject to homogeneous loads. If, however, two contacts of the same orientation are in similar locations, but in different systems,

their positions can be considered as equivalent in the statistical sense. Forces on such contacts can be postulated as being *a priori* equiprobable and the distribution of forces on contacts with orientation θ:

$$P_\theta(\underset{\sim}{f},\underset{\sim}{r})d\underset{\sim}{f} \tag{3.38}$$

can be introduced to give the probability of a force being in the range $\underset{\sim}{f} \div \underset{\sim}{f}+d\underset{\sim}{f}$. The postulate on equal *a priori* probabilities is a necessary beginning of any statistical analysis [35]. In the present theory it is motivated by the continuum mechanics approach, according to which all systems in the considered ensemble will be viewed as being identical, with identical force characteristics in similar spatial locations. The theory here recognizes microscopic differences in the considered systems, but postulates similar locations in such systems as being statistically equivalent. It can be regarded as a precaution that not all contacts in such conditions, but only those with similar orientations, are viewed as being equivalent. It is for the developed theory to determine whether contacts of different orientations are equivalent in the statistical sense or not. It will be seen shortly that in static equilibrium all contacts are equivalent under hydrostatic loads and not equivalent under deviatoric loads.

3.12 Ensemble Average of the Phenomenological Stress Tensor

Due to generally non-uniform loads on systems of the ensemble, the phenomenological stress tensor depends on the volume size and position of the volume to which $\hat{\sigma}_{ij}(r)$ is referred to. A point characteristic of the ensemble can be obtained as

$$\sigma_{ij}(r) = \lim_{V\to 0} \bar{\hat{\sigma}}_{ij}(V) \tag{3.39}$$

where $\bar{\hat{\sigma}}$ is an ensemble average. It is convenient to calculate the required

average when $\hat{\sigma}_{ij}(V)$ for each system is referred to a volume with only one contact. Such volumes can always be selected near a certain point r and will be of varying sizes with a certain distribution $Z(v)dv$. Since there are on average $\frac{1}{2}\gamma n_v$ contacts per unit volume, the average volume per contact is such that $\frac{1}{2}\gamma n_v \bar{v} = 1$, so that

$$\int_0^\infty \frac{1}{v} Z(v)dv = \frac{1}{2}\gamma n_v \tag{3.40}$$

Let $P_v(\theta, \underset{\sim}{f})d\underset{\sim}{f}dv$ be the probability that there is a contact with orientation θ and force $\underset{\sim}{f}$ in an arbitrarily selected system of the ensemble with the volume of interest v. The ensemble average is of the form

$$\bar{\sigma}_{ij} = \int_{(v,\theta,\underset{\sim}{f})} \frac{1}{v}\sigma^c_{ij} P_v(\theta,\underset{\sim}{f})Z(v)dvd\theta d\underset{\sim}{f} \tag{3.41}$$

where integration is performed over the entire range of volumes, contact orientations and forces (possible for a contact), and $\sigma^c_{ij} = \frac{d_o}{2} f_i n_j$ is the contact force tensor introduced in section 3.5. The distribution $P_v(\theta,\underset{\sim}{f})$ can be given in terms of conditional distributions (3.37-3.38) in the form

$$P_v(\theta,\underset{\sim}{f}) = P_{\theta}(\underset{\sim}{f},\underset{\sim}{r})S(\theta)$$

and (3.41) be written in the form

$$\bar{\sigma}_{ij} = \frac{d_o}{2}\int_0^\infty \frac{1}{v}\left\{\int_0^{2\pi} S(\theta)n_j(\theta)\left[\int_{-\infty}^{+\infty} f_i P_{\theta}(\underset{\sim}{f},\underset{\sim}{r})d\underset{\sim}{f}\right]d\theta\right\}Z(v)dv \tag{3.42}$$

Introducing an average force for the contacts with the same orientation and at similar locations r within different systems

$$\bar{\underset{\sim}{f}}(\theta,\underset{\sim}{r}) = \int_{-\infty}^{+\infty} \underset{\sim}{f}\, P_{\theta}(\underset{\sim}{f},\underset{\sim}{r})d\underset{\sim}{f} \tag{3.43}$$

and performing integration with respect to v in (3.42) using (3.40), one can obtain

$$\bar{\sigma}_{ij}(r) = \frac{1}{2}\gamma d_o n_v \int_0^{2\pi} \bar{f}_i(\theta,\underset{\sim}{r})n_j(\theta)S(\theta)d\theta \tag{3.44}$$

Due to the selection of a small volume with one contact, the necessity

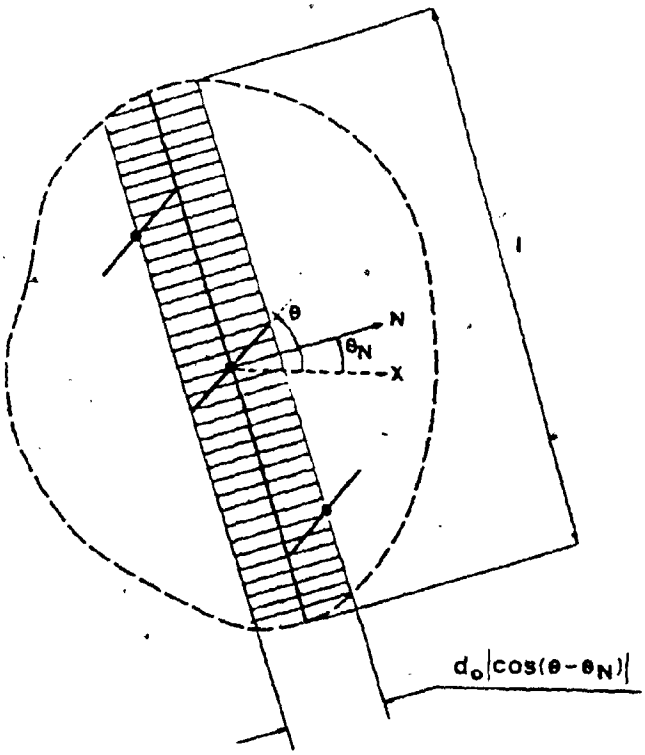

FIGURE 3.9

INTERSECTION OF RANDOM SEGMENTS WITH A LINE

was eliminated of performing a limiting transition (3.39) and a point characteristic of the ensemble was developed. The form of (3.44) is similar to the phenomenological stress tensor for an infinite assembly, although (3.44) is position-dependent.

3.13 Ensemble Average of Forces on Plane Elements

In order to show that properties of the ensemble average of the phenomenological stress tensor are similar to those of the stress tensor of continuum mechanics, it is necessary to calculate average force acting on an element of plane in similar positions in different systems of the considered ensemble. The two-dimensional case is considered first and the average force one element $\underset{\sim}{l}$ within volumes containing one contact is calculated. These volumes were defined in the preceding section and their averages (3.40) are known.

The probability that there is a force on a line element depends on whether the segment related to the contact of interest intersects the line element or not (see section 3.10). To determine this probability, note that the segment corresponding to a certain contact will intersect the line if its center is within the shaded area in Fig. 3.9. The probability of an intersection (calculated as a geometrical probability [18]) is the ratio of the shaded area in Fig. 3.9 to the total area, i.e.

$$I_v(\theta) = \frac{d_o l}{v} |\cos(\theta-\theta_N)| \quad . \tag{3.45}$$

$I_v(\theta)$ is the probability of intersection and θ_N is the orientation of the normal to the line element.

As in the preceding section, let $P_v(\theta, \underset{\sim}{f})$ be the probability that there will be a contact with orientation θ and force $\underset{\sim}{f}$ in the volume v of

an arbitrarily selected system. The probability that this force is applied to the line element $\underset{\sim}{l}$ is

$$P_v(\theta,\underset{\sim}{f})I_v(\theta)d\underset{\sim}{f}d\theta ,$$

i.e. it is calculated as a joint probability of two independent events related to occurrence of contact orientation θ with force $\underset{\sim}{f}$ and to intersection of the line element $\underset{\sim}{l}$. The above probability is for events in fixed volume v. Since the probability of selecting a system with volume v is $Z(v)dv$, the average force on $\underset{\sim}{l}$ can be calculated as follows:

$$\overline{F}_i = \int_{(v,\theta,\underset{\sim}{f})} f_i P_v(\theta,\underset{\sim}{f})I_v(\theta)Z(v)dvd\theta d\underset{\sim}{f} , \qquad (3.46)$$

i.e. similar to (3.41). Note that integration must be performed over the interval $\theta_N-\frac{\pi}{2}\le\theta\le\theta_N+\frac{\pi}{2}$ representing orientations of contacts contributing forces on the line element with orientation θ_N (section 3.10). $S(\theta)$ must also be temporarily defined and normalized on this interval. In this case the modulus in (3.45) can be dropped and (3.46) can be given in the form

$$\overline{F}_i = d_o \int_0^{\infty} \frac{l}{v} \int_{\theta_N-\frac{\pi}{2}}^{\theta_N+\frac{\pi}{2}} \left\{S(\theta)\cos(\theta-\theta_N)\overline{f}_i(\theta,\underset{\sim}{r})d\theta\right\}Z(v)dv$$

where the average force (3.43) was introduced by performing integration with respect to v using (3.40). The above relationship can be given with $l = 1$ in the form

$$\overline{F}_i = \frac{1}{2}\gamma d_o n_v \int_{\theta_N-\frac{\pi}{2}}^{\theta_N+\frac{\pi}{2}} \overline{f}_i(\theta,\underset{\sim}{r})\cos(\theta-\theta_N)S(\theta)d\theta$$

Noting that both cosine and $\overline{f}_i(\theta,\underset{\sim}{r})$ change sign simultaneously when substitution $\theta \to \theta+\pi$ is made; integration in the above expression can be extended over the entire range of θ. The ensemble average of forces acting per

unit length of line element l can be given in the form

$$\bar{F}_i = \frac{1}{2}\gamma d_o n_v \int_0^{2\pi} \bar{f}_i(\theta,r)\cos(\theta-\theta_N)S(\theta)d\theta \qquad (3.47)$$

As a check, it is noted that $\sigma_{ij}(r)$ in the form (3.44) gives the above force as follows:

$$\bar{F}_i = \bar{\hat{\sigma}}_{ij}N_j \qquad (3.48)$$

All the above calculations are valid in the three-dimensional case if l in (3.45) is the area of the plane element with normal vector N.

3.14 Description of Statistical Ensembles

Tensor $\sigma_{ij}(r)$

continuum mechanics stress tensor (3.48) and it is defined for any point of the region common to all systems in the ensemble.

To make the analogy with the continuum mechanics stress tensor complete, it is necessary to show that (3.44) also satisfies the equations of static equilibrium (in the absence of body forces).

$$\frac{\partial \bar{\hat{\sigma}}_{ij}}{\partial r_j} = 0 \qquad (3.49)$$

which the continuum mechanics stress tensor satisfies.

To do this it is necessary to calculate the left-hand side of (3.49) using (3.44) and integrate over an arbitrary volume V with boundary S.

If the order of integration with respect to θ and spatial variables r is reversed, the result of these calculations is

$$\int_V \frac{\partial \bar{\hat{\sigma}}_{ij}}{\partial r_j}\,dv = \frac{1}{2}\gamma d_o n_v \int_0^{2\pi} S(\theta)\left[\int_V \frac{\partial \bar{f}_i}{\partial r_j} n_j dV\right]d\theta \qquad (3.50)$$

Note that n_j is a function of θ, but for internal integration it is a constant. It can be shown using the Green-Gauss theorem that (3.50) can be given in the form

$$\int_V \frac{\partial f_i}{\partial r_j} n_j dV = \int_S f_i \cos(\theta-\theta_N) dS \qquad (3.51)$$

where θ_N is orientation of the normal on the boundary. Substituting (3.51) into (3.50) and again inverting the order of integration, the relationship follows:

$$\int_V \frac{\partial \bar{\sigma}_{ij}}{\partial r_j} dV = \int_S dS\left[\frac{1}{2}\gamma d_o n_v \int_0^{2\pi} \bar{f}_i(\theta, \underset{\sim}{r}) \cos(\theta-\theta_N) S(\theta) d\theta\right] = \int_S \bar{F}_i(N, \underset{\sim}{r}) dS$$

where (3.47) was employed to identify the term in brackets. The left-hand side of the above relationship represents an ensemble average of forces acting on the surface of an arbitrary volume. Since each system of the ensemble is in static equilibrium, the total force acting on the contour is zero, and the same is true of the ensemble average. Therefore, the left-hand side of (3.50) is zero for any arbitrary volume V, indicating that the integrand is also zero and $\bar{\underset{\sim}{\sigma}}_{ij}(\underset{\sim}{r})$ in the form (3.44) satisfies the equations of equilibrium of continuum mechanics, provided $\bar{f}(\theta, \underset{\sim}{r})$ in (3.44) corresponds to states of static equilibrium. Tensor (3.44) is therefore a micro-mechanical analogue of the stress tensor of continuum mechanics. It is imperative to realize that stress tensor (3.44) is a point characteristic of an ensemble of similar systems and not of any one discrete assembly. The possibility of such description is related to the postulate on equal *a priori* probabilities of forces in similar locations within different systems. The existence of distribution (3.38) was assumed and the postulate resulted in a "continuum description for the ensemble of systems".

This result is of great practical significance to the present theory, since it indicates that ensemble averages can be calculated using methods of continuum mechanics and knowledge of averages of the (3.44) type is necessary to recover the form of the ensemble average for forces $\underset{\sim}{f}(\theta,\underset{\sim}{r})$ which carry important information on distribution function (3.38) introduced *a priori* into the theory. The possibility of obtaining $\bar{\hat{\sigma}}(\underset{\sim}{r})$ using methods of continuum mechanics requires knowledge of "constitutive relationships" for the ensemble. It is one of the objectives of the theory to present methods for their development.

If the system is subject to external loads corresponding to $\bar{\hat{\sigma}}_{ij} = \text{const.}$, i.e. a uniform state of stress for the ensemble, $\bar{\underset{\sim}{f}}(\theta,\underset{\sim}{r}) = \bar{\underset{\sim}{f}}(\theta)$ and the expression for the ensemble average of the phenomenological stress tensor (3.44) coincides with the expression for the phenomenological stress tensor for infinite assemblies (3.29). This fact simplifies the problem of developing constitutive relationships and distribution functions by allowing one to study infinite systems on the basis of equations of mechanics. The result of such analysis - constitutive relationships and contact force distributions - can be used for solving problems for finite systems with ensemble interpretation of results.

In further analyses a common notation will be used for the ensemble average of the phenomenological stress tensor and for its limit for infinite systems, i.e. $\bar{\hat{\sigma}}_{ij} = \tilde{\sigma}_{ij} = \sigma_{ij}$ and generally

$$\sigma_{ij} = \frac{1}{2}\gamma d_o n_v \int_0^{2\pi} \bar{f}_i(\theta,\underset{\sim}{r}) n_j(\theta) S(\theta) d\theta \qquad (3.52)$$

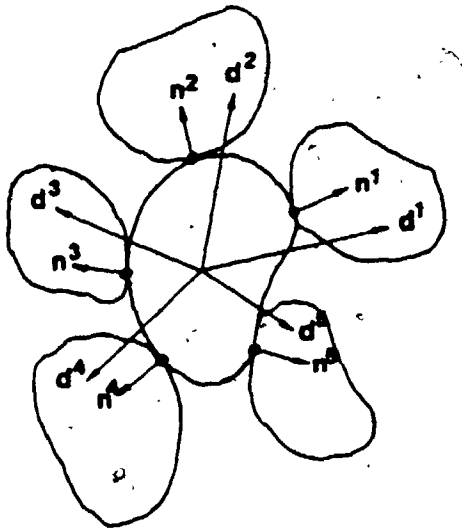

FIGURE 3.10

CONTACT VECTORS FOR IRREGULAR SHAPE PARTICLES

3.15 Assemblies of Varying Size Particles

The above geometrical technique supports the conclusion based on analytical methods that the expression for the stress tensor must depend only on the distance between the centers of two particles. Volume-additive identities (3.10) were developed for spheres and the technique was based on selection of particle centers as reference points within the particle volume, multiplication of equations of equilibrium for each particle (3.6) by components of the reference vector of the particle r^k and summation for all particles with the final result of (3.7). If any arbitrary point within the volume is selected instead of a particle center as a reference point, the resulting volume-additive identities will be of the form

$$\sum_{\beta \in B} f_i^\beta r_j^\beta = \sum_{c \in V} \frac{1}{2} d_i^c f_j^c .$$

Vectors d_i^c for a particle's neighbours are shown in Fig. 3.10. They coincide with the normal vectors of a contact only for spherical particles, regardless of the shape of the two particles in contact. To develop an expression for the stress tensor for this case presents no difficulty and for an infinite assembly σ_{ij} is given, without proof, in the form

$$\sigma_{ij} = \frac{1}{2} \gamma m_v \int_0^{2\pi} \left[\int_0^\infty d\bar{f}_i(d,\theta) P(d)\, \delta d \right] n_j(\theta) S(\theta)\, d\theta .$$

Note that in this case contacts of the same orientation are not necessarily equivalent, since contact stiffness, generally, depends on particle diameter. That is why the average force on a contact of the same orientation depends on the distance between the centers of the particles in contact. In the following analysis contact stiffnesses will be assumed fixed which numerically-wise is a realistic approximation for bonded particles only (more on that in the next chapter). In such a case $\bar{f}_i(d,\theta) =$

$\overline{f}_i(\theta)$ and (3.29) follows, but $\overline{d}$, the average distance between particle centers, appears instead of constant particle diameter d_o. This characteristic can always be worked out on the basis of particle size distribution. For particles of shapes other than spherical, the analysis becomes more complicated. It will be only mentioned that the distribution of particle orientations for elliptical or ellipsoidal particles will enter the analysis. In the case of isotropy in particle orientations and assuming unbiased formation of contacts, (3.29) will result in redefined d_o. Note that the mentioned assumptions are only realistic for small particle eccentricities.

Particles other than spheres will not be considered here. All results presented here for assemblies of identical spheres and discs bonded at contact points are applicable to assemblies of varying size spheres and discs provided contact stiffnesses are independent of particle diameters.

3.16 Discussion and Conclusions

The phenomenological stress tensor introduced in the present chapter is the main conceptual and analytical instrument with which granular assemblies will be studied in this work.

The presentation of the material reflects an attempt to study large mechanical systems initially only on the basis of equations of equilibrium with subsequent introduction of additional concepts and postulates.

For a mechanical problem to be properly posed for granular assemblies, it is necessary to prescribe external actions on the boundaries of a studied system. Boundary contact forces were specified in terms of a tensor

of the second rank σ^{β}_{ij} in an attempt to simulate conditions known in continuum mechanics as uniform state of stress. Tensor σ^{β}_{ij}, however, is not identified with the stress tensor of continuum mechanics.

Analysis of equations of static equilibrium leads to relationships between σ^{β}_{ij} and forces on all contacts of the assembly. An important feature of relationships (3.11) is their volume-additive nature, when each contact makes a small contribution to σ^{β}_{ij} regardless of its position within the assembly.

It can be expected that if such combinations of contact forces are evaluated for large sub-volumes of the system, the result will not differ significantly from σ^{β}_{ij} in the case of homogeneous systems. The intuitive idea lead to the definition of the phenomenological stress tensor $\hat{\sigma}_{ij}(V)$ as a certain function defined for any sub-volume of the system. If V the total volume, $\hat{\sigma}_{ij}(V) = \sigma^{\beta}_{ij}$. Properties of the phenomenological stress tensor were examined and it was shown that it coincides formally with the average stress tensor defined in continuum mechanics and represented here through volume-additive relationships developed on the basis of the concept of two-phase continuum.

The expression for the phenomenological stress tensor was further given in the form (3.27), which involved contact orientation distributions for a studied volume and average forces on contacts of the same orientation.

Further development of the theory required clarification of the intuitive notion of homogeneity, which actually resulted in the introduction of the phenomenological stress tensor as a function of volume.

There were two theoretical options on the basis of which homogeneity were introduced. A probabilistic approach to this definition required a

fundamental measure-theoretical construction reflecting *a priori* equivalence of different locations of the assembly and their physical properties. Such an approach to a single system of interest violated a basic theoretical premise: the possibility of studying the system on the basis of equations of equilibrium.

The other option was to study an infinite system and to define homogeneity as equivalence in physical properties of any infinite part of an infinite assembly. This approach did not contradict mechanical determinism of a studied system and was considered acceptable from a physical point of view. Both approaches were used in the theory within the theoretical framework defined above and homogeneous states of a single system were studied by passing to the limit of an infinite assembly. The probabilistic approach was reserved for the analysis of inhomogeneous states of an ensemble of macroscopically similar systems. Statistical analysis of an ensemble did not contradict mechanical determinism of each system of the ensemble.

Homogeneous states of a single system were analyzed first and the expression for the phenomenological stress tensor was given in the form (3.27) which involved contact orientation distribution for a studied volume and average forces on contacts of the same oerientation.

Average forces, as defined here, are not statistical averages introduced in connection with a certain random process and defined as "empirical averages", sums of contact forces divided by the number of terms in the sum.

Transition to an infinite assembly in exact relationships developed for an arbitrary large, but finite system was not rigorously justified and limits were assumed for average forces, contact orientation distribution, etc., as well as a continuous form of the mentioned orientation distribu-

tions*.

The phenomenological stress tensor for an infinte assembly δ_{ij} is a unique charactersitic of average contact forces in the system. Geometrical analysis of gross forces F acting per unit area of plane elements with normal N indicated that such forces can be obtained using relationship $F_i = \delta_{ij}N_j$ which indicates a close relationship between the introduced quantity and the stress tensor of continuum mechanics.

For infinite homogeneous systems this property of δ_{ij} is of no practical interest. Its major physical importance is the fact that δ_{ij} is also the tensor which defines boundary loads on infinity and specification of boundary forces impose restrictions on average contact forces. In the next chapter considerable information on average forces will be obtained on the basis of these constraints. Knowledge of average forces enables to recover information on distribution functions of contact forces using additional statistical postulates.

The above theoretical scheme is not adequate for analysis of inhomogeneous boundary loads. In such conditions it is impossible to assume equivalence of infinite samples of an infinite assembly and another theoretical construction is necessary.

An idea of this construction is related to the practical success of continuum mechanics in treating macroscopically similar systems as iden-

---

*Rigorous application of existing ergodic theories which study such limits proved to be impossible, since it required mathematical features of studied systems which can be physically obtained by considering their history which leads to homogeneity. Any asusmption in this respect made in a rigorous mathematical form is ultimately related to intuitive physical notions. Specific mathematical constructions do not result in such conditions in sizable physical advantages, so that their final result was simply assumed.

tical. If a collection of macroscopically identical, but microscopically different systems is considered, it is reasonable to consider identical locations in different systems as statistically equivalent, provided systems of the statistical ensemble are subject to identical boundary loads.

Development of this concept proceeded with the introduction of the postulate on equal *a priori* probabilities of forces on contacts of the same orientation which are in identical geometrical locations in different systems of the considered ensemble. The introduced probability density $P_\theta(\underset{\sim}{f},\underset{\sim}{r})$ enables to evaluate averages of the phenomenological stress tensor over an infinitesimal volume of systems in the ensemble. The calculated average $\bar{\bar{\sigma}}_{ij}(r)$ is a point characterstic of an ensemble and it is shown that it has all properties of the continuum mechanics stress tensor. The ensemble of systems can ,therefore, be described as "continuum". This results provides a statistical interpretation of continuum mechanics, although its significance to the present theory lies in the possibility of using powerful methods of continuum mechanics to calculate continuous fields of the ensemble average of the phenomenological stress tensor.

With an expression for $\bar{\bar{\sigma}}_{ij}(r)$ in terms of the ensemble average of contact forces (3.52) it will be possible to obtain information on average forces and, finally, their fluctuations in identical locations of different systems of the ensemble. The present theory is also capable of developing constitutive relationships describing average gross response over systems of the ensemble.

As a conclusion to this chapter, it is emphasized that:

(1) The developed theoretical scheme based on the analysis of con-

tact forces in granular assemblies resulted in a tensorial characteristic of granular systems with all properties of the stress tensor of continuum mechanics, but describing either an infinite homogeneous system or an ensemble of similar systems under identical, generally inhomogeneous loads.

(2) Regardless of whether an ensemble logic is employed or an infinite homogeneous system is considered, the respective postulates and related specific methods of analysis result in identical expressions for the introduced stress tensor in terms of average forces on contacts of the same orientation and contact orientation distribution.

(3) Both logical schemes, while employing different concepts and methods of analysis (analytical and geometrical), point to the significance of average forces on contacts of the same orientation and contact orientation distribution. The identified elements of mechanical description are independent of a particular particle shape, although a specific form of relationship between the above quantities and the stress tensor is affected by particle shape.

The above analysis and conclusions indicate that the theory must provide for adequate methods of describing average forces and contact orientations. The next chapter considers average forces using a rather general form of contact orientations for plane systems. Statistico-geometrical analysis of contact orientation distributions is presented later.

CHAPTER IV

AVERAGE CONTACT FORCES

4.1 Introduction

The preceding chapter considered contact forces in an ensemble of macroscopically similar systems under identical gross loads. It was shown that the average of forces over similar contacts in different systems is related to the ensemble average of the phenomenological stress tensor. This tensor satisfies equations of equilibrium of continuum mechanics indicating that the ensemble can be described, on average, in continuum terms. Other ingredients of continuum mechanics description (e.g. strain tensor) must appear naturally in problems with prescribed external forces, once particle deformational properties are specified and systems are analyzed on the level of those deformations.

A continuum type description for ensembles of systems can, however, be expected. In this case methods of continuum mechanics enable one to determine the stress tensor at each point of a region occupied by systems of the ensemble. If this is the case, average forces on similar contacts in different systems cannot be arbitrary and their average is related to the stress tensor according to (3.52). Although it is not yet justified that the stress tensor describing the ensemble of systems can be determined, tensor σ_{ij}^{β} is *a priori* known for a single system subject to boundary tractions $p_i = \sigma_{ij}^{\beta} n_j$. It means that certain constraints are imposed on volume-additive combinations of contact forces.

Whatever the deformational properties of particles or precise features of contact orientations may be, the mentioned constraints must

be satisfied. Knowledge of such constraints is of utmost importance if the statistics of contact forces is to be developed. With a complete set of constraints on contact forces available, any set of contact forces satisfying these constraints can be assumed to be *a priori* equiprobable, and the most probable distribution of contact forces can be determined.

Classical statistical mechanics of dynamic systems is based on this scheme. In the case of conservative dynamic systems, there is a natural volume-additive constraint, energy of the system. Statistical mechanics operates on a premise that only the energy constraint is physically important.

In the present theory, a volume-additive constraint was identified in connection with externally specified loads. The integral form of this constraint (3.52) indicated the possibility that average forces on contacts of similar orientations are also constrained to a certain extent regardless of particle deformational properties.

Considering the diversity of deformational properties of granular systems, it is important to realize which features of granular assemblies are independent of the type of deformational behavior. Only plane assemblies of discs are analyzed in this chapter, while assemblies of spheres with specified particle deformational properties are treated later.

To concentrate attention on the main features of plane systems, equal size discs are considered. Final relationships obtained here are applicable to discs of varying sizes if the average distance between disc centers is substituted for disc diameters.

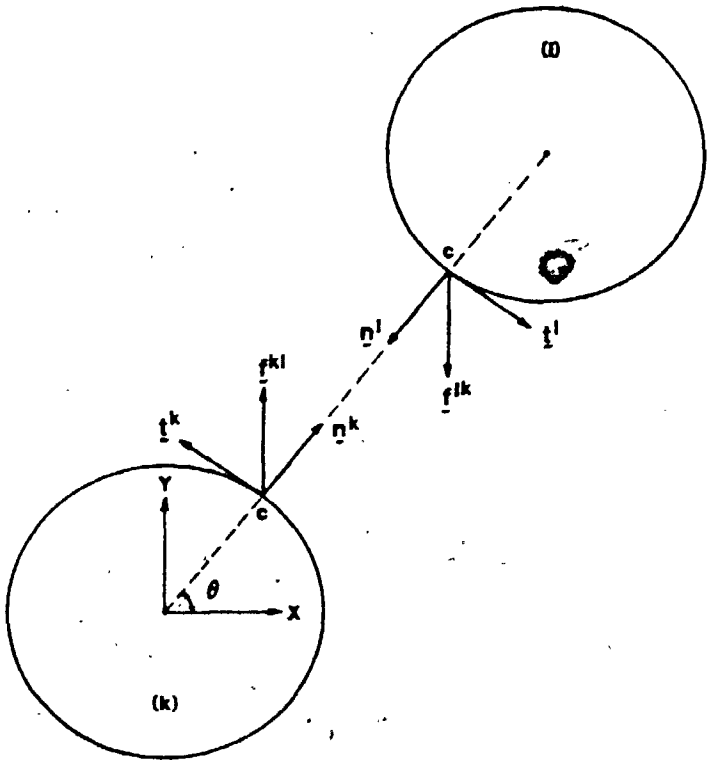

FIGURE 4.1

LOCAL COORDINATE SYSTEM OF A CONTACT

4.2 Condition of Symmetry for the Stress Tensor

It is convenient to present the relationships between average forces and the stress tensor (3.52) in a slightly different form. Consider two particles k and l and the force $\underset{\sim}{f}^{kl}$ with which particle l acts on particle k. If components of this force are considered in a local coordinate system of a contact (Fig. 4.1) with normal and tangential directions

$$\underset{\sim}{n} = \{\cos\theta,\ \sin\theta\};\quad \underset{\sim}{t} = \{-\sin\theta, \cos\theta\}, \tag{4.1}$$

both contact forces can be represented in the form

$$\underset{\sim}{f}^{kl} = f_n^c \underset{\sim}{n}^k + f_t^c \underset{\sim}{t}^k;\quad \underset{\sim}{f}^{lk} = f_n^c \underset{\sim}{n}^l + f_t^c \underset{\sim}{t}^l \tag{4.2}$$

where f_n^c , f_t^c are normal and tangential components of contact forces. Since $\underset{\sim}{f}^{kl} = -\underset{\sim}{f}^{lk}$ and unit vectors $\underset{\sim}{n}$, $\underset{\sim}{t}$ also change sign on both sides of the contact, components f_n^c, f_t^c are characteristics of the contact and are the same on both sides of it. As for stresses, note that positive f_n^c indicates tension in the contact and positive f_t^c indicates that a contact force tends to induce counter-clockwise rotation on the particle. With contact forces (4.2) the stress tensor (3.52) can be given in the form

$$\sigma_{ij} = \frac{1}{2}\gamma d_o n_v \int_0^{2\pi} [\bar{f}_n(\theta)\ n_i n_j + \bar{f}_t(\theta)\ t_i n_j] S(\theta) d\theta \tag{4.3}$$

where $\bar{f}_n(\theta)$, $\bar{f}_t(\theta)$ are normal and tangential components of the average force on contacts with orientation θ. In the case of ensemble averages, average forces are generally position-dependent. Note that (4.3) can be expressed in three dimensions with the only difference being that $\underset{\sim}{t}(\theta)$ is *a priori* unknown and can be viewed as the average tangential direction of forces on contacts with normal $\underset{\sim}{n}$.

It was shown in section 3.7 that the assumption of load transmission by means of contact forces with no contact couples results in a symmetrical stress tensor. Expression (4.3) for the stress tensor is, however,

generally not symmetrical and it is important to establish conditions for $S(\theta)$, $\bar{f}_n(\theta)$ and $\bar{f}_t(\theta)$ which assure symmetry of the stress tensor.

The first term in (4.3) related to the average normal force is symmetrical, but the second term is not as $t_i n_j \neq n_j t_i$. The tensor (4.3) would be symmetrical if

$$\sigma_{ij} - \sigma_{ji} = \frac{1}{2} \gamma d_o n_v \int_0^{2\pi} \bar{f}_t(\theta)[t_i n_j - t_j n_i] S(\theta) d\theta = 0$$

The above relationship also holds for the three-dimensional case. In the plane case, the tangential direction (4.1) is *a priori* known and the above condition gives

$$\int_0^{2\pi} \bar{f}_t(\theta) S(\theta) d\theta = 0 \tag{4.4}$$

This condition imposes severe limitations on the form of the expressions for the average tangential forces and the contact orientations.

4.3 Stress Tensor Invariants

The expression for the stress tensor (4.3) was introduced because of the importance of the normal and tangential force components in that they are directly related to frictional and deformational properties of particles. Both $\bar{f}_n(\theta)$, $\bar{f}_t(\theta)$ are scalars and can be related to the invariants of the stress tensor. Such relationships and subsequent analysis are considerably simplified if the invariants are selected as Mohr's circle parameters

$$\sigma_t = \left[\left(\frac{\sigma_{11} - \sigma_{22}}{2}\right)^2 + \sigma_{12}^2\right]^{1/2}$$
$$\sigma_n = \frac{1}{2}(\sigma_{11} + \sigma_{22}) \tag{4.5}$$

Let $\underset{\sim}{n}^p = \{\cos\theta_p, \sin\theta_p\}$ be the major principal direction of the stress tensor (3.30) whose orientation can be given as follows:

$$\sin 2\theta_p = \frac{\sigma_{12}}{\sigma_t}, \quad \cos 2\theta_p = \frac{\sigma_{11} - \sigma_{22}}{2\sigma_t} \tag{4.6}$$

Invariants σ_n, σ_t of the plane stress tensor can be expressed as

$$\sigma_{ij} n_j^p n_i^p = \sigma_n + \sigma_t \tag{4.7}$$

and also

$$\sigma_{ij} n_j^p t_i^p = 0 \tag{4.8}$$

where t^p is the second principal direction obtained by counter-clockwise rotation of n^p by $\frac{\pi}{2}$.

Direct substitution of the expression for stress tensor (4.3) into (4.5) enables one to obtain σ_n which can be further used to evaluate σ_t from (4.7) to obtain

$$\begin{aligned} \sigma_n &= \frac{\rho\gamma}{\pi d_0} \left[\int_0^{2\pi} n(\theta) S(\theta) d\theta\right] \\ \sigma_t &= \frac{\rho\gamma}{\pi d_0} \left[\int_0^{2\pi} n(\theta) \cos 2(\theta - \theta_p) S(\theta) d\theta - \int_0^{2\pi} t(\theta) \sin 2(\theta - \theta_p) S(\theta) d\theta\right] \end{aligned} \tag{4.9}$$

where $\rho = n_v \frac{\pi d_0^2}{4}$ is the area density of the assembly (the ratio of the area filled with discs to the total area of the assembly) and

$$\begin{aligned} n(\theta) &= \bar{f}_n(\theta) S(\theta) \\ t(\theta) &= \bar{f}_t(\theta) S(\theta) \end{aligned} \tag{4.10}$$

Substituting (4.3) into (4.8) and making use of the symmetry condition (4.4) one can obtain

$$\int_0^{2\pi} n(\theta) \sin 2(\theta - \theta_p) S(\theta) d\theta + \int_0^{2\pi} t(\theta) \cos 2(\theta - \theta_p) S(\theta) d\theta = 0 \tag{4.11}$$

It should be noted that the functions which describe contact forces and orientations of contacts enter equations (4.9) as products (4.10), so that only two functions $n(\theta)$, $t(\theta)$ which specify the stress tensor are required. Since orientations of contacts θ and $\theta+\pi$ are equivalent

and $n(\theta)$, $t(\theta)$ are scalars, they must be periodic with period π and can be decomposed into Fourier series of the form

$$n(\theta) = \frac{a_o^n}{2} + \sum_{k=1}^{\infty} a_{2k}^n \cos 2k(\theta-\theta_p) + b_{2k}^n \sin(\theta-\theta_p)$$
$$t(\theta) = \frac{a_o^t}{2} + \sum_{k=1}^{\infty} a_{2k}^t \cos 2k(\theta-\theta_p) + b_{2k}^t \sin 2k(\theta-\theta_p) \qquad (4.12)$$

where without loss of generality θ_p can be selected as a reference direction.

If (4.12) is substituted into (4.9) and integration is performed, stress invariants take the form

$$\sigma_n = \frac{p\gamma}{d_o} a_o^n$$
$$\sigma_\tau = \frac{p\gamma}{d_o} (a_2^n + b_2^t)$$

The above general considerations lead to the conclusion that the magnitude of stress invariants depends on the Fourier components of $n(\theta)$, $t(\theta)$ of the order not higher than 2. Moreover, if the deviatoric invariant is not zero, at least one of second Fourier coefficients a_2^n or b_2^t is not zero. This fact results in an important conclusion that, under deviatoric loads, either the contact force distribution must be direction-dependent, or contacts must be distributed anisotropically if the force distribution is isotropic. Generally, however, one must expect that both distributions can be anisotropic if the assembly is free to form or to alter contacts (the particles are not bonded).

4.4 Strength Components in Anisotropic Assemblies

Consider an anisotropic plane assembly with distribution of contact orientations

$$S(\theta) = \frac{1}{2\pi}(1 + a \cos 2(\theta-\theta_0)) \qquad (4.13)$$

2

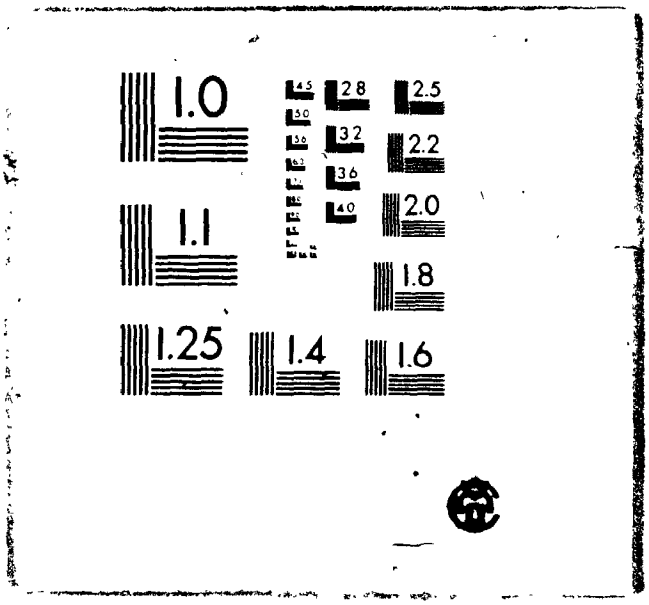

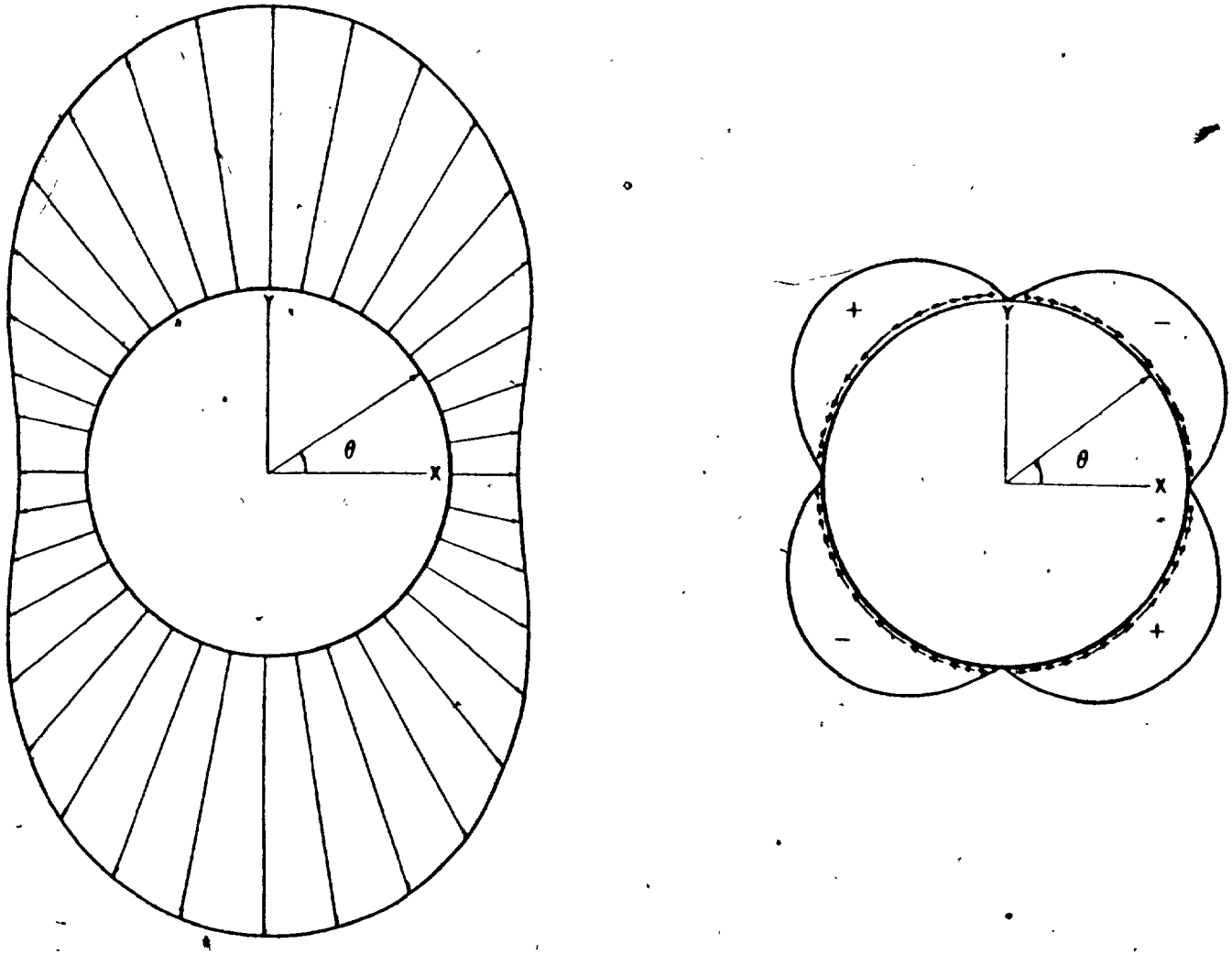

FIGURE 4.2

ORIENTATIONAL DISTRIBUTION OF AVERAGE NORMAL AND TANGENTIAL FORCES

shown in Fig. 2.3.

It will be shown that such a contact orientation distribution is natural for stable irregular anisotropic structures. At this point it can be viewed as an approximation based on only the second Fourier component of the contact orientation distribution.

Assume also direction-dependent average forces on contacts with orientation θ to be in the form

$$\begin{aligned} \bar{f}_n(\theta) &= f_n^o(1 + a_f \cos 2(\theta-\theta_o)) \\ \bar{f}_t(\theta) &= -f_t^o \sin 2(\theta-\theta_o) \end{aligned} \tag{4.14}$$

Such average forces have the same preferential directions as contact orientations and also can be represented by a truncated Fourier series. Note that if a constant term is present in the above $\bar{f}_t(\theta)$, the condition of symmetry (4.4) will not be satisfied. Physically this situation corresponds to non-compensated moments. Fig. 4.2 shows the above orientational distributions of average forces "applied to a generic particle". It can be seen that parameter a_f controls eccentricity in normal force distributions. It is convenient to select coefficients f_n^o, f_t^o in the form $f_t^o = f_n^o a_\mu$, where a_μ is a nondimensional coefficient. Coefficients a, a_f, a_μ, which define anisotropy in contact orientations and average forces, can be assumed small; so that, their products can be neglected in further computations. Substitution of (4.13-4.14) and integration gives

$$\begin{aligned} \sigma_{11} &= \frac{\rho\gamma}{\pi d_0} f_n^o \left(1 + \frac{1}{2}(a + a_f + a_\mu)\cos 2\theta_0\right) \\ \sigma_{22} &= \frac{\rho\gamma}{\pi d_0} f_n^o \left(1 - \frac{1}{2}(a + a_f + a_\mu)\cos 2\theta_0\right) \\ \sigma_{12} &= \frac{\rho\gamma}{\pi d_0} f_n^o \left(\frac{1}{2}(a + a_f + a_\mu)\sin 2\theta_0\right) \\ \sigma_{21} &= \sigma_{12} \end{aligned} \tag{4.15}$$

The form of the stress tensor (4.15) indicates that its principal direction is θ_o, i.e. exactly as the common direction of anisotropy in contact orientations and average forces.

Stress invariants can be evaluated either directly or by using (4.9). Such calculations give

$$\sigma_n = \frac{\rho\gamma}{\pi d_0} f_n^{\ell}$$
$$\sigma_t = \frac{\rho\gamma}{\pi d_0} f_n^{\ell} \frac{1}{2} (a + a_f + a_\mu) \tag{4.16}$$

Coefficients f_n^{ℓ} and particular parameters of the assembly can be eliminated from the above relationships if one is divided by the other to obtain the following expression

$$\frac{\sigma_t}{\sigma_n} = a_\sigma = \frac{1}{2} (a + a_f + a_\mu) \tag{4.17}$$

where a_σ (always less than unity) is a characterstic of deviatoric loads on the system. It is clear that, if a granular assembly is subject to deviatoric loads, its ability to resist such external actions is related to the possibility of having anisotropic distributions of contacts (a), normal forces (a_f), tangential forces (a_μ). Moreover, all three "anisotropies" equally contribute to the "strength" of an assembly. For cohesionless assemblies a_σ rarely exceeds 0.7 (which corresponds to the angle of internal friction* $\phi = \arcsin a_\sigma \simeq 45°$). Assuming $a = a_f = a_\mu$, magnitudes of these coefficients are approximately 0.5.

In the above analysis, distributions (4.14) were simply assumed. If, however, higher Fourier components in distributions (4.14) are considered, only the fourth Fourier components of $\overline{f}_n(\theta)$, $\overline{f}_t(\theta)$

*The angle of internal friction is defined here as $\sin \phi = (\sigma_1-\sigma_2)/(\sigma_1+\sigma_2) = \sigma_t/\sigma_n < 1$; σ_1, σ_2 are principal stress components.

contribute terms to (4.16) and these terms combine to form products with a. Contributions of these terms to a_0 can be neglected.

It will be shown that Fourier components of average contact forces of the order higher than two do not appear in linear systems, and, as it was pointed out, contributions of these components to the strength of assemblies is not dominant for any but linear systems.

Relationships (4.16) show that the amplitude of normal forces f_n^o is uniquely related to hydrostatic stress. For a system with specified structure (a is known), average contact forces are considerably constrained by external loads. Only the amplitude of tangential forces $f_t^o = a_\mu f_n^o$ (or coefficient a_μ) is not prescribed uniquely by external loads and depends on deformational or frictional properties of particles. In the above example, directions of anisotropy of forces and contact orientations were chosen to coincide. If such is not the case and the stress tensor with arbitrary direction is specified, the direction of force anisotropy can be found using (4.11).

In further analysis deformational properties of particles will be considered.

4.5 Linear Contact Model

Contact interactions of granular materials are sufficiently complicated and no attempt will be made here to present a realistic model of a contact for any specific material.

Contact force-interparticle displacement relationships are generally non-linear due to variation of the area of contact with the level of normal contact force.

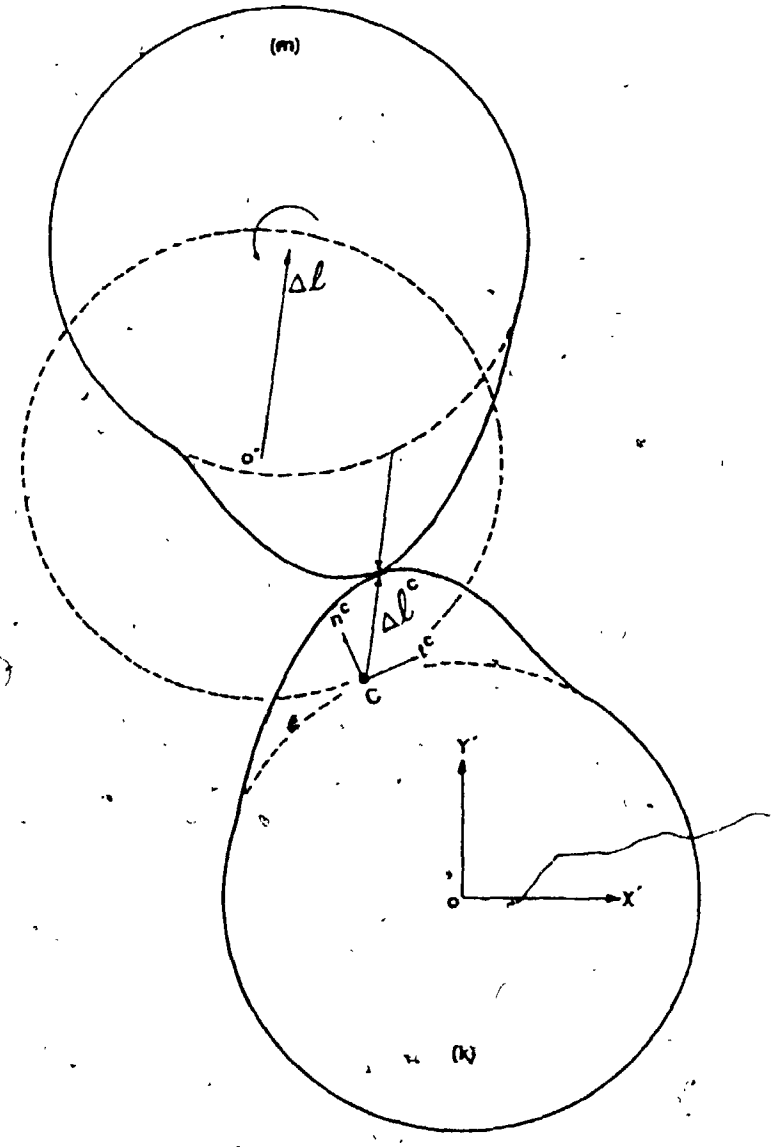

FIGURE 4.3

LOCAL DEFORMATIONS IN CONTACTS

The mechanism of load transmission in granular assemblies can be approximated by considering particles with a linear relationship between contact forces and interparticle displacements. Such a model can also be considered as a realistic approximation for systems of bonded particles when the area of each contact does not vary with the level of contact forces. Even in situations when the area of a contact varies, the statistical features of surface asperities may result in linear response of a contact [1].

The linear contact model is sometimes employed for computer simulations of granular systems [7] and in the present work it carries considerable analytical advantages. Details of a linear contact model for three-dimensional particles are presented in Appendix A. The present section will explore the features of the plane case.

Consider two particles shown in Fig. 4.3 and let the motion of particle m be observed in a coordinate system rigidly connected with the center of particle k. The motion of particle m can always be decomposed into translation of its center $\Delta \underset{\sim}{l}$ and rotation $\Delta \underset{\sim}{\omega}$ about its own center, which may also rotate in the considered coordinate system of particle k.

The force acting on particle k is related to the translation $\Delta \underset{\sim}{l}^c$ of the contact point c with respect to the center of particle k (Fig. 4.3). It is important to realize that both translation and rotation contribute to the magnitude of the vector $\Delta \underset{\sim}{l}^c$ which can be expressed in the form

$$\Delta \underset{\sim}{l}^c = \frac{1}{2}\Delta \underset{\sim}{l} + \frac{d_0}{2}\left[\underset{\sim}{n} \times \Delta \underset{\sim}{\omega}\right] \tag{4.18}$$

where $\underset{\sim}{n}^c$ is the vector normal to the contact on particle k and the above cross product contributes a component in the tangential direction of the contact, since $\Delta \underset{\sim}{\omega}$ in the plane case is perpendicular to the plane of the

assembly and has only one component $\Delta\omega$, positive for counter-clockwise rotation of particle m. The coefficient of 1/2 in (4.2) indicates that relative displacements Δl between two particle centers are due to identical deformations in the area of contact in both particles. Normal and tangential components of Δl^c, in the local coordinate system of a contact, can be obtained by scalar multiplication of (4.1) by unit vectors n^c, t^c of the local coordinate system of a contact. Scalar multiplication gives the following expressions

$$\Delta l_n^c = \frac{1}{2}\,\Delta l_n$$
$$\Delta l_t^c = \frac{1}{2}\,(\Delta l_t + d_o \Delta\omega) \tag{4.19}$$

where Δl_n^c, Δl_t^c are normal and tangential components of the contact point displacement. These two parameters define contact forces through normal (k_m') and tangential (k_t') contact stiffnesses as follows

$$f_n^c = k_n' \Delta l_n^c$$
$$f_t^c = k_t' \Delta l_t^c$$

where f_n^c, f_t^c are scalar components of contact force.

According to (4.19) the above relationships can be written in the form

$$f_n^c = (\frac{1}{2}\, k_n' d_o)\, \frac{\Delta l_n}{d_o}$$
$$f_t^c = (\frac{1}{2}\, k_t' d_o)\, (\frac{\Delta l_t}{d_o} + \Delta\omega) \tag{4.20}$$

It is convenient to redefine contact stiffnesses introducing new quantities

$$k_n = \frac{1}{2}\, k_n' d_o\,, \quad k_t = \frac{1}{2}\, k_t' d_o \tag{4.21}$$

and also introducing relative displacements between particle centers per distance between centers d_o, i.e.

$$\delta_n^c = \frac{\Delta l_n}{d_o} \qquad \delta_t^c = \frac{\Delta l_t}{d_o}$$

Relationships (4.20) can now be rewritten in the form

$$\begin{aligned} f_n^c &= k_n \delta_n^c \\ f_t^c &= k_t(\delta_t^c + \Delta\omega) \end{aligned} \tag{4.22}$$

Stiffnesses which enter can be determined from simple experiments shown in Fig. 4.4, where particles are not allowed to rotate.

Potential energy stored in one physical contact with forces f_n^c, f_t^c can be calculated as

$$w^c = \int_0^{\Delta l_t^c} k_n' \Delta l_n \, d(\Delta l_n) + \int_0^{\Delta l_t^c} k_t' \Delta l_t \, d(\Delta l_t)$$

The above potential energy is calculated with rotations prevented as in the "experiment" in Fig. 4.4. If the above integration is performed and the result expressed in terms of contact forces and stiffnesses (4.4), the following expression is obtained

$$w_f^c = d_o \left[\frac{(f_n^c)^2}{2k_n} + \frac{(f_t^c)^2}{2k_t} \right] \tag{4.23}$$

With potential energy expressed in terms of relative displacements and rotations by using (4.22) the result contains rotations explicitly. The expression for potential energy in the three-dimensional case is identical to (4.23) Note that for linear systems complementary work of internal deformations coincides with potential energy.

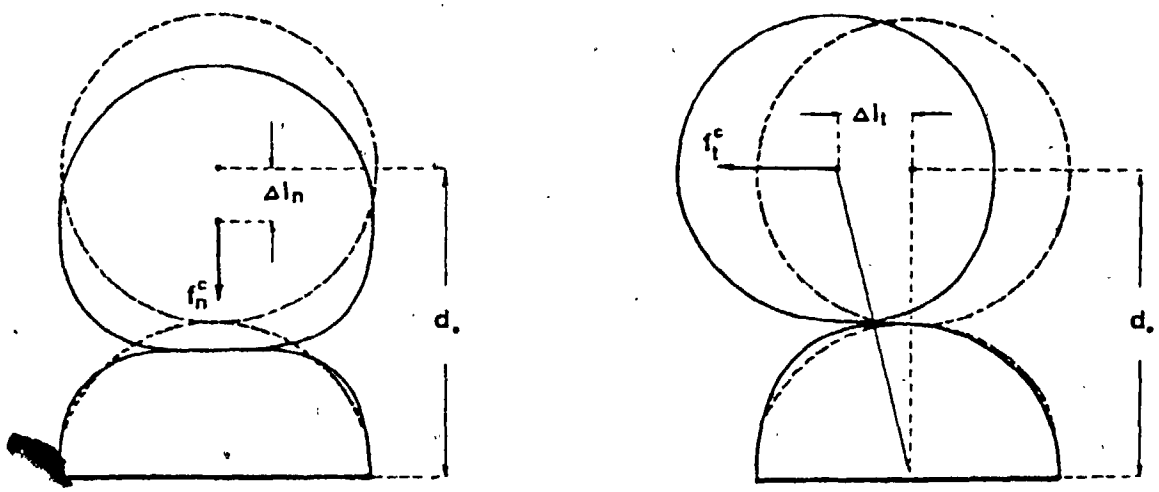

FIGURE 4.4

NORMAL AND TANGENTIAL RELATIVE DISPLACEMENTS

4.6 Particle Rotations and Deformations of Granular Materials

Consider the problem of determining contact forces and particle displacements in an exact form. Deformations of a system of N particles (e.g. spheres) can be described in terms of $3N$ components of displacement vectors of particle centers and $3N$ components of rotation vectors. Contact forces can be expressed in terms of these $6N$ unknowns of the problem and $6N$ equations of force and moment equilibrium can be solved if forces on boundary particles or their displacements are specified. Rotational degrees of freedom are as essential to the above formulation as their translational degrees of freedom. Particle's rotations are largerly responsible ror a local moment equilibrium, but on the other hand, no global motion results from these local rotations. An entirely different condition would result if contacts are capable of transmitting moments. This possibility is not considered here due to small contact areas.

Consider a group of contacts with the same orientation θ and calculate average forces over contacts of this group. For the linear contact model (4.22) gives

$$\begin{aligned} \bar{f}_n(\theta) &= k_n \bar{\delta}_n(\theta) \\ \bar{f}_t(\theta) &= k_t(\dot{\bar{\delta}}_t(\theta) + \Delta\bar{\omega}) \end{aligned} \tag{4.24}$$

where $\delta_n(\theta)$, $\delta_t(\theta)$ are average relative displacements.

Note that $\Delta\omega$ in (4.22) is the rotation of one particle in the coordinate system rotating with another particle in contact. It is shown (Appendix A) that $\Delta\omega = \Delta\omega_1 + \Delta\omega_2$ where $\Delta\omega_1$ and $\Delta\omega_2$ are rotations of both particles about their own centers. In the case of no rigid body rotations, the average rotation over all particles is zero. If average rotation is calcu-

lated over large groups of particles scattered in different parts of the assembly, the result must also be zero. This is the case of rotation $\Delta\bar{\omega}$ in (4.24) which is zero and average forces can be given in the form

$$\bar{f}_n(\theta) = k_n \bar{\delta}_n(\theta)$$
$$\bar{f}_t(\theta) = k_t \bar{\delta}_t(\theta) \tag{4.25}$$

i.e. defined by average relative displacements between particles forming contacts with orientation θ.

The statement that $\Delta\bar{\omega}$ in (4.24) is zero is, so far, an assumption and will be verified below. Note that the possibility of obtaining relationships between group averages of forces and relative displacements is due to the linearity of (4.22). In non-linear cases, a relationship between group averages cannot be established directly and a distribution function of relative displacements is necessary.

For the linear model, group averages can be calculated first and the distribution function of forces of the same orientation group can then be determined.

4.7 Average Relative Displacements Between Particles

In section 4.6 a mechanical problem for an assembly of bonded particles was posed in terms of kinematic variables. Such a formulation is not absolutely necessary and the problem can be considered in terms of contact forces on the basis of the theorem on minimum of complementary work of internal deformations. Such an attitude is logical within the present theory based on specification of boundary forces. With this approach deformational

features of an assembly (strains) must appear automatically.

In the present section a heuristic approach is considered that is based on the notion of strain as defined in continuum mechanics. This discussion is necessary in order to clarify the meaning of certain unspecified parameters encountered in the rigorous consideration of the problem of deformations of bonded particles to be presented in the next chapter.

Consider a homogeneous continuum subject to boundary displacements of the form $l_i^B(R) = \varepsilon_{ij} R_j$ where R represents a point on the boundary of the continuum. With ε_{ij} constant for all points of the boundary, a uniform displacement field with displacement gradients ε_{ij} will exist within the continuum. If L^o is a certain vector with orientation θ in undeformed configuration, this vector following deformation will be of the form

$$L = L^o + \Delta L$$

where ΔL can be calculated as follows:

$$\Delta L_i = |L^o| \varepsilon_{ij} n_j$$

where n is the unit vector in the direction of vector L^o. Normal and tangential components of ΔL per unit length of the vector can be calculated as scalar products of ΔL with vectors n, t, i.e.

$$\delta_n = \frac{(\Delta L \cdot n)}{|L^o|} = \varepsilon_{ij} n_j n_i$$
$$\delta_t = \frac{(\Delta L \cdot t)}{|L^o|} = \varepsilon_{ij} n_j t_i \qquad (4.26)$$

Relative displacements are direction-dependent, and if θ is the orientation of vector L^o, calculation according to the above relationships gives

$$\delta_n = \frac{1}{2} (\varepsilon_n + \varepsilon_t \cos 2(\theta - \theta_\varepsilon))$$
$$\delta_t = \frac{1}{2} (\varepsilon_\omega - \varepsilon_t \sin 2(\theta - \theta_\varepsilon))$$

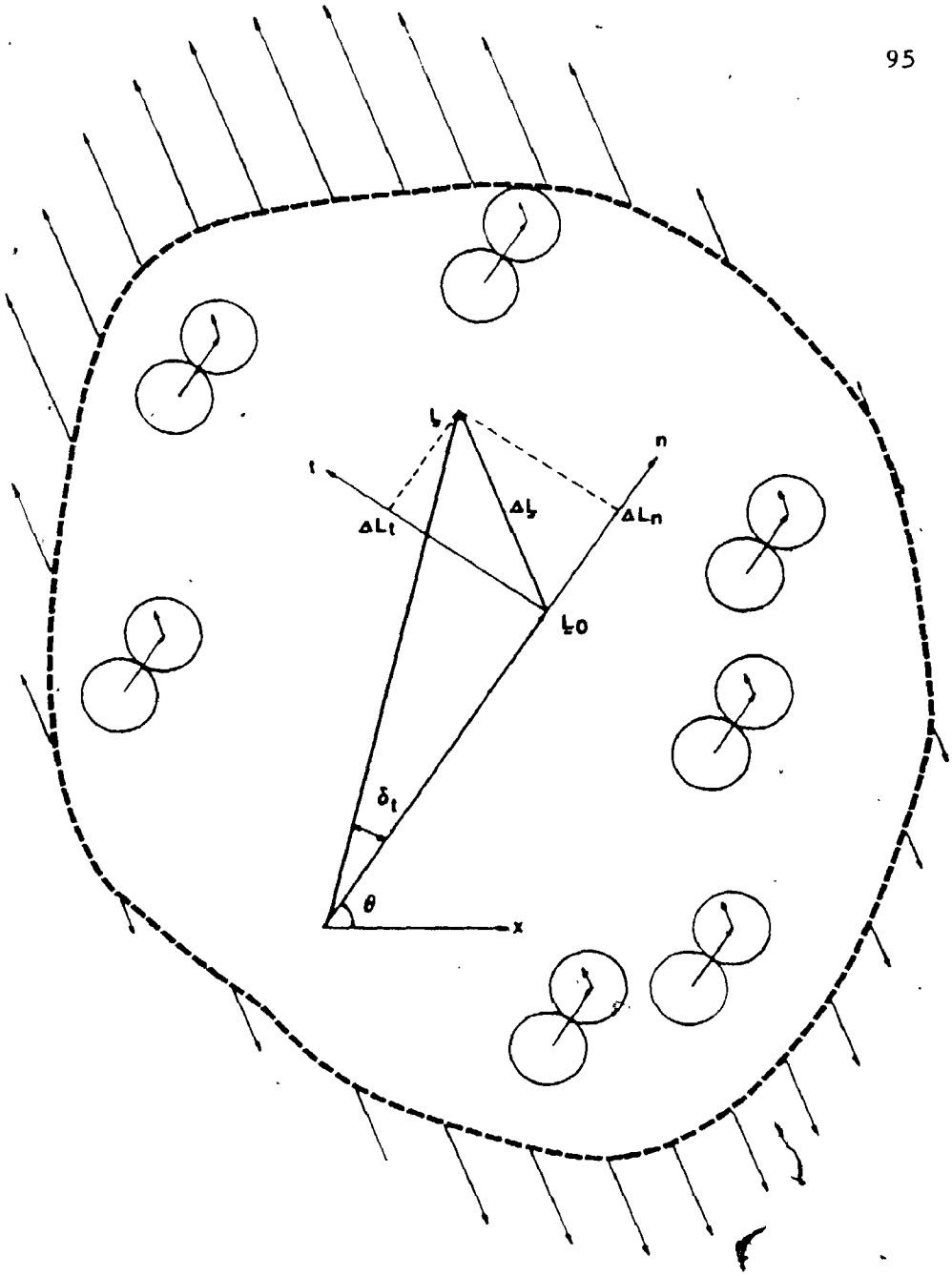

FIGURE 4.5

AVERAGE INTERPARTICLE DISPLACEMENTS IN CONTINUUM

where

$$\varepsilon_n = \varepsilon_{11} + \varepsilon_{22}$$
$$\varepsilon_t = [(\varepsilon_{11}-\varepsilon_{22}) + (\varepsilon_{21}+\varepsilon_{12})]^2 \qquad (4.27)$$
$$\varepsilon_\omega = \varepsilon_{21} - \varepsilon_{12}$$

are invariants of ε_{ij}. Note that ε_n is volumetric strain, ε_t is the shearing strain intensity, and ε_ω gives rigid body rotations, positive when counter-clockwise. Major principal direction can be calculated from the expression

$$sin2\theta_\varepsilon = \frac{\varepsilon_{21} + \varepsilon_{12}}{\varepsilon_t} \quad , \quad cos2\theta_\varepsilon = \frac{\varepsilon_{11} - \varepsilon_{22}}{\varepsilon_t} \qquad (4.28)$$

If a structure of the considered continuum is recognized and a group of contacts with orientation θ is selected (Fig. 4.5), it is reasonable to expect that average relative displacements between particle centers will be proportional to relative displacements which can be calculated according to (4.24). Relative displacements between centers of particles forming contacts of the same orientation will fluctuate from contact to contact and the proportionality relative to displacements calculated from continuum mechanics considerations can be assumed only on the average, i.e.

$$\bar{\delta}_n(\theta) = \xi \frac{1}{2} (\varepsilon_n + \varepsilon_t cos2(\theta-\theta_\varepsilon))$$
$$\bar{\delta}_t(\theta) = \xi \frac{1}{2} (\varepsilon_\omega - \varepsilon_t sin2(\theta-\theta_\varepsilon)) \qquad (4.29)$$

where ξ is a certain coefficient of proportionality which reflects the structure of the assembly. The meaning of coefficient ξ will be thoroughly investigated further. It need only be mentioned now that $\xi<1$ for systems with irregular structures. This parameter will be of considerable importance below. this stage, (4.29) is merely an assumption which enables one to obtain

average forces on contacts of the same orientation using (4.25) which gives

$$\begin{aligned} \overline{f}_n(\theta) &= k_n \xi \frac{1}{2} [\varepsilon_n + \varepsilon_t cos2(\theta-\theta_\varepsilon)] \\ \overline{f}_t(\theta) &= k_t \xi \frac{1}{2} [\varepsilon_\omega - \varepsilon_t sin2(\theta-\theta_\varepsilon)] \end{aligned} \tag{4.30}$$

A similiar form (4.14) of average forces with preffered direction coincident with the direction of anisotropy has already been considered.

Previous analysis in simplified conditions showed that the magnitude of contact forces, defined by f_n^o in (4.14), is uniquely related to hydrostatic stress according to (4.16). It is convenient to introduce the same parameter f_n^o into (4.30) and to rewrite the equations in the form

$$\begin{aligned} \overline{f}_n &= \frac{\pi d_0}{\rho\gamma} \sigma_n [a_n + a_f cos2(\theta-\theta_f)] \\ \overline{f}_t &= \frac{\pi d_0}{\rho\gamma} \sigma_n [a_\omega - a_\mu sin2(\theta-\theta_f)] \end{aligned} \tag{4.31}$$

where $\theta_f = \theta_\varepsilon$ and

$$\begin{aligned} a_n &= K \frac{\varepsilon_n}{\sigma_n} & a_f &= K \frac{\varepsilon_t}{\sigma_n} \\ a_\omega &= \frac{K}{r} \frac{\varepsilon_\omega}{\sigma_n} & a_\mu &= \frac{K}{r} \frac{\varepsilon_t}{\sigma_n} \end{aligned} \tag{4.32}$$

$$K = \frac{1}{2} k_n \xi \frac{\rho\gamma}{\pi d_0} \tag{4.33}$$

$$r = \frac{k_t}{k_n} \tag{4.34}$$

To obtain a physical interpretation for the above quantities, it is necessary to compare average forces (4.31) with their simplified form (4.14) and note that a_n was taken as unity in (4.14). It was shown previously that the form of average forces with $a_n = 1$ corresponds to a system with small anisotropy and subject to loads in the direction of anisotropy. The form of forces with $a_n = 1$ is, therefore, an exact for isotropic assemblies and the first formula in (4.32) gives $\sigma_n = K \varepsilon_n$ thus indicating that K

given by (4.33) is a bulk modulus defined by normal contact stiffness and geometrical features of an assembly. This interpretation of K useful, since it indicates how parameter ξ, introduced empirically in (4.29), can be measured experimentally*.

Average forces (4.31) are, generally, direction-dependent and their directional variation is controlled by parameters a_f, a_μ referred to further as "coefficients of force anisotropy" (for normal and tangential forces, respectively). Directional variation of $\overline{f}_n(\theta)$, $\overline{f}_t(\theta)$ is about a certain average level defined by coefficients a_n, a_ω called "coefficients of contact force intensity". For an isotropic assembly $a_n = 1$ and the average level of forces is defined only by hydrostatic stress. For anisotropic assemblies a_n will depend on parameters of anisotropy and deviatoric loads. Coefficient a_n is related to volumetric strain according to (4.32). For an incompressible assembly ε_v is zero, indicating that normal contact forces in incompressible assemblies have only a direction-dependent component and the average normal force over contacts of all directions is zero.

Comparison of (4.31) and 4.14) shows that the coefficient of tangential force intensity a_ω is zero when loads on an assembly are in the direction of anisotropy. This is a consequence of moment equilibrium. For other types of deviatoric loads, a_ω is not zero and is related (for a linear contact model) to the rotational part of the displacement gradient. It will be shown in the next section that when external loads are not

---

* It will be shown in the chapter VI that ξ is related to the second moment of force distribution on contacts of the same orientation. Numerical assesment of this quantity enables to study fluctuations of phenomenological parameters. The theory, at present, provides no means of calculating ξ and relates it to contact stiffness and bulk modulus (both are measurable parameters).

in the direction of anisotropy , macro-rotations will be always present.

Magnitudes of normal and tangential forces (4.30) can be independently varied by volumetric and deviatoric strains. The form of average forces (4.31) underlines the fact that directional parts of both distributions are controlled by parameters a_f, a_μ which, according to (4.32) are proportional, i.e.

$$a_\mu = \frac{k_t}{k_n} a_f = r\, a_f \tag{4.35}$$

where $r = k_t/k_n$ will designate the ratio of tangential to normal stiffnesses. In section 4.4 coefficient a_μ was introduced, but was unspecified. Its form 4.34 is due to the adopted model of a contact.

The preferred direction of forces $\theta_f = \theta_\varepsilon$ is determined by the principal direction of the strain tensor.

In the following section parameters (4.32) are related to invariants of the stress tensor and physical consequences of these relationships are discussed.

4.8 Average Contact Forces in Plane Anisotropic Assemblies

Forces between deformable solids depend upon their deformations and it is natural to expect that contact forces are related to the global deformations. For systems of bonded particles with unlimited strength at their contacts the mentioned mode of deformation is the only one possible.

For cohesionless assemblies or, generally, for systems with contacts of limited strength, global deformations are also related to rearrangement in structure ("plastic deformations"). Such strains are not related

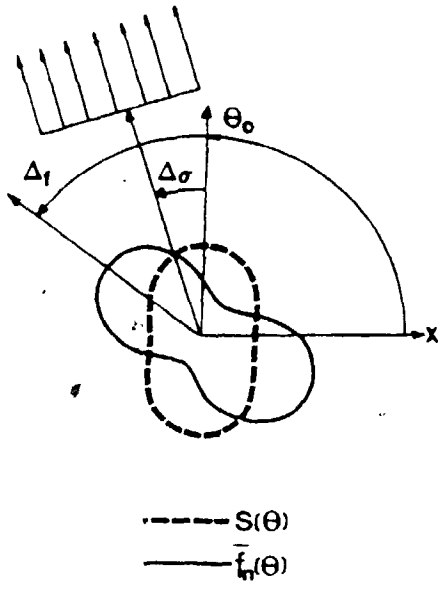

FIGURE 4.6

PREFERRED DIRECTION OF AVERAGE FORCE WITH RESPECT TO DIRECTION OF ANISOTROPY

directly to contact forces defined by local particle deformations. In this case it is no longer possible to associate parameters defining average forces (4.30) with the strain tensor. It is, perhaps, possible to link parameters defining average forces with the "elastic part" of strains, although decomposition of the strain tensor into "elastic" and "plastic" parts is artificial. For any physical system the possibility of such an approach must be thoroughly investigated.

Average forces can be investigated in the form (4.31) which does not explicitly contain a reference to heuristic logic that leads to (4.30). With this approach the form of average forces (4.30) can be viewed as an approximation based on the second Fourier component in decomposition of average contact forces. The most general form of such a decomposition can be considered as follows:

$$f_n(\theta) = A_o + A_1 cos2(\theta-\theta_1)$$
$$f_t(\theta) = A_2 + A_3 sin2(\theta-\theta_2)$$

where angles θ_1 and θ_2 are, generally, different. For isotropic systems, substitution of the above forces into (4.11) immediately gives $\theta_1 = \theta_2$. This case will be considered further for anisotropic systems also. Its justification will be presented in Chapter 6 where energy methods will be introduced.

Average forces (4.31) are described in terms of five parameters a_n, a_f, a_μ, a_ω, θ_f and systems will be studied under conditions with the stress tensor prescribed by external conditions. In the plane case studied here, all five parameters cannot be uniquely determined by three components of the plane stress tensor and one condition of symmetry. One parameter is always a characteristic of a specific system, as it is the case of linear

contacts when a_μ and a_f are proportional

$$a_\mu = r\, a_f \tag{4.36}$$

It is convenient to consider a_μ in the above form, but not associate r with the ratio of tangential to normal stiffnesses as for the linear contact model. This, however, suggests that r is also related to particle properties for systems more general than that considered above. This parameter, by definition, reflects proportionality in directional variation of normal and tangential forces. It will be shown that it entirely controls the magnitudes of tangential forces. Both features indicate that r must be related to a coefficient of interparticle friction for frictional systems.

The following analysis is independent of specific interpretation of r which does not affect qualitative conclusions on the nature of average forces.

Average normal and tangential forces are invariant scalars and must, therefore, be related to invariants of the stress tensor. Contact orientation distribution will be considered in the form

$$S(\theta) = \frac{1}{2\pi}\left[1 + a\cos 2(\theta-\theta_0) + b\cos 4(\theta-\theta_0)\right]$$

i.e. with a fourth Fourier component. It is convenient to refer all orientations to the direction of anisotropy θ_0 and to introduce an angle $\Delta\sigma = \theta_\sigma - \theta_0$ between the major principal direction θ_σ of the stress tensor and direction of anisotropy. Similarly, $\Delta_f = \theta_f - \theta_0$ is the preferred orientation of forces measured from the direction of anisotropy. Note that θ_f is not necessarily interpreted as the major principal direction of the strain tensor. Both angles are shown in Fig. 4.6.

The presence of a constant term in the expression for tangential forces indicates the possibility of non-compensated moments on particles.

Since the stress tensor must be symmetrical, the distribution of tangential forces must be such that the condition of symmetry 4.4 be satisfied. Substitution of $\bar{f}_t$ from (4.31) into (4.4) gives

$$a_\omega = -\frac{1}{2} a\, a_\mu \sin 2\Delta_f \tag{4.37}$$

The same condition written in terms of strain tensor invariant can be obtained using (4.32) in the form

$$\varepsilon'_\omega = -\frac{1}{2} a\, \varepsilon_t \sin 2\Delta_\varepsilon \tag{4.38}$$

where $\Delta_\varepsilon = \Delta_f$ is the deviation of the principal direction of the strain tensor from the direction of anisotropy. For a system of bonded particles with linear contact interactions the above condition imposes a certain constraint on components of the strain tensor.

To explain the physical meaning of the above constraint, assume for a moment that tangential forces (4.30) do not have a constant term ε_ω (or a_ω in (4.31)) and suppose that loads on anisotropic material are not imposed in the direction of anisotropy. Fig. 4.7[a] illustrates the described situation. A preferred direction of contact forces must be such as to correspond to external loads. Suppose that such a direction was found with tangential force without a constant term (Fig. 4.7[a]). The gross effect of average forces with orientation θ is determined by the amount of these contacts in the assembly, i.e. by $S(\theta)$, also shown in Fig. 4.7[a] within a "generic particle". It may be seen that with symmetrical distribution of $\bar{f}_t(\theta)$ without a constant term, there will be a non-compensated clockwise moment due to a larger amount of contacts corresponding to forces producing this moment. Orientations of these contacts correspond to the shaded areas of $S(\theta)$ in Fig. 4.7[a]. In order to compensate for such moments, deformations must proceed in such away as to reduce tangential forces on contacts

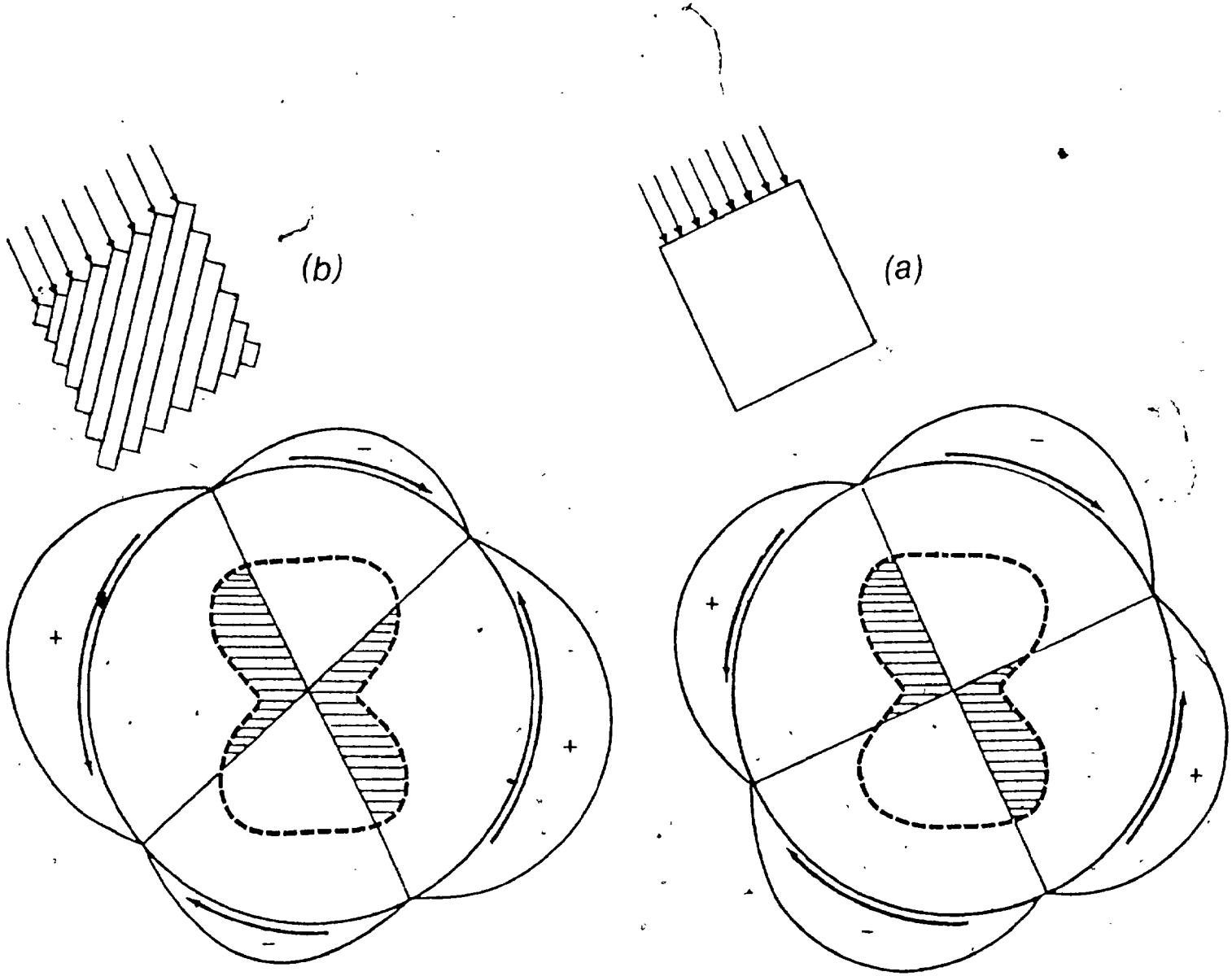

FIGURE 4.7

BALANCE OF MOMENTS AND CONSTRAINT DEFORMATIONS

of greater availability and to increase tangential forces on contacts which are present in smaller ammounts. This would result in a tangential force distribution as shown on fig. 4.7[b] which also shows a deformation mode of such an anisotropic material. One can immediately recognize DeJong's [9] "double sliding mechanism" and (4.32) indicate a clockwise rotation, as indicated on fig. 4.7[b]. An interpretation of sliding is relevant to cohesionless materials only. The described mechanism is general for anisotropic systems.

Gross rotations presented here are related to the deformational part of the strain tensor according to (4.33). Tangential forces are determined by the "constitutive part" of displacement gradient related to deviatoric strains ε_t. Rotations ε_ω can be excluded from (4.30) using (4.33) and the average tangential force depends on deviatoric strains as follows:

$$\overline{f}_t(\theta) = -k_t \xi \frac{1}{\varepsilon} \varepsilon_t [0.5\, a\, sin2\Delta_\varepsilon + sin2(\theta-\theta_\varepsilon)]$$

Similarly, a_ω can be excluded from (4.31) using (4.32) to obtain

$$\overline{f}_t(\theta) = -f_n^o\, a_\mu [0.5\, a\, sin2\Delta - sin2(\theta-\theta_\varepsilon)]$$

Taking a_μ in the form (4.34) it can be seen that tangential forces are entirely controlled by a_μ ,or equivalently, by r.

The remaining parameters of average contact forces a_n, a_f, Δ_f can be linked directly to invariants of the stress tensor using relationships (4.9-4.11). Substitution of (4.31) into (4.9-4.11), straightforward integration and rather tedious transformations finally give

$$a_n = 1 - \frac{a^2}{2c_f(1+r)} (R\, cos2\Delta_\sigma - 1)$$

$$a_f = \frac{a}{c_f(1+r)} \sqrt{D} \qquad (4.39)$$

$$cos2\Delta_f = \frac{R\, cos2\Delta_\sigma - 1}{\sqrt{D}}$$

where

$$R = \frac{2a_\sigma}{a}$$

$$D = R^2 - 2R\cos 2\Delta_\sigma + 1 + \left[\left(\frac{c_f}{c_\mu}\right)^2 - 1\right] R^2 \sin^2 2\Delta_\sigma \tag{4.40}$$

and

$$c_f = 1 - \frac{a^2}{2}\frac{1}{1+r} + \frac{b}{2}\frac{1-r}{1+r}$$

$$c_\mu = 1 - \frac{a^2}{2}\frac{r}{1+r} - \frac{b}{2}\frac{1-r}{1+r} \tag{4.41}$$

Physical interpretation of the above results will be greatly facilitated if potential energy of a system of bonded particles with the above average forces is calculated. This calculation can be perfomed now using continuum mechanics considerations (the validity of this approach will be justified in the next chapter).

Potential energy per unit area of the considered plane system can be given in the form

$$U = \frac{1}{2}\sigma_{ij}\varepsilon_{ij} = \frac{1}{2}\left[\sigma_n\varepsilon_n + \sigma_t\varepsilon_t\cos 2(\theta-\theta_\sigma)\right]$$

Expressing potential energy in terms of parameters (4.32) one can obtain

$$U = \frac{\sigma_k}{2K}\left[a_n + a_f a_\sigma \cos 2(\theta_\sigma - \theta_\varepsilon)\right] \tag{4.42}$$

Substitution of (4.39-4.40) into the above expression and simple transformations give

$$U = \frac{\sigma_n^2}{2K_n}\left\{1 + \frac{a^2}{2c_f(1+r)}\left[R^2 - 2R\cos 2\Delta_\sigma + 1 + \frac{c_f - c_\mu}{c_\mu} R^2 \sin 2\Delta_\sigma\right]\right\} \tag{4.43}$$

The above results indicate that average forces are controlled mainly by parameter R which defines the level of deviatoric loads in relation to anisotropy in contact distributions, so that according to the definition of R (4.40), $a_\sigma = R\frac{1}{2}a$ and R will be called "coefficient of deviatoric load". Various terms in (4.39-4.41) and (4.43) are of different

orders of magnitude with respect to the parameter of anisotropy a. Terms quadratic with respect to a and b can be neglected with no effect on the numerical values of parameters of interest or on qualitative features. Although the expression for a_n (4.39) contains a quadratic term, this term is, however, of the form $O(a^2R) = O(a\ a_\sigma)$ and is of the second order of magnitude for small deviatoric loads.

Extensive numerical investigations show that no loss of qualitative information occurs if such terms of the order $O(a^2)$, $O(a\ a_\sigma)$, $O(b^2)$, $O(b\ a_\sigma)$, $O(a\ b)$ are neglected in expressions (4.39-4.41). Such terms cannot be neglected in the expression for potential energy which is quadratic by definition, so that only cubic terms $O(b\ a^2)$ are neglected to obtain a simplified form of the above expressions

$$\begin{aligned} a_n &= 1 \\ a_f &= \frac{a}{1+r}\sqrt{R^2 - 2R\cos 2\Delta_\sigma + 1} \\ \cos 2\Delta_f &= \frac{R\cos 2\Delta_\sigma - 1}{\sqrt{R^2 - 2R\cos 2\Delta_\sigma + 1}} \\ U &= \frac{\sigma_n^2}{2K}\left[1 + \frac{a^2}{2(1+r)}(R^2 - 2R\cos 2\Delta_\sigma + 1)\right] \end{aligned} \qquad (4.44)$$

The above expressions contain all major features of average contact forces. Note that parameter b is not present in (4.44), although its influence is important for problems involving non-homogeneous stress distributions. The exact form of average forces will be considered below, however, at this point (4.44) is sufficiently accurate.

It is interesting to note that the preferred direction of forces Δ_f is independent of parameter r which is a characteristic of a specific system. Parameter a_n which defines average force over all contacts is

practically unaffected by anisotropy of contact orientations and the main effect of anisotropy on directional variation of contact forces is controlled by a_f.

An isotropic case can be recovered from (4.37) and (4.43) when $a \to 0$, $R \to \infty$ and $a_\sigma = \frac{1}{2} R\, a = const$. This limiting transition gives

$$a_\omega = 0;\ a_n = 1;\ a_f = 2\,\frac{a_\sigma}{1+r};\ \Delta_f = \Delta_\sigma \qquad (4.45)$$

For systems of bonded particles the last formula means that principal directions of stress and strain coincide.

Average forces in this case can be written in a form based on (4.31) and (4.39).

$$\begin{aligned} \bar{f}_n(\theta) &= \frac{\pi d_o}{\rho\gamma}\,\sigma_n\,[1 + \frac{2}{1+r}\,a_\sigma cos2(\theta-\theta_\sigma)] \\ \bar{f}_t(\theta) &= \frac{\pi d_o}{\rho\gamma}\,\sigma_n\,[\frac{2r}{1+r}\,a_\sigma sin2(\theta-\theta_\sigma)] \end{aligned} \qquad (4.46)$$

To give a simple interpretation of the above average forces, consider gross forces per unit length of a macro-element with normal $N(\theta)$ and tangential direction $T(\theta)$. Such forces are of the form

$$\begin{aligned} F_n(\theta) &= \sigma_{ij} N_j N_i = \sigma_n[1 + a_\sigma cos2(\theta-\theta_\sigma)] \\ F_t(\theta) &= \sigma_{ij} N_j T_i = -\sigma_t[a_\sigma sin2(\theta-\theta_\sigma)] \end{aligned} \qquad (4.47)$$

Comparison of (4.46) and (4.47) indicates that average forces on contacts of orientation θ follow a trend of gross forces on plane elements with orientation θ. Direct proportionality exists only for $r = 1$, which for a linear contact model is the case of equal normal and tangential contact stiffnesses.

The magnitude of forces is controlled by hydrostatic stress and geometrical parameters of the packing. Redistribution of forces between normal and tangential components is related to parameter r (for the linear

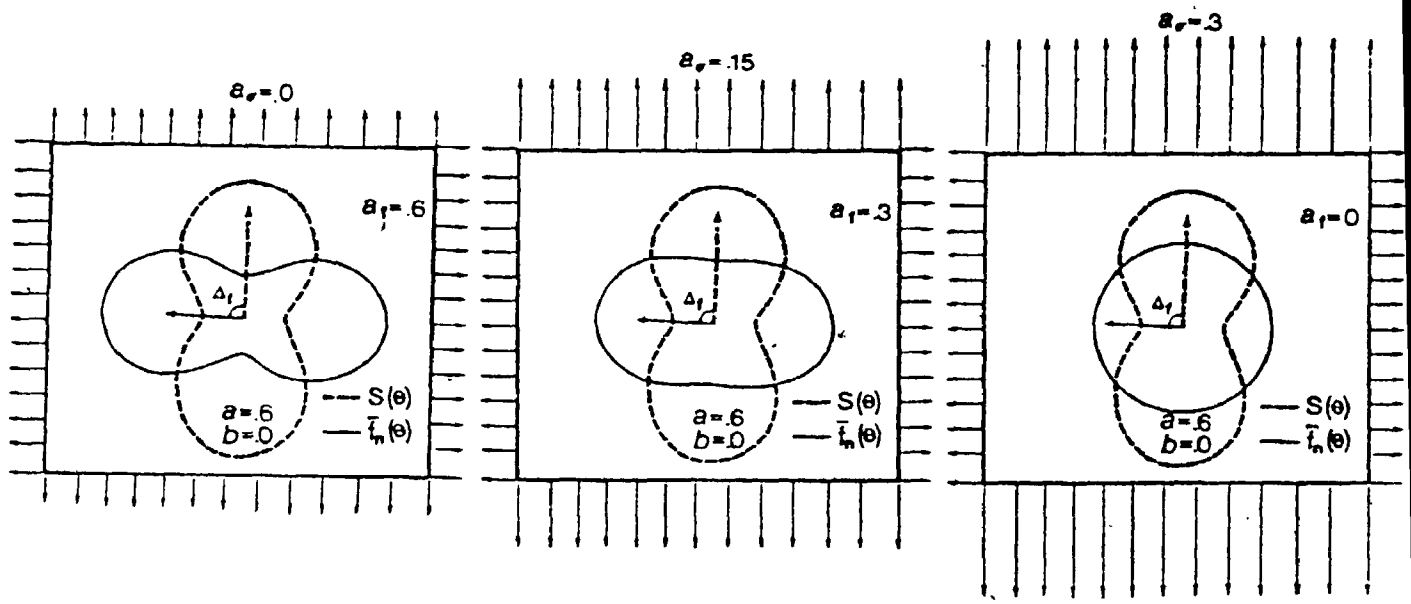

FIGURE 4.8

EFFECT OF ANISOTROPY ON AVERAGE FORCES

contact model, to the ratio of tangential to normal contact stiffnesses). Isotropic structure of a system has no effect on directional variation of average forces which is entirely controlled externally by σ_{ij} or, more specifically, by its principal direction and a_σ.

Consider now anisotropic systems and let initially the principal direction of the stress tensor coincide with the direction of anisotropy, i.e. $\Delta\sigma = 0$ and (4.44) gives

$$a_f = \frac{a}{1+r}\,|R-1|$$
$$\cos 2\Delta_f = sign(R-1) \qquad (4.48)$$

Note first that under hydrostatic loads $a_\sigma = 0$ $(R = 0)$, average forces are direction-dependent due to intrinsic anisotropy in contact orientations. In this case (4.48) gives $\Delta_f = \frac{\pi}{2}$ and distribution of average forces is shown on Fig. 4.8. When deviatoric loads increase ($a_\sigma > 0$, $R > 0$), directional variation induced externally reduces the existing intrinsic variation due to anisotropy (Fig. 4.8^b). When $R = 1$, i.e. $a_\sigma = \frac{1}{2}\,a$, externally induced force anisotropy compensates anisotropy of contacts due to varying contact orientations and $a_f = 0$ (Fig. 4.8^c). When $R > 1$ $(a_\sigma > \frac{1}{2}\,a)$, externally induced directional variation of forces exceeds intrinsic and, according to (4.48), $\Delta_f = 0$, i.e. the preferred direction of forces coincides with the direction of anisotropy. In this case anisotropy in contacts reduces induced anisotropy in contact forces. The mentioned reduction of forces on contacts in the direction of anisotropy is understanfable, since there are more contacts in that direction to support the load, so that the force per contact is less compared to other directions which contain less contacts. For large coefficients of deviatoric load

R, the influence of anisotropy in contact orientations disappears. Such response of anisotropic systems is reflected in peculiar variations of potential energy with the level of external loads. For $\Delta_\sigma = 0$, the last expression in (4.44) gives

$$U = \frac{\sigma_n^2}{2K_n}\left[1 + \frac{a^2}{2(1+r)}(R-1)^2\right],$$

i.e. potential energy decreases within the range $0 \leq R \leq 1$ and has an isolated minimum for $R=1$. It then increases with R.

If potential energy stored in the system is intuitively associated with the degree of stability of the system, the most stable state of considered anisotropic systems is the one with $R=1$, i.e. under deviatoric load with $a_\sigma = \frac{1}{2}a$ and not under hydrostatic load as for isotropic systems. This fact will be employed when the theory of earth pressure at rest will be presented for cohesionless materials.

Consider now a pattern of contact forces when the major principal direction of stress does not coincide with the direction of anisotropy. The preferred direction of forces deviates from both the direction of anisotropy and external load. The angle of deviation from the direction of anisotropy is given by (4.44) and is shown in Fig. 4.9 for a series of values of R. In all cases the preferred direction of force deviates from the direction of anisotropy more than the principal direction of the stress tensor. This way the system of forces compensates for a reduced number of contacts in the direction of maximum gross load Response of an anisotropic assembly is sharply different for $R<1$ and $R>1$. In the first case, an externally induced variation of forces is less than the one which intrinsically exists under hydrostatic loads. Consider a conceptual experiment in which the major principal direction Δ_σ is kept fixed with respect

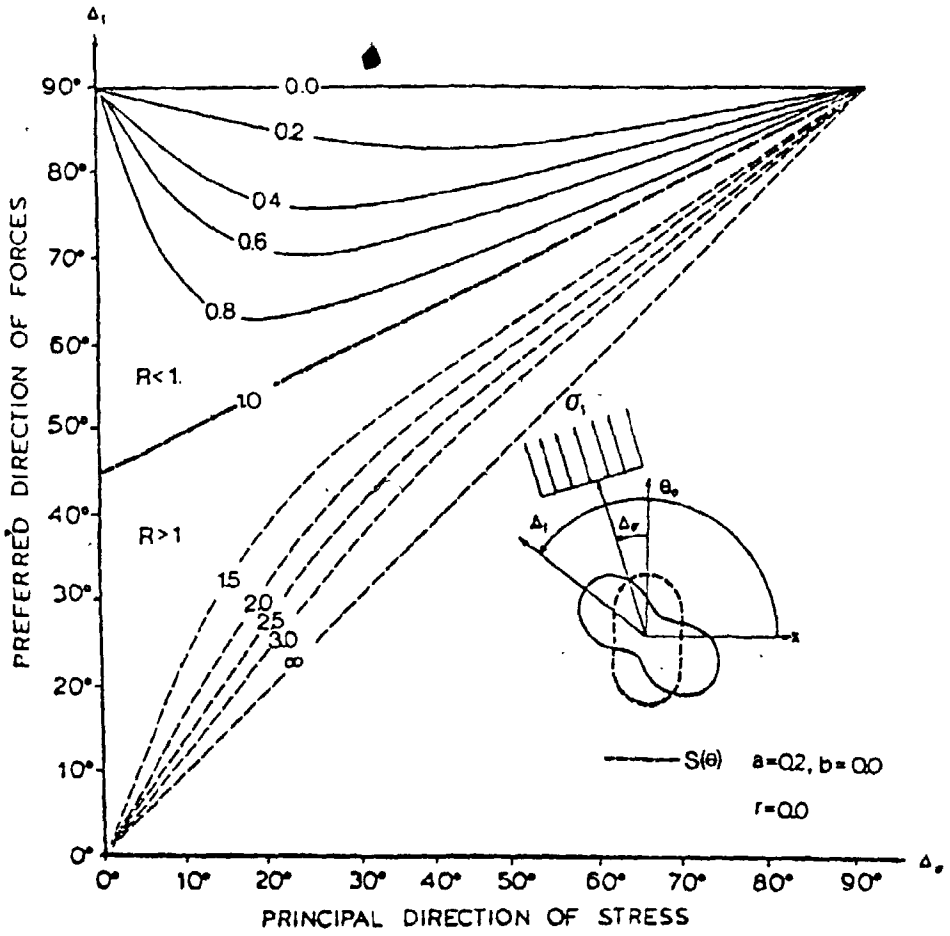

FIGURE 4.9

PREFERRED DIRECTION OF AVERAGE FORCES
VS.
PRINCIPAL DIRECTION OF STRESS

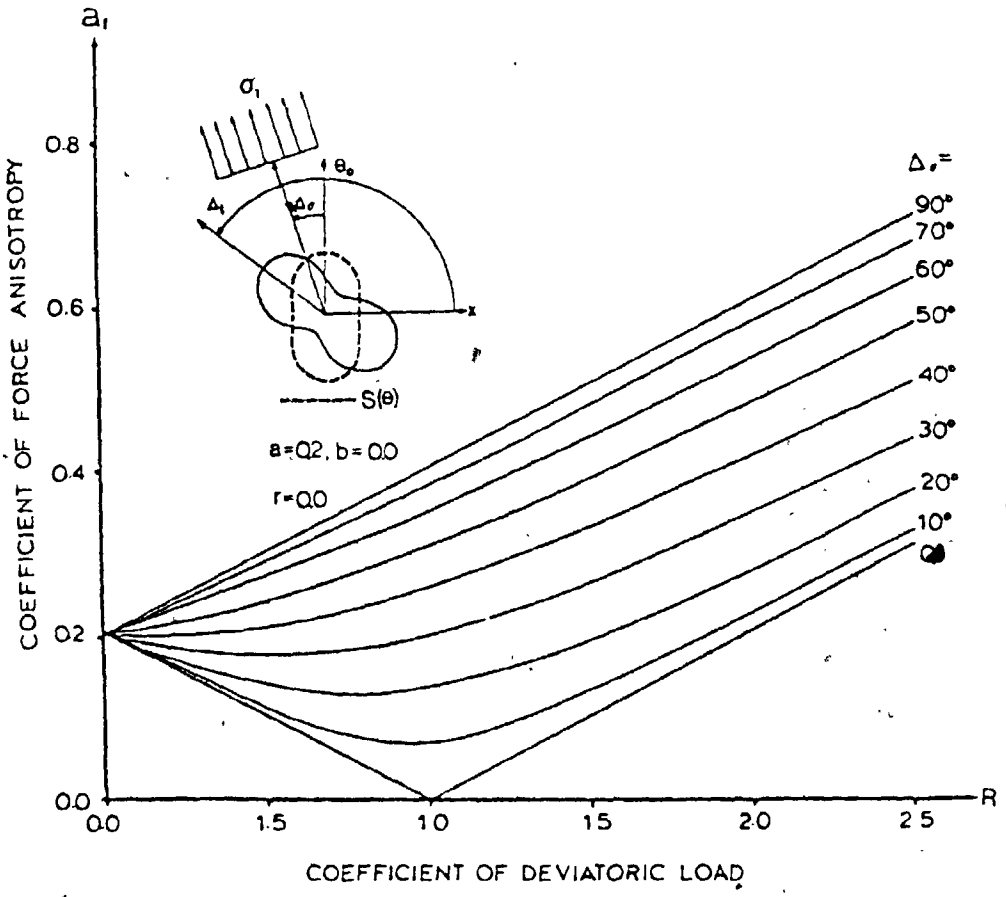

FIGURE 4.10

COEFFICIENT OF FORCE ANISOTROPY VS. COEFFICIENT OF DEVIATORIC LOAD

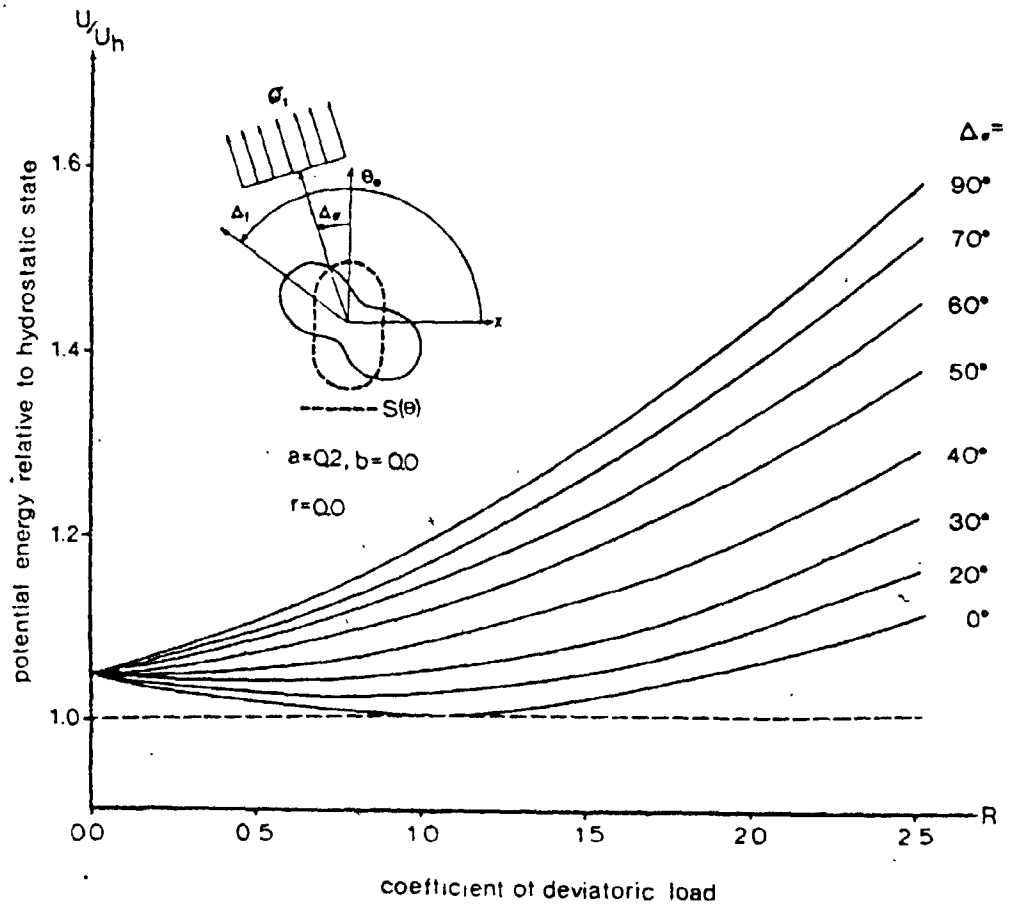

FIGURE 4.11

POTENTIAL ENERGY OF AN ANISOTROPIC SYSTEM VS. COEFFICIENT OF DEVIATORIC LOAD

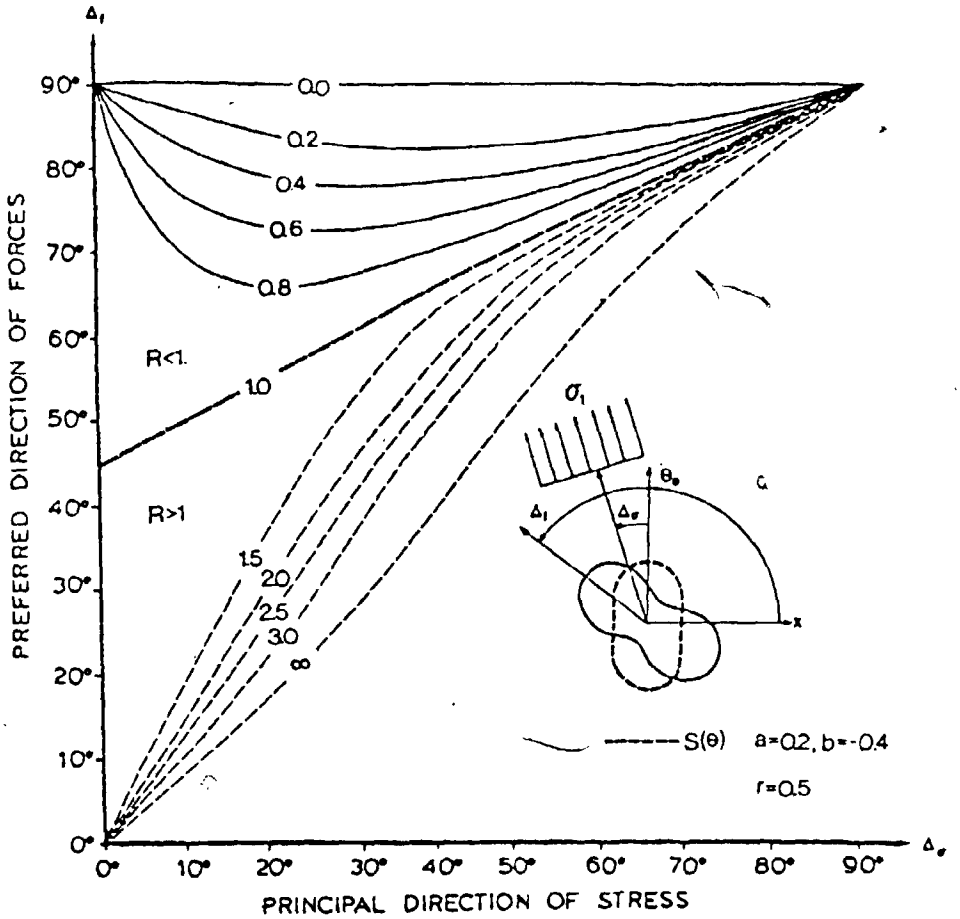

FIGURE 4.12

PREFERRED DIRECTION OF FORCES VS.

PRINCIPAL DIRECTION OF STRESS FOR b≠0

to the direction of anisotropy and deviatoric load increases from a hydrostatic state (R increases). Fig. 4.10 shows variation in the coefficient of force anisotropy a_f with R for fixed Δ_σ. It can be seen that for small Δ_σ, a_f initially deceases. A pattern of potential energy (Fig. 4.11) indicates that deacrease in a_f is equivalent to reduction in the system's potential energy.

For a certain deviatoric load corresponding to $R = cos2\Delta_\sigma$, the coefficient of force anisotropy a_f and potential energy are both minima and further increase in deviatoric load increases a_f and the potential energy of the system. In the described process of deviatoric load increase, the preferred direction of forces rotates towards the direction of external force (Fig. 4.9). In an experiment with fixed deviatoric load ($R = const.$), an increase in deviation of maximum load from the direction of anisotropy results in an increase in force anisotropy (Fig. 4.10). Also, the preferred direction of force initially rotates towards the direction of load, but after a certain point when deviations are minimum, the opposite trend is observed (Fig. 4.9).

For $R>1$, when directional variation of average forces induced by deviatoric load is greater than intrinsic under hydrostatic load, the behavior of the system is "normal" in the sense that increase in deviatoric load causes an increase in anisotropy of forces with a corresponding increase in potential energy.

In the above analysis, only the influence of the coefficient of anisotropy a was investigated (the influence of b was neglected for qualitative analysis). The influence of b on the preferred direction of forces is shown in Fig. 4.12. Visual comparison with the same graph points to minor qualitative differences, although the basic trends remain unchanged.

Specific influence of b on gross stiffness properties of anisotropic systems will be studied in the next chapters. Average forces considered in this chapter were developed with no reference to specific properties of contacts, although one parameter (r), which defines redistribution of forces between normal and tangential components, can be determined when properties of contacts are specified.

4.9 Discussion and Conclusions

Average forces investigated in the present chapter are either averages over contacts of similar orientation in one infinite homogeneous system subject to loads on infinity prescribed by the stress tensor, or averages over contacts of similar orientation and in identical locations of different, but macroscopically similar systems. The stress tensor in this case is assumed to be known at the investigated location.

The theory at this stage does not present a method for calculation of stress fields and the developed analysis is also based on the concept of strain tensor as defined in continuum mechanics. This heuristic approach established the form of directional variation for average forces. The assumed form of average forces will be proven to be correct for systems of bonded particles with linear contacts. On the other hand, the investigated form of average forces can be viewed as an approximation for other systems. The accuracy of this approximation has been checked by considering Fourier components of the order higher than the second in the form of average forces. It was found that the relationships developed will not be significantly different quantitatively or qualitatively.

Parameters which define average forces were shown to be related to invariants of the stress tensor. One parameter (r) of average forces cannot be related to the stress tensor and the example of linear contacts suggests that the mentioned parameter, which defines redistribution of contact forces between normal and tangential components, is related to specific properties of contacts. For linear contacts, normal and tangential average forces are proportional to respective contact stiffnesses. The analysis based on the form of contact forces assumed above can be considered as sufficiently general, so that its physical consequences can be used for theoretical modelling of systems under conditions when a complete and rigorous analysis is of prohibitive complexity.

The main physical conclusions of the above analysis are the following:

(1) The magnitude of average contact forces in both isotropic and anisotropic systems is determined mainly by the hydrostatic part of the stress tensor and average coordination number of the assembly.

(2) Directional variation of average forces in isotropic systems is controlled by the deviatoric part of the stress tensor, or, more specifically, by the parameter of deviatoric loads $a_\sigma = \sigma_t/\sigma_n$. The preferred direction of force for isotropic systems coincides with the major principal direction of the stress tensor.

(3) Directional variation of average forces in anisotropic systems is strongly influenced by anisotropy in contact orientations. Average forces in anisotropic systems under hydrostatic stress

are direction-dependent due to varying availability of contacts of different orientations in the system.

Deviatoric loads change the pattern of average forces which exist under hydrostatic stress. The influence of deviatoric loads on average forces is controlled by the coefficient of deviatoric load R which defines the level of deviatoric loads in relation to anisotropy in contact orientations ($a_\sigma = R\,\frac{1}{2}\,a$)

The above analysis shows that for each direction of load application with respect to the direction of anisotropy there is a corresponding level of deviatoric load for which directional variation of average forces is minimal. If the direction of load application coincides with the direction of anisotropy, the deviatoric load with $a_\sigma = \frac{1}{2}\,a$ ($R=1$) corresponds to the state with no directional variation of forces and minimum of potential energy compared to states under deviatoric loads.

(4) If relative levels of potential energy under different loads are intuitively related to the stability of the system under the given load, the conclusion follows that for anisotropic systems a state under deviatoric stress $a_\sigma = \frac{1}{2}\,a$ is more stable than a state under hydrostatic loads, as is the case of isotropic materials.

(5) In the case of the linear contact model, when parameters defining average forces are related to invariants of the strain tensor directly, it has been shown that the symmetry of the stress tensor requires gross rotational motion of particles.

CHAPTER V

PHENOMENOLOGICAL DISPLACEMENT GRADIENT TENSOR

5.1 Introduction

The preceding chapters considered external mechanical control over granular assemblies by means of forces on boundary particles. The introduction of the phenomenological stress tensor was related to the idea of simulating boundary forces which result in a uniform state of stress if applied to a continuum. Deformational response in such conditions can be expected in terms of a quantity similar to the strain tensor of continuum mechanics. An *a priori* introduction of the phenomenological displacement gradient tensor is not absolutely necessary and this quantity appears automatically as a conjugate tensor in the expression of complementary work of internal deformations w_f which will be obtained in the next chapter for linear systems in the form

$$w_f = \frac{1}{2} \sigma_{ij} \lambda_{ij} \tag{5.1}$$

where λ_{ij} is a certain tensor which appears formally after minimization of complementary work expressed in terms of contact forces. The form (5.1) suggests that λ_{ij} has the meaning of a strain tensor, although a more direct interpretation is desirable. Moreover, complementary work is minimized in the next chapter under a very strong, and far from obvious, assumption related to statistical features of contact forces.

A priori introduction of a continuum mechanics analogue of the strain tensor presented in this chapter clarifies the meaning of the mentioned assumptions used in the statistical analysis that follows.

Only plane assemblies of discs are considered here and the pheno-

menological displacement gradient tensor for three-dimensional systems will be introduced formally on the basis of (5.1).

5.2 Displacement of Boundary Particles and the Principle of Virtual Work

The technique for introducing the phenomenological displacement gradient tensor is formally similar to that employed in Chapter III for the phenomenological stress tensor. In physical terms there are, however, substantial differences. The quantity to be introduced here describes the kinematics of deformations and it must be ensured that the described process is possible for the considered media. To avoid difficult questions relative to the creation and destruction of contacts in cohesionless assemblies, material discs treated below are assumed bonded at contacts.

A uniform displacement field within a continuum can be described in terms of a displacement vector $\underset{\sim}{l}(r)$ of the form

$$l_i = \varepsilon_{ij} r_j \tag{5.2}$$

where ε_{ij} is a certain second rank tensor.

A uniform displacement field within a granular assembly can be simulated by imposing displacements of boundary contact points

$$l_i^\beta = \varepsilon_{ij}^\beta r_j^\beta \tag{5.3}$$

where ε_{ij}^β is a tensor which gives displacements $\underset{\sim}{l}^\beta$ of external contact points $\underset{\sim}{r}^\beta$ and can be called the "boundary displacement tensor".

Suppose that a granular assembly is subject to external forces specified in terms of the tensor σ_{ij}^β. Consider work δW_e of boundary forces (3.3) on infinitesimal variation in displacements of external contacts

$$\delta l_i^\beta = \delta\varepsilon_{ij}^\beta r_j^\beta$$

This work is of the form:

$$\delta W_e = \sum_{\beta \in B} f_i^\beta \delta l_i^\beta = \sum_{\beta \in B} f_i^\beta \epsilon_{ij}^\beta r_j^\beta = \epsilon_{ij} \sum f_i^\beta r_j^\beta$$

Making use of identity (3.5) for forces specified in terms of tensor σ_{ij}^β the above relationship can be given in the form

$$\delta W_e = V \sigma_{ij}^\beta \delta \epsilon_{ij}^\beta \tag{5.4}$$

This demonstrates consistency in definition of tensors σ_{ij}^β, ϵ_{ij}^β as being conjugate variables. According to the principle of virtual work (Appendix A), the work of external forces (considered further per unit volume, i.e. $\delta w_e = \delta W_e / V$) is related to work δw_f of contact forces on virtual displacements δl^c of contact points, i.e.

$$\delta w_f = \frac{1}{V} \sum_{c \in V} (f^c \cdot \delta l^c) = \sigma_{ij}^\beta \delta \epsilon_{ij}^\beta \tag{5.5}$$

If δl_i^c are contact displacements of contact points related to contact forces through normal and tangential stiffnesses k_n, k_t, according to (4.23),

$$w_f = \frac{d_o}{V} \sum_{c \in V} \left[\frac{(f_n^c)^2}{2k_n} + \frac{(f_t^c)^2}{2k_t} \right] \tag{5.6}$$

and

$$\delta w_f = \sigma_{ij}^\beta \delta \epsilon_{ij}^\beta \tag{5.7}$$

where w_f is complementary work of internal deformations which coincide with the system's potential energy in the considered linear case.

5.3 Relationship between the Boundary Displacement Tensor and Displacements of Boundary Particles

Relationship (5.2) gives boundary displacements in terms of ϵ_{ij}^β.

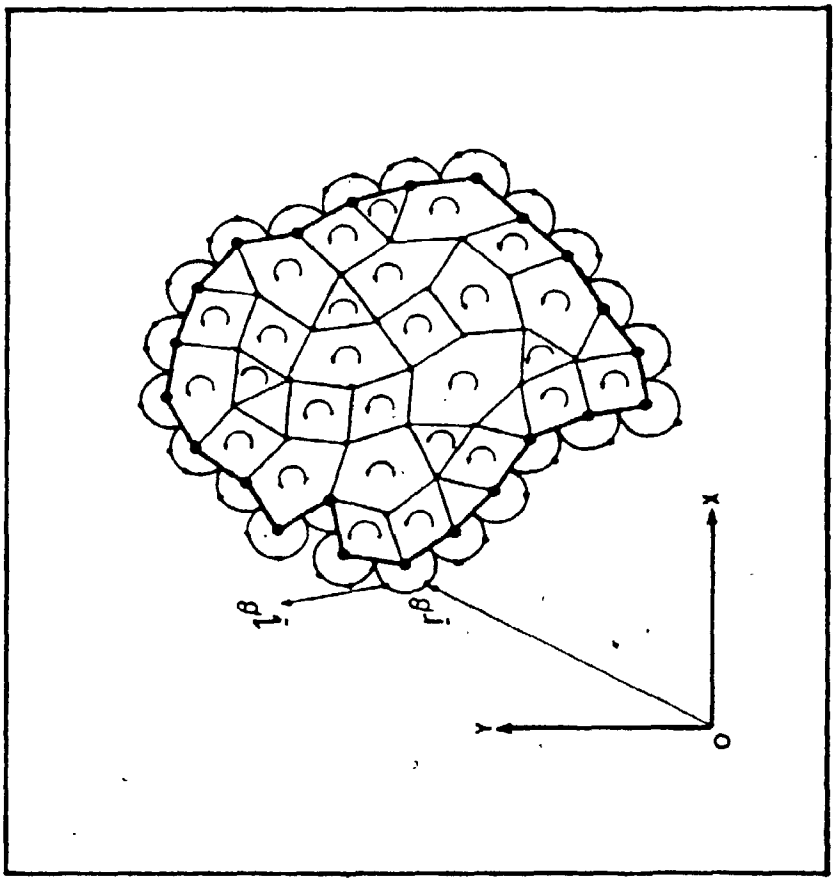

FIGURE 5.1

ORIENTED NETWORK OF SEGMENTS

For further analysis it is necessary to obtain an expression for ε_{ij}^{β} in terms of boundary displacements. To avoid undue complications, a large assembly of discs will be considered and displacements of external contacts of boundary particles will be regarded as coincident with displacements of boundary particle centers. It can be shown using a method similar to that employed in section 3.2 that the resulting error is negligible for large assemblies.

Consider an assembly of discs (Fig. 5.1) where only segments connecting boundary particles are shown. A "continuous" boundary B of the assembly consists of segments connecting the centers of boundary particles. Let all polygons within the assembly be given counter-clockwise orientations, so that the boundary B is an oriented contour. Let $\underset{\sim}{l}(r)$ be a continuously differentiable function defined on the boundary B and in the region surrounded by it. Let $d\underset{\sim}{l}/dt$ be the derivative of $\underset{\sim}{l}$ in the direction tangential to the boundary. It can be shown, using integration by parts and application of the two-dimensional form of the Green-Gauss theorem, that

$$\int_B \frac{dl_i}{dt}\,\hat{r}_j\,dB = \int_V \frac{\partial l_i}{\partial r_j}\,dV \qquad (5.7)$$

where $\underset{\sim}{r} = \{x_1, x_2\}$ and $\underset{\sim}{\hat{r}} = \{-x_2, x_1\}$ is the vector perpendicular to $\underset{\sim}{r}$. Integration in the left-hand side of (5.7) is over the area V surrounded by the boundary B. Let $\underset{\sim}{l}$ be selected according to (5.2). Since $\underset{\sim}{l}$ is linear with respect to x_1, x_2, the derivative in the tangential direction on each segment of the boundary is constant for the segment between particles β and $\beta + 1$ and is of the form

$$\frac{dl_i}{dt} = \frac{l_i^{\beta+1} - l_i^{\beta}}{d_o},$$

since the length of each segment on the boundary is d_o. According to the interpretation of l^{β} as displacemnt of particle β, the numerator above is the relative displacement Δl_i^{β} between particles β and $\beta + 1$ viewed from particle β. Substitution of (4.1) into the left-hand side of (4.3) and further integration gives

$$\sum_{\beta \in B} \Delta l_i^{\beta} \hat{r}_j^{\beta} = V \epsilon_{ij}^{\beta} \qquad (5,8)$$

where

$$\hat{r}_i^{\beta} = \frac{1}{d_o} \int_{\beta}^{\beta+1} \hat{r}_j dB$$

is a point on the part of the contour of integration between β and $\beta + 1$. Relationship (4.5) relates tensor ϵ_{ij} specifying displacements of boundary particles to their relative displacements. Note that (5.8) is similar to the expression for the phenomenological stress tensor (3.5).

5.4 Volume-Additive Identities for a Geometrically Compatible Assembly of Discs

Consider once more an assembly of discs represented by segments connecting particle centers. Let there be a total of K numbered and oriented polygons and $l^{k,m}$ be referred to the m-th side of the k-th polygon. During a deformation process, $l^{k,m}$ varies, but compatibility requires that

$$\sum_{m=1}^{m_k} l_i^{k,m} = 0 \qquad (i = 1,2)$$

where m_k is the number of sides forming the polygon k. The above equality is correct in initial (i) and final (f) configurations, and if $l_f = l_i + \Delta l$, the following set of compatibility conditions can be written:

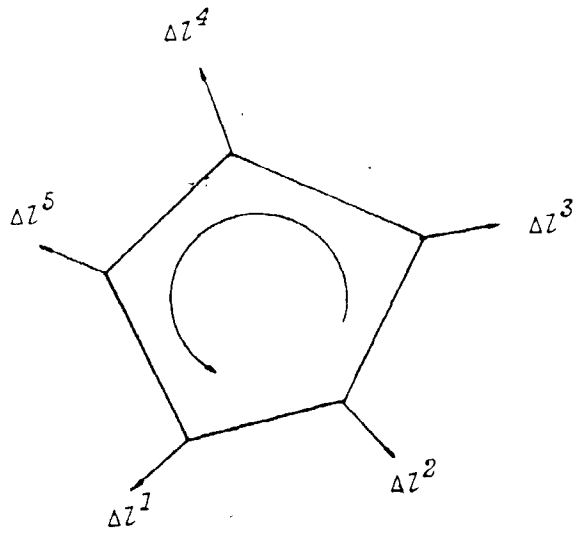

FIGURE 5.2

COMPATIBILITY CONDITION FOR A POLYGON

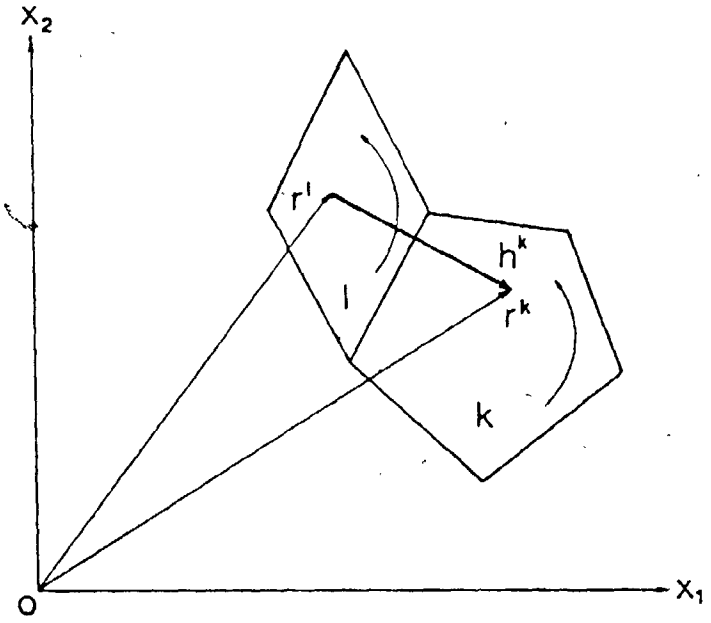

FIGURE 5.3

COMPATIBILITY CONDITION FOR A POLYGON

$$\sum_{m=1}^{m_k} \Delta l_i^{k,m} = 0 \quad (i = 1,2 \; ; \; k = 1,\ldots,K) \tag{5.9}$$

Note that vectors $\Delta \underset{\sim}{l}^{k,m}$ correspond to vectors of relative displacement between disc's centers. It is also of interest to note that equations (5.9) are of the same type as equations of static equilibrium, but written for polygons as if a force were applied on the sides of a polygon (Fig. 5.2). This analogy suggests a type of transformations to be performed on (5.9) which lead to volume-additive identities of section 3.3.

To perform these transformations, select an arbitrary point r_j^k within each of the K polygons and multiply (5.9) by r_j^k. Further summation with respect to all polygons gives four identities of the form

$$\sum_{k=1}^{K} \sum_{m=1}^{m_k} \Delta l_i^{k,m} r_j^k = 0 \qquad (i,j = 1,2) \tag{5.10}$$

Each internal segment of the assembly contributes two terms with relative displacements of opposite sign. Consider a pair of terms in (5.10) corresponding to two ajacent polygons k and l ($\Delta \underset{\sim}{l}^{kl} = -\Delta \underset{\sim}{l}^{lk}$) and transform them as follows:

$$\Delta l_i^{kl} r_j^k + \Delta l_i^{lk} r_j^l = \frac{1}{2} \left[\Delta l_i^{kl} (r_j^l - r_j^k) + \Delta l_i^{lk} (r_j^k - r_j^l)\right] \tag{5.11}$$

Let $\underset{\sim}{h}^k$, $\underset{\sim}{h}^l$ ($\underset{\sim}{h}^k = -\underset{\sim}{h}^l$) be vectors which connect two points between adjacent polygons in such a way that h^k points in the direction tangential to the contact (Fig. 5.3). Relationship (5.11) can be rewritten in the form

$$\Delta l_i^{kl} r_j^k + l_i^{lk} r_j^l = -\frac{1}{2} \left[\Delta l_i^{kl} h_j^k + \Delta l_i^{kl} h_j^l\right] \tag{5.12}$$

Separating terms in (5.10) corresponding to internal and boundary segments and making use of (5.12), (5.10) can be written in the form

$$\sum_{\beta \in B} \Delta l_i^{\beta} r_j^{\beta} = \frac{1}{2} \sum_{c \in V} \Delta l_i^c h_j^c \tag{5.13}$$

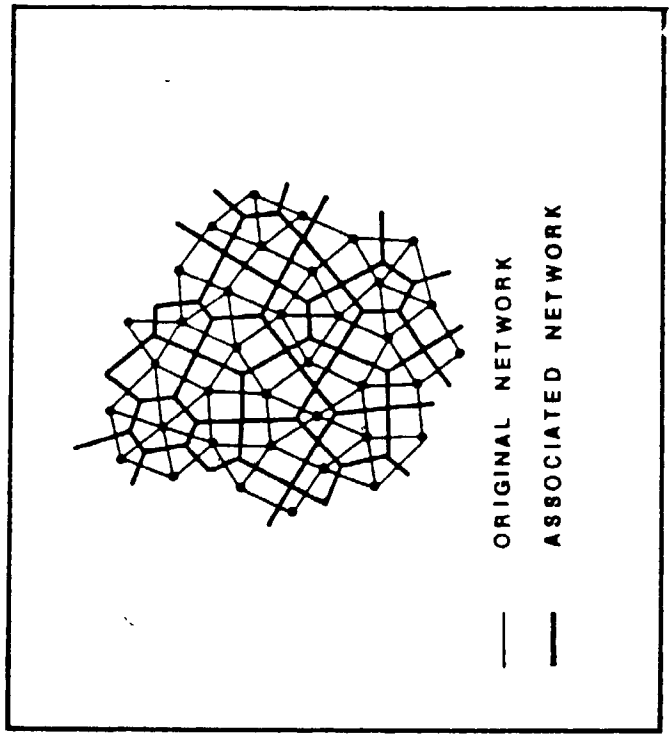

FIGURE 5.4

ASSOCIATED NETWORK OF SEGMENTS

The sum in the left-hand side of (5.13) contains two numerically identical terms corresponding to two adjacent sides of polygons. The above volume-additive identities are valid for any specification of points r_j^k within the polygons.

5.5 Associated Network of Segments

To make full use of relationships (5.13) vectors h^c must be specified by convenient selection of points r^k within each polygon. Such a selection will be made by considering a network of segments perpendicular to the sides of considered polygons (Fig. 5.4). Consider the construction of such a network. Let there be K original polygons with N vertices (N is the number of particles) and M sides (M here is the number of physical contacts). The above quantities are related by Euler's identity for polygons $K = M-N+1$ (proven independently in section 9.4). For large assemblies it can be used in the form $K = M-N$. In order to construct a network of segments orthogonal to original segments, it is necessary to select $2K$ coordinates of vectors r^k related to each polygon and to choose them in such a way that M orthogonality conditions are satisfied. This can generally be done if $2K<M$. Using Euler's identity, the last condition can be written in the form $M>2N$. Introducing the average coordination number $\gamma = 2M/N$, the condition for the existence of an orthogonal network of segments can be written in the form $\gamma \geq 4$. This condition does not assure that the position of initial points of the orthogonal segments will always be within the polygons, and actually nothing in the derivation of the volume-additive relationship required the presence of r^k within each polygon. With such construction of the orthogonal network, each vector h^c is in the

tangential direction defined at each contact. If h^c is the length of the corresponding vector, volume-additive identities can be written in the form

$$\sum_{\beta \in B} \Delta l_i^\beta r_j^\beta = \frac{1}{2} \sum_{c \in V} h^c \Delta l_i^c t_j^c$$

where

$$\underset{\sim}{r} = \{x_1, x_2\}$$

$$\underset{\sim}{t} = \{\sin\theta^c, -\cos\theta^c\}$$

It is convenient to rewrite the above relationships in terms of contact normal vectors. This can be achieved by a formal substitution in the above relationships of vectors orthogonal to r^β and t^c . respectively. Finally

$$\sum_{\beta \in B} \Delta l_i^\beta \hat{r}^\beta = \frac{1}{2} \sum_{c \in V} h^c \Delta l_i^c n_j^c \qquad (5.14)$$

where

$$\underset{\sim}{\hat{r}}^\beta = \{-x_2, x_1\}$$

$$\underset{\sim}{n}^c = \{\cos\theta^c, \sin\theta^c\}$$

Identities (5.14) are applicable to plane assemblies of discs with coordination number $\gamma > 4$. Only for such assemblies an orthogonal network of segments can exist. It will be shown later that assemblies with $\gamma < 4$ are unstable.

5.6 Phenomenological Displacement Gradient Tensor

Consider geometrically compatible deformations prescribed according to (5.3). Taking into account that boundary relative displacements are related to ε_{ij}^β according to (5.8) and specifying r_j^c to be as in (5.8), (5.14) can be given in the form

$$\varepsilon_{ij}^\beta = \frac{1}{V} \sum_{c \in V} \frac{h^c}{2} l_i^c n_j^c \quad . \qquad (5.15)$$

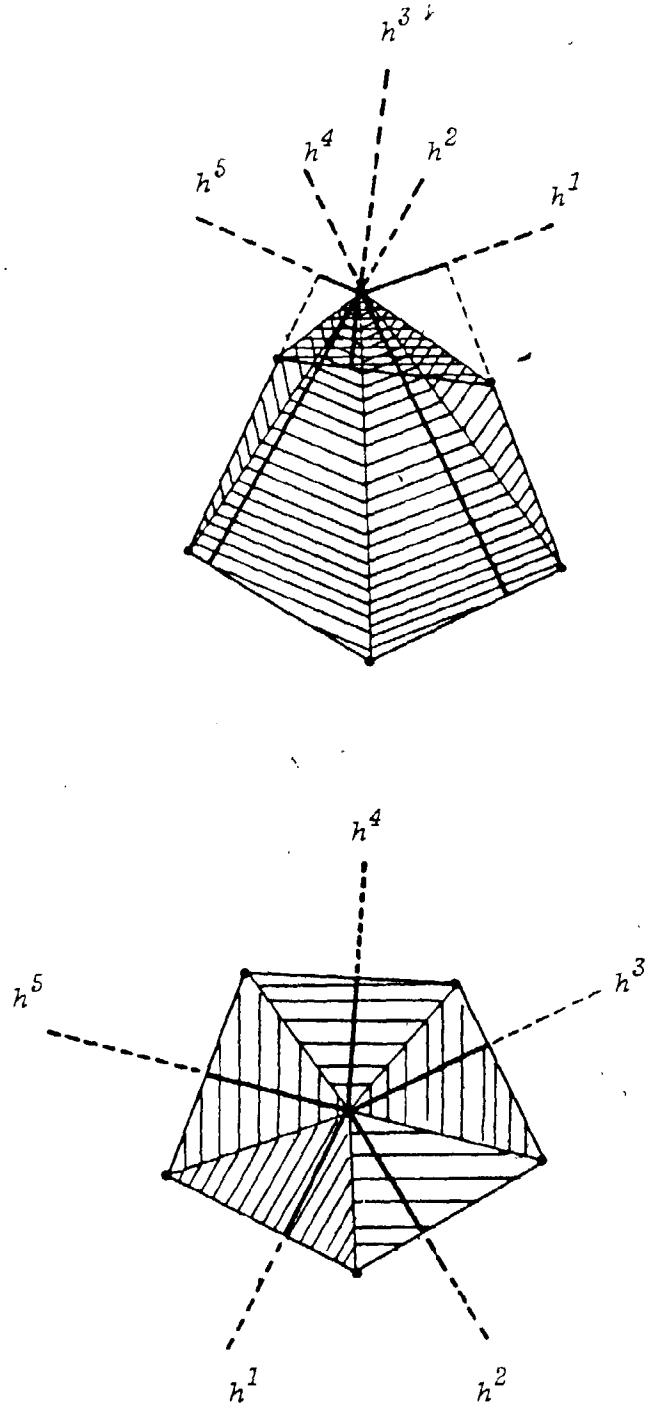

FIGURE 5.5

BALANCE OF AREA FOR A POLYGON

The above expression is identical to (3.12) for the boundary tensor σ^{β}_{ij}, but it contains vectors of relative displacements between particles forming contacts instead of forces and the length of segments of the associated network instead of the length of segments connecting particle centers. In the present case, segments h^c are of different length which corresponds to the expression for the boundary stress tensor for an assembly of unequal diameter discs.

Relationships (5.15) are valid as long as compatibility conditions (5.9) are satisfied during the deformation process. In this case (5.15) are valid for any orthogonal network of segments h^c. Such insensitivity of (5.15) to a specific selection of an associated network is related to the geometrical fact that for any polygon k with sides m_k

$$\frac{1}{2} d_o \sum_{c=1}^{m_k} h^c = V_k \qquad (5.16)$$

where V_k is the area of the polygon.

Fig. 5.5[a] illustrates this identity based on area balance for the polygon. Note that the identity holds for any point O selected outside of the polygon if distances h^c are understood in the analytico-geometrical sense as the distance between a point and oriented line. Fig. 5.5[b] illustrates this case with h^3 taken as negative. It is precisely in this sense that h^c must be understood when the transition from (5.11) to (5.13) is performed. Those comments illustrate the independence of (5.15) from a specific orthogonal network used in the derivation of (4.11). The fact of its existence is imperative.

If (5.15) are added for all polygons of the original network, the following relationships for the sum of all segment lengths in the

associated network are obtained

$$\frac{1}{2} d_o \sum_{c \in V} h^c = V$$

where V is now the total sum area of the assembly. Since the total number of segments is M, the average length of segments for any associated network

$$\bar{h}^c = \frac{2V}{d_o M} = \frac{\pi d_o}{\rho \gamma} \tag{5.17}$$

If the volume of the assembly is expressed on the basis of (5.17) and relative displacements per unit distance between disc centers $\underline{\delta}^c = \Delta \underline{l}^c / d_o$ are introduced, (5.15) can be given in the form

$$\varepsilon^{\beta}_{ij} = \frac{2}{M} \sum_{c \in V} \eta^c \delta^c_i n^c_j \tag{5.18}$$

where

$$\eta_c = \frac{h^c}{\bar{h}^c}$$

represents segments of the associated network scaled to give the average length 1. Note that M above is twice the number of physical contacts and equal to the number of terms in the above sum.

Relationships (5.18) were developed for a specific type of boundary particle displacement and they relate boundary tensor ε^{β}_{ij} with relative displacements between all particles of the assembly. Consider now an arbitrary region of the assembly of the area V. The following function of the selected area is introduced by definition:

$$\hat{\varepsilon}_{ij}(V) = \frac{2}{M} \sum_{c \in V} \eta^c \delta^c_i n^c_j \tag{5.19}$$

where the summation is with respect to all contacts in the considered volume. The difference between (5.18) and (5.19) is that $\hat{\varepsilon}_{ij}(V)$ is defined

for any arbitrary area of the assembly and is called the "phenomenological displacement gradient". As a function of volume, $\hat{\varepsilon}_{ij}$ will fluctuate from volume to volume, but the fluctuations will be small for large volumes due to the volume-additive form of (5.19).

The phenomenological displacement gradient is introduced here in a similar way as the phenomenological stress tensor in section 3.4. Definition (5.19) does not imply that the given system is subject to uniform boundary displacement.

Homogeneous deformations can be studied by considering an infinite assembly and obtaining a limit of (5.19) for $V \to \infty$, thus developing a unique deformational characteristic of a homogeneous system. The set of assumptions under which this limit exists has been described in section 3.8. In the present section emphasis is on specifics pertinent to the analysis of deformations.

To perform transition to an infinite assembly, contacts must be classified into G orientation groups, so that within each group orientations of contacts are within θ_g and $\theta_g + \Delta\theta$. Selecting $\Delta\theta$ small enough, orientations of contact normals within each orientation group can be considered as identical and terms in (5.18) can be reorganized to obtain

$$\varepsilon_{ij} = 2 \frac{1}{M} \sum_{g=1}^{G} \left(\frac{1}{M_g} \sum n^c \delta_i^c \right) \Delta M_g \tag{5.20}$$

where $M_g = \Delta M_g = M\, S(\theta_g)\Delta\theta$. Introducing the following group average,

$$\overline{n\delta}_i(\theta_g) = \frac{1}{M_{c\in\theta_g}} \sum n^c \delta_i^c, \tag{5.21}$$

(5.20) can be given in the form

$$\hat{\varepsilon}_{ij} = 2 \sum_{g=1}^{G} \overline{n\delta}_i(\theta_g) n_j S(\theta)\Delta\theta \tag{5.22}$$

Assuming that the limit of (5.20) for $V \to \infty$, $\Delta\theta \to 0$ exists, (5.22) can be given in integral form

$$\varepsilon_{ij} = 2 \int_0^{2\pi} \overline{\eta\delta_i}(\theta) n_j(\theta) S(\theta) d\theta \qquad (5.23)$$

The above expression can be rewritten in terms of normal and tangential components of relative displacements as follows:

$$\varepsilon_{ij} = 2 \int_0^{2\pi} [\overline{\eta\delta}_n(\theta) n_i n_j + \overline{\eta\delta}_t(\theta) t_i n_j] S(\theta) d\theta \qquad (5.24)$$

Several comments should be made regarding factors η^c and their averages. According to their definition, η^c are proportional to the length of segments of the associated network and have an average *1* over all segments of the network. For different orientation groups, $\overline{\eta}(\theta)$ is, generally, direction-dependent and

$$\int_0^{2\pi} \eta(\theta) S(\theta) d\theta = 1$$

For an isotropic assembly $\overline{\eta}=1$, i.e. it is direction-independent.

Expressions (5.23) contain certain average of the product $\overline{\eta\delta_i}$ and there is no reason to assume that η and δ_i are statistically independent for the same group of contacts. A statistical bias between the length of segments in an associated network and relative displacements between particles corresponding to these segments occurs due to the following reason. Observation of an associated network in Fig. 5.4 indicates that h^c are smaller in the vicinity of dense regions and longer in regions with lower density, i.e. h^c reflect local structure near a contact. Contact deformations are controlled not only by contact stiffnesses, but also to a large extent by geometrical structure of a local environment of a contact which is reflected in h^c (or η^c). Ultimately, macro-stiffness of an assembly depends on both contact stiffness and its "geometrical stiffness".

It was mentioned previously that the expression for ε^{β}_{ij} is formally identical to the expression for tensor σ^{β}_{ij} for an assembly of varying size particles, and h^c in this analogy correspond to interparticle distances, while relative displacements correspond to contact forces. In this case the expression for the stress tensor is of the form

$$\sigma_{ij} = \frac{1}{2}\gamma\eta_v \int_0^{2\pi} \overline{df}_i(\theta) n_j(\theta) S(\theta) d\theta$$

The reason for a bias in contact forces and particle diameters is that contact stiffness is a function of diameter. This effect is not considered here for simplicity and the problem was avoided by considering linear contacts with constant stiffnesses. For a more realistic contact model, redistribution of forces is affected by varying contact stiffnesses. A "varying geometrical stiffness" cannot be excluded, since it is an inherent property of irregular systems and the problem of a bias between local contact environment and contact deformations is unavoidable. In subsequent analysis $\overline{\eta\delta}_i(\theta) \neq \overline{\eta}(\theta)\overline{\delta}_i(\theta)$ and (5.23) cannot be simplified further without the risk of physical contradictions.

To check relationships (5.23) consider a "quasi-isotropic" regular array of particles shown in Fig. 5.6 .Although $\gamma = 4$ in the considered example, an associated network for this assembly exists and has the same form as the original network. Contact orientation distribution for this array is of the form

$$S(\theta) = \frac{1}{4}\sum_{c=1}^{4} \delta(\theta-\theta_c) \qquad (5.25)$$

where $\theta_1 = \frac{\pi}{4};\ \theta_2 = \frac{3\pi}{4};\ \theta_3 = \frac{5\pi}{4};\ \theta_4 = \frac{7\pi}{4}$

Let particles be rigid and only tangential components of relative

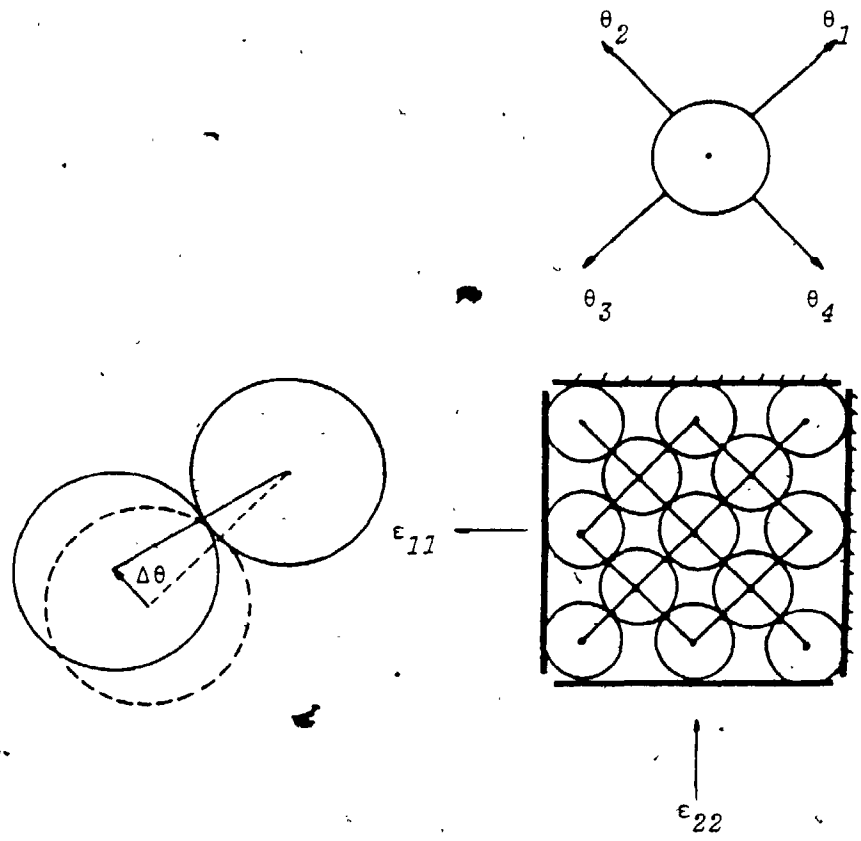

FIGURE 5.6

QUASI-ISOTROPIC REGULAR ARRAY

displacements exist. In this case

$$\delta_t(\tfrac{\pi}{4}) = \delta(\tfrac{5\pi}{4}) = \Delta\theta$$
$$\delta_t(\tfrac{5\pi}{4}) = \delta(\tfrac{7\pi}{4}) = -\Delta\theta \qquad (5.26)$$

where $\Delta\theta$ is shown in Fig. 5.6 for contact $\theta^c = \frac{3\pi}{4}$.

Since $\overline{\eta\delta}_t(\theta) = \delta_t(\theta)$ in the present case, substitution of (5.25) into (5.24) gives

$$\varepsilon_{11} = \Delta\theta \qquad \varepsilon_{12} = 0$$
$$\varepsilon_{21} = 0 \qquad \varepsilon_{22} = -\Delta\theta,$$

as expected.

In the considered case all relative displacements on contacts of the same orientation are identical, as well as factors $\eta^c = 1$, so that formally $\overline{\eta\delta}(\theta) = \overline{\eta}\ \overline{\delta}(\theta)$. Analysis in the next chapter will show that if the same be assumed for an assembly with irregular structure, contact forces and relative displacements on contacts of the same orientation will be identical, as for a regular array. This is an obvious contradiction.

5.7 Relative Displacements Between Macro-Separated Points

The phenomenological displacement gradient was introduced by definition and it is necessary to study its properties. For an infinite assembly its limit (5.19) is a unique deformational characteristic of the system and it is necessary to establish as to what extent ε_{ij} can be interpreted as a displacement gradient.

It will be demonstrated using geometrical methods that $\Delta_i = \varepsilon_{ij}\hat{N}_j$ is the vector of relative displacements per unit length of an infinite line with unit vector $\hat{N}$ parallel to it.

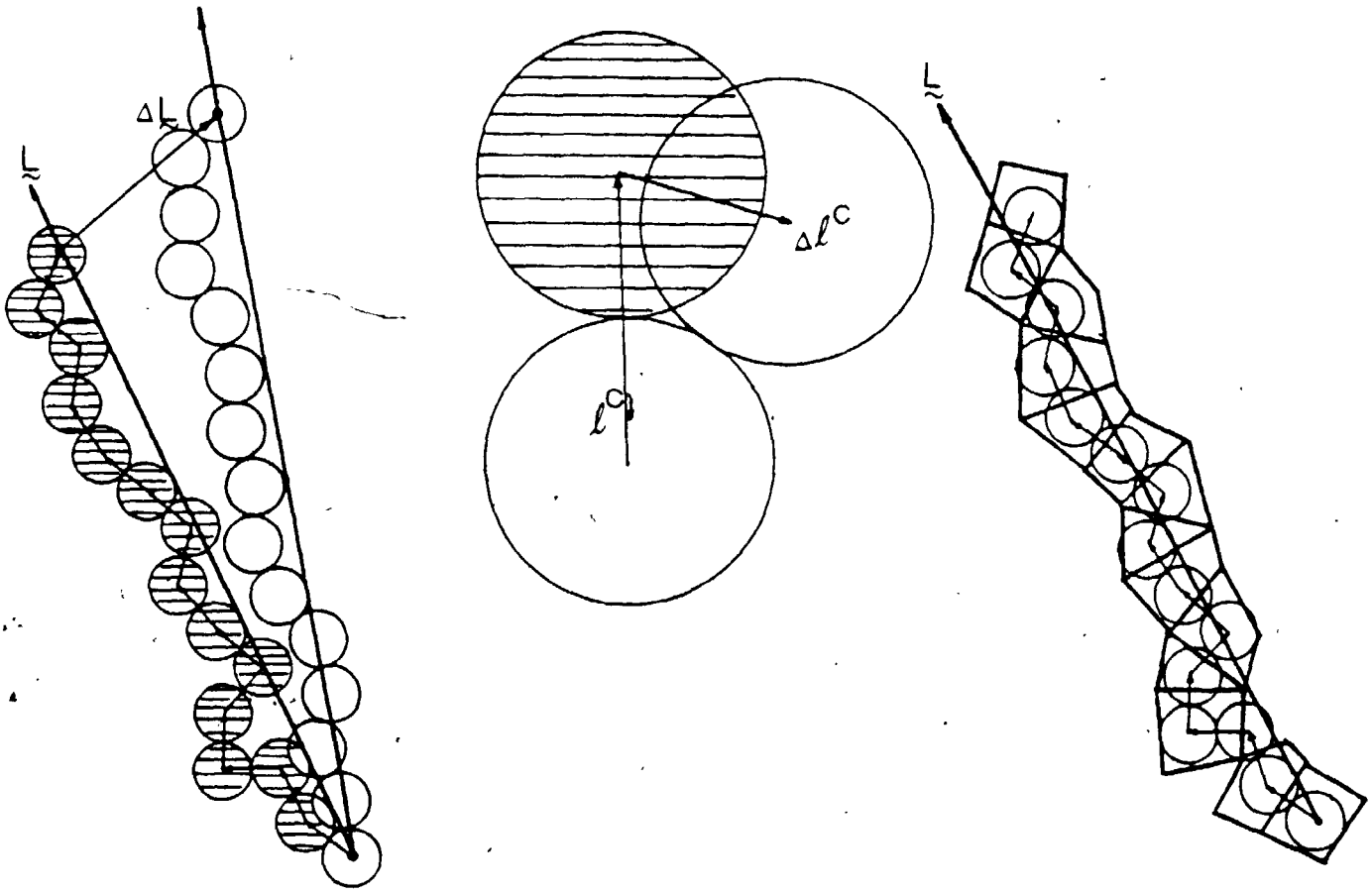

FIGURE 5.7

DEFORMATIONS OF A CHAIN OF PARTICLES

To present the idea of this analysis, consider a chain of particles shown in Fig. 5.7[a]. Recall that this geometrical element has already been employed in section 3.10 when gross loads acting on chains of particles were calculated as $F_i = \sigma_{ij} N_j$, where N_j is the normal vector of the chain. Consider initially a finite chain C. During the deformation process, vectors connecting particle centers $\underset{\sim}{l}^c_i$ are such that

$$\underset{\sim}{L} = \sum_{c \in C} \underset{\sim}{l}^c$$

After deformation all vectors $\underset{\sim}{l}^c$ are incremented by $\Delta \underset{\sim}{l}^c$ and

$$\Delta \underset{\sim}{L} = \sum_{c \in C} \Delta \underset{\sim}{l}^c \qquad (5.27)$$

where $\Delta \underset{\sim}{l}^c$ is the vector of relative displacements between neighbouring particles of the chain (Fig. 5.7[b]). Let $dN_c(\theta|\hat{N})$ be the number of segments with orientations between Θ and $\theta + \Delta\theta$ in the chain with unit vector parallel to it. The vector of relative displacements (5.27) between points of the chain can be given in the form

$$\Delta \underset{\sim}{L} = \int_{\theta_-}^{\theta_+} \Delta \underset{\sim}{l}^c dN(\theta|N) \qquad (5.28)$$

where θ_- and θ_+ denote limits of segment orientations in the chain. Note that for a finite chain $dN_c(\theta|\hat{N})$ cannot be continuous. It may be expected that (5.28) can be also represented in the form $|L| \cdot \varepsilon_{ij} \hat{N}_j$ where $|L|$ is the length of the chain. Practical use of (5.28) requires an explicit form of $dN_c(\theta|\hat{N})$ which is not available. Segments of an associated network help to avoid this uncertainty. Fig. 5.7[c] features polygons formed by segments of an associated network. According to the way the associated network is constructed, each polygon of it contains a center of one and only one particle.

If polygons of the associated network are intersected by a transect line, particle centers which are within intersected polygons form the considered chain of particles. The analysis of chains of particles is equivalent to the transect analysis of segments of an associated network.

Elements of transect analysis have already been presented in section 3.9 for segments of equal length. Segments of the associated network do not fall into this category and can be characterized by a certain length distribution density $H_\theta(h)$ which gives the number of segments associated with contacts of orientations $\theta+\theta+d\theta$ and with length between h and $h+dh$. Since there are a total of $M\,S(\theta)\,d\theta$ segments with orientation θ, the number of associated segments with length near h can be given in the form

$$dM(\theta,h) = M H_\theta(h) S(\theta) d\theta dh$$

This group of associated segments has the same length and orientations and the number of them dM_L intersected by the transect line is proportional to their density, length of the transect line, and projection on the direction perpendicular to the transect line (Fig. 5.8), i.e.

$$dM_L = |L|\frac{M}{V} h H_\theta(h) |\cos(\theta-\theta_N)| S(\theta) d\theta \qquad (5.29)$$

Let $\Delta l(\theta,h)$ be the average relative displacement between particles corresponding to contacts with orientation θ and associated with segment of the length h.

The total contribution of these segments to gross relative displacement is $\Delta l(\theta,h) dM_L$ where dM_L is given by (5.29). A total relative displacement results from all segments of the chain and can be obtained by integration with respect to all possible h and θ, i.e.

$$\Delta L_i = \frac{M}{V}|L| \int_{\theta_{\hat{N}}-\frac{\pi}{2}}^{\theta_{\hat{N}}+\frac{\pi}{2}} \left[\int_0^{\infty} h\, l_i(\theta,h) H_\theta(h)\, dh \right] \cos(\theta-\theta_{\hat{N}}) S(\theta)\, d\theta$$

Note that θ above is the orientation distribution of non-directed segments defined for any arbitrary interval π selected in the above integral as $\theta_{\hat{N}}-\frac{\pi}{2}$ + $\theta_{\hat{N}}+\frac{\pi}{2}$. Integration above can be formally extended over the range of θ 0+2π, since both $l_i(\theta,h)$ and $\cos(\theta-\theta_{\hat{N}})$ change sign simultaneously when θ is substituted for $\theta+\pi$. The term in brackets above is the average $\overline{hl}_i(\theta)$. Noting that $M = \frac{1}{2}\gamma N$, introducing relative displacements per unit distance between particle centers $\delta_i = l_i/d_o$ and also introducing factors η as in (5.24), the above relationship can be given in the form

$$\delta_i = \frac{L_i}{|L|} = 2 \int_0^{2\pi} \overline{\eta\delta}_i(\theta) \cos(\theta-\theta_{\hat{N}}) S(\theta)\, d\theta \qquad (5.30)$$

Strictly speaking, the above relationship is exact only for infinite lines within an infinite homogeneous assembly. Direct calculation of $\varepsilon_{ij}\hat{N}_j$ using (5.23) gives (5.30). This result indicates that the phenomenological displacement gradient can be interpreted as the displacement gradient introduced in continuum mechanics.

For a simple homogeneous assembly the above interpretation is valid only when the assembly is infinite. If an ensemble of macroscopically similar systems under identical non-homogeneous deformations is considered, an ensemble average of the phenomenological displacement gradient becomes a point characteristic of the ensemble, i.e. $\varepsilon_{ij}(r)$. Using methods similar to that in section 3.14, it is possible to show that $\varepsilon_{ij}(r)$ obtained as an ensemble average of the phenomenological displacement gradient satisfies compatibility conditions for the strain tensor of continuum mechanics. The proof is tedious and is not presented here. The final result, however,

should be expected, since the phenomenological displacement gradient was, in fact, introduced on the basis of compatibility conditions on a micro-level.

In further development of the theory, the phenomenological displacement gradient will be considered either for an infinite assembly or as an ensemble average. It was demonstrated that these averages have all properties of the continuum mechanics displacement gradient, so that there is no reason to distinguish the mentioned averages from the corresponding continuum mechanics parameters. The analysis in this chapter and in chapter III for the stress tensor resulted in physical interpretations of continuum mechanics parameters as ensemble averages of corresponding micro-mechanical quantities.

5.8 Invariants of the Displacement Gradient

Invariants of the displacement gradient (4.27) can be expressed in terms of average relative displacements similarly to the way invariants of the stress tensor were developed in section 4.3. The results of calculations are the following:

$$\varepsilon_n = 2\int_0^{2\pi} \overline{\eta\delta}_n(\theta)S(\theta)d\theta$$
$$\varepsilon_t = 2\int_0^{2\pi} \overline{\eta\delta}_n(\theta)\cos 2(\theta-\theta_\varepsilon)S(\theta)d\theta - 2\int_0^{2\pi} \overline{\eta\delta}_t(\theta)\sin 2(\theta-\theta_\varepsilon)S(\theta)d\theta \qquad (5.31)$$

5.9 Average Relative Displacements Between Particles Forming Contacts of the Same Orientation

Consider application of the developed concepts to isotropic systems of bonded particles.

For an isotropic system the lengths of segments of an associated network are direction-independent, so that $\overline{\eta}(\theta) = 1$, although still $\overline{\eta\delta_i}(\theta) \neq \overline{\delta}(\theta)$. Since η represents geometrical features of the system and is independent of imposed deformations, the average $\overline{\eta\delta_i}(\theta)$ must be proportional to $\overline{\delta}_i(\theta)$ and can be given in the form

$$\overline{\eta\delta_i}(\theta) = \frac{1}{\xi}\,\overline{\eta}\,\overline{\delta}_i(\theta) = \frac{1}{\xi}\,\overline{\delta}_i(\theta) \tag{5.32}$$

where ξ is a certain coefficient of proportionality which reflects structure of the system.

Invariants of the strain tensor (4.27) can be given for this case as follows:

$$\begin{aligned}
\varepsilon_n &= \frac{2}{\xi}\int_0^{2\pi}\overline{\delta}_n(\theta)S(\theta)\,d\theta \\
\varepsilon_t &= \frac{2}{\xi}\left\{\int_0^{2\pi}\overline{\delta}_n(\theta)\cos 2(\theta-\theta_\varepsilon)S(\theta)\,d\theta - \int_0^{2\pi}\overline{\delta}_t(\theta)\sin 2(\theta-\theta_\varepsilon)S(\theta)\,d\theta\right\}
\end{aligned} \tag{5.33}$$

where $S(\theta) = \frac{1}{2\pi}$.

In this form expressions for invariants of the strain tensor are similar to invariants (4.9) of the stress tensor. Consider the form of average relative displacements $\overline{\delta}_n(\theta)$ $\overline{\delta}_t(\theta)$. If these averages are decomposed into infinite Fourier series, their substitution into (5.33) will result in relationships between amplitudes of Fourier components and invariants of the strain tensor. The form of (5.33) shows that integration will not result in contributions of Fourier components of the order higher than the second, so that average relative displacements can be considered in the form

$$\begin{aligned}
\overline{\delta}_n(\theta) &= A_1 + A_2\cos 2(\theta-\theta_\varepsilon) + A_3\sin 2(\theta-\theta_\varepsilon) \\
\overline{\delta}_t(\theta) &= A_4 - A_5\cos 2(\theta-\theta_\varepsilon) - A_6\sin 2(\theta-\theta_\varepsilon)
\end{aligned}$$

Negative signs are introduced for convenience.

Substitution of the above relationships into (5.33) and integration gives

$$\frac{1}{2}\,\xi\,\varepsilon_n = A_1$$

$$\frac{1}{2}\,\xi\,\varepsilon_t = \frac{1}{2}\,(A_2 + A_6)$$

Integrals corresponding to coefficients A_3, A_4, A_5 vanish, which means that their corresponding terms contribute nothing to macro-deformations. For a system of bonded particles which act according to the principle of minimum potential energy, it is reasonable to expect that terms in $\overline{\delta}_n(\theta)$ $\overline{\delta}_t(\theta)$ which are not fixed by external constraints, but can result in extra potential energy, will not appear. Even in this case, coefficients A_2, A_6 cannot be determined uniquely.

It is convenient to select $A_6 = r'A_2$, where r' is undetermined. Using the above relationships, average relative displacements can be given in the form

$$\overline{\delta}_n(\theta) = \frac{1}{2}\,\xi\,\left[\varepsilon_n + \frac{2}{1+r'}\,\varepsilon_t cos2(\theta-\theta_\varepsilon)\right]$$

$$\overline{\delta}_t(\theta) = -\frac{1}{2}\,\xi\,\left[\frac{2r'}{1+r'}\,\varepsilon_t sin2(\theta-\theta_\varepsilon)\right] \qquad (5.34)$$

Consider, however, average contact forces related to the stress tensor according to (4.46) rewritten here (noting that $a_\sigma = \sigma_t/\sigma_n$) in the form

$$\overline{f}_n(\theta) = \frac{\pi d_o}{\rho\gamma}\left[\sigma_n + \frac{2}{1+r}\,\sigma_t cos2(\theta-\theta_o)\right]$$

$$\overline{f}_t(\theta) = -\frac{\pi d_o}{\rho\gamma}\,\left[\frac{2r}{1+r}\,\sigma_t sin2(\theta-\theta_o)\right] \qquad (5.35)$$

Since for the linear contact model $\overline{f}_n(\theta) = k_n\overline{\delta}_n(\theta)$ and $\overline{f}_t(\theta) = k_t\overline{\delta}_t(\theta)$, comparison of (5.34) and (5.35) gives $\theta_\varepsilon = \theta_\sigma$

$$\sigma_n = \frac{1}{2}\,k_n\xi\,\frac{\rho\gamma}{\pi d_o}\,\varepsilon_n$$

$$\sigma_t = \frac{1}{2} k_t \xi \frac{r'}{r} \frac{1+r}{1+r'} \varepsilon_t$$

$$\sigma_t = \frac{1}{2} k_n \xi \frac{1+r}{1+r'} \varepsilon_t$$

The first of the above equations reflects the proportionality of volumetric strain and hydrostatic stress. In the last two equations,

if $r = \frac{k_t}{k_n} r'$, then

$$\sigma_n = K \varepsilon_n$$

$$\sigma_t = G \varepsilon_t$$

where

$$K = \frac{1}{2} k_n \xi \frac{\rho\gamma}{\pi d_0} \qquad (5.36)$$

$$G = \frac{1}{2} k_n \xi \frac{1+\frac{k_t}{k_n} r'}{1+r'} \frac{\rho\gamma}{\pi d_0}$$

are bulk and shear moduli, respectively. These macro-parameters are still to be determined, as neither ξ nor r' are known. In the next chapter r' will be determined from the minimization of complementary work (which will give $r' = 1$), but coefficient ξ will remain unspecified. As established in the above analysis of this chapter, ξ reflects a bias between deformations of particles and local density of the assembly. In the case of an absolutely uniform assembly with no local fluctuations of density, $\xi = 1$. This, however, is not possible for irregular systems.

The analysis presented in the next chapter will formally show that fluctuations of contact forces are directly related to ξ. Geometrical analysis of the material in this chapter will demonstrate this fact. The theoretical derivation of is a problem of great complexity and will not be attempted here.

The definition of parameter ξ contained in (3.32) enables one to

establish that $\xi \leq 1$, since for any two random variables X, Y, always $\overline{X \cdot Y} \geq \overline{X} \cdot \overline{Y}$. According to (5.36) this means that the macro-stiffness of an assembly can be reduced only by recognizing the irregularity in its structure.

5.10 Existence of Constitutive Relationships for Assemblies of Bonded Particles

If external actions on a certain granular assembly are specified in terms of a boundary tensor ε^{β}_{ij}, relative displacements between all particles can be determined by solving equations of equilibrium and compatibility. For a plane system of N particles, there are $3N$ equations of static equilibrium and the number of equations of geometrical compatibility (5.9) is $2P$, where P is the number of polygons formed by segments connecting particle centers. Since $P = M-N$ (according to Euler's identity, section 5.5), there is a total of $3N + 2(M-N) = N + 2M$ equations of equilibrium and compatibility for $2M$ components of relative displacements and N angles of rotation, so that the number of unknowns is equal to the number of equations. For a linear contact model, these equations will be linear with coefficients which are sines and cosines of contact orientations and include normal and tangential stiffnesses. If the system of equations is solved for relative displacements, the latter will be linear functions of ε^{β}_{ij} components. Coefficients of this linear combination must be functions of orientations of all contacts in the assembly and ratio of normal to tangential stiffnesses. Contact forces can be expressed in terms of obtained relative displacements and rotations and gross loads can be claculated using relationships (3.11) for σ^{β}_{ij}, so that finally

$$\sigma^{\beta}_{ij} = \hat{A}_{ijkl}\varepsilon^{\beta}_{ij} \qquad (5.37)$$

where $\hat{A}_{ijkl}$ is a certain second rank tensor which depends on contact orien-

tations of all particles, the number of contacts, and contact stiffnesses. The relationships cannot be viewed as "constitutive", since $\hat{A}_{ijkl}$ is a characteristic of a specific system and depends on its precise structure.

If transition to an infinite assembly is performed, it can be expected that the influence of a precise pattern of contact orientations will disappear and the corresponding tensor $\hat{A}_{ijkl}$ for an infinite assembly will depend on the contact orientation distribution $S(\theta)$, average coordination number and contact stiffnesses. In the considered limit

$$\sigma_{ij} = A_{ijkl}\varepsilon_{kl} \tag{5.38}$$

and (5.38) is a characteristic of a class of systems with identical structural characteristics $S(\theta)$, γ, k_n, k_t. In this case (5.38) can be viewed as constitutive relationships for an infinite assembly.

A unique characteristic for finite systems can be obtained only as average over an ensemble of similar systems. Constitutive relationships, as understood in continuum mechanics, must be regarded in physical terms as avereage characteristics of a class of macroscopically similar systems.

5.11 Complementary Work in Terms of the Boundary Tensor

The established relationship between boundary tensors σ^{β}_{ij} and ε^{β}_{ij} enables one to obtain an expression for complementary work of internal deformations in terms of σ^{β}_{ij}. This can be done by inverting (5.37) and calculating variations of $\delta\varepsilon^{\beta}_{ij}$ entering (5.7) in terms of variations $\delta\sigma^{\beta}_{ij}$. If boundary loads increase from zero to a certain level σ^{β}_{ij}, integration of complementary work results in the following expression:

$$w_f = \frac{1}{2}\hat{A}^{-1}_{ijkl}\sigma^{\beta}_{ij}\sigma^{\beta}_{kl} \tag{5.39}$$

For an infintie system this expression gives complementary work

in terms of σ_{ij}. The above expression is of no practical use, since the tensor elasticity is unknown. It theoretical significance, however, is considerable. It indicates that sums of the squares of contact forces representing w_f are uniquely fixed according to (5.39). This fact will be employed later.

5.12 Discussion and Conclusions

The concept of the phenomenological displacement gradient arises from an attempt to simulate a uniform displacement field by prescribing displacements of boundary particles in such a way that there be a uniform displacement field in a continuum if the displacements are specified on its boundary. Further analysis of the equations of compatibility in contacts results in the conclusion that the boundary tensor ε_{ij}^{β} is related to volume-additive combinations of relative displacements between particle centers.

Considering that such combinations of a system's micro-parameters do not fluctuate significantly between similar large volumes, the phenomenological displacement gradient was introduced by definition as a function of volume related to all relative displacements between particles in the considered volume. Its properties were studied and it was concluded that the phenomenological displacement gradient for infinite assemblies is a unique characteristic of the deformational state of the system and has the usual properties of the displacement gradient in continuum mechanics. For brevity the term "strain tensor" was suggested.

In the present theory granular assemblies are mainly studied in conditions with specified external forces. It will be shown in chapter VI that the strain tensor appears directly from the minimization of complementary work as a conjugate tensor. The above analysis also shows that the introduced ε^{β}_{ij} is also a tensor conjugate to the boundary stress tensor σ^{β}_{ij}. This fact will be used for the interpretation of formal results when the strain tensor appears implicitly and its meaning must be recognized.

The above analysis facilitates this step and provides a much deeper understanding of the concept of the strain tensor than results from formal analysis based on minimization of complementary work. The present analysis of an assembly's compatibility is conducted for plane assemblies using geometrical representation of the assembly as a network of segments connecting particle centers. Equations of compatibility written for polygons representing the original assembly resulted in the necessity of considering an associated network with segments perpendicular to the original network. Lengths of these segments entered realtionship (5.15) between the boundary tensor and relative displacements between particles. Visual examination of an associated network in Fig. 5.4 indicated that the length of associated segments is related to local particle density in the vicinity of contacts.

This fact suggested the possibility of a statistical bias between deformations of contacts and local density, reflected in the length of associated segments. Further analysis of contact forces will show that coefficient ξ, which characterizes the mentioned correlation, also controls fluctuations of contact forces. In the above analysis, geomet-

rical representations of assemblies provided an interpretation for the coefficient ξ as a coefficient related to irregularity in the system's structure. This interpretation of ξ is invaluable, since it will appear in the analysis of contact forces as a parameter controlling the dispersion of contact forces, but with no direct physical meaning. This is the main contribution of this chapter to the development of this thesis.

CHAPTER VI

STATISTICS OF CONTACT FORCES

6.1 Introduction

The preceding analysis provided general means for a phenomenological description of granular assemblies, but the theory so far has not yet achieved its objective of developing constitutive relationships for considered systems and providing tools for studying fluctuations of phenomenological parameters. Both topics are intimately related: the statistical theory of contact forces to be developed in this chapter accomplishes the above objective.

The present statistical theory is conceptually based on an axiomatic approach to statistical description of dynamic systems adopted now almost universally [35] after W. Gibbs [13]. Static and dynamic situations are, however, inherently different and specific statistical methods outlined here are substantiated by resorting to concepts of the information theory. Both mentioned conceptual sources of the present theory are non-contradictive and classical statistical mechanics of dynamic systems will be presented from the point of view of the information theory [14]. It should be noted that any new application of the information theory outside of its traditional realm [4] requires considerable physical judgement in assessing its results. Well-tested concepts of classical statistical mechanics are of great value in this respect.

Before presenting the theory, it is preferable to demonstrate what statistical results are necessary and how they can be applied to develop constitutive relationships. The next section attempts to solve the problem

of deformations for systems of bonded particles directly and indicates a point where no further development is possible without adequate statistical analysis.

6.2 Complementary Work of Internal Deformations

All contact forces for a system of N particles can be determined if $6N$ equations of equilibrium are solved for $6N$ kinematic variables, components of the displacements of particle centers and their rotations. To set up a system of equations it is encessary to express contact forces in terms of kinematic variables of the system and substitute them into the equations of static equilibrium.

In the present theory, based mainly on analysis of contact forces, the problem of obtaining a complete solution should preferably be posed in terms of contact forces only. This methodology followed from the theorem on minimum complementary work of internal deformations (Appendix A). According to this energy principle (which follows directly from the equations of static equilibrium and considerations of kinematics of deformations), a set of contact forces corresponding to the state of static equilibrium can be obtained by minimizing complementary work of internal deformations on all possible sets of statically admissible contact forces corresponding to fixed external loads (Appendix A).

Practical application of the noted principle is hindered by the necessity of describing statically admissible forces, i.e. all possible solutions of equations of static equilibrium for the system of interest. Each such solution corresponds to a virtual state of the system wherein the geometrical compatibility of particles in contacts is violated. When complement-

ary work is a minimum, a statically admissible state is geometrically compatible, i.e. a true state of static equilibrium. For linear systems, direct application of this principle is not as simple as a direct solution of the problem without the principle. It is fortunate that considerable simplifications occur for the more complex mechanical systems.

To clarify this point, consider complementary work per unit volume which consists of contributions of the (4.23) type from all contacts of the system, i.e.

$$w_f = \frac{d_o}{V} \sum_{c \in V} \left[\frac{(f_n^c)^2}{2k_n} + \frac{(f_t^c)^2}{2k_t} \right] \tag{6.1}$$

Note that for linear systems the complementary work is precisely the potential energy.

Let a single infinite homogeneous system subject to homogeneous loads on infinity be considered. To present (6.1) in a form more convenient for analysis, contacts of the assembly must be classified according to their orientations and G groups of contacts with similar orientations be considered.

If there are

$$\Delta M_g = MS(\theta_g)\Delta\theta \tag{6.2}$$

contacts in each group, terms in (6.1) corresponding to contacts of similar orientations can be grouped together and (6.1) be rewritten in the form

$$w_f = \frac{d_o}{V} \sum_{g=1}^{G} \left\{ \frac{1}{M_g} \sum_{c \in \theta_g} \left[\frac{(f^c)^2}{2k_t} + \frac{(f_n^c)^2}{2k_n} \right] \right\} \Delta M_g \tag{6.3}$$

where $M_g = \Delta M_g$.

If group averages are introduced as follows

$$\overline{f_n^2}(\theta_g) = \frac{1}{M_g} \sum_{c \in \theta_g} (f_n^c)^2 \tag{6.4}$$

$$\overline{f_t^2}(\theta_g) = \frac{1}{M_g} \sum_{c \in \theta_g} (f_t^c)^2 \tag{6.5}$$

using (6.2) with $M = \frac{1}{2} \gamma N$, (6.3) can be rewritten in the form

$$w_f = \frac{1}{2} \gamma d_o n_v \sum_{G=1}^{G} \left[\frac{\overline{f_n^2}(\theta_g)}{2k_n} + \frac{\overline{f_t^2}(\theta_g)}{2k_t} \right] S(\theta) \Delta\theta \tag{6.6}$$

where $n_v = N/V$.

Passing to the limit of an infinite assembly in (6.6) and assuming the existence of limits (3.28) and also limits of the form

$$\overline{f_n^2}(\theta) = \lim_{\Delta\theta \to 0} \lim_{V \to \infty} \frac{1}{M_g} \sum_{c \in \theta_g} (f_n^c)^2 , \tag{6.7}$$

and similarly for f_t, (6.6) can be written in an integral form

$$w_f = \frac{1}{2} \gamma d_o n_v \int_0^{2\pi} \left[\frac{\overline{f_n^2}(\theta)}{2k_t} + \frac{\overline{f_t^2}(\theta)}{2k_t} \right] S(\theta) d\theta \tag{6.8}$$

If boundary loads are specified on infinity with σ_{ij}, all statically admissible contact forces satisfy constraints (4.3) related to boundary loads and can be rewritten here for reference purposes as

$$\sigma_{ij} = \frac{1}{2} \gamma d_o n_v \int_0^{2\pi} [\overline{f}_n(\theta) n_i n_j + \overline{f}_t(\theta) t_i n_j] S(\theta) d\theta . \tag{6.9}$$

The expression for complementary work (6.8) inidcates that individual contact forces do not enter w_f, which depends only on group averages. Although the theorem on minimum of complementary work requires minimization with respect to all statically admissible contact forces, the individual contact forces, for large systems, do not contribute significantly to the complementary work and only group averages have meaning defining the magnitude of w_f. It can, therefore, be minimized with respect to group averages which

must be statically admissible as the mentioned theorem on complementary work requires.

With external loads prescribed, group averages are not independent for different groups and must satisfy (6.9). To obtain average forces in the state of static equilibrium, (6.8) must be minimized subject to constraints related to fixed external loads.

A straightforward minimization of w_f cannot be performed, since (6.8) and constraints (6.9) depend on different arguments. A relationship between $\overline{f_n^2}(\theta)$, $\overline{f_t^2}(\theta)$ and $\overline{f}_n(\theta)$, $\overline{f}_t(\theta)$ can be obtained if the distribution function $P_\theta(f_n, f_t)$ of forces on contacts of the same orientation group is known. This distribution is not *a priori* known and it is necessary to establish the form of this distribution before complementary work can be efficiently minimized.

At this stage no information on $P_\theta(f_n, f_t)$ is available. A simple exponential distribution will be assumed for illustration purposes to outline the minimization procedure:

$$P_\theta(f_n, f_t) = \frac{1}{\overline{f}_n \overline{f}_t} \exp\left\{ - \frac{f_n}{\overline{f}_n} - \frac{f_t}{\overline{f}_t} \right\} .$$

For this distribution function, $\overline{f_n^2} = 2\overline{f}_n^2$, $\overline{f_t^2} = 2\overline{f}_t^2$. To analyze a case which ultimately will have a physical meaning, it will be assumed that the averages of squares and squares of averages are in the form

$$\frac{\overline{f_n^2}}{2k_n} + \frac{\overline{f_t^2}}{2k_t} = \frac{\overline{f}_n^2}{2\xi k_n} + \frac{\overline{f}_t^2}{2\xi k_t} \qquad (6.10)$$

where ξ is a certain non-dimensional parameter. Note that the above exponential distribution results in $\xi = 0.5$.

Complementary work (6.8), can now be rewritten in the form:

$$w_f[\bar{f}_n(\theta),\ \bar{f}_t(\theta)] = \frac{1}{2}\gamma d_o n_v \int_0^{2\pi}\left[\frac{\bar{f}_n^{\,2}}{2\xi k_n} + \frac{\bar{f}_t^{\,2}}{2\xi k_t}\right] S(\theta)\,d\theta \qquad (6.11)$$

Note that the above functional and $\sigma_{ij}[\bar{f}_n(\theta),\bar{f}_t(\theta)]$ given by (6.9) are both functions of the same vaiables $\bar{f}_n(\theta)$, $\bar{f}_t(\theta)$ with respect to which (6.11) is to be minimized subject to constraints (6.9).

6.3 Minimization of Complementary Work

Minimization of complementary work can be approached using the method of Lagrangian multipliers [40]. According to the technique, extremim of a functional $W[f_1,\ldots,f_k]$ defined on functions $f_1,\ldots,f_k$ which satisfy functional constraints

$$\Phi_i[f_1,\ldots,f_k] = 0 \qquad i = 1,\ldots,I \qquad (6.12)$$

can be performed as unconstrained minimization of a functional

$$L[f_1,\ldots,f_k] = W - \sum_{i=1}^{I}\lambda_i\Phi_i$$

where $\lambda_1,\ldots,\lambda_I$ are constants which must be determined. The procedure is usually applied as follows: L is minimized with respect to $f_1,\ldots,f_k$ which gives a set of functions depending on unspecified constants λ_i. The latter are chosen in such a way that I constraints (6.12) are satisfied.

In the present problem there are generally 9 constraints λ_{ij} related to components of σ_{ij} (6.9). In the three-dimensional case, minimization of w_f must be performed not only with respect to $\bar{f}_n(\theta)$, $\bar{f}_t(\theta)$, but also with respect to the vector $\underset{\sim}{t}(\theta)$ which gives the direction of tangential forces. There are therfore additional constraints related to normalization of the vector $\underset{\sim}{t}(\theta)$ and its orthogonality to the normal vector $\underset{\sim}{n}(\theta)$, i.e.

$$\Phi_1 = (\underset{\sim}{t}\cdot\underset{\sim}{t}) - 1 = 0$$
$$\Phi_2 = (\underset{\sim}{t}\cdot\underset{\sim}{n}) = 0 \qquad (6.13)$$

Minimization here is performed for an arbitrary, but fixed $S(\theta)$. This enables one to rewrite (6.13) in an integral form

$$\begin{matrix}\int_0^{2\pi} S(\theta)[(\underset{\sim}{t}(\theta)\cdot\underset{\sim}{t}(\theta) - 1]d\theta \\ \int_0^{2\pi} S(\theta)[(\underset{\sim}{t}(\theta)\cdot\underset{\sim}{n}(\theta)]d\theta\end{matrix} \qquad (6.14)$$

Since $S(\theta)$ is arbitrary, (6.14) is equivalent to (6.13). Lagrangian functional can be given in the form

$$L(f_n, f_t, \overline{f}) = w_f - \lambda_{ij}\sigma_{ij} - \mu_1\Phi_1 - \mu_2\Phi_2$$

where μ_1, μ_2 are Lagrangian multipliers related to constraints (6.14). Note that all Lagrangian multipliers are constants and can be introduced into the integral to obtain

$$L = \frac{1}{2}\gamma d_o n_v \int_0^{2\pi} S(\theta)\left\{\frac{\overline{f_n}^2}{2\xi k_n} + \frac{\overline{f_t}^2}{2\xi k_t} - \lambda_t f_n - \lambda_t f_t - \mu_1[(\underset{\sim}{t}\cdot\underset{\sim}{t})-1] - \mu_2(\underset{\sim}{t}\cdot\underset{\sim}{n})\right\}d\theta$$

where $\lambda_t = \lambda_{ij}n_j n_i$, $\lambda_t = \lambda_{ij}n_j t_i$.

Variation of L with respect to $\overline{f_n}$, $\overline{f_t}$ immediately gives that at the "stationary point" of L

$$\overline{f}_n(\theta) = \xi k_n[\lambda_{ij}n_i n_j]$$
$$\overline{f}_t(\theta) = \xi k_t[\lambda_{ij}n_j t_i] \qquad (6.15)$$

Variation with respect to t and elimination of multipliers μ_1, μ_2 using (6.13) gives

$$t_k(\theta) = \mu[\lambda_{ki}n_i - (\lambda_{ij}n_i n_j)n_k] \qquad (6.16)$$

where μ is a normalization constant.

The form of average forces (6.15) can be readily interpreted. If (6.15) are multiplied by $\overline{f}_n(\theta)$, $\overline{f}_t(\theta)$, respectively; and, if stiffnesses are introduced into the left-hand side anf both equations are added and integrated

with $S(\theta)$, the following expression results

$$\int_0^{2\pi}\left[\frac{\bar{f}_n^{\,2}}{2\xi k_n}+\frac{\bar{f}_t^{\,2}}{2\xi k_t}\right]S(\theta)d\theta=\frac{1}{2}\lambda_{ij}\sigma_{ij}$$

The left-hand side of the above relationship is the complementary work of internal deformations and comparison with (5.39) indicates that Lagrangian multipliers are components of the strain tensor.

For the plane case (6.15) can be written in the form

$$\bar{f}_n(\theta)=\frac{1}{2}\xi k_n[\lambda_n+\lambda_t\cos 2(\theta-\theta_\lambda)]$$

$$\bar{f}_t(\theta)=\frac{1}{2}\xi k_t[\lambda_\omega-\lambda_t\sin 2(\theta-\theta_\lambda)]$$

where λ_n, λ_t, λ_ω are invariants of tensor λ_{ij} similar to (4.27). Comparison with average forces (4.30) obtained from continuum mechanics considerations indicates once again that the tensor formed by Lagrangian multipliers can be interpreted as the strain tensor.

Expression (6.16) for the direction of average tangential forces also has an interesting interpretation. Vector $\lambda_{ki}n_i$ which enters (6.16) is the vector of relative displacements between a pair of points forming a segment of orientation θ and of unit length. The expression in brackets in (6.16) is therefore a tangential component of this vector. This indicates that the average direction of tangential forces coincides with the tangential direction of the vector of relative displacements calculated according to continuum mechanics rules.

The use of analogies with continuum mechanics is therefore justified, though only partly at this stage. Minimization of complementary work was performed assuming a relationship between averages (6.10). This is a very strong assumption which requires a considerable effort to be justified. Note that constitutive relationships here can be obtained from the

above results. All that is necessary is to substitute average forces (6.15) into the expression for the stress tensor (6.9) and a tensorial relationship between σ_{ij} and $\varepsilon_{ij} = \lambda_{ij}$ will follow.

The main objective of this chapter, however, remains the justification of (6.10).

6.4 Distribution of Forces on Contacts of the Same Orientation

Consider a finite assembly and select a group of contacts with orientations between θ and $\theta + \Delta\theta$. Let there be M_g contacts in the group. The number of contacts ΔM_g with forces between $f_n + f_n+\Delta f_n$, $f_t + f_t+\Delta f_t$ can be given in the form

$$\Delta M_g = P_g(f_n, f_t)\Delta f_n \Delta f_t$$

where $P_g(f_n, f_t)$ is a generally discontinuous function for a finite assembly where a spectrum of contact forces is expected to be discrete.

For an infinite assembly with an infinite number of contacts of the same orientation θ, $P_\theta(f_n, f_t)$ can be assumed to be continuous and $P_\theta(f_n, f_t)df_n df_t$ can be interpreted as the probability that an arbitrarily selected contact with orientation θ has force components in ranges $f_n + f_n+df_n$, $f_t + f_t+df$.

It is worth noting that P_θ for a single deterministic system can be associated with a probability density function with certain reservations, only in relation to an artificial process of "random selection of contacts". In physical terms $P_\theta(f_n, f_t)$ is the density of a spectrum of contact forces assumed to be continuous for an infinite system. The probabilistic language used in relation to such a density is convenient, since the usual rules of probability are applicable to such distribution densities, termed sometimes "ergodic" [28].

The exact determination of $P_g(f_n, f_t)$ is a problem of enormous complexity and it can be shown that $P_g(f_n, f_t)$ is related to the vibrational spectrum of the system, i.e. a spectrum of eigenvalues of a stiffness matrix. Literature on the subject is very limited [12] and, to the best of the knowledge of the author, only limited studies of the vibrational spectrum of a plane irregular system are available and these are based on computer analysis [5].

Under such circumstances further description of granular systems on the basis of equations of mechanics only becomes non-feasible and it is necessary to introduce some statistical postulates to obtain a measure of the form of the distribution function of forces on contacts of the same orientation.

6.5 Statistical Analysis of Granular Assemblies in Conditions of Incomplete Mechanical Description

The preceding analysis indicated that the description of granular assemblies on the level of constitutive relationships does not require considerable information as to the precise structure of the system. Specification of certain micro-structural averages like $S(\theta)$, n_v, γ is all that is necessary for an adequate description of geometrical structure in constitutive relationships. A description of contact forces in terms of distribution $P_\theta(f_n, f_t)$ is basically on the same level as the description of the structure, since both $S(\theta)$ and P_θ describe, respectively, the number of contacts with certain orientations per unit volume or forces on these contacts. In both cases , the precise position of the contact within the assembly is irrelevant, since gross actions or the response are related only to the number of contacts with specific properties. If precise infor-

mation on the structure, a set of all particle positions, be available, it would be redundant and disappear once gross response would be calculated on the basis of $S(\theta)$, $P_\theta(f_n, f_t)$. In such conditions systems of microscopically different, but macroscopically similar structures may result in the same $P_\theta(f_n, f_t)$. From the point of view of a "macroscopic observer" interested in constitutive relationships and, possibly, fluctuations in phenomenological response, all systems resulting in the same P_θ are identical, or nearly so, once fluctuations are of interest. Statistics can be initiated not with respect to situations within the system, but with respect to different systems.

A question can be asked: what are the chances of selecting a system with a specified distribution P_θ. If it is shown that for a vast majority of similar systems P_θ is nearly the same and such distributions can be found, the answer can be viewed as acceptable. This is a compromise with the precise demands of the laws of mechanics for which classical statistical mechanics has given a solution for dynamic systems [35]. Basically the same point of view is adopted here, although a lack of "randomness in time" for problems of static equilibrium makes direct application of the methods of classical statistical mechanics less direct.

It is convenient to take a more formal point of view on statistics of equilibrium related to the principles of the information theory [16]. An attempt is made to provide a physical interpretation for the procedure based on information theory principles.

Description of contact forces in terms of distribution P_θ contains an inherent uncertainty, the same distribution can describe the contact forces in a large number of systems. Having only P_θ, it is impossible

to answer precisely what system is being described by this function. Any system with the same forces, but on contacts differently scatterred within an assembly can produce the same P_θ. An attempt to assess the number of such systems leads to the notion of missing information associated with the distribution P_θ. If the problem of assessing how many systems correspond to the same P_θ is solved, a final statistical answer gives a function P_θ which can describe the maximum number of systems. The reason for such a choice within a statistical scheme is clear: the chance that the system of actual interest is described by P_θ is the greatest.

Information theory [16] adopts a formalized scheme of assessing the amount of "missing information" associated with any distribution function. In applications to statistical physics the amount of "missing information" is a measure of the number of similar systems which can be described with a certain distribution.

Consider how this "missing information" can be calculated for the problem of interest. It is convenient to consider a finite system with G groups of contacts of similar orientations. To calculate the amount of "missing information" consider first of all how the information can be "lost".

Let a complete solution for contact forces be known and the problem is to determine a distribution P_θ for a certain group of contacts by plotting a histogram of forces. The complete range of forces, a plane with coordinates f_n, f_t, is subdivided into elementary cells of the size $\Delta f_n \Delta f_t$ Each of M_g contacts of this group is examined one after another and a mark is placed on an elementary cell corresponding to the recorded force. When all contacts are examined, the number of marks M_i corresponding to the

elementary cell i is calculated and an empirical distribution P_g is obtained by calculating numbers M_i/M_g. For all selected elementary cells

$$\sum_i M_i = M_g$$

This can be done for all groups of contacts. If the same is performed with a collection of similar systems with exactly the same number of contacts in each group, one can expect that similar empirical distributions P_g can be found.

If now the original pattern of contact forces is to be reconstructed, all possible combinations must be tried until the right combination will be found the one corresponding to the state of static equilibrium. The total number of combinations of forces can be assessed [16]. There are total of

$$K_g = \frac{M_g!}{M_1! \ldots M_N!} \qquad (6.17)$$

combinations and only one correct combination; N in (6.17) is the number of elementary cells. The number K_g gives an indication of the amount of "missing information" associated with the distribution P_g, or, equivalently, with the set of numbers M_i. The amount of "missing information" is by definition

$$E_g = \log K_g \qquad (6.18)$$

The reason for such a definition is the following. If $K_g = 1$, a hypothetical case in the considered interpretation corresponding to no "missing information", then $E_g = 0$. If the group of contacts be subdivided into two subgroups with M_{g1} and M_{g2} contacts with corresponding numbers K_{g1}, K_{g2}, it can be shown that $K_g = K_{g1} \cdot K_{g2}$, and according to (6.18), $E_g = E_{g1} + E_{g2}$. Definition (6.18) again corresponds to an intuitive notion of "missing information" (the total "missing information" about the group

is the sum of missing information about its parts). This property of missing information enables one to present the amount of "missing information" about the whole system of contact forces in the form

$$E_v = \sum_{g=1}^{G} E_g[P_g]$$

where $E_g[P_g]$ is the amount of missing information about one group of contacts. This amount of missing information corresponds to the total of

$$K = \prod_{i=1}^{G} K_g$$

trials before the correct pattern of forces in the system is found.

Formulae (6.17) are rather inconvenient for direct calculations and can be simplified when all numbers M_i are large, for a large system. All M_i can be given in the form

$$M_i = M_g P_g(i) \Delta f_n \Delta f_t$$

where $P_g(i)$ symbolically denotes $P_g(f_n, f_t)$ for forces of an elementary cell i, and $\Delta f_n \Delta f_t$ is the size of elementary cells. It can be shown [16] using asymptotics for factorials that the total amount of missing information associated with the description with distributions P_g can be given in the form

$$E_v \simeq -\sum_{g=1}^{G} M_g \Big[\sum_{i=1}^{N} P_g(i) \log P_g(i)\Big] \Delta f_n \Delta f_t - \log \Delta f_n \Delta f_t$$

The accuracy of the above approximation increases with the size of the system. The above "missing information" will be used to assess relative values of E for different P_g, so that the term above related to the size of an elementary cell can be neglected (although it is infinite when the size of an elementary cell tends to zero).

If there are $M_g = \frac{1}{2} \gamma n_v \cdot V S(\theta_g) \Delta\theta$ contacts in each group in the

assembly of volume V, the above missing information can be given in the form

$$E_v = -\frac{1}{2}\gamma n_v V \sum_{g=1}^{G} S(\theta)\left\{\left[\sum_{i=1}^{N} P_g(i)\log P_g(i)\right]\Delta f_n \Delta f_t\right\}\Delta\theta \qquad (6.19)$$

It can be seen that the missing information is proportional to the volume of the system. For an infinite assembly the total missing information tends to infinity, but it can be assumed that "specific missing information" $e_v = \frac{E_v}{V}$ tends to a finite limit.

For conceptual reasons it is convenient to represent (6.19) in integral form which is strictly correct only for infinite assemblies when $V\to\infty$, $\Delta f_n \Delta f_t \to 0$, $P_g \to P_\theta$. For a finite assembly the following expression is correct if integration is understood in a generalized sense:

$$E_v = -\frac{1}{2} n_v V \int_0^{2\pi} S(\theta)\left[\int_{-\infty}^{+\infty} P_g \log P_g \, df_n df_t\right]d\theta \qquad (6.20)$$

For a finite assembly both $S(\theta)$ and P_g are discontinuous.

E_v is frequently called "information-entropy", although the use of this term in the present context is not advocated. This quantity is referred to as "missing information" associated with a specific description of contact forces with statistical element $P_g(f_n, f_t)$. So far E_v (6.20) is the $\log$ of the number of all possible combinations of contact forces which are compatible with distribution P_θ. For a single system only one such combination corresponds to static equilibrium.

Consider now a physical premise on the basis of which E_v can be utilized for the problem of interest.

Suppose an ensemble of large macroscopically similar systems is considered with the same number of contacts in each orientation group. Let all systems be subject to the same external load specified in terms

of σ_{ij}^{β}. An exact number of systems in this ensemble is difficult to assess, although one can expect that this number is large. Each system will be characterized by a certain distribution P_g, or, equivalently, by numbers of contacts corresponding to forces within elementary cells of the size $\Delta f_n \Delta f_t$. For all these N cells, $\sum_{i=1}^{N} M_i^g = M_g$, but each number M_i will, generally, depend on the size of the cell (fixed for the purpose of this discussion). All systems of the ensemble can be classified according to distributions $P_g\{M_i^g\}$. It is also assumed that the number of systems with identical $P_g\{M_i^g\}$ is also large*. If an attempt is made to reconstruct contact forces for the group of systems with the same P_g, not every combination, obviously, would correspond to a correct system of forces in a given system with considered P_g. It can, however, be expected that the greater the number of combinations of forces for given P_g, the greater the number of systems in the group corresponding to distribution P_g.

The last statement is difficult to argue against, but the major question is whether direct proportionality can be assumed or not. Let it be the case for the time being. In this case the largest number of systems in the considered ensemble corresponds to the function P_g which admits the greatest possible number of combinations of forces when their reconstruction is attempted for a given P_g.

Since this number of combinations is proportional to E_v (6.20), this quantity must be maximized to obtain contact force distributions which have an overwhelming chance to be observed. The reason that this chance

*Their exact number also depends on the size of the cell $\Delta f_n \Delta f_t$. The smaller the tolerance with which systems are grouped, the fewer the systems in the group.

is overwhelming lies in the proportionality of E_v to the volume. It the part of E_v given by integrals in (6.20) has even a small relative maximum, it will be greatly magnified by the factor containing the volume of the system. In the limit of an infinite assembly, the most probable P_g is, perhaps, the one which follows from the laws of mechanics. This, however, is an unsubstantiated guess. Within classical statistical mechanics of dynamic systems, ultimate justification of a similar procedure is based only on experiments and heuristic logic similar to that presented above*.

The situation is more uncertain with respect to the present theory of static equilibrium due the the assumed direct proportionality between the number of systems in the ensemble corresponding to the set of distributions P_g and the number of different combinations of forces compatible with this set of P_g.

6.6 Maximum of Missing Information

To determine the most probable distribution of contact forces, missing information must be maximized on an admissible set of contact force distributions. It is convenient to present maximization when (6.20) is given in integral form in the limit of an ensemble of infinite systems. In this case missing information is infinite and specific missing information $e_v = E_v/V$

$$e_v = -\frac{1}{2}\gamma n_v \int_0^{2\pi} S(\theta) \left\{ \int\int_{-\infty}^{+\infty} P_\theta \log P_\theta \, df_n df_t \right\} d\theta \qquad (6.21)$$

will be maximized with respect to P_θ subject to constraints

*An interesting account of attempts to justify the classical statistical mechanical procedure is presented by C. Truesdell [37].

$$\sigma_{ij} = \frac{1}{2}\gamma d_o n_v \int_0^{2\pi} S(\theta)\left\{\int_{-\infty}^{+\infty} P_\theta\left[f_n n_i n_j + f_t t_i n_j\right] df_n df_t\right\} d\theta \quad (6.22)$$

$$w_f = \frac{1}{2}\gamma d_o n_v \int_0^{2\pi} S(\theta)\left\{\int_{-\infty}^{+\infty} P_\theta\left[\frac{f_n^2}{2k_n} + \frac{f_t^2}{2k_t}\right] df_n df_t\right\} d\theta \quad (6.23)$$

The reason for making use of the above constraints now will be carefully discussed.

First of all, systems of the considered ensemble are subject to loads on infinity specified in terms of σ_{ij}. In this situation, as was shown in Chapter III, certain volume-additive combinations of the system's contact forces are fixed regardless of the type of particle deformational properties. This absolute constraint on contact forces is given for an infinite assembly in the form (4.3) and average forces on contacts of the same orientation in (4.3) are presented in (6.22) as averages with distribution P_θ.

Another constraint that will be employed is the complementary work of internal deformations (5.1) which coincides with the system's potential energy. The reason for making use of this constraint is the fact that the level of potential energy of the system is fixed when external loads are specified. The particular magnitude of w_f (5.1) is unknown, but the fact that this quantity is fixed was established in Chapter V. Since the considered ensemble is characterized by the same $S(\theta), \gamma, n_v$, (6.22-6.23) are identical for all systems of the ensemble and P_f which maximizes (6.21) must not violate these constraints.

The question, however, remains whether constraints (6.22-6.23) are the only constraints which must be imposed. Are there any other combinations of forces or their averages which must be constrained? First of all,

each considered system is deterministic and, once all solutions are known, an infinite combination of forces can be formed and employed as constraints in the minimization problem. Such an approach, however, violates the principle on which the procedure has been based. It should be remembered that the formulation of the problem in terms of contact forces is a practical necessity. The distribution of forces, however, reflects the statistics of different systems in the ensemble, i.e. different microstructures with the same $S(\theta)$, γ, n_v. Contact forces are used here as an indirect reflection of microstructure. The more constrained P_θ, the fewer systems result in equilibrium with this P_θ.

The two constraints presented above indicate very basic structural properties of systems and one of them is completely independent of particle deformational properties. The form of the second constraint w_f follows from the principle of virtual work the formulation of which is again independent of specific deformational properties. Stiffnesses enter (6.23) as a reflection of geometrical compatibility of particles in the system.

It also should be mentioned that both the maximized functional (6.21) and the constraints follow from relationships of volume-additive nature. These quantities are considered per unit volume in the problem, but their volume-additive origin remains in the coefficient $\frac{1}{2}\gamma n_v$ which is the number of contacts per unit volume (usually a large quantity). Any other constraint of non-volume-additive nature will have an effect on P_θ, but the effect will be proportional to the number of contacts represented by this constraint per unit volume.

Classical statistical mechanics of dynamic systems invariably operates with only one volume-additive constraint—total energy. Beginning

with the introduction of this discipline, the use of only this constraint axiomatically introduced by Gibbs [13] has been a topic of may serious discussions [35 , 37]. Classical statistical mechanics does not follow as an exact consequence of the laws of mechanics and the axiomatic treatment of the subject by Gibbs resulted in supported conclusions from experiments.

The use of constraints (6.22-6.23) is not justified rigorously, but is based on the heuristic logic presented above and the experience of classical statistical mechanics. The additional volume-additive constraint (6.22) reflects the difference between static and dynamic cases.

Maximization of missing information will be performed in this section for plane systems. The three-dimensional case contains interesting details and treated in the next section. There are four Lagrangian multipliers λ^{*}_{ij} associated with constraints (6.22) and one λ_{w} associated with complementary work. To simplify calculations it is convenient to construct a Lagrangian functional as follows:

$$L[P_{\theta}] = d_{o}e_{v} + \frac{1}{\lambda_{w}}\left[w_{f} + \lambda^{*}_{ij}\sigma_{ij}\right]$$

Calculation of the variation of the above functional with respect to P_{θ} gives the following Gaussian distribution presented in normalized form:

$$P_{\theta} = \frac{1}{2\pi\sqrt{k_{n}k_{t}}\,\lambda_{w}}\exp\left\{-\frac{(f_{n}-\bar{f}_{n})^{2}}{2k_{n}\lambda_{w}} - \frac{(f_{t}-\bar{f}_{t})^{2}}{2k_{t}\lambda_{w}}\right\} \qquad (6.24)$$

where

$$\bar{f}_{n} = k_{n}\lambda^{*}_{ij}n_{j}n_{i}$$
$$\bar{f}_{t} = k_{t}\lambda^{*}_{ij}t_{j}n_{i} \qquad (6.25)$$

The above distribution automatically predicts the form of directional variation for average forces which was assumed on the basis of continuum mechanics analogies and was obtained assuming the relationship (6.10) between

the first and second moments of P_θ. The second moments of (6.24) can be given in the form

$$\overline{f_n^2}(\theta) = \overline{f}_n^2(\theta) + k_n\lambda_w$$
$$\overline{f_t^2}(\theta) = \overline{f}_t^2(\theta) + k_t\lambda_w \qquad (6.26)$$

Lagrangian multipliers λ^*_{ij} can be obtained by substituting average forces (6.25) into the expressions for the stress tensor (6.9). The resulting set of linear equations can be solved for λ^*_{ij} to obtain this tensor in terms of σ_{ij}. To obtain λ_w, complementary work must be calculated on the basis of (6.26) to obtain

$$w_f = \frac{1}{2}\gamma d_o n_v\left\{\int_0^{2\pi} S(\theta)\left[\frac{\overline{f}_n^2}{2k_n} + \frac{\overline{f}_t^2}{2k_t}\right]d\theta + \lambda_w\right\} \qquad (6.27)$$

If complementary work is known, λ_w can be calculated from the above relationship and the distribution of contact forces can be completely specified in terms of the stress tensor. Complementary work, however, is given by (5.39) in terms of an unknown tensor of elasticity which also must be found.

To obtain the form of λ_w, note that it must be a quadratic function of σ_{ij}, since the rest of terms in (6.27) are quadratic. If this function is obtained and σ_{ij} are given in terms of average forces using (6.9), then λ_w is a certain functional of $\lambda_w = \lambda_w[\overline{f}_n(\theta), \overline{f}_t(\theta)]$. It can be shown that λ_w can be resented in the form

$$\lambda_w = \int_0^{2\pi} S(\theta)\Phi(\overline{f}_n, \overline{f}_t)d\theta$$

Dimensional considerations require that Φ above be a quadratic:

$$\Phi = \alpha_1\overline{f}_n^2 + \alpha_2\overline{f}_n\overline{f}_t + \alpha_3\overline{f}_t^2 \qquad (6.28)$$

Limited information on coefficients α_1, α_2, α_3 can be recovered.

Complementary work (6.27) must have a minimum under constraints (6.9). By constructing a Langrangian functional with multipliers λ_{ij} associated with (6.9) and equating its variation to zero, it is easy to obtain

$$\frac{\overline{f}_n}{k_n} + \frac{\partial \Phi}{\partial \overline{f}_n} = \lambda_{ij} n_j n_i$$
$$\frac{\overline{f}_t}{k_t} + \frac{\partial \Phi}{\partial \overline{f}_t} = \lambda_{ij} n_j t_i \qquad (6.29)$$

As average forces must have directional variation (6.25), the only alternative for α_2 in (6.28) is seen to be zero. Further comparison of (6.29) with (6.25) indicates that coefficients in (6.28) must be of the form

$$\alpha_1 = \frac{1}{2k_n}\frac{1-\xi}{\xi}\,; \qquad \alpha_2 = \frac{1}{2k_t}\frac{1-\xi}{\xi}$$

where ξ is a certain parameter which remains unspecified.

The form of Φ and λ_w is now known and complementary work (6.27) can be given in the form

$$w_f = \frac{1}{2}\gamma d_o n_v \int_0^{2\pi} S(\theta)\left[\frac{\overline{f}_n^2}{2k_n\xi} + \frac{\overline{f}_t^2}{2k_t\xi}\right]d\theta \qquad (6.30)$$

The parameter λ_w of distribution (6.24) is now of the form

$$\lambda_w = (1-\xi)\left[\frac{1}{2}\gamma d_o n_v\right]^{-1} w_f \qquad (6.31)$$

Before continuing the discussion of the statistical analysis, an example will be given to clarify the meaning of the obtained results. Consider a plane isotropic assembly subject to a hydrostatic load. Complementary work of the system in this case is

$$w_f = \frac{\sigma_n}{2K} \qquad (6.32)$$

where K is the bulk modulus of the system given by (4.33). Coefficient ξ in that formula has the same meaning as here with the difference that

it was introduced heuristically in chapter IV. To calculate dispersion of contact forces, relationships (6.26) can be used to obtain

$$D_n = \overline{f_n^2} - \overline{f}_n^2 = k_n(1-\xi)\left[\frac{1}{2}\gamma d_o n_v\right]^{-1} w_f$$
$$D_t = \overline{f_t^2} - \overline{f}_t^2 = k_t(1-\xi)\left[\frac{1}{2}\gamma d_o n_v\right]^{-1} w_f \qquad (6.33)$$

Noting that for a plane system

$$\frac{1}{2}\gamma d_o n_v = 2\,\frac{\rho\gamma}{\pi d_o}$$

and making use of (6.32-6.33), (4.33) it is easy to obtain

$$D_n = \frac{1-\xi}{2\xi} \cdot \sigma_n^2 \Big/ \left[\frac{\rho\gamma}{\pi d_o}\right]^2$$

Dispersion of contact forces is proportional to the level of contact forces. The coefficient of variation of forces, however, must represent only the structure of an assembly for linear systems. Noting the expression for average forces (4.31), the coefficient of variation of contact forces can be given in the form

$$c_n^2 = \frac{\overline{f_n^2} - \overline{f}_n^2}{\overline{f}^2} = \frac{1-\xi}{2\xi} \qquad (6.34)$$

Note that the same expression holds in the three-dimensional case. This example clarifies the physical meaning of the above theory. Fluctuations of contact forces are a reflection of the irregularity in a system's structure. Considerable information has been accumulated on contact forces and their averages have been employed to study the structure of a system, but the ultimate result proved to be a coefficient which analysis failed to predict theoretically. This comes as no surprise, since the methods used were indirect.

In the geometrical analysis used in chapter V there was a clear

indication that the same paramter ξ in (6.34) controls a bias between deformations of contacts and their local environment, indicating that ξ is a geometrical characteristic of the system.

The theory also indicates how parameter ξ can be assessed experimentally. Parameter ξ reduces stiffness of the system due to its irregularity, as compared to a regular system of particles with the same stiffness properties. For a regular system $\xi=1$, as shown by the example in chapter V of a regular array. Relationship (6.34) for $\xi=1$ gives $C_n = 0$, i.e. no fluctuations of forces.

If the bulk modulus of an irregular assembly is determined experimentally as well as its contact stiffness, (4.33) can be used to obtain and to calculate the coefficent of variation of contact forces.

The procedure is indirect, but that is the price to pay for making use of indirect methods.

6.7 Distribution of Contact Forces in Three-Dimensional Assemblies

Three-dimensional systems have an extra degree of freedom which increases the possible number of geometrical structures that can be formed with identical macroscopic properties.

In the present approach a variety of different structures is determined indirectly by calculating a variety of different systems of contact forces compatible with external actions and geometrical structures of considered systems.

Any contact force in the three-dimensional case has three components and this fact must be taken into account. Normal and tangential

force components still are the most important, since they are directly related to particle deformations. The tangential direction of contact forces, however, is not fixed, as for plane systems, and its distribution must also be determined by maximization of missing information associated with distribution $P_\theta(f_n, f_t, t)$. Note that the orientation θ is now given by a pair of angles $\theta = \{\xi, \phi\}$, although all previous relationships preserve their form.

Further calculations are much more simple when Cartesian components of contact forces are considered $\underset{\sim}{f} = \{f_1, f_2, f_3\}$ instead of a triple $\{f_n, f_t, t\}$.

Missing information per unit volume e_v is defined as previously

$$e_v = -\frac{1}{2}\gamma n_v \int_\Omega S(\theta) \left[\int_\infty P_\theta \log P_\theta \, df_1 df_2 df_3 \right] d\Omega \qquad (6.35)$$

where $d\Omega = \sin\xi \, d\xi d\phi$ is an element of surface of a unit sphere.

Maximization constraints exist as previously indicated, but are written in terms of Cartesian force components. Noting $f^2 = f_n^2 + f_t^2$, complementary work can be given in the form

$$w_f = \frac{1}{2}\gamma d_o n_v \int_\Omega S(\theta) \left\{ \int P_\theta \left[\frac{f^2}{2k_t} + \frac{f_n^2}{2k_*} \right] df_1 df_2 df_3 \right\} d\Omega \qquad (6.36)$$

where $\frac{1}{k_*} = \frac{1}{k_t} - \frac{1}{k_n}$. The constraint related to fixed external loads will be written in the form (3.29) which includes Cartesian force components

$$\sigma_{ij} = \frac{1}{2}\gamma d_o n_v \int_\Omega S(\theta) \left\{ \int P_\theta f_i n_j(\theta) \, df_1 df_2 df_3 \right\} d\Omega$$

The method of Lagrangian multipliers gives

$$P_\theta = A \exp\{-\Psi\}$$

where

$$\Psi = \frac{1}{\lambda_w} \left[\frac{f_i f_i}{2k_t} + \frac{(f_i n_i)^2}{2k_*} - \lambda^*_{ij} n_j f_i \right] \qquad (6.37)$$

and A is a normalization constant.

Lagrangian multipliers are as previously given for the plane case. The form of the above distribution is Gaussian, although the Cartesian force components are correlated. It can be shown that (6.37) can be given in the form

$$\Psi = \frac{1}{2} k^*_{ij} (f_i - \bar{f}_i)(f_j - \bar{f}_j) + const. \tag{6.38}$$

where

$$\bar{f}_i = k_t \lambda^*_{il} n_l + (k_n - k_t)(\lambda^*_{kl} n_k n_l) n_i \tag{6.39}$$

$$k^*_{ij} = \frac{1}{k_t} \lambda_\omega [\delta_{ij} - (1-r) n_i n_j]; \; r = \frac{k_t}{k_n}$$

and the constant depends on Lagrangian multipliers. It will disappear after the distribution is normalized.

With Ψ of the form (6.38) distribution P_θ takes a standard Gaussian form and k^*_{ij} in (6.38) is the inverse of the correlation matrix. To normalize (6.38), k^*_{ij} must be inverted to obtain

$$k_{ij} = k_n \lambda_\omega [r\delta_{ij} + (1-r) n_i n_j] \tag{6.40}$$

Its determinant $\Delta = \lambda_\omega^3 k_n^3 r^2$ defines the normalization constant. The complete distribution of forces on contacts of similar orientation is of the form

$$P_\theta(f_1, f_2, f_3) = \frac{1}{r(2\pi k_n \lambda_\omega)^{3/2}} \exp\left\{ -\frac{1}{2} k_{ij} (f_i - \bar{f}_i)(f_j - \bar{f}_j) \right\} \tag{6.41}$$

Correlation matrix (6.40) determines the central second moments as follows:

$$E[(f_i - \bar{f}_i)(f_j - \bar{f}_j)] = k_{ij} \tag{6.42}$$

where E denotes expectation of the quantity in brackets.

The following averages can be determined using (6.42):

$$\overline{f^2} = \bar{f}^2 + \lambda_\omega k_n (2r+1) \tag{6.43}$$

$$\overline{f_n^2} = \bar{f}_n^2 + \lambda_\omega k_n$$

The average of the square of tangential force is of the form

$$\overline{f_t^2} = \overline{f^2} - \overline{f_n^2} = \overline{f}_t^2 + 2\lambda_\omega k_t \qquad (6.44)$$

The above relationship indicates a basic difference between plane and three-dimensional systems. Averages of normal forces are related to λ_ω similarly to the case of plane systems (*c.f.* (6.26)). The average of tangential force (6.44) is of the same form as (6.26), but contains an additional multiplier which reflects two degrees of freedom associated with tangential forces.

Dispersion of tangential forces

$$\overline{f_t^2} - \overline{f}_t^2 = 2\lambda_\omega k_t \qquad (6.45)$$

is greater in three-dimensional systems than in the plane case.

Relationships (6.43) and (6.45) enable one to calculate the complementary work in the form

$$\omega_f = \frac{1}{2}\gamma d_o n_v \left\{ \int_\Omega \left[\frac{\overline{f}_n^2}{2k_n} + \frac{\overline{f}_t^2}{2k_t} \right] S(\theta) d\Omega + \frac{3}{2}\lambda_\omega \right\}$$

The above relationship is similar to (6.31) and a similar logic enables to establish that λ_ω must be proportional to the integral in the expression above. If it is not the case, minimization of complementary work will not result in directional variation of forces (6.39). The coefficient of proportionality remains unspecified and can be selected in such a way that complementary work be of the form (6.30). This selection of the mentioned coefficient results in λ_ω of the form

$$\lambda_\omega = \frac{2}{3}(1-\xi)\left[\frac{1}{2}\gamma d_o n_v\right]^{-1}\omega_f \qquad (6.46)$$

The expression for complementary work (6.30), identical in the two- and three-dimensional cases, makes use of the results presented in section 6.3 where complementary work was minimized in this form. Ex-

3

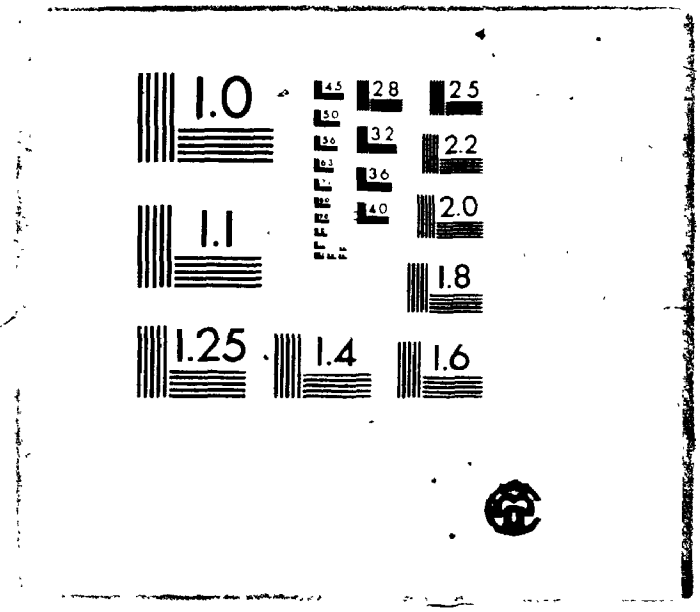

pression (6.15) for average forces is correct in both two and three dimensions, although the tangential direction of forces in the latter case is given by (6.16). It can readily be shown that a combination of (6.15) and (6.16) results in the expression for average forces of the (6.39) type. Lagrangian multipliers in (6.16) are equivalent to the components of the strain tensor, but λ^*_{ij} in (6.30) do not have that interpretation. Comparison of both expressions for average forces gives

$$\lambda^*_{ij} = \xi\lambda_{ij} = \xi\varepsilon_{ij}$$

where ε_{ij} is the strain tensor.

Finally, average forces on contacts of the same orientation can be written in three dimensions in the form

$$\bar{f}_i(\theta) = \xi k_t \varepsilon_{il} n_l + \xi(k_n - k_t)(\varepsilon_{kl} n_l n_k) n_i \qquad (6.47)$$

where n is the common orientation of contacts in the group. In the plane case it is more convenient to work with normal and tangential components and to retain the form of average forces (6.15) rewritten here for comparison with (6.47)

$$\begin{aligned} \bar{f}_n(\theta) &= \xi k_n \varepsilon_{kl} n_l n_k \\ \bar{f}_t(\theta) &= \xi k_t \varepsilon_{kl} n_l t_k \end{aligned} \qquad (6.48)$$

Coefficient ξ reflects a system's irregularity leading to apparent reduction in particle stiffnesses. Using experimental data it will be numerically assessed later to show that the stiffness reduction is drastic and fluctuations of contact forces, also controlled by ξ, are very high.

The form of the distribution of contact forces (6.41) is slightly complicated due to a bias between Cartesian components. It can be shown that normal and tangential components are statistically independent and distributed in the three-dimensional case according to (6.24), as in the

plane case, but with λ_ω given by (6.46).

At this stage the theory is ready for applications, although there are several points of conceptual significance which will be clarified in the following discussion.

6.8 Discussion

No new results will be presented in this section discussing the proposed approach to statistical description of contact forces and alternative ways of constructing the theory.

The main result of the above statistical analysis is the distribution function of forces on contacts of the same orientation. This function, however, is not a characteristic of any particular system, but rather characterizes a collection of systems with similiar macroscopic structures. If a system of this ensemble is selected for examination, the chance that the developed distribution indeed describes the contact forces in this system must be overwhelming, provided the postulates of the theory conform to reality. The possibility that a system of the ensemble will have a distribution markedly different from the most probable distribution obtained above is not ruled out, but such circumstances can be neglected. This compromise with the exact character of the laws of mechanics has, most likely, to be accepted [35].

The determination of the most probable distribution required enumeration of macroscopically similiar systems corresponding to any possible distribution of contact forces. It was performed on the premimise that a variety of different micro-structures, with the same $S(\theta), \gamma, n_\nu$ can be described by a variety of different systems of forces. This premise is used in

a very specific form: it is postulated that any combination of contact forces compatible with selected constraints can *a priori* equiprobably appear in a certain system of the ensemble.

The postulate on equal *a priori* probability is the starting point of any statistical investigation. It is always necessary to describe the outcomes of all possible elementary events related to the studied phenomena or problem. Equal chances of elementary events are assigned on the basis of judgement. In an experiment of flipping a coin, the probabilities of 0.5 for heads and tails are assigned only after investigation shows that the coin is not "loaded".

The present theory started from the same point assigning equal *a priori* probabilities to all combinations of contact forces compatible with constraints directly following from the equations of mechanics. The total number of all possible combinations is assessed and the most probable combination is determined from the conditions with prescribed external loads.

One major point, however, was left out. It was not checked that an assignment of equal *a priori* probabilities to all possible systems of contact forces is physically meaningful. If this is not the case, predictions of the above theory would be as unreasonable as it would be to expect that a "loaded" coin would not be biassed toward showing heads or tails.

Obviously, any theory is only as good as its postulates. Neither this theory, nor classical statistical mechanics [35] have the means to experimentally support their major postulates , however classical statistical mechanics has the enormous advantage of Loiuville's theorem [35]

which indicates persistently, though not directly, how equal *a priori* probabilities must be assigned to different states of dynamic systems. The present theory lacks such a powerful aid and only experimentally may its results be checked.

There are, however, difficulties in this respect. Constant ξ which controls stiffness of granular systems and its deformational properties remained undetermined, so that deformation moduli cannot be calculated precisely. Fortunately, Poisson's ratio for isotropic assemblies is independent of the unspecified parameter and is only controlled by the ratio of tangential to normal contact stiffnesses, as will be shown in the analysis of constitutive relationships in the next chapter. With experimental data on Poisson's ratios of granular systems available, the theory predicts the correct range for granular materials. i.e. between zero and 1/4.

Precise data on contact stiffnesses are not available, however this comparison is tought to be reasonable, though not decisive. At this point the validity of the introduced postulate can be assessed by judging the character of the conclusions resulting from the introduced postulate. Average contact forces were developed in this work using several different approaches, including statistical analysis. In all approaches the same expression appears, but statistical analysis shows that average forces are also the most probable. There is obviously no good reason as to why this should necessarily be so, although the result is intuitively satisfying. It can be shown that this result will not be obtained with different assignment of equal *a priori* probabilities.

The theory also does not contradict its basic physical premise.

Contact forces are used here as an agent to learn about the structure of the system. For studied linear systems variations of external loads alter contact forces proportionately. Once it is assumed that the fluctuations are due to irregularities in structure, the coefficient of variation for the contact force distribution, as a ratio of force averages, must be independent of the level of the external load and must reflect a system's irregularity. It is, indeed, the case, as shown by expression (6.34) for the coefficient of variation.

The above are physical concepts which form the framework of the statistical theory, however the theory is presented largely from the point of view of information theory. The reason for such a presentation is the following. The present theory is based on a guess, and the necessity of guessing is related to incomplete theoretical knowledge regarding the object of studies. Information theory provides a reasonable theoretical procedure for making the best guesses under circumstances related to incomplete knowledge of the systems studied.

In section 6.2 it was reasonably shown that the theory cannot proceed further without a distribution function of forces on contacts of the same orientation, so that it must be either simply assumed with no justification whatsoever, or certain postulates must be introduced. The first alternative is not very attractive because of the possible adverse effect such an action may have on its use. If an exponential distribution of forces assumed, relationships between second moments would be uniquely fixed with $\xi=0.5$ (section 6.2). This would immediately fix the coefficients of variation for contact forces which must be a function of a system's structure.

If it is necessary to make an educated guess, it should be made in such a way that the least information be produced that is not based on precise knowledge. The distribution of forces P_θ which conveys certain information of the system was the quantity that was assumed. Suppose a choice must be made between two such functions, both compatible with precise available knowledge: energy of the system and constraints related to external loads. If the two functions have different amounts of missing information associated with the functions, the one which corresponds to the smaller amount of missing information conveys more knowledge than the one with the large amount of missing information. The extra knowledge conveyed by one of the two functions is unsubstantiated by available information (constraints). Selection of the function with the larger amount of missing information assures the least amount of possibly adverse information which can result from an unsubstantiated guess.

This is the non-physical logic underlying the principle of the best guess [16]. The principle does not assure that the result of its application be correct or reasonable. In any particular application it is up to the user of this principle to determine how the principle is to be applied.

The specific way of applying the principle here was motivated by physical considerations resulting in expression (6.20) for missing information. Consider now an alternative way of applying the principle of the best guess to systems of interest.

Specification of loads on an assembly immediately results in a situation where certain information on contact forces must be recovered. Such

information was obtained in chapter IV where average forces on contacts of the same orientation were developed in terms of stress tensor invariants, i.e. first moments of the distribution function $P_\theta(f_n, f_t)$ became known

$$\bar{f}_n(\theta) = \int_{-\infty}^{+\infty} f_n P_\theta(f_n, f_t) df_n df_t$$
$$\bar{f}_t(\theta) = \int_{-\infty}^{+\infty} f_t P_\theta(f_n, f_t) df_n df_t \qquad (6.48)$$

If no other information is available and $P_\theta(f_n, f_t)$ must be guessed, the best choice would be one which carries the least information in addition to that confidently available. This choice corresponds to the maximum of missing information associated with $P(f_n, f_t)$.

Missing information associated with a single group of contacts and its distribution P is of the form

$$E_\theta = -\int_{-\infty}^{+\infty} P_\theta(f_n, f_t) \log P_\theta(f_n, f_t)\, df_n df_t \qquad (6.49)$$

To determine P_θ, (6.49) must be maximized subject to constraints (6.48) and a normalization condition.

It can be readily shown that, with first moments known, the choice corresponding to maximum missing information is given by the following exponential distribution:

$$P_\theta(f_n, f_t) = \frac{1}{\bar{f}_n \bar{f}_t} \exp\left\{-\frac{f_n}{\bar{f}_n} - \frac{f_t}{\bar{f}_t}\right\} \qquad (6.50)$$

Examination of (6.50) shows that contact force components must have the same sign as their averages (to have a negative argument of the exponent). This, perhaps, is reasonable for normal force components where the above distribution implies that all normal force components, under a compressive hydrostatic load on an isotropic assembly, are compressive and

there are no contacts under tension. The distribution of normal forces reasonably reflects what can be accepted for cohesionless materials.

The distribution of tangential forces is, however, physically meaningless. To illustrate, consider a case of hydrostatic compression of an isotropic assembly. Without any analysis it is clear that the average of tangential forces is zero in this case. An exponential distribution of tangential forces immediately implies that all tangential forces are strictly zero with a zero average which is physically impossible.

The above attempt to apply the principle of maximum missing information to function P_θ for each fixed θ resulted in physically unrealistic predictions. In mathematical terms the reason, perhaps, is that the maximization problem was over-constrained, and missing information was maximized for each group separately.

In the present theory constraints on total missing information are much less severe, so that the resulting distribution corresponds to much higher missing information, i.e. much more systems can correspond to the Gaussian distribution developed in the preceding section.

In any case, physical justification for constraining each group average was not found. Constraints used in the present theory are related to very general structural properties of systems which are basically independent of particle deformational properties. As shown in chapter III, average forces are prescribed only with specification of particle deformational properties.

This example shows that a formal application of the information theory principle requires considerable judgement in evaluating results. The adopted scheme based on volume-additive constraints yields reasonable results

that cannot be rejected outright.

The following conclusions can be made on the basis of the above statistical analysis related to systems of bonded particles with linear contacts:

(1) The distribution of forces on contacts of the same orientation was developed as a characteristic of an ensemble of systems. For an arbitrary system of the ensemble this distribution is the most probable. Circumstances, under which the developed distribution does not describe a large system of actual interest, are viewed as negligible. The distribution can, therefore, be accepted as a characteristic of any infinite system with structure described by a contact orientation distribution, average coordination number and particle density.

(2) Normal and tangential force components are independently distributed and the distribution is Gaussian. Averages of the distribution (average forces on contacts of the same orientation) are expressed in terms of stress or strain tensors. Dispersion of contact forces is related to the system's potential energy and ξ, a structural parameter that reflects a bias between the systems local density and contact deformations. This parameter affects the system's response as if particle stiffnesses were reduced.

(3) The distribution of Cartesian components of contact forces is also Gaussian, but different force components are correlated.

The correlation matrix is presented and it will be employed to study fluctuations in phenomenological parameters.

(4) Plane and three-dimensional systems of discs and spheres have similar forms of contact force distributions, although disperion of forces is greater in three-dimensional systems due to an extra degree of freedom.

CHAPTER VII

CONSTITUTIVE RELATIONSHIPS FOR SYSTEMS OF BONDED PARTICLES

7.1 Introduction

The foregoing chapters present the concepts of a micro-mechanical description of granular assemblies. Major emphasis was placed on careful development of concepts leading to a continuum mechanics type description, but with the possibility of developing constitutive relationships with parameters admitting explicit physical interpretation. Stress and strain tensors, as understood here, have all properties of similar quantities defined in continuum mechanics, but are interpreted as averages of phenomenological stress and strain tensors over infinitesimal volume in identical locations in macroscopically similar systems.

The latter tensors are defined as functions of volume and fluctuate for identical volumes of similar systems subject to identical loads. Fluctuations of phenomenological parameters are studied in the next chapter, while relationships between stress and strain tensors are derived here for small elastic deformations of assemblies of discs and spheres with linear contacts characterized by stiffness coefficients k_n, k_t.

It should be emphasized that constitutive relationships characterize an ensemble of similar systems and not a single system. For large systems, fluctuations in phenomenological parameters can be neglected and a continuum mechanics description of individual systems follows as an approximation.

7.2 Isotropic Assemblies of Spheres

Constitutive relationships for three-dimensional assemblies of spheres are presented for the isotropic case only. The reason for this limitation is not related to deficiencies in the preceding analysis which is perfectly applicable to anisotropic three-dimensional systems. All the relationships, however, contain a contact orientation distribution $S(\theta)$ which is unknown for anisotropic assemblies. In the isotropic case, $S(\theta) = const = 1/4\,\pi$ and the theory can be applied.

The form of $S(\theta)$ for anisotropic systems is considered only in the plane case.

The relationship between stress and strain tensors can be obtained by making use of the expression for average forces (6.47) in terms of the strain tensor

$$\bar{f}_i(\xi,\phi) = \xi\, k_n\, \varepsilon_{il} n_l + \xi(k_n - k_t)(\varepsilon_{kl} n_k n_l) n_i \tag{7.1}$$

and substituting it into the relationship between the stress tensor and average forces (3.29) rewritten here in the form

$$\sigma_{ij} = 3\,\frac{\rho\gamma}{\pi d_o^{\,2}} \int_0^{2\pi}\int_0^{\pi} S(\xi,\phi)\,\bar{f}_i n_j \sin\xi\, d\xi d\phi \tag{7.2}$$

Note that for assemblies of spheres the factor $1/2\,\gamma\, d_o n_v$ in (3.29) is $3\,\frac{\rho\gamma}{\pi d_o^{\,2}}$. Integration in the above expression is performed in the limits

$$0<\xi<\pi; \quad 0\le\phi\le 2\pi$$

corresponding to all contact orientations. Note also that components of vector n in the spherical coordinate system (Fig. 3.7)

$$n_1 = \sin\xi\cos\phi$$

$$n_2 = \sin\xi\sin\phi$$

$$n_3 = \cos\xi$$

Substitution of (7.1) into (7.2) gives

$$\sigma_{ij} = 3\frac{\rho\gamma}{d_o^2}\xi\left[k_t A_{kj}\varepsilon_{ik} + (k_n-k_t)A^2_{ijkl}\varepsilon_{kl}\right] \qquad (7.3)$$

where

$$4\pi A^1_{kl} = \int_0^{2\pi}\int_0^{\pi} n_k n_j \sin\xi\, d\xi d\phi$$

$$4\pi A^2_{ijkl} = \int_0^{2\pi}\int_0^{\pi} n_i n_j n_k n_l \sin\xi\, d\xi d\phi$$

The form of constitutive relationships (7.3) indicates that, generally, σ_{ij} is non-symmetrical, unless certain constraints are imposed on ε_{kl}. This effect was discussed in chapter IV. For an isotropic assembly, σ_{ij} (7.3) is symmetrical and constitutive relationships will take the form of Hooke's law

$$\sigma_{ij} = K\varepsilon_{kk}\delta_{ij} + 2G(\varepsilon_{ij} - \tfrac{1}{3}\varepsilon_{kk}\delta_{ij})$$

where K and G are bulk and shear moduli. This fact can be checked directly by calculating coefficients A^1_{kl}, A^2_{ijkl}. Several important coefficients which define elastic moduli are

$$A^1_{11} = \frac{1}{4\pi}\int_0^{\pi}\int_0^{2\pi} \sin^3\xi\, \cos^2\phi\, d\phi d\xi = \frac{1}{3}$$

$$A^2_{1111} = \frac{1}{4\pi}\int_0^{\pi}\int_0^{2\pi} \sin^5\xi\, \sin^2\phi\, \cos^2\phi\, d\phi d\xi = \frac{1}{15}$$

Straightforward calculations give

$$K = \frac{1}{3}\frac{\rho\gamma}{\pi d_o^2}\xi k_n \qquad (7.4)$$

$$G = \frac{1}{5}\frac{\rho\gamma}{\pi d_o^2}\xi k_n\left(1+\frac{3}{2}r\right) \quad ; \quad r = \frac{k_t}{k_n} \qquad (7.5)$$

Both moduli have the dimensionality of stress, since contact stiffnesses have dimensions of force.

Both elastic moduli are proportional to ξ which remains unknown. Expression (7.4) for K will be employed to determine ξ using experiments.

Since K/G is related to Poisson's ratio, it is independent of ξ and can be given in the form

$$\nu = \frac{1 - r}{4 + r} \tag{7.6}$$

Poisson himself considered the question of determining ν [27] by considering central atomic interactions. His analysis corresponds to zero tangential stiffness and the above formula gives $\nu = 1/4$, as obtained by Poisson.

The analysis is more general here and it can be seen that Poisson's ratio (7.6) is a function of the ratio of tangential to normal stiffnesses. This implies that $r>0$, which immediately shows that Poisson's ratio for granular materials is less than or equal 1/4.

Strictly speaking, the above analysis is applicable to bonded particles only. A perfect example is concrete for which $\nu \approx 0.10 - 0.15$.

Empirical constitutive relationships for elastic deformations of cohesionless materials presented by Rowe [30] do not give a unique interpretation for Poisson's ratio, since the same non-linear curves describing wide ranges of loads can be fitted by different combinations of his constant, including a power constant for stress. For reasonable power constants close to 2/3 (which follows from Hertz's theory of an elastic contact), the coefficient in Rowe's relationships, corresponding to Poisson's ratio, is less than 1/4.

The present theory was not developed for polycrystalline metals, so that it is impossible to expect a high Poisson's ratio near $\nu = 0.3$.

If particles are such that tangential stiffness is much greater than normal stiffness, $r \to \infty$ and (7.6) gives $\nu = -1$, so that Poisson's ratio

determined here satisfies the so-called "thermodynamic restrictions".

It is usually mentioned that materials with a negative Poisson's ratio are not encountered in reality. The above theory suggests how a material with a negative Poisson's ratio can be constructed by making particles very stiff in the tangential direction. Real particles do not possess this property. The topic will be only slightly touched upon in the next section.

The major significance of relationships (7.4-7.5) is that they give a chance to determine parameter ξ which determines the magnitude of elastic moduli and will be called the "stiffness reduction coefficient".

7.3 Determination of the Stiffness Reduction Coefficient

The above theory is developed for a linear contact model and its application to non-linear situations, strictly speaking, is unwarranted. However, if non-linear contact force-relative displacement relationships are considered, the relationships are linear for each load increment and contacts respond according to the linear contact model, although contact stiffnesses are not identical in all contacts due to fluctuation of contact forces, as is the case in the above theory.

At this point there are indications that the effect of varying stiffnesses leads to further reduction in the global stiffness of the assembly expressed in its deformation moduli. Moreover, there are indications that additional randomness in the system, whether related to varying particle size, stiffness or to some other unspecified factor, results in further reduction in stiffness. This conclusion follows by analogy with the influence of fluctuations in local density on global

stiffness.

Considering the complexity of a complete formulation of the problem, it will be assumed that relationships (7.4-7.5) for systems of varying size, shape and stiffness particles preserve their form with respect to averages and a cumulative effect of additional irregularities is contained in ξ.

Under this assumption analysis of experimental data is possible to determine ξ. Consider the expression for stiffness coefficients of ideally elastic spheres which follows from Hertz's theory of an elastic contact. By transforming expressions for the solution of Hertz's problem for elastic spheres [22], it can be shown that tangential stiffness of a non-linear contact can be given in the form

$$k_n = \frac{d_o^2 E_p}{2(1-\nu_p^2)} \frac{d_c}{d_o} \tag{7.7}$$

where E_p, ν_p are elastic parameters for granules and d_c/d_o is the ratio of the contact diameter to the diameter of the particle, so that

$$\frac{d_c}{d_o} = \left[f_n \frac{3(1-\nu_p^2)}{E_p d_o^2} \right]^{1/3} \tag{7.8}$$

where f_n is the contact force which will be taken as the average contact force for assemblies of particles.

Simple analysis shows that average normal contact force for an isotropic assembly can be given in the form

$$\overline{f}_n = \frac{\pi d_o^2}{\rho\gamma} \sigma_n \tag{7.9}$$

where σ_n is hydrostatic stress. The above relationship is similar to the one developed for plane systems, but with the second power of the particle's

diameter (which is required by dimensionality considerations).

Making use of (7.7-7.9) the bulk modulus (differential or tantengial modulus) can be given in the form

$$K = K_p \frac{1-2\nu_p}{1-\nu_p^2} \left(\frac{d_c}{d_o}\right) \frac{\rho\gamma}{\pi} \xi \tag{7.10}$$

where

$$\frac{d_c}{d_o} = \left[\frac{1-\nu_p^2}{1-2\nu_p} \frac{\pi}{\rho\gamma} \frac{\sigma_n}{K_p}\right]^{1/3} \tag{7.11}$$

and K_p is the bulk modulus of particles.

An interesting property of the above relationship is its independence of a particle's diameter, but the combination of structural parameters $\rho\gamma$ has decisive influence, as well as ξ. Note that practical application of the above relationships requires knowledge of the average coordination number-particle density relationship. This relationship will be developed for plane assemblies; for spheres a semi-empirical relationship developed in [38] will be used.

Noting that particle density ρ considered here is related to void ratio e

$$\rho = \frac{1}{1+e} \quad ,$$

the expression for the average coordination number given in [38] can be presented in the form

$$\rho\gamma = 26.5\rho - 10.7$$

The experimental data on hydrostatic compression are taken from [10].

It should be mentioned that the 2/3 power law for hydrostatic compression is not usually satisfied exactly due to formation of new contacts. Under higher stress level, when it can be expected that all potential contacts are formed, a new problem may arise. Due to the increasing area

of contacts under high loads, Hertz's theory may not be applicable.

In the opinion of the author, the 2/3 power law is pronounced in the mentioned experiments for a range of hydrostatic loads between σ_n + 300 - 625 kPA, and the tangential modulus is recovered as

$$K = 116 \ MPa$$

for $\sigma_n = 625 KPa$

and void ratio $e = 0.59$. The material tested was quartz sand with K_p = 36.9 GPa $\nu_p = 0.17$ [17]. Particle diameters of the tested material are irrelevant according to (7.10-7.11). Note that the size distribution and variations in stiffnesses are viewed as being included in ξ.

Calculations give $\xi = 0.1$ which indicates a drastic reduction in stiffness due to irregularity of the system's properties. The above estimate of ξ will be employed to study fluctuations of phenomenological parameters later.

7.4 Constitutive Relationships for Plane Anisotropic Assemblies

For plane assemblies of discs, average forces (6.48) are related to components of the strain tensor as follows:

$$\begin{aligned} \overline{f}_n(\theta) &= k_n \xi \, \varepsilon_{kl} n_l n_k \\ \overline{f}_t(\theta) &= k_t \xi \, \varepsilon_{kl} n_l t_k \end{aligned} \tag{7.12}$$

Stress tensor (3.29) can be given in the form

$$\sigma_{ij} = 2 \frac{\rho \gamma}{\pi d_o} \int_0^{2\pi} [\overline{f}_n(\theta) n_i n_j + \overline{f}_t(\theta) t_i n_j] S(\theta) d\theta \tag{7.13}$$

The contact orientation distribution will be considered with second and fourth Fourier components as follows:

$$S(\theta) = \frac{1}{2\pi}[1 + a \cos 2(\theta - \theta_o) + b \cos 4(\theta - \theta_o)] \tag{7.14}$$

Substitution of (7.12) into (7.13) results in the relationship between stress and strain tensors in the form

$$\sigma_{ij} = 2 \frac{\rho\gamma}{\pi d_o} \xi \left[k_n A^1_{ijkl} + k_t A^2_{ijkl}\right] \epsilon_{kl}$$

where

$$A^1_{ijkl} = \int_0^{2\pi} S(\theta) n_i n_j n_k n_l d\theta \qquad (7.15)$$

$$A^2_{ijkl} = \int_0^{2\pi} S(\theta) t_i n_j t_k n_l d\theta$$

Note that

$$\underset{\sim}{n} = \{\cos\theta,\ \sin\theta\}$$

$$\underset{\sim}{t} = \{-\sin\theta,\ \cos\theta\}.$$

Calculation of tensors (7.15) results in a set of relationships which can be better observed in a matrix form

$$\begin{Bmatrix} \sigma_{11} \\ \sigma_{12} \\ \sigma_{21} \\ \sigma_{22} \end{Bmatrix} = \frac{1}{4} \frac{\rho\gamma}{\pi d_o} k_n \xi \begin{vmatrix} A_{11} & A_{12} & A_{13} & A_{14} \\ A_{21} & A_{22} & A_{23} & A_{24} \\ A_{31} & A_{32} & A_{33} & A_{34} \\ A_{41} & A_{42} & A_{43} & A_{44} \end{vmatrix} \begin{Bmatrix} \epsilon_{11} \\ \epsilon_{12} \\ \epsilon_{21} \\ \epsilon_{22} \end{Bmatrix} \qquad (7.16)$$

where

$A_{11} = 3+r+2a\cos2\theta_o+(1-r)b\cos4\theta_o$ $\quad A_{12} = (1+r)a\sin2\theta_o+b(1-r)\sin4\theta_o$

$A_{21} = (1+r)a\sin2\theta_o+(1-r)b\sin4\theta_o$ $\quad A_{22} = 1+3r-2ar\cos2\theta_o-(1-r)b\cos4\theta_o$

$A_{31} = (1-r)a\sin2\theta_o+(1-r)b\sin4\theta_o$ $\quad A_{32} = (1-r)-(1-r)b\cos4\theta_o$

$A_{41} = (1-r)-(1-r)b\cos4\theta_o$ $\quad A_{42} = (1-r)a\sin2\theta_o-(1-r)b\sin4\theta_o$

$A_{13} = (1-r)a\sin2\theta_o+(1-r)b\sin4\theta_o$ $\quad A_{14} = (1-r)-(1-r)b\cos4\theta_o$

$A_{23} = (1-r)-(1-r)b\cos4\theta_o$ $\quad A_{24} = (1-r)a\sin2\theta_o-(1-r)b\sin4\theta_o$

$A_{33} = (1+3r)+2ar\cos2\theta_o-(1-r)b\cos\theta_o$ $\quad A_{34} = (1+r)a\sin2\theta_o-(1-r)b\sin4\theta_o$

$A_{43} = (1+r)a\sin2\theta_o-(1-r)b\sin4\theta$ $\quad A_{44} = 3+r-2a\cos2\theta_o+(1-r)b\cos4\theta_o$

In the above form anisotropic stress-strain relationships are valid for an arbitrary coordinate system (which explains their slightly complicated structure).

Stress tensor (7.16) is, generally, non-symmetrical, unless components of ε_{ij} are specially constrained. Since the symmetry of σ_{ij} reflects moment equilibrium, strain components cannot be independent.

The above constitutive relationships contain a wealth of information on the behavior of anisotropic assemblies. Only several aspects relevant to further applications will be discussed. Consider, first of all, a limiting case of an isotropic assembly ($a = 0$, $b = 0$). The stress tensor then is unconditionally symmetrical and (7.16) can be given in the form

$$\begin{aligned}
\sigma_{11} &= \frac{1}{4}\frac{\rho\gamma}{\pi d_o}\xi k_n(3+r)\left[\varepsilon_{11} + \frac{1-r}{3+r}\varepsilon_{22}\right] \\
\sigma_{22} &= \frac{1}{4}\frac{\rho\gamma}{\pi d_o}\xi k_n(3+r)\left[\varepsilon_{22} + \frac{1-r}{3+r}\varepsilon_{11}\right] \\
\sigma_{12} &= \frac{1}{4}\frac{\rho\gamma}{\pi d_o}\xi k_n 2(1+r)\varepsilon_{12}
\end{aligned} \tag{7.18}$$

The above relationships are similar to plane strain equations in three-dimensional elasticity. Bulk and shear moduli for a plane assembly can be calculated by presenting (7.18) in the form

$$\begin{aligned}
\frac{\sigma_{11} + \sigma_{22}}{2} &= K(\varepsilon_{11} + \varepsilon_{22}) \\
\sigma_{11} - \sigma_{22} &= 2G(\varepsilon_{11} - \varepsilon_{22}) \\
\sigma_{12} &= 2G\,\varepsilon_{12}
\end{aligned} \tag{7.19}$$

$$K = \frac{1}{2}\frac{\rho\gamma}{\pi d_o}\xi k_n; \qquad G = \frac{1}{4}\frac{\rho\gamma}{\pi d_o}\,k_n(1+r) \tag{7.20}$$

Consider as to what extent constitutive relationships for plane systems can be used in the analysis of plane strain conditions for three-

dimensional systems. This possibility can be expected, but not automatically assumed.

With constitutive relationships for three-dimensional assemblies of spheres it can be checked directly. Taking $\varepsilon_{33} = \varepsilon_{13} = \varepsilon_{23} = 0$ in the expression for Hooke's law and making use of moduli (7.4-7.5), stress compnents relevant to plane strain problems can be given in the form

$$\sigma_{11} = \frac{1}{5}\frac{\rho\gamma}{\pi d_o^2}\xi k_n \frac{1}{5}[3+2r][\varepsilon_{11} + \frac{1-r}{3+2r}\varepsilon_{22}]$$
$$\sigma_{22} = \frac{1}{5}\frac{\rho\gamma}{\pi d_o^2}\xi k_n \frac{1}{5}[3+2r][\varepsilon_{22} + \frac{1-r}{3+2r}\varepsilon_{11}] \qquad (7.21)$$
$$\sigma_{12} = \frac{1}{5}\frac{\rho\gamma}{d_o^2}\xi k_n \frac{1}{5}[2+3r]\varepsilon_{12}$$

Direct comparison of (7.21) and (7.18) shows that both systems are qualitatively equivalent only for $r = 0$ (zero tangential stiffness). In this case similarity in both stress and strain fields is assured in all problems involving elastic deformations.

This result cannot be checked for anisotropic assemblies, since constitutive relationships for three-dimensional anisotropic systems are not available. Note that the case $r = 0$ corresponds to Poisson's ratio $\nu = 0.25$. This is a reasonable Poisson's ratio for elastic deformations of cohesionless materials [30].

In the case of zero tangential stiffness ($r=0$), constitutive relationship (7.16) results in a symmetrical stress tensor (also for anisotropic systems) and strain components may be independent. Only in this case solutions of boundary value problems of continuum mechanics are relatively simple and well-explored. The developed constitutive re-

lationships are strictly valid for systems of bonded particles. Their application to the analysis of stress fields in cohesionless materials will be based on theoretical considerations presented in chapter X. In the meantime this case will be given the most attention.

Strictly speaking, the above constitutive relationships for $r = 0$ describe an irregular pin-jointed truss, i.e, an irregular network of segments, as in Fig. 2.2, jointed in vertices with pins. Such connection of truss members assures no tangential forces in its members, with only axial forces acting. These forces correspond to normal contact forces considered here*.

Constitutive relationships (7.16) take a simple form if written in a coordinate system with horizontal x-axis and a direction of anisotropy $\frac{\pi}{2}$ with respect to the y-axis (in the positive direction of - axis. In this case (7.16)(for $\theta_o = \frac{\pi}{2}$, $r = 0$) can be given in the form:

$$\begin{aligned} \sigma_{11} &= \frac{K}{2}\,[c_1\varepsilon_{11} + c_o\varepsilon_{22}] \\ \sigma_{22} &= \frac{K}{2}\,[c_o\varepsilon_{11} + c_2\varepsilon_{22}] \\ \sigma_{12} &= \frac{K}{2}\,[2c_o\varepsilon_{12}] \end{aligned} \tag{7.22}$$

where

$$\begin{aligned} c_1 &= 3 - 2a + \frac{b}{2} \\ c_2 &= 3 + 2a + \frac{b}{2} \\ c_o &= 1 - \frac{b}{2} \\ K &= \frac{1}{2}\,\frac{\rho\gamma}{d_o}\,\xi\,k_n \end{aligned}$$

*This comment contains a hint as to how the theory presented above can be checked explicitly using computer simulations of large irregular trusses.

Constants c_1, c_2, c_o depend on the geometry of contact orientations only. The bulk modulus K of corresponding isotropic assembly is non-essential and retained for dimensional consistency. Note that the form of (7.22) is only in the specifically selected coordinate system.

To gain some physical insight into the material described by (7.22) it is convenient to investigate its stiffness properties in different directions.

Suppose a rectangular sample of the material is cut as shown in Fig. 7.1[a] and subject to a load in the direction forming an angle Δ_σ with the direction of anisotropy. Consider an elongation of the sample in the direction of the load. Analysis can be conducted on the basis of (7.22), but it is easier to make use of results of chapter IV which placed principal emphasis on average forces in anisotropic systems.

Since parameters describing contact forces (4.31) are related (for the linear contact model) to invariants of the strain tensor according to (4.32), a combination of solutions (4.39) gives the following relationships between invariants of the stress and strain tensors:

$$\begin{aligned} \varepsilon_n &= \frac{\sigma_n}{K}\left[1 - \frac{a^2}{2c_f(1+r)}\left(R\cos 2\Delta_\sigma - 1\right)\right] \\ \varepsilon_t &= \frac{\sigma_n}{K}\left[\frac{a}{c_f(1+r)}\sqrt{D}\right] \\ \cos 2\Delta_\varepsilon &= \frac{R\cos 2\Delta_\sigma - 1}{\sqrt{D}} \end{aligned} \tag{7.23}$$

where $R = \frac{2a_\sigma}{a}$ and D, c_f are given by(4.40-4.41);Δ_ε is the principal direction of the strain tensor with respect to the direction fo anisotropy.

Relationships between invariants of both tensors can be obtained from (7.22) directly, but transformations are tedious.

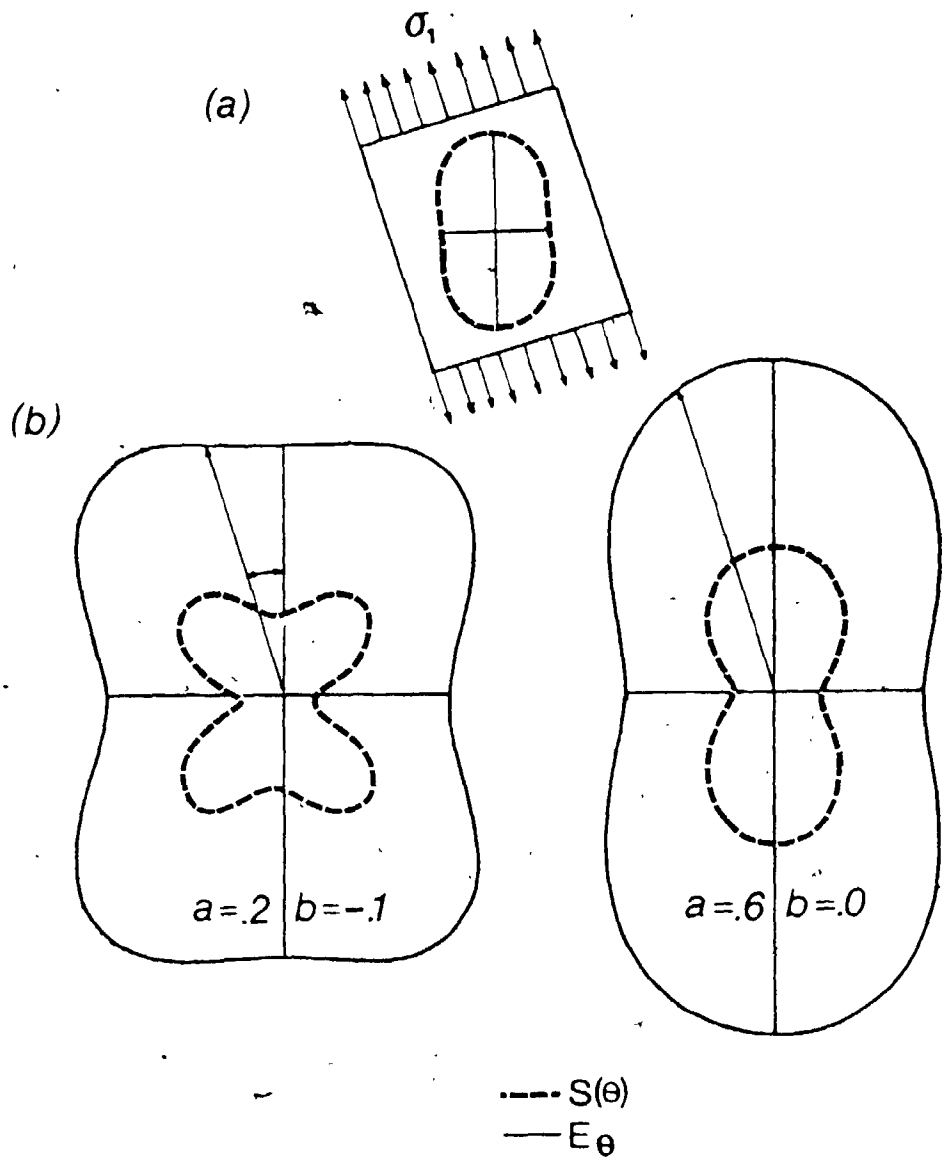

FIGURE 7.1

DIRECTIONAL STIFFNESS OF ANISOTROPIC ASSEMBLIES

If the material be subject to unidirectional load σ_1 per unit length of a plane boundary, σ_1 is the major principal stress and $\sigma_2 = 0$. Parameter $a_\sigma = \frac{\sigma_t}{\sigma_n} = 1$, since

$$\sigma_t = \frac{|\sigma_1 - \sigma_2|}{2}; \quad \sigma_n = \frac{\sigma_1 + \sigma_2}{2}$$

Elongation (or contraction) in any direction θ per unit length can be calculated as

$$\delta(\theta) = \varepsilon_{ij} n_j n_i = \frac{1}{2} [\varepsilon_n + \varepsilon_t \cos 2(\theta - \theta_\varepsilon)].$$

In the present case a response in the direction of the load is of interest, i.e. $\theta = \theta_\sigma$ where θ_σ is the principal direction of stress. The above relationship gives

$$\delta_1 = \frac{1}{2} [\varepsilon_n + \varepsilon_t \cos 2(\theta_\sigma - \theta_\varepsilon)]$$

Note that δ_1 is not a principal strain component. Making use of (7.22) one can obtain for a general case with r present the following relationship:

$$\delta_1 = \frac{\sigma_1}{E_\theta}$$

where

$$E_\theta^{-1} = \frac{1}{4K} \left[e_o - e_2 \cos 2(\theta_\sigma - \theta_o) - e_4 \cos 4(\theta - \theta_\sigma) \right] \quad (7.24)$$

and

$$e_o = 1 + \frac{1}{1+r} \left(\frac{1}{c_f} + \frac{1}{c_\mu} + \frac{2}{(1+r)} \right)$$

$$e_2 = \frac{2a}{c_f(1+r)}, \quad e_4 = \frac{1}{1+r} \left(\frac{1}{c_\mu} - \frac{1}{c_f} \right) \quad (7.25)$$

If $r=0$ and anisotropies are small (quadratic terms with respect to a, b are neglected), the following relationship is obtained

$$E_\theta = E_o [1 + a \cos 2(\theta_\sigma - \theta_o) + \frac{b}{2} \cos 4(\theta_\sigma - \theta_o)]$$

where $E_o = 2K$.

It may be seen that directional macro-stiffness for small anisotropies follows the trend of a contact orientation distribution. From the above relationship it may also be seen that the influence of b is less pronounced. Examination of the form of constants c_μ, c_f in (7.25) given by (4.41) shows that b does not influence stiffness properties of the material when $r=1$ (which corresponds to zero Poisson's ratio). This case will not be considered here. Fig. 7.1 shows several shapes of directional stiffness E_θ. It can be qualitatively observed that variation in E_θ is much more smooth compared to variations in contact distributions.

Average forces in systems governed by constitutive relationships (7.16) were studied in chapter IV. Everything said there is applicable to the considered systems of bonded particles if r be interpreted as k_t/k_n. Considerations of chapter IV are for arbitrary systems and in the present case the preferred direction of forces coincides with the major principal direction of strain.

Deviations of the major principal directions of stress and strain are shown in Fig. 4.9 and 4.11. An explanation for the existence of constraints on strain components was presented in section 4.8. In further applications only the case of zero tangential stiffness will be considered, in which case no restrictions on strain components exist.

7.5 Discussion and Conclusions

Constitutive relationships for linear systems of bonded particles were developed on the basis of expressions for average forces in terms of strain components. Stress-strain relationships are of the form con-

sidered in linear elasticity, but with explicit expressions for elastic moduli in terms of structural characteristics of assemblies and particle stiffnesses.

Three-dimensional systems were investigated only in the isotropic case due to a lack of information on the contact orientation distribution. The most interesting result is the expression for Poisson's ratio in terms of the ratio of tangential to normal stiffnesses. The developed expression is automatically within thermodynamic limits for this quantity.

Plane assemblies of discs were analyzed in the most general anisotropic case. The developed stress-strain relationships resulted in a non-symmetrical stress tensor which indicated that arbitrary deformation of the material violates moment equilibrium, so that there must be a restriction on deformation modes. This restriction was developed in chapter IV together with its physical explanation.

Allowable modes of deformation basically correspond to the "double-sliding model" [9]. In the present case there is no sliding, however, and deformations are elastic.

Deformations of considered isotropic systems are unrestricted when the tangential contact stiffness is zero. In this case tangential forces are zero and cannot create a moment which requires a special type of compensating deformation. This case is intended for further applications.

It was also shown that for systems with zero tangential stiffness constitutive relationships for isotropic assemblies of spheres degenerate,

in the plane case, to constitutive relationships for discs. This result is not valid for $r \neq 0$.

For $r = 0$ constitutive relationships take a simple form in a special coordinate system intended for solving problems of a point load on the considered media. The solution of this problem is, in fact, available in the literature [24], although the solution cannot be properly interpreted relative to the present theory as there is no information available as to the parameters a, b.

CHAPTER VIII

FLUCTUATIONS OF PHENOMENOLOGICAL PARAMETERS

8.1 Introduction

The distribution of forces on contacts of the same orientation permits an approach to the problem of assessing fluctuations of phenomenological parameters in finite volumes. Such fluctuations are, generally, due to irregularities in the structure of considered systems. The objective here is to evaluate the probability that the phenomenological stress tensor for a finite volume

$$\hat{\sigma}_{ij}(V) = \frac{1}{V} \sum_{c \in V} \frac{d_o}{2} f_i n_j \tag{8.1}$$

deviates from its average by a specified amount. The mentioned average is either an ensemble average of $\hat{\sigma}_{ij}$ (in this case fluctuations between similar volumes in different systems are studied) or $\hat{\sigma}_{ij}$ for an infinite homogeneous assembly (in this case fluctuations between similar volumes of the same system can be considered).

For non-homogeneous problems averages can be obtained using methods of continuum mechanics. It will be shown here that fluctuations of the stress tensor are related to the potential energy of the system and controlled by the number of contacts within the assembly and by the stiffness reduction coefficient ξ.

8.2 Variance of the Phenomenological Stress Tensor

Terms in the sum (8.1) representing $\hat{\sigma}_{ij}(V)$ can be reorganized

to group terms related to contacts of the same orientation

$$\hat{\sigma}_{ij}(V) = \frac{1}{V} \sum_{g=1}^{G} \hat{\sigma}^{g}_{ij} M_g \tag{8.2}$$

where

$$\hat{\sigma}^{g}_{ij} = \frac{1}{M_g} \sum_{c \in g} \frac{d_o}{2} f^{c}_{i} n^{c}_{j} \tag{8.3}$$

is the part of $\hat{\sigma}_{ij}$ related to contacts of the group g and M_g is the number of contacts in the group for the considered volume.

Let $P(\hat{\sigma}^{g}_{ij}/M_g)$ be the distribution of the sum (8.3) for a fixed number of contacts in the group. Considering that statistical analysis is performed with respect to different systems with similar micro-structure, forces on contacts of the same orientation group can be considered as statistically independent.

In this case $\hat{\sigma}^{g}_{ij}$ is the sum of independently distributed random variables and, if the number of contacts in the group be large, distribution $P(\hat{\sigma}^{g}_{ij}/M_g)$ is necessarily Gaussian due to the central limit theorem [26]. In the present case contact forces have Gaussian distribution and $P(\hat{\sigma}_{ij}/M_g)$ is also Gaussian, even for a small number of contacts in the group.

An average of this distribution coincides with the common average for each term in the sum (8.3), i.e.

$$\overline{\hat{\sigma}}^{g}_{ij} = \overline{f}_i n_j$$

Variance of σ^{g}_{ij} is, however, reduced and due to statistical independence

$$D[\hat{\sigma}^{g}_{ij}] = \frac{1}{M_g} n_i^2 D[f_i] = \frac{1}{M_g} n_i^2 (\overline{f_i^2} - \overline{f}_i^2) \tag{8.4}$$

where D denotes corresponding variances or, in physical terms, disper-

sions of corresponding quantities.

The above result is totally based on the assumed statistical independence of contact forces within the same orientation group. Consider a physical explanation of the assumed feature of contact forces for a single assembly. Due to irregularity in structure, contacts of the same orientation must be spatially separated, and the stricter the criterion for selecting contacts in an orientation group (the smaller the $\Delta\theta$), the greater the separation of contacts. The assumption of statistical independence is then equivalent to the assumption that forces on contacts are defined by an immediate environment of a contact (and level of boundary loads). Since it is reasonable to assume that micro-structures in distant localities are not correlated, the assumption of statistical independence of forces on contacts of the same orientation is physically warranted.

The dispersion of contact force components can be obtained from the correlation matrix (6.40) and expression (6.46). These results enable to rewrite (8.4) in the form

$$D(\hat{\sigma}^{g}_{ij}) = \frac{1}{M_g}\frac{2}{3}(1-\xi)k_n[\frac{1}{2}\gamma d_o n_v]^{-1} w_{f_c}[n_j^2 r + (1-r)n_i^2 n_j^2]\frac{d_o^2}{4} \quad (8.5)$$

where w_f is the complementary work per unit volume.

Consider now a dispersion of the phenomenological stress tensor given in the form (8.2). Calculation of the dispersion is easy only if $\hat{\sigma}^{g}_{ij}$ for different groups are statistically independent. This can hardly be the case, however. Forces on one group of contacts cannot be completely independent of all the remaining groups, since all groups form a total structure for which a gross balance of forces must be satisfied.

Complete independence of all groups of contacts is, however, not necessary to assess the dispersion of $\hat{\sigma}_{ij}$ and it is sufficient to assume a pair-wise independence. This assumption is more reasonable, since contacts of any two groups can still be considered as sufficiently spatially separated.

Consider how dispersion for the sum of random variables

$$\hat{X} = \sum \hat{x}_i$$

can be calculated in this case. First of all,

$$\bar{\hat{X}} = \sum \bar{\hat{x}}_i$$

and

$$\overline{(\hat{X} - \bar{\hat{X}})^2} = \sum_i (\hat{x}_i - \bar{\hat{x}}_i)^2 + \sum_{i,j} (\hat{x}_i - \bar{\hat{x}}_i)(\hat{x}_j - \bar{\hat{x}}_j)$$

It may be seen from the above relationships that only pair correlations between variables $\hat{x}_i$ entered the expression for the dispersion.

If random variables are pair-wise independent, then

$$\overline{(\hat{X} - \bar{\hat{X}})^2} = \sum_i (\hat{x}_i - \bar{\hat{x}}_i)^2$$

If pair-wise independence is assumed for different groups of contacts, dispersion of $\hat{\sigma}_{ij}$ given in the form (8.2) can be calculated as follows:

$$D[\hat{\sigma}_{ij}] = \frac{1}{V^2} \sum_{\epsilon=1}^{G} D[\hat{\sigma}_{ij}]\, M_g^2$$

With expression (8.5) and noting that $M_g = \Delta M_g = MS(\theta)\,\Delta\theta$, the dispersion of σ_{ij} can be given in an integral form when $\Delta\theta \to 0$:

$$D[\hat{\sigma}_{ij}] = \frac{1}{\gamma N} \frac{1-\xi}{\xi} \left[\frac{1}{3} \frac{\rho\gamma}{\pi d_o^2} \xi k_n \right] \phi_{ij} w_f \qquad (8.6)$$

where

$$\phi_{ij} = 3 \int_0^{\pi} \int_0^{2\pi} S(\xi, \nu) \left[r n_j^2 + (1-r) n_i^2 n_j^2 \right] \sin\xi \, d\xi d\nu$$

For an isotropic assembly $S = 1/4\pi$ and the last tensor is

$$\phi_{ij} = [r + \frac{1-r}{5}(1+2\delta_{ij})] \tag{8.7}$$

Note that the quantity in brackets in (8.6) is the bulk modulus (7.4) and that (8.2) can be expressed in terms of Poisson's ratio according to (7.6). Expression (8.6) can finally be given in the form

$$D[\hat{\sigma}_{ij}] = \frac{1}{\gamma N} \cdot \frac{1-\xi}{\xi} K \phi_{ij} w_f \tag{8.8}$$

where

$$\phi_{ij} = \frac{1}{1-\nu}[(1-4\nu) + \frac{3}{5}(1+2\delta_{ij})]$$

Dispersion of phenomenological stress components is proportional to the potential energy of the system and decreases with the number of contacts per unit volume.

Note that the bulk modulus in (8.8) is a characteristic of an ensemble of systems. As an example, consider an experiment in which the bulk modulus is to be determined using hydrostatic compression. Suppose the experiment is strain-controlled and a corresponding load is measured. To calculate dispersion of results in this test (repeated on macroscopically similar samples), note that $w_f = \sigma_n^2/2K$ and , assuming independence of fluctuations of stress components, (8.7) gives

$$s_o^2 = \frac{D[\sigma_n]}{\sigma_n^2} = \frac{1}{\gamma N} \frac{1-\xi}{2\xi} \cdot \frac{3}{5} \frac{5-11\nu}{1-\nu}$$

The coefficient of variation for bulk modulus measurements is

$$s_o = \left[\frac{\overline{(K-\overline{K})^2}}{\overline{K}}\right]^{1/2}$$

A 1000 cm^3 assembly of 1 mm diameter particles contains 1.19×10^6 particles for assumed void ratio 0.6. The empirical density - coordination number relationship [38] gives $\gamma = 9.38$, so that there are roughly

10^7 contact points. Taking an estimate for the stiffness reduction coefficient $\xi = 0.1$ (based on calculations of chapter VI) and arbitrarily selecting $\nu = 1/4$, $s_o = 8.5\,10^{-4}$. A "3 sigma" interval is about 0.25%. Standard deviation varies inversely proportional to the square root of the considered volume. This is a usual pattern of fluctuations [23] for "intensive" phenomenological parameters, such as pressure, stress, temperature, density.

8.3 Discussion and Conclusions

Fluctuations of the phenomenological stress tensor in finite volumes were investigated for isotropic three-dimensional assemblies of spheres. Variances of stress components were expressed in terms of potential energy of the system, the number of contacts in the studied volume and the stiffness reduction coefficient.

Although the considered systems were assemblies of spheres, the final formula is expressed in terms of the bulk modulus and Poisson's ratio. This fact suggests that the range of applicability of the derived relationships is greater than for merely assemblies of spheres.

Fluctuations were assessed assuming statistical independence of contact forces within the same orientation group and pair-wise independence of different orientation groups. It should be mentioned that different stress components are not statistically independent and their correlation can be assessed using the correlation matrix (6.40) for different force components.

The developed relationships indicate that the coefficient of varia-

tion of stress components decreases as the inverse of the square root of the number of contacts in the considered volume.

The numerical analysis of a test in which the bulk modulus was measured in hydrostatic compression showed that fluctuations in test results are not high for the selected "apparatus" (of the size of a "Proctor mold") and 1 mm particle diameter. The obtained "3 sigma" range was 0.25%.

In spite of the rather low level of fluctuations in the considered example, fluctuations of contact forces cannot be discarded from a practical point of view. Any instrumentation installed within granular systems reacts only to forces transmitted from a limited number of particles. The present theory can be useful in assessing fluctuations in such conditions.

It should be emphasized that the above derivations are not applicable to "plastic deformations of granular materials", where fluctuations can be expected to be higher. The reason for this conclusion is the following.

The above analysis showed that the variance of stress depends on the number of contacts in the system. This quantity entered calculations due to the mentioned assumptions of statistical independence of contact forces and the term γN in (8.8) is the number of statistically independent entities considered in the analysis.

It was observed [9] that during plastic deformations particles slide in blocks and such blocks may contain a substantial amount of particles. If statistics of such motion be considered, fluctuations must depend on the number of sliding blocks, and not on the number of

contacts.

The mechanism forming such conglomerates of sliding particles requires a level of analysis much higher that that considered so far. Geometrical methods considered further are also insufficient to attack the problem of fluctuations during significant rearrangements in the structure of considered systems.

CHAPTER IX

STATISTICAL GEOMETRY OF PLANE ASSEMBLIES OF DISCS

9.1 Introduction

The preceding analysis of mechanical equilibrium in granular assemblies pointed to the exceptional significance of the orientational distribution of contacts within granular systems. The outlined analysis was able only to proceed above generalities. This was due to the assumed shapes of the contact orientation distribution without indicating how the average coordination number of the assembly, which appeared in almost every relationship, can be measured.

Even with assumed shapes of the contact orientation distributions, the theory could not be applied, as the parameters describing the contact orientation distribution remained unspecified. There was even no qualitative indication as to how these parameters could be selected for assemblies of different densities. The answer to this question is the immediate objective of the present chapter. Its long-term objectives are much broader.

This work only touches upon the means of phenomenological description of granular assemblies and does not provide all answers regarding the extremely diversified responses of granular systems. The range from a liquid type behavior of cohesionless assemblies under shearing loads to the solid type response under hydrostatic compression.

In all cases involving static equilibrium, the mechanical concepts of stress and strain, developed by contact forces and local contact deformation levels, are perfectly applicable to all ranges of material

response, since they are based only on equations of static equilibrium and compatibility of the contacts. Applications of these concepts to descriptions of granular systems with aribitrary conditions at the contacts are perfectly legitimate, but the difficulties in practical analysis stem from lack of adequate description of the geometry of a system.

The long-term objective of this chapter is to provide the means of geometrical description which will ultimately permit the study of all ranges of mechanical response of granular systems under static equilibrium.

Deformations of cohesionless systems are complicated processes which involve significant structural changes. Before any analysis of such systems can be performed, it is necessary to answer a basic question: what configurations of particles may appear in this process? In other words, what structures are stable enough to survive under given external conditions and what new structures can be created under such conditions? Restrictions on the shapes of particle conglomerates are proposed here and, as a consequence of these restrictions, the shapes of contact orientation distributions can no longer be arbitrary. Parameter b, previously unspecified, will be a function of parameter a and the average coordination number. Parameter a remains a free parameter describing systems with different anisotropies and the theory must provide the means of measuring it.

Chapter IX will only indicate how this can be done with a "theoretical experiment" by transecting an assembly with a straight line. More feasible ways of determining this parameter will be presented later. The theory presented in this chapter is for plane assemblies of discs and generalizations for three-dimensional systems will not be attempted.

9.2 Geometrical Representation of an Assembly of Discs and Geometrical Condition of Stability

This geometrical representation of a plane assembly as a network of segments connecting particle centers has already been considered on several occations in this work. In the following geometrical analysis of plane systems, an original representation of assemblies in terms of particles is irrelevant and networks of segments are studied with practically no reference to their origin. Segments of networks will be considered of unequal lengths, although only small variations in their lengths will be studied. Such networks correspond to assemblies of discs with particles of slightly varying diameter.

Each segment of a considered (infinite) network can be characterized by its length τ and orientation θ. The entire network will be described by a density $T(\theta,\tau)$ which gives the number of segments per unit area $dm_v(\theta,\tau)$ with orientations close to θ and lengths close to τ in the form .

$$dm_v(\theta,\tau) = m_v T(\theta,\tau)\, d\theta d\tau \tag{9.1}$$

where m_v is the number of segments per unit area. This quantity is defined through a limiting operation

$$m_v = \lim_{V\to\infty} \frac{M(V)}{V}$$

where $M(V)$ is the number of segments in the area V. Considered networks are assumed to be homogeneous in the sense that the above limiting operation gives the same results for different infinite parts of the network. Distributions $dm_v(\theta,\tau)$, $T(\theta,\tau)$ are defined through the same limiting operation but are performed for segments with orientations in the range

between θ and $\theta + d\theta$ and length between τ and $\tau + d\tau$. The mentioned distributions are assumed to be continuous with respect to θ according to the hypothesis of "perfect irregularity", introduced previously.

Segments will be considered non-directed and all their orientations can be described in an arbitrary interval of the length π. $T(\theta,\tau)$ is defined to be normalized; i.e.

$$\int_0^{\pi}\int_0^{\infty} T(\theta,\tau)d\theta d\tau = 1$$

In all operations $T(\theta,\tau)$ will be considered in the form

$$T(\theta,\tau) = T(\tau)S(\theta),$$

i.e. no bias between a segment length and its orientation is assumed.

Note that $T(\tau)$ is not a distribution of particle diameters but can be related to it. If a particle size is known, $T(\tau)$ can be determined assuming a mechanism of contact formation. The simplest case is to assume that any two particles can form contacts equiprobably. In this case τ is the sum of two identically distributed random variables $\tau = \frac{1}{2}(d_1+d_2)$ where d_1, d_2 are diameters of particles in contacts. The distribution of $T(\tau)$ can be obtained as a convolution of particle size distributions.

If considered particles are of shapes other than discs, calculations may not be straightforward. However, the fact that is emphasized here is that it is not a specific form of considered particles that affects both mechanical response and geometrical analysis, but the above-mentioned distribution of segments.

Networks of segments studied here are not arbitrary, but subject to a geometrical restriction related to an intuitive concept of mechanical stability of corresponding assemblies. Fig. 9.1 shows conglomerates

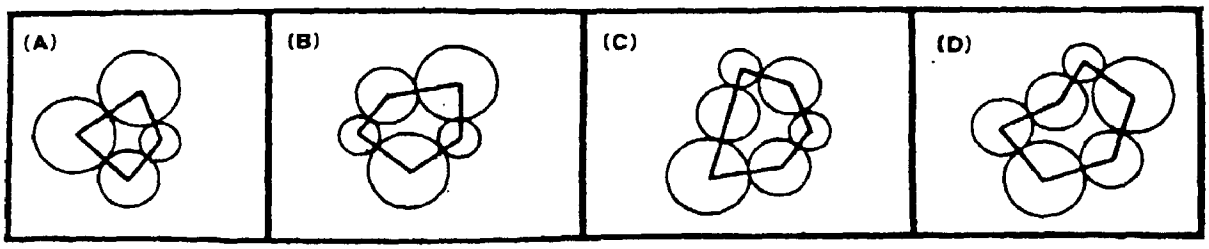

FIGURE 9.1

STABILITY OF PARTICLE CONGLOMERATES

of particles forming closed "voids" which can be characterized by a polygon connecting particle centers. It can be seen that conglomerates A, B can be intuitively ruled as stable, while conglomerate D is clearly unstable. Conglomerate C can be said to be on the verge of instability. It is readily noticed that a polygon corresponding to the "unstable" conglomerate D is non-convex, while the rest of the polygons, referred to as in the stable category, are convex.

In further analysis only networks of segments forming convex polygons will be considered as those representing stable equilibrium of plane granular assemblies. The objects of study are, therefore, irregular tessellations of a plane into convex polygons.

9.3 Transect Analysis of Segment Networks

Intersection of segments by a transect line has already been considered in sections 3.9 and 5.7 in connection with interpretations of phenomenological stress and strain tensors. This analysis is briefly repeated now and slightly different notations will be used.

Segments of the studied network are considered as non-directed segments. Orientational distribution of these segments can be described by the function $S(\theta)$ in (9.1), defined for any interval $\theta \div \theta + \pi$.

Suppose an infinite network is considered and a certain area V is selected that contains $M(V)$ segments. Let there be $dM_V(\theta, \tau)$ segments with close lengths in the interval $\tau \div \tau + d\tau$ and orientations $\theta \div \theta + d\theta$.

Consider the number of segments $dM_L(\theta, \tau | \alpha)$ intersected by a transect line L which makes an angle α with the x-axis of a fixed coordinate system. Let a series of lines parallel to L be drawn and let the spacing of lines be

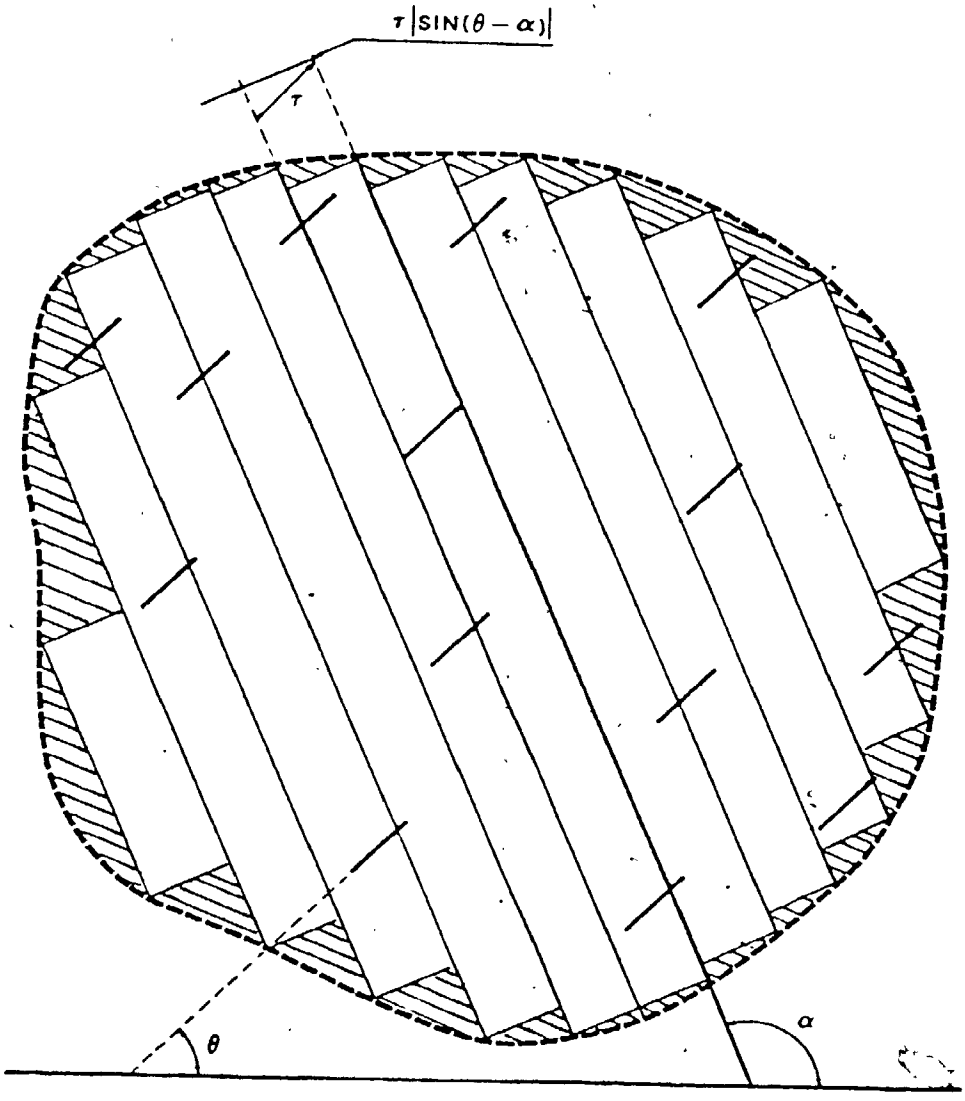

FIGURE 9.2

TRANSECT ANALYSIS OF SEGMENTS

such that each segment of the considered group be intersected only once and no segment be missed (Fig. 9.2). Spacing of such lines is $\tau\,|sin(\theta-\alpha)|$. Let $\sum L_\alpha$ be the length of all parallel lines in region V. Fig. 9.2 shows that

$$(\sum L_\alpha)\tau|sin(\theta-\alpha)| = V - v$$

where v is the shaded area in Fig. 9.2 representing an "edge effect" in the count of segments in a finite region. The above relationship can be given in an equivalent form

$$\frac{dM_V}{\sum L_\alpha} = \frac{dM_V}{V}\,\frac{1}{(1-v/V)}\,\tau\,|sin(\theta-\alpha)| \qquad (9.2)$$

Since all ΔM_V segments are intersected, the left-hand side of (9.2) is the number of intersections per unit length of all lines. A special notation for this quantity is introduced as follows:

$$dm_l(\theta,\tau|\alpha) = \frac{dM_V(\theta,\tau)}{\sum L_\alpha} \qquad (9.3)$$

Also let

$$dm_v(\theta,\tau) = \frac{dM_V(\theta,\tau)}{V} \qquad (9.4)$$

be the number of considered segments per unit area. For finite areas both Δm_l, Δm_v will fluctuate due to irregularities of the network; however, in the limit for an infinite area, fluctuations can be assumed to disappear. Hence, the ratio v/V will tend to zero and the following relationship is obtained:

$$dm_l(\theta,\tau|\alpha) = dm_v(\theta,\tau)\,\tau\,|sin(\theta-\alpha)| \qquad (9.5)$$

As all infinite parallel transect lines are equivalent for an infinite homogeneous network, $dm_l(\theta,\tau|\alpha)$ can be considered as the number of intersected segments of the length τ and orientation θ per unit length of the transect line; $dm_v(\theta,\tau)$ in (9.5) is the number of

segments in the considered group per unit area. Using (9.1), (9.5) can be given in the form

$$dm_l(\theta,\tau\ \alpha) = m_v\tau\,|sin(\theta-\alpha)|T(\theta,\tau)d\theta d\tau \qquad (9.6)$$

where m_v is the number of segments per unit area of an infinite network.

The total number of intersected segments per unit length of the transect line can be obtained by integrating (9.5) with respect to θ,τ. Making use of (9.6), the total number of intersections is as follows:

$$m_\alpha = m_v \int_{\alpha-\frac{\pi}{2}}^{\alpha+\frac{\pi}{2}} \int_0^\infty \tau|sin(\theta-\alpha)|\,T(\theta,\tau)d\theta d\tau \qquad (9.7)$$

Note that the range of contact orientations was selected for convenience as a symmetrical interval of the length π about the direction of the transect line. If $T(\theta,\tau)$ is represented as a product, the above relationship gives

$$m_\alpha = \bar{\tau}\ m_v \int_{\alpha-\frac{\pi}{2}}^{\alpha+\frac{\pi}{2}} |sin(\theta-\alpha)|S(\theta)d\theta \qquad (9.8)$$

where $\bar{\tau}$ is the average length of segments.

As an example, consider an isotropic assembly with

$$S(\theta) = \frac{1}{\pi}$$

Relationship (9.8) gives

$$m_\alpha = \frac{2}{\pi}\bar{\tau}\,m_v \qquad (9.9)$$

The above is the well-known result of geometrical probability [18] associated with Buffon's needle problem. In the present context this results remains valid. This was demonstrated by the specific logic of derivation based on formation of groups of segments and an explicit counting procedure.

Relationship (9.9) can be checked using the network in Fig. 2.1

consisting of 474 segments (including edge segments). The length of segments is 0.8 cm and the area occupied by the network is 144 cm^2. A set of lines of the length 12 cm was used to transect the assembly in both vertical and horizontal directions. The following results were recorded.

Vertical direction			Horizontal direction		
Number of intersections	Intersections per unit length	Average Experiment	Number of intersections	Intersections per unit length	Average experiment
18	1.500	1.500	19	1.583	1.708
19	1.583		21	1.250	
17	1.417		21	1.250	
18	1.500		21	1.750	

For the same direction of transect lines it can be seen that results do not fluctuate significantly, although there is a consistent difference in the number of intersections for vertical and horizontal directions. If the assemblies are assumed to be isotropic, (9.9) gives 1.676 intersections per unit length. The average over both directions of transect lines is 1.604.

An explanation for such a difference in "experimental" and theoretical results can be clearly seen from Fig. 2.2 which shows $S(\theta)$ for the considered assembly. That distribution can hardly be considered isotropic. To obtain a correction for anisotropy of the system, consider

$S(\theta)$ in the form

$$S(\theta) = \frac{1}{\pi}\left[1 + a\cos 2(\theta-\theta_o) + b\cos 4(\theta-\theta_o)\right] \tag{9.10}$$

where θ_o for the considered assembly is obviously $\frac{\pi}{2}$ with respect to the horizontal direction (Fig. 2.2). If (9.10) is substituted into (9.8) and the integration is performed, the number of intersections is directionally dependent and is of the form

$$m(\alpha) = \frac{2}{\pi}\bar{\tau} m_v \left[1 - \frac{a}{3}\cos 2(\alpha-\theta_o) - \frac{b}{15}\cos 4(\theta-\theta_o)\right]$$

The transect line is in the direction of anisotropy ($\alpha = \frac{\pi}{2}$)

$$m(\tfrac{\pi}{2}) = \frac{2}{\pi}\bar{\tau} m_v\left(1 - \frac{a}{3} - \frac{b}{15}\right) \tag{9.11}$$

and for the horizontal direction

$$m(0) = \frac{2}{\pi}\bar{\tau} m_v\left(1 + \frac{a}{3} - \frac{b}{15}\right) \tag{9.12}$$

With experimental intersections in two directions, parameters a, b can be estimated using (9.11-12)

$$\frac{m(0) - m(\frac{\pi}{2})}{2} = \frac{2}{\pi}\bar{\tau} m_v \frac{a}{3}$$

$$\frac{m(0) + m(\frac{\pi}{2})}{2} = \frac{2}{\pi}\bar{\tau} m_v\left(1 - \frac{b}{15}\right)$$

Statistical treatment of the histogram in Fig. 2.2 using least squares fit (with respect to a, b assuming the shape of $S(\theta)$ (9.10)) results in the following comparison of parameters a, b determined using two different techniques.

$a = 0.42$
$b = 0.60$ least squares fit (9.13)

$a = 0.39$
$b = 0.64$ transect analysis (9.14)

The agreement is rather close considering the small size of the sample (474 segments).

The above relationships will be employed further to check theoretical relationships between a and b.

9.4 Average Number of Sides per Polygon

For applications of segment network analysis to assemblies of discs, it is necessary to relate the average number of sides per polygon to the average coordination number of a plane assembly.

To relate these quantities note that each particle is related to a vertex of a polygon and each segment corresponds to a contact between particles.

Suppose a considered area contains P_i polygons with i sides. The total number of segments can be given as follows:

$$2M = \sum_i i P_i \qquad (9.15)$$

The coefficient 2 indicates that each segment is a common side of two polygons. Since the sum of internal angles for a polygon with i sides is $(i-2)\,\pi$, the total number of internal angles of all polygons is equal to $2\pi N$ where N is the number of particles, i.e.

$$2\pi N = \pi \sum_i (i-2) P_i \qquad (9.16)$$

and also

$$\sum_i P_i = P \qquad (9.17)$$

where P is the total number of polygons in the considered region.

Combination of (9.16-9.18) gives

$$M - N = P \qquad (9.18)$$

The above expression is a simplified form of Euler's identity which relates the numbers of polygon vertices to the sides of a connected graph. An exact form of this identity is $P = M - N + 1$, but for large

systems (9.18) is sufficiently accurate. Inaccuracy in the presented derivation appears in (9.16), since the complete circumference of boundary particles was considered and it does not correspond to the internal angles of the polygons.

If the average coordination number γ is introduced, $M = \frac{1}{2}\gamma N$ and, dividing (9.18) by area V, it is easy to obtain

$$N_P = \frac{1}{2}(\gamma-2)n_v \tag{9.19}$$

where n_p, n_v are the numbers of particles and polygons per unit area. The average number of sides per polygon is $\bar{n}_c = 2M/P$ and can be given in terms of the average coordination number using (9.18-9.19) to obtain

$$\bar{n}_c = \frac{2\gamma}{\gamma-2} \tag{9.20}$$

9.5 Chains of segments

Chains of segments are considered in sections 3.9 and 5.7 as analogues of line elements on which gross forces are calculated using the stress tensor and whose deformations are expressed in terms of the strain tensor. In the present section these entities are analyzed geometrically in greater detail.

Consider a transect line which intersects a certain number of segments. Fig. 9.3[a] shows the polygons associated with the intersected segments. Due to the convexity of the considered polygons, the number of intersected segments is exactly equal to the number of intersected polygons.

Consider chains of segments corresponding to particles which run "on average" parallel to the transect line (Fig. 9.3[b]). The chains con-

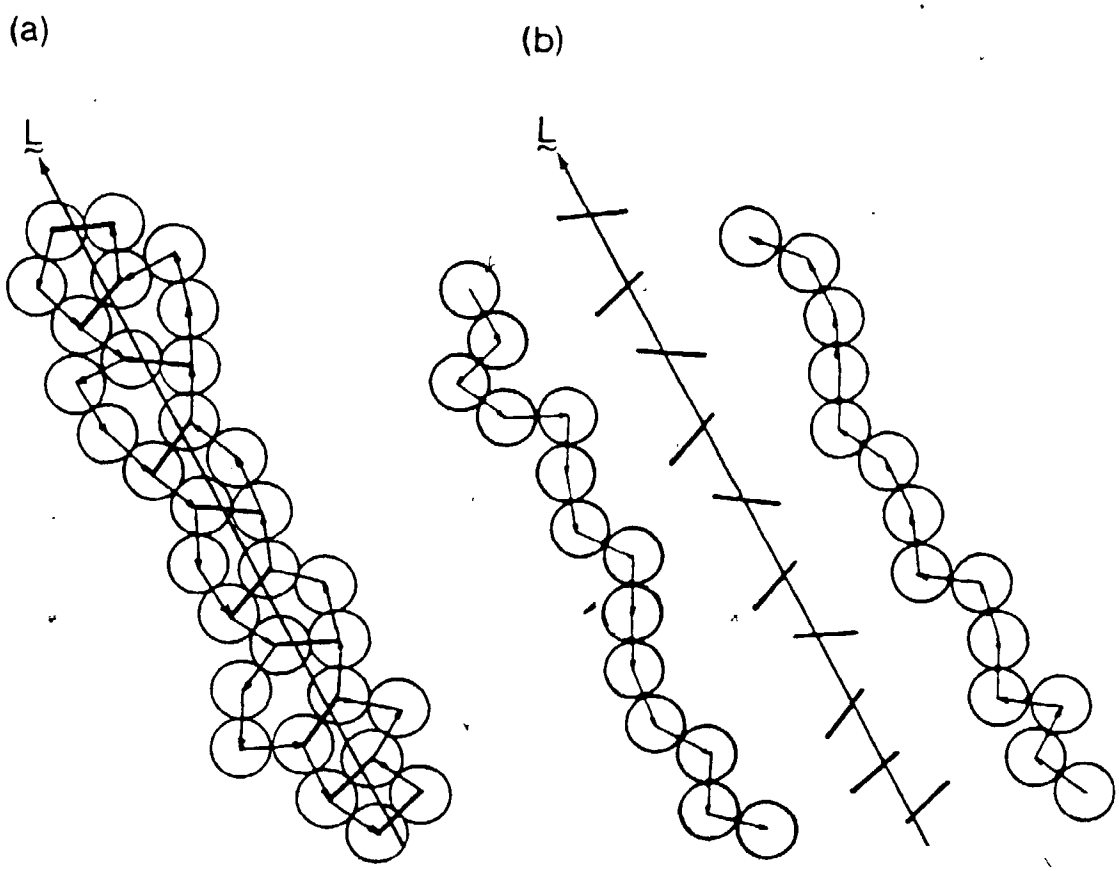

FIGURE 9.3

CHAINS OF PARTICLES

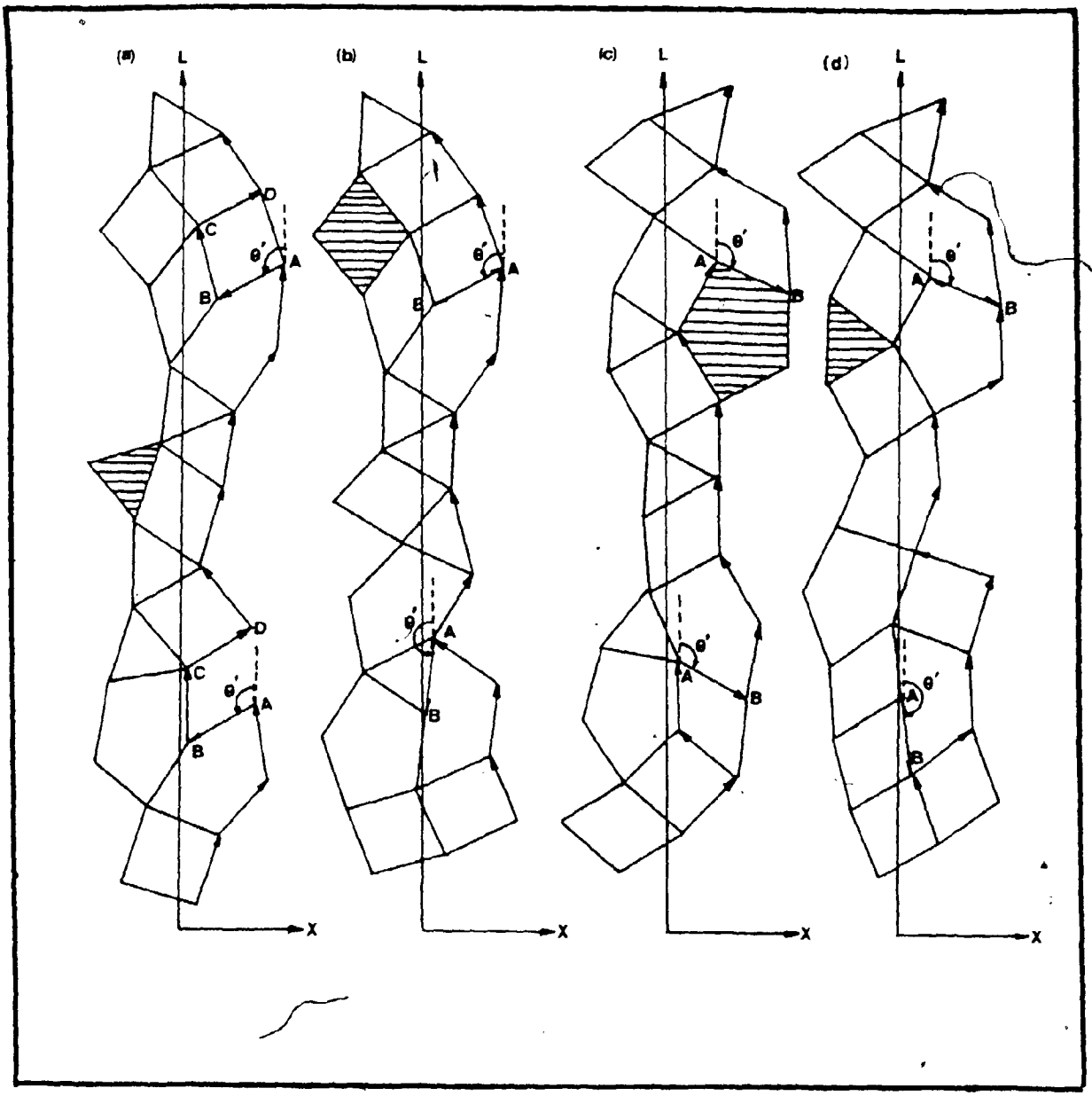

FIGURE 9.4

CHAINS OF SEGMENTS

sist of segments which

(i) belong to intersected polygons;

(ii) are not intersected by the transect line.

The two chains are formed by segments with the above properties and which are on opposite sides of the transect line. It is necessary to develop a distribution function of segments for any chain associated with a transect line of arbitrary orientation α.

Note that the majority of segments in the considered chains are oriented "along" the transect line and do not "run in the opposite direction". Fig. 9.4 shows several chains of particles with directed segments. Consider initially a distribution of non-directed segments in the chain. Such distribution $dm_c(\theta,\tau|\alpha)$ gives the number of segments per unit length of the chain with orientations between $\theta \div \theta+d\theta$ and lengths between $\tau \div \tau+d\tau$. This distribution, however, cannot supply information as to whether a segment runs "along" the chain or "in the opposite direction".

To determine this distribution consider polygons intersected by the transect line and a distribution of sides for these polygons. Let this distribution be $dp_l(\theta,\tau|\alpha)$. If this distribution is available, then

$$dp_l = 2dm_c + 2dm_c \tag{9.21}$$

where $dm_c(\theta,\tau|\alpha)$ is the distribution of intersected segments. The above relationship expresses the fact that all sides of intersected polygons consist either of segments which belong to the chains, or of intersected segments. The number 2 in front of dm_c indicates that there are two chains associated with intersected polygons.

The same coefficient for intersected segments distribution indicates that each intersected segment is counted twice in the distribution of polygon sides, since it corresponds to adjacent sides of two polygons. If dp_l in (9.21) be known, then the required distribution of segments in the chain can be obtained.

Consider how dp_l can be determined. The sides of all polygons in the assembly (per unit area) have a distribution

$$dp = 2m_v T(\theta,\tau)\, d\theta d\tau,$$

i.e. the original distribution of segments, but counted twice. Now consider the following question: is there anything special about the intersected polygons that makes the distribution of their sides different from the sides of all other polygons? Indeed, intersected polygons, in a certain sense, are special with respect to the transect line, since it picks polygons with the orientation and lengths of sides which are more favourable to intersection. On the other hand, it can easily be imagined that the complete assembly can be "disassembled" into blocks parallel to the transect line (like the four blocks of polygons in Fig. 9.4). If this decomposition is possible in such a way that all polygons be associated with a certain transect line and there be no "redundant" blocks, as shaded in Fig. 9.4, which do not form considered chains, then, due to statistical equivalence of different chains, the distributions of polygon sides will be identical in all blocks. Since the entire assembly is decomposed into such blocks, the distribution of polygonal sides in each block must be the same as the distribution of segments in the whole network.

Several attempts to perform this decomposition of the assembly presented in Fig. 2.2 fails, but the number of "redundant" polygons shaded in Fig. 9.4 was found to be small.

In the following analysis, the sides of polygons intersected by the transect line will be considered as distributed like all other segments of the considered network. Soon there will be the possibility to assess the accuracy of this approximation.

To determine the form of the required distribution exactly, note that the number of sides in intersected polygons can be obtained by multiplication of m_α by the average number of sides per polygon (9.20). Since the number of intersected polygons m_α is given by (9.8), finally,

$$dp_l = \frac{2\gamma}{\gamma-2} m_\alpha T(\theta,\tau)\, d\theta d\tau$$

The distribution of non-directed segments in the chain can be obtained using (9.21) which gives

$$dm_c(\theta,\tau|\alpha) = \frac{\gamma}{\gamma-2} m_\alpha - dm_l(\theta,\tau|\alpha)$$

If expressions (9.6-7) be used for dm_l, m_α the above distribution can be given in the final form

$$dm_c(\theta,\tau|\alpha) = \frac{1}{2}\gamma n_v \left\{ \frac{\gamma}{\gamma-2}\bar{\tau} \int_{\alpha-\frac{\pi}{2}}^{\alpha+\frac{\pi}{2}} S(\theta)\,|\sin(\theta-\alpha)|\,d\theta - \tau|\sin(\theta-\alpha)| \right\} S(\theta)T(\tau)\,d\theta d\tau \tag{9.22}$$

This distribution is crucial for the following analysis.

As an example, consider an isotropic assembly with $S(\theta) = 1/\pi$ and obtain an orientational distribution of segments with no regard to their lengths. Integration of (9.22) with respect to τ gives

$$dm_c = m_c S_c(\theta-\alpha)\,d\theta$$

$$m_c = \frac{2\gamma}{\gamma-2}\frac{n_v\bar{\tau}}{\pi}$$

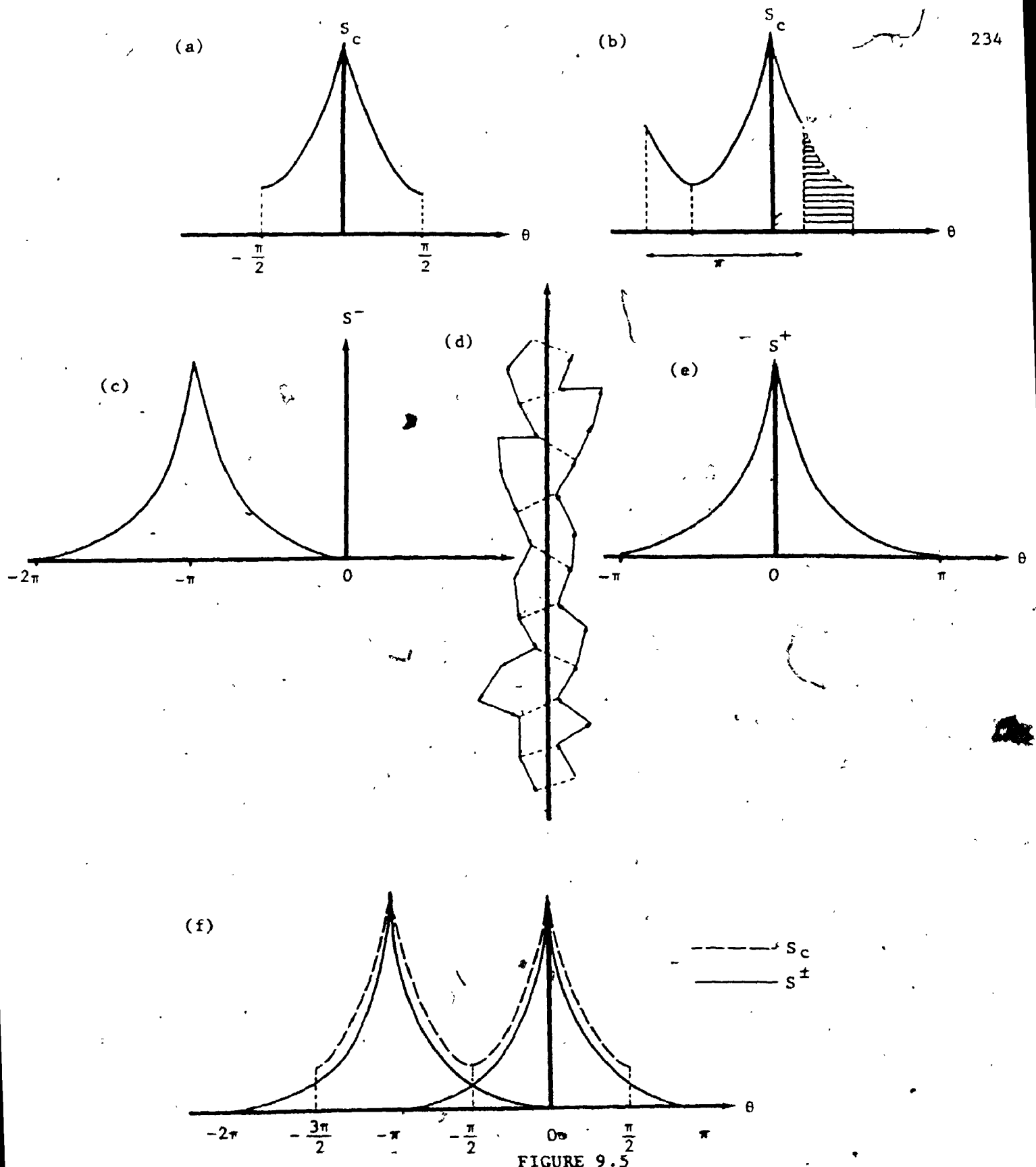

FIGURE 9.5

ORIENTATIONAL DISTRIBUTIONS OF SEGMENTS IN CHAINS

and $$S_c(\theta) = \frac{\gamma-2}{4}\left[\frac{\gamma}{\gamma-2}\cdot\frac{2}{\pi} - |\sin\theta|\right] \qquad (9.23)$$

Note that m_c above is the toal number of segments in the chain and $S_c(\theta)$ is the normalized orientational distribution of segments. Orientations of segments in (9.23) are measured from the transect line. Since the assembly is isotropic, $S_c(\theta)$ is independent of the orientation of the transect line. The shape of $S_c(\theta)$ is shown on Fig. 9.5[a] for an interval of the length π symmetrical about the transect line. $S_c(\theta)$, however, describes non-directed segments and in any other interval of the length π it will have a different form, as , for example, in Fig. 9.5[b].

The foregoing transect analysis of non-directed segments gives no indication as to how segments are directed within the chain. $S_c(\theta)$ gives their total number for any θ or $\theta + \pi$.

Now let segments of the chain be directed, as shown in Fig. 9.5[d]. There are actually two chains associated with each transect line. They are statistically equivalent, but with segments directed differently. The distribution of directed segments in both chains can be described by two distributions $S_c^+(\theta)$ and $S_c^-(\theta)$. It is quite clear that these distributions must have sharp maxima, one in the direction of the transect line ($S_c^+(\theta)$ on Fig. 9.5[e]) and the other in the direction opposite to the transect line ($S_c^-(\theta)$ on Fig. 9.5[c]). The shape of both distributions must be identical and

$$S_c^-(\theta) = S_c^+(\theta+\pi)$$

Although the majority of segments in each chain must be in the direction of the transect line (for S_c^+), the possibility of occasional segments having negative projections on the direction of the transect

line cannot be ruled out. Fig. 9.4 features situations where segments of the chain deviate significantly from the direction of the transect line (segments *AB* on Fig. 9.4[a-d]). This is why distributions $S^+(\theta)$, $S^-(\theta)$ are defined for intervals of the length 2π. It can, however, be expected that the "tails" of these distributions, corresponding to negative projections on the direction of the transect line, must be small.

It is necessary now to relate the distribution of non-directed segments to $S^+(\theta)$, $S^-(\theta)$. The distribution of non-directed segments actually never contains any information as to how the segments are organized in the chain. It was obtained by subtracting segments intersected by the transect line (dashed segments on Fig. 9.5[d]) from all segments corresponding to the sides of intersected polygons. In a certain sense both chains were "mixed up" in this procedure.

The only fact that remained certain for any interval of the length π is

$$S_c(\theta) = S_c^+(\theta) + S_c^-(\theta)$$

This relationship is illustrated on Fig. 9.5[f] with $S_c(\theta)$ shown with a dashed line. If an interval of θ be selected as symmetrical about the transect line, as in Fig. 9.5[a], then $S_c(\theta)$ contains mostly segments of the chain running in the direction of the transect line. In this case only a "tail" of the other chain is included in $S_c(\theta)$, which in this interval represents directed segments of one chain (approximately, of course). When the interval of θ was shifted, as in Fig. 9.5[b], a significant part corresponding to the other chain appeared.

The magnitude of "tails" of distributtions is difficult to assess exactly; although some information can be obtained. It can be seen that the minimum of $S_c(\theta)$ (at the point $\theta = -\frac{\pi}{2}$ on Fig. 9.5[f]) is twice the $S^+(-\frac{\pi}{2})$

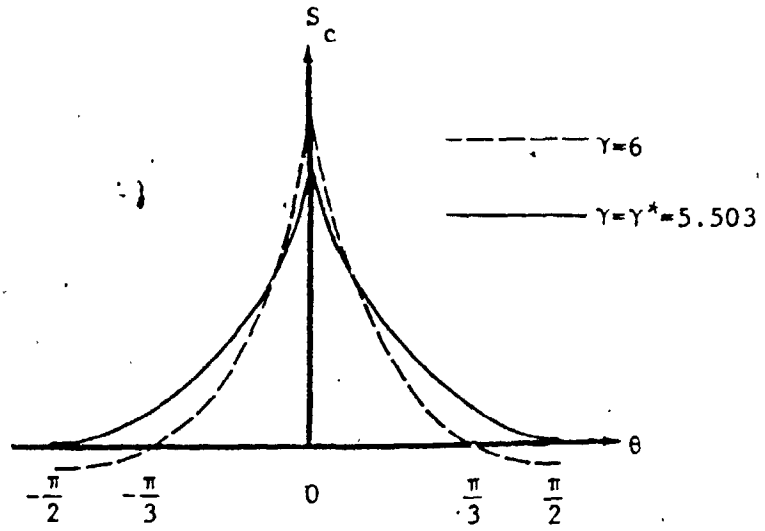

FIGURE 9.6

ORIENTATIONAL DISTRIBUTION OF SEGMENTS FOR DENSEST RANDOM STATE

at this point and, according to (9.23)

$$S_c^+(-\tfrac{\pi}{2}) = \tfrac{1}{2}S_c(-\tfrac{\pi}{2}) = \frac{\gamma-2}{\theta}\left[\frac{\gamma}{\gamma-2}\cdot\frac{2}{\pi} - 1\right]$$

Since it is reasonable to assume that $S_c^+(\theta)$ decreases monotonically, the above is an estimate for its magnitudes for $|\theta|>\frac{\pi}{2}$. For $\gamma = 4$, the following estimate is obtained

$$S_c^+(\theta)<0.068$$

and for greater coordination numbers the "tail" is of even smaller magnitude.

If the "tails" of the distribution of directed segments be neglected, distributions $S_c^+(\theta)$ and $S_c^-(\theta)$ will not overlap, as on Fig. 9.5[f]; and, for a proper selection of interval θ for $S_c(\theta)$ it will coincide with the distribution of directed segments.

For the considered isotropic assembly distribution (9.21) represents directed segments of the chain for

$$\alpha - \frac{\pi}{2} <\theta< \alpha + \frac{\pi}{2} \qquad (9.24)$$

where α is the orientation of the transect line. This is an approximation whose *a priori* accuracy is difficult to assess.

There is an extremely intersting feature associated with the above approximation. For the coordination number

$$\gamma^* = \frac{2\pi}{\pi-2} = 5.5039 \qquad (9.25)$$

distribution (9.23) is such that $S_c(\pm\frac{\pi}{2}) = 0$ (Fig. 9.6) which means that the "tail" of the distribution of directed segments does not exist and all segments in the chain have positive projections on the direction of the transect line. Moreover, $S_c(\theta)$ becomes negative for when θ is such that $\gamma>\gamma^*$. It is shown in Fig. 9.6 for $\gamma = 6$, i.e. for regular hexagonal packing.

Negative values of $S_c(\theta)$ are physically contradictive and the nature of this contradiction is obvious: for $\gamma>\gamma^*$ an assembly cannot be described by the contact orientation distribution $S(\theta) = \frac{1}{\pi}$. For $\gamma=6$ (closely packed assembly), there are only six possible directions for contact orientations and not the whole spectrum of contact orientations, as for $S(\theta) = \frac{1}{\pi}$.

The above result indicates that a uniform spectrum of contact orientations is impossible for $\gamma>\gamma^*$. This can be interpreted as the maximum coordination number corresponding to a "random" assembly.

There will be more support to this conclusion presented later, including experimental support. The above analysis of segment orientations in chains is only for isotropic assemblies. In anisotropic assemblies a preferred direction of segments in the chain does not generally coincide with the direction of the transect line and a selection of the interval of orientations for directed segments is not as simple.

In any case, the length of this interval must be π and it will be considered in a form similar to (9.24)

$$\alpha - \frac{\pi}{2} + \Delta(\alpha) \leq \theta \leq \alpha + \frac{\pi}{2} + \Delta(\alpha) \qquad (9.26)$$

i.e. shifted by an angle $\Delta(\alpha)$ which must be found considering equations of geometrical compatibility developed in the next section.

9.6 Equations of Geometrical Compatibility

By definition, chains of directed segments run parallel to the transect line. Their total projection on the direction of the transect line must be equal to its length and to zero on the perpendicular direction.

On the basis of distribution (9.22) developed per unit length of the transect line, the following relationships are obtained:

$$\int_0^{\infty} \int_{\alpha-\frac{\pi}{2}+\Delta}^{\alpha+\frac{\pi}{2}+\Delta} \tau \cos(\theta-\alpha)\, dm_c(\theta,\tau|\alpha) = 1$$

$$\int_0^{\infty} \int_{\alpha-\frac{\pi}{2}+\Delta}^{\alpha+\frac{\pi}{2}+\Delta} \tau \sin(\theta-\alpha)\, dm_c(\theta,\tau|\alpha) = 0 \qquad (9.27)$$

The above equations must be satisfied for any orientation of the transect line. The form of the equations which will follow becomes considerably more simple, if parameter

$$\chi = \frac{8\gamma}{\pi(\gamma-2)} - 4$$

be introduced instead of coordination number γ. If $\gamma = \gamma^* = 2\pi/(\pi-2)$, $\chi = 0$. The case $\chi = 1$ corresponds to coordination number

$$\gamma_* = \frac{10\pi}{5\pi-8} = 4.0757 \qquad (9.28)$$

It will be shown that the theory predicts the existence of irregular assemblies with stable structures within limits

$$0 \le \chi < 1$$

which correspond to

$$\gamma_* \le \gamma \le \gamma^*$$

i.e. the range between 4 and 5.5.

If distribution (9.21) is substituted into (9.3) and resulting integrals are slightly reorganized and the following equations are obtained:

$$(4+\chi)\bar{\tau}_0^{-2}\, \hat{F}_z^{11} S\, \hat{F}_z^{0} S - 4\bar{\tau}_0^{2}\, \hat{F}^{12} S = \frac{\pi}{2\rho}\, \frac{\pi\chi+4\pi-8}{4+\chi}$$

$$(4+\chi)\bar{\tau}_0^{-2}\, \hat{F}_z^{21} S\, \hat{F}_z^{0} S - 4\bar{\tau}_0^{2} \hat{F}^{22} S = 0 \qquad (9.29)$$

where

$$\hat{F}_z^{11} S = \frac{\pi}{2} \int_{-\frac{\pi}{2}+\Delta(z)}^{\frac{\pi}{2}+\Delta(z)} \cos x \, S(x+z)\, dx \qquad \hat{F}_z^{12} = \frac{\pi}{2} \int_{-\frac{\pi}{2}+\Delta(z)}^{\frac{\pi}{2}+\Delta(z)} \cos x \, |\sin x| \, S(x+z)\, dx$$

$$\hat{F}_z^{21} S = \frac{\pi}{2} \int_{-\frac{\pi}{2}+\Delta(z)}^{\frac{\pi}{2}+\Delta(z)} \sin x \, S(x+z)\, dx \qquad \hat{F}_z^{22} = \frac{\pi}{2} \int_{-\frac{\pi}{2}+\Delta(z)}^{\frac{\pi}{2}+\Delta(z)} \sin x \, |\sin x| \, S(x+z)\, dx \qquad (9.30)$$

$$F^{\rho} S(x+z) = \frac{\pi}{2} \int_{-\frac{\pi}{2}}^{+\frac{\pi}{2}} |\sin x| \, S(x+z)\, dx$$

Also

$$\bar{\tau}_o = \frac{1}{\sqrt{\overline{d_o^2}}} \int_0^{\infty} \tau \, T(\tau)\, d\tau$$

$$\bar{\tau}_o^2 = \frac{1}{\overline{d_o^2}} \int_0^{\infty} \tau^2 T(\tau)\, d\tau \qquad (9.31)$$

where $\overline{d_o^2}$ is the average of the square of particle diameters. Note that this quantity is introduced artificially into equations to have non-dimensional variables as $\bar{\tau}_o$, as well as to introduce area density of the assembly

$$\rho = n_v \frac{\pi}{4} \overline{d_o^2}$$

Both relationships depend on the variable z which measures orientation of the transect line with respect to the direction of anisotropy, i.e. $z = \alpha - \theta_o$. The variable of integration x in the integral operators was introduced after substituting $x = \alpha - \theta$ in the integrals in (9.30). This eliminated α from the limits of integration in (9.30).

Distribution $T(\theta,\tau)$ was taken as a product and integration with respect to τ was performed, so that the moments of $T(\tau)$ appeared.

Equations (9.29) contain two unknown functions $S(\theta)$, $\Delta(z)$, and also the unknown parameter ρ which must be determined. Simple applications of these equations will now be considered.

9.7 Density of Plane Isotropic Assemblies

9.7.1 Equal Size Discs

Consider an isotropic assembly of equal size discs. All segments of the network are of the same length, therefore

$$\overline{\tau}_o = 1, \quad \overline{\tau_o^2} = 1$$

The contact orientation distribution is $S(\theta) = 1/\pi$ and $\Delta(z) = 0$ (due to symmetry of all chains of segments). Integrals (9.30) can be calculated as follows:

$$F_z^{11} S = 1 \qquad F_z^{12} S = \frac{1}{2}$$
$$F_z^{21} S = 0 \qquad F_z^{22} = 0 \tag{9.32}$$
$$F_z^{o} = 1$$

Substitution of the above relationships into (9.29) shows that the second equation is satisfied identically and the first equation may be satisfied if ρ be the following function of χ

$$\rho_o = \frac{\pi}{2} \frac{\pi\chi + 4\pi - 8}{\chi^2 + 6\chi + 8}$$

The subscript indicates the density of equal size particles. If parameter χ is expressed in terms of γ, the following density - average

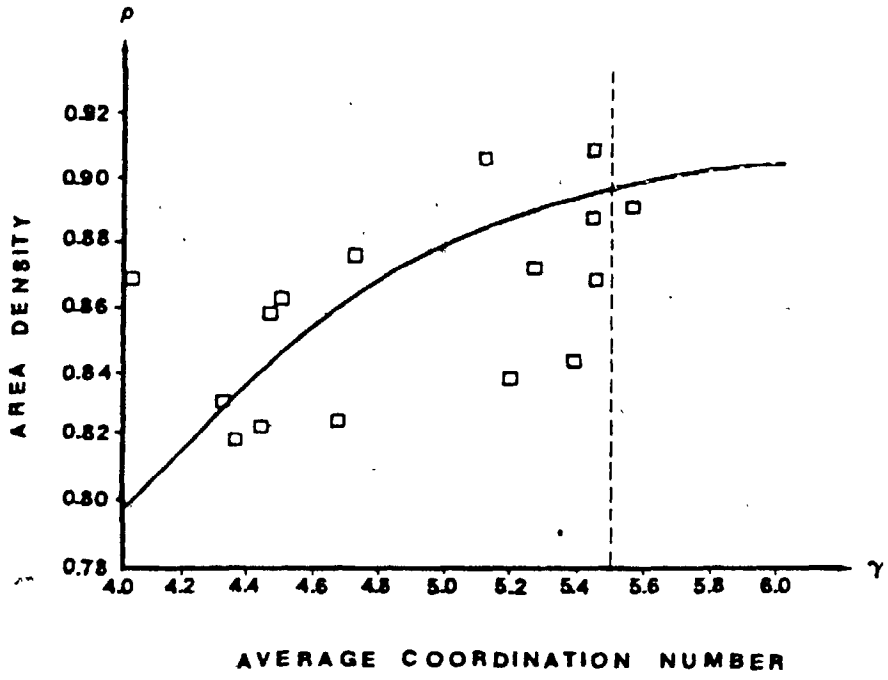

FIGURE 9.7

DENSITY - AVERAGE COORDINATION NUMBER RELATIONSHIP

coordination number relationship is obtained:

$$\rho_o(\gamma) = \frac{\pi^2}{4}\,\frac{\gamma-2}{\gamma}\,\frac{1}{1+\left(\frac{2}{\pi}-\frac{1}{2}\right)\gamma} \qquad (9.33)$$

Consider certain numerical values

$$\rho_o(6) = \frac{\pi^3}{72-12\pi} = 0.9039$$

For $\gamma = 6$ an assembly is a regular array for which

$$\rho_{reg}(6) = \frac{\pi}{2\sqrt{3}} = 0.9069$$

The above numbers differ by only 0.32%. Note that by using (9.33) for a regular array, the equations of compatibility were tested beyond their range of validity which could account for the slight error. Solution (9.33) is vaild for irregular systems only for $\gamma<\gamma^* = 5.505$

$$\rho_o^*(\gamma^*) = \frac{\pi}{4}(\pi-2) = 0.8966$$

The above expression is the maximum "random density" of a plane assembly.

For $\gamma = 4$ it is possible to compare "random density" with the density of a "quasi-isotropic" regular array

$$\rho_o(4) = \frac{\pi^3}{64-8\pi} = 0.7977$$

$$\rho_{reg}(4) = \frac{\pi}{4} = 0.7854$$

The difference here is 1.04%. Exact coincidence, of course, should not be expected.

Fig. 9.7 shows the density - average coordination number relationship compared with experimental results obtained by [29] and shown in Fig. 9.7 as presented in [32]. Considering the scatter of experimental points, the comparison can be said to be favourable.

It can be seen that the experimental data have no points for $\gamma>5.6$. This fact is in agreement with the conclusion that $\gamma = \gamma^* = 5.5039$ is the maximum coordination number for which an assembly of discs may

have a continuous spectrum of contact orientations, i.e. be perfectly irregular.

9.7.2 Varying Size Discs

In this case $S(\theta) = \frac{1}{\pi}$ and integrals (9.30) are the same. Averages $\bar{\tau}_o$, $\overline{\tau_o^2}$ depend on the particle size distribution and calculations will be performed without their specification.

Transformations as above give

$$\rho = \rho_o(\chi) C_\tau$$

where

$$C_\tau = \left\{ \frac{\bar{\tau}_o^2}{\overline{\tau_o^2}} \left[1 - \frac{2}{2+\chi} \left(\frac{\overline{\tau_o^2} - \bar{\tau}_o^2}{\bar{\tau}_o^2} \right) \right] \right\}^{-1}$$

The density of varying size discs is therefore controlled by the coefficient of variation of the segment size distribution.

The above expression for density indicates that an increase in the coefficient of variation increases the density of the assembly for the same coordination number. This trend is obvious and it is supported experimentally. On the other hand, the coefficient C_τ can even become infinite for a certain coefficient of variation of the segment size distribution.

The reason for this inconsistency lies in the nature of the approximations made. It was assumed that the polygons intersected by the transect line have the same length-orientation distribution as all the rest of the segments in the assembly. The accuracy of this approximation decreases with variations in segment lengths, since polygons intersected by the transect line statistically have longer sides than those not intersected. This effect does not appear to such an extent for equal size segments.

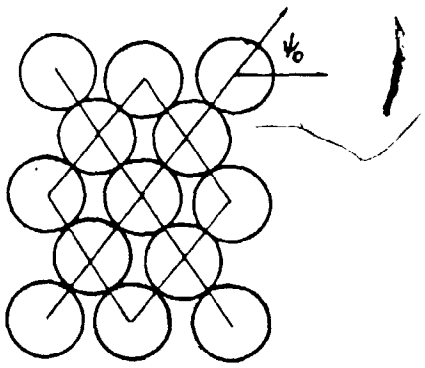

FIGURE 9.8

REGULAR ARRAY OF PARTICLES

Generally the probability for a polygon to be intersected is proportional to its perimeter. Polygons with a large number of sides in an equal size segment network have a greater probability of being intersected. For networks of equal size segments, only the orientational distribution of segments matters and the probability for a polygon of being intersected depends only on its perimeter. This explains why chain equations are accurate for equal size segments and can also be applied to segments of varying length only when the coefficient of variation is small.

9.7.3 Regular Array of Particles

Although the equations of geometrical compatibility were developed for irregular networks, there is no reason for them not be be valid for regular networks, as on Fig. 9.8.

The contact orientation distribution in this case is

$$S(\theta) = \frac{1}{4}[\delta(\theta-\psi_o) + \delta(\theta+\psi_o) + \delta(\theta-\psi_o-\pi) + \delta(\theta+\psi_o+\pi)]$$

where ψ_o is shown on Fig. 9.8.

It can be shown that orientations of directed segments in the chain are, indeed, within limits of the (9.26) type, where Δ is a certain discontinuous function. Substitution of the above contact orientation into chain equations indicates that they can be satisfied only when

$$(4+\chi)\frac{\pi}{16} - 1 = 0$$

$$\rho = \frac{\pi}{4\sin 2\psi_o}$$

The first of the above relationships results in χ corresponding to $\gamma = 4$ and the second equation gives the density of a regular array. It should be mentioned that transformations leading to the above result

are tedious and unlike those for irregular structures for which chain equations are more natural.

9.8 Contact Orientation Distribution for Anisotropic Assemblies and Their Density

Equations (9.29) are applied to anisotropic networks of equal size segments. A correction for minor variations of segment length will also be indicated.

Equations of geometrical compatibility for $S(\theta)$ are of a very complicated analytical nature and no attempt is made here to investigate the uniqueness of their solutions. The existence of these solutions was demonstrated for isotropic assemblies and a regular array, indicating that solutions of these equations are not unique. This comes as no surprise, since the existence of regular assemblies is a fact and the existence of perfectly irregular structures is a reasonable assumption. The question as to whether there are stuctures with contact orientations other than those indicated is very interesting, but no attempt will be made here to investigate such a possibility.

In short, it is not clear whether (9.29) are integral equations with solutions only for certain types of relationship between ρ and χ (an eigenvalue type problem), or whether (9.29) must simply be viewed as integral restrictions. In the author's opinion, based on analytical work with these relationships, they can be considered as integral equations. The fact that two solutions have already been found suggests that there may be a perfect spectrum of solutions which can be expected considering the possible diversity of geometrical structures.

The objective here is to find a solution that corresponds to a continuous distribution describing anisotropic structure. The solution will be attempted only for small anisotropies and no attempt will be made to consider Fourier components of the order higher than the fourth, i.e. a solution will be sought in the form (9.10) and it is necessary to investigate whether equations will be satisfied for all a, b, or whether there will be a restriction on these parameters. Only small degrees of anisotropy will be considered and an attempt will be made to satisfy equations (9.29) with accuracy $0(a^2)$, $0(b^2)$. To achieve higher accuracy of solutions, higher Fourier components in $S(\theta)$ must be considered. Even after invoking approximations in parameters a and b, the procedure is very tedious, especially for the coordination number γ^* (suspected to be the maximum coordination number). In this case, where $\chi = 0$, anisotropic perturbations near $\chi = 0$ result in drastic directional variations in the assembly structure. The strategy for the solution is the following:

(i) to substitute the form of $S(\theta)$ into the second equation (9.29) which will be then an algebraic equation for $\Delta(z)$ and the solution must depend on all parameters of the equation, i.e. $\Delta = \Delta(z, a, b, \chi)$;

(ii) to substitute $\Delta(z, a, b, \chi)$, $S(\theta)$ into the first equation (9.31), to decompose the result into Fourier series, and to attempt to equate to zero Fourier coefficients which are linear with respect to a, b.

This way the first equation will be satisfied with accuracy $0(a^2)$, $0(b^2)$. An attempt to implement this strategy immediately reveals peculiar

features of equations (9.31).

If $S(\theta)$ is substituted into the second equation (9.29), the resulting algebraic equation

$$\Phi_2(\Delta, z, a, b, \chi) = 0 \tag{9.34}$$

is transcendental and cannot be solved analytically. Computer analysis showed that the solution does exist. To determine an approximate solution analytically, note that $\Delta = 0$ corresponds to the isotropic case, when $a = 0$, $b = 0$. This suggests that Δ will be of the first order of magnitude with respect to a, b and a solution of (9.34) can be obtained by decomposing Φ_2 into a power series. Retaining only linear terms, the solution is as follows:

$$\Delta(z) = \frac{2}{3}\frac{a}{\chi}(1+\chi)\sin 2z + \frac{4}{15}\frac{b}{\chi}(1-\chi)\sin 4z \tag{9.35}$$

According to the introduction of $\Delta(z)$, it restricts orientations of segments in the chain with orientation z (z is the orientation of the transect line with respect to the direction of anisotropy). The function $\Delta(z)$ carries indirect information on contact orientations in the assembly.

It can be seen that the above solution contains a singularity when $\chi = 0$, i.e. near the densest "random" state. This singularity is only due to considerations of only linear terms with respect to Δ terms in (9.34). The above solution suggests that the linear approximation is physically inadequate in the vicinity of $\chi = 0$.

Extensive numerical analysis showed that the following approximation for Φ_2 in (9.34) is sufficiently accurate:

$$A_3\Delta^3 + A_1\Delta + A_0 = 0 \tag{9.36}$$

where

$$A_3 = \frac{4-\chi}{6}$$

$$A_1 = \chi$$

$$A_0 = -\frac{2a}{3}(1+\chi)\sin 2z + \frac{4b}{15}(1-\chi)\sin 4z$$

Note that the exact form of coefficients A_3, A_1, A_0 contains close to 30 terms which were neglected after a check that equation (9.34) with coefficients (9.36) is satisfied with accuracy $0(a^2)$ (b^2) for χ not close to zero and with accuracy $0(a^{4/3})$ for $\chi \doteq 0$. A numerical check, however, showed that the solution based on (9.36) is very accurate for all ranges of χ.

The above tedious details were presented to examine the singularity with respect to χ. The final solution for $\Delta(z)$ is continuous with respect to all parameters, although its derivatives with respect to a, b, χ for $\chi = 0$ are singular. The solution of the above cubic equation can be given in analytical form.

The first equation of (9.29) is of the form

$$\Phi_1(z,\ a,\ b,\ \chi,\ \Delta(z)) = \frac{\pi}{2\rho}\,\frac{\pi\chi + 4\pi - 8}{4 + \chi} \qquad (9.37)$$

after substitution of $S(\theta)$, $\Delta(z)$. Function Φ_1 is extremely complicated near $\chi = 0$, but for χ not close to zero, it is automatically quadratic with respect to a, although it contains terms linear with respect to b.

An analytical reason for such a form with respect to a is the following. Suppose $S(\theta)$ is taken in the form

$$S(\theta) = \frac{1}{\pi}\,[1 + a\cos(\theta-\theta_0)] \qquad (9.38)$$

i.e. b is neglected. If χ is not close to zero, Δ given by (9.35) is linear with respect to a and it can be shown that Φ_1 (9.37), as a function

of $\Delta(z)$, is quadratic with respect to Δ, so that the influence of Δ on (9.37) for $\chi \neq 0$ can be neglected.

It can also be shown that operator F_z^{12} is quadratic with respect to a, but F_z^{11}, F_z^{ρ} are of the form

$$F_z^{11} = (1 + \frac{a}{3} \cos 2z)$$

$$F_z^{\rho} = (1 - \frac{a}{3} \cos 2z)$$

Their product, which enters the original equations, is, therefore, quadratic with respect to a.

This fact has an important physical meaning. The shapes of distributions (9.38) are natural for anisotropic networks. If terms with b are added into (9.38), analysis shows that their influence on equations is linear. In order to satisfy equations of compatibility in the considered approximation, b cannot be independent. For $\chi \neq 0$ analysis shows that the equations of compatibility are satisfied with accuracy $0(a^2)$ $0(b^2)$ when

$$b = b(a,\chi) = -\frac{5}{12} a^2 \frac{2+\chi^2}{\chi - \chi^2} \tag{9.39}$$

$$\rho = \rho(a,\chi) = \rho_o(\chi) C_a(a,\chi) \tag{9.40}$$

where

$$C_a(a,\chi) = 1 + \frac{a^2}{18} \frac{3\chi^2 + 8\chi + 2}{\chi^2 + \chi}$$

The above relationship for b contains two singularities: one related to the densest state for $\chi = 0$, the other related to the loosest state for $\chi = 1$; $\chi = 1$ corresponds to $\gamma_* = 4.076$. When $\chi = 1$, the equations of compatibility are satisfied with accuracy $0(a^2)$ $0(b^2)$ for arbitrary a and b.

Consider the physical meaning of the foregoing. An assembly of N discs has $2N$ geometrical degrees of freedom (positions of particle centers). Suppose the position of a particle is perturbed slightly. Consider the possibility that a variation in the position of a particle is possible without disruption of contacts. If contacts are preserved under perturbations, the positions of all particles during these perturbations must satisfy M conditions of compatibility in M contacts.

If $M>2N$, the number of contact constraints exceeds the number of degrees of freedom which means that perturbations are impossible in the position of a particle without disruption of contacts. In this case an assembly can be viewed as being geometrically stable, i.e. it cannot be continuously transformed into another assembly.

If $M<2N$, i.e. the number of contact constraints is less than the number of degrees of freedom, the geometry of the system can be continuously changed without disruption of contacts. Such an assembly is geometrically unstable.

The case $M=2N$ is the boundary of geometrical instability which corresponds to coordination number $\gamma = 2M/N = 4$. The singularity at $\gamma_* = 4.076$ is most probably related to the said geometrical instability. The fact that the above instability appears at $\gamma_* = 4.076$ instead of $\gamma = 4$ is a reflection of the approximations made when the equations were derived and solved. The error is certainly not significant. Note that a system of cohesionless frictionless particles is statically determinate for $\gamma = 4$.

When $\gamma<4$, static equilibrium cannot be maintained and a system with such a low coordination number is a "plane liquid". For $\gamma>4$ the system

is statistically indeterminate and stable. The case $\gamma = 4$ corresponds to liquid - solid phase transition for plane systems (the fact is experimentally supported in [29]).

Relationship (9.39) for b shows that it must change sign passing through $\gamma_* = 4.076$ and be positive for $\gamma<\gamma_*$. In the assembly in Fig. 2.1, the average coordination number is between 3.82-3.85 (depending on the treatment of boundary contacts). Parameters a and b were estimated in section 9.3. If a is assumed correct, the following comparison of estimates can be given:

$a = 0.405 \quad b = 0.60$ for $\gamma = 3.83$ (according to (9.39))

$a = 0.405 \quad b = 0.62$ for $\gamma = 3.83$ (average of (9.13-14))

The agreement is quite satisfactory. Relationships (9.39) are valid for loose states only.

A complete analysis based on the solution of cubic equation (9.36) for $\Delta(z)$ results in a rather complicated, but interesting expression for b:

$$b(a,\chi) = -\frac{5}{24}\,\frac{\tilde{a}\,\frac{18\chi}{1-\chi}\,\phi_4\!\left(\frac{\chi}{\tilde{a}}\right) - \tilde{a}^3\,\frac{4+\chi}{(1+\chi^2)(1-\chi)}}{1-\frac{\tilde{a}}{4}\left[\frac{14-9\chi}{1-\chi}\,\phi_8\!\left(\frac{\chi}{\tilde{a}}\right) + \frac{7\chi-2}{1-\chi}\,\phi_0\!\left(\frac{\chi}{\tilde{a}}\right)\right]} \qquad (9.41)$$

where

$$\tilde{a}^3 = 2a^2(1+\chi)^2$$

and

$$\phi_{2n}(x) = \frac{2}{\pi}\int_0^{\frac{\pi}{2}} \tilde{\Delta}(z,x)\cos 2nz\,dz$$

$$\tilde{\Delta}(z,x) = \left[\cos z + \sqrt{\cos^2 z + x^3}\,\right]^{2/3} + \left[\cos z - \sqrt{\cos^2 z + x^3}\,\right]^{2/3} - 2x$$

The above solution was obtained using the outlined strategy of decomposition of $\phi_1(z,a,b,\chi,\Delta(z))$ into Fourier series and equating to

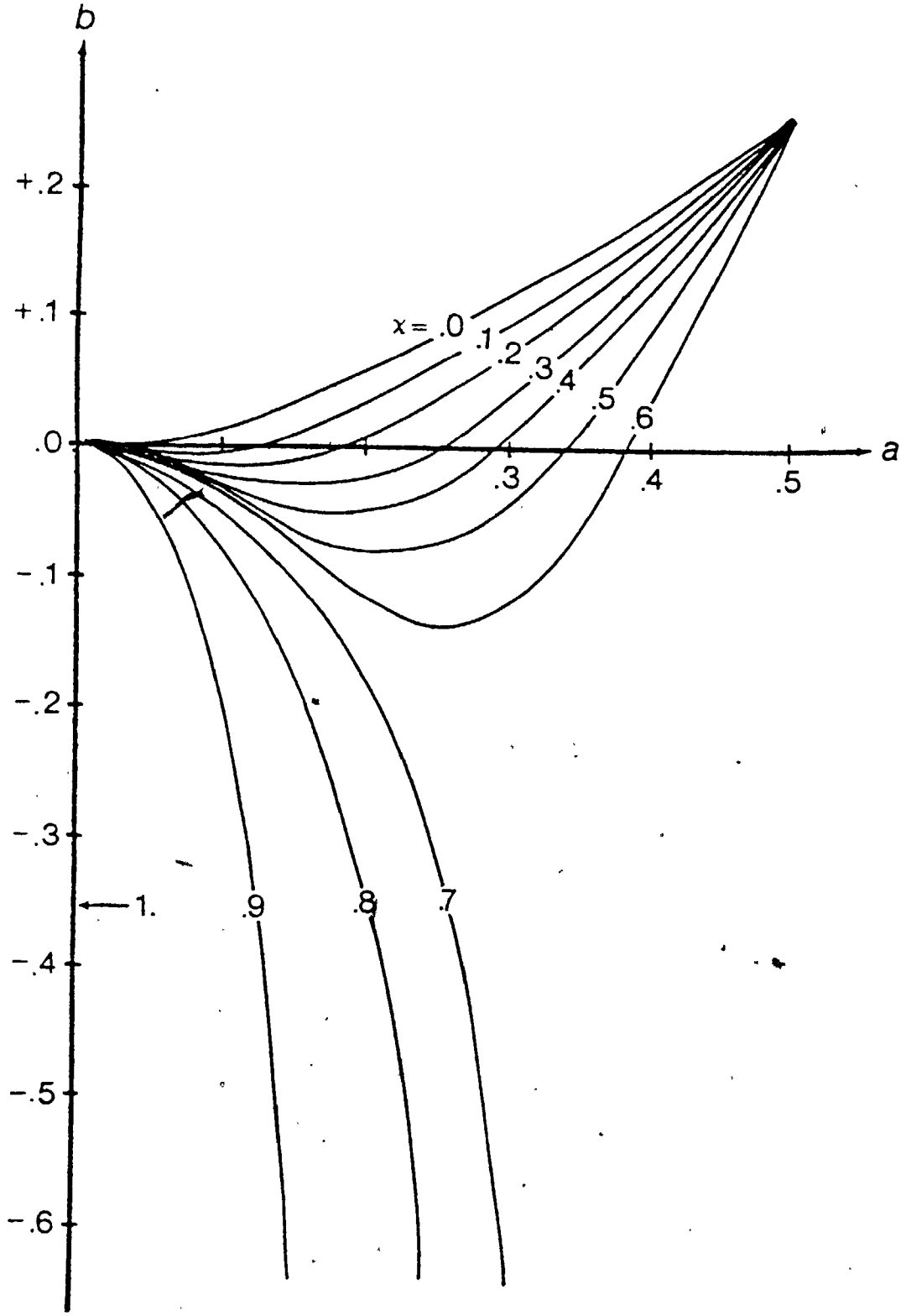

FIGURE 9.9

RELATIONSHIP BETWEEN PARAMETERS OF ANISOTROPY

zero a term which contains b linearly (fourth Fourier component of Φ_1). Function Δ is the form of the solution of (9.36) and ϕ_{2n} are its Fourier components.

For small anisotropies when $a<<\chi$, the argument of ϕ_{2n} in (9.41) is large and these functions have asymptotic expansions as follows:

$$\phi_0 = \frac{2}{9}\, x^{-2}; \quad \phi_4 = \frac{1}{9}\, x^{-2}; \quad \phi_8 = O(x^{-4})$$

Relationship (9.39) follows for small anisotropies and when $\chi \neq 0$.

The relationship for b (9.41) covers the entire range of densities and is shown on Fig. 9.9. It can be seen that there are two distinct patterns characteristic of dense ($0 \leq \chi \leq 0.6$) and loose ($0.6 \leq \chi \leq 1.$) assemblies.

It is difficult to present a precise qualitative explanation for such peculiar features of microstructure; however, an attempt will be made. In a dense state the structure of an assembly consists of closely packed particles which correspond to triangles in the network of segments. If an assembly is anisotropic and dense (Fig.9.10[a]), its structure must basically correspond to hexagonal packing with "lateral contacts" disintegrated. This explains the sharp minimum of $S(\theta)$ in the direction corresponding to these contacts. Moreover, with excessive disintegration of lateral contacts, the stability of the system is endangered, so that there is a small number of contacts in the direction perpendicular to the direction of anisotropy, thus providing "lateral support" to particles.

The situation is very different for loose assemblies, where the structure corresponds to a greater extent to arrangements with four neighbours. In an isotropic state, these arrangements corresponding to

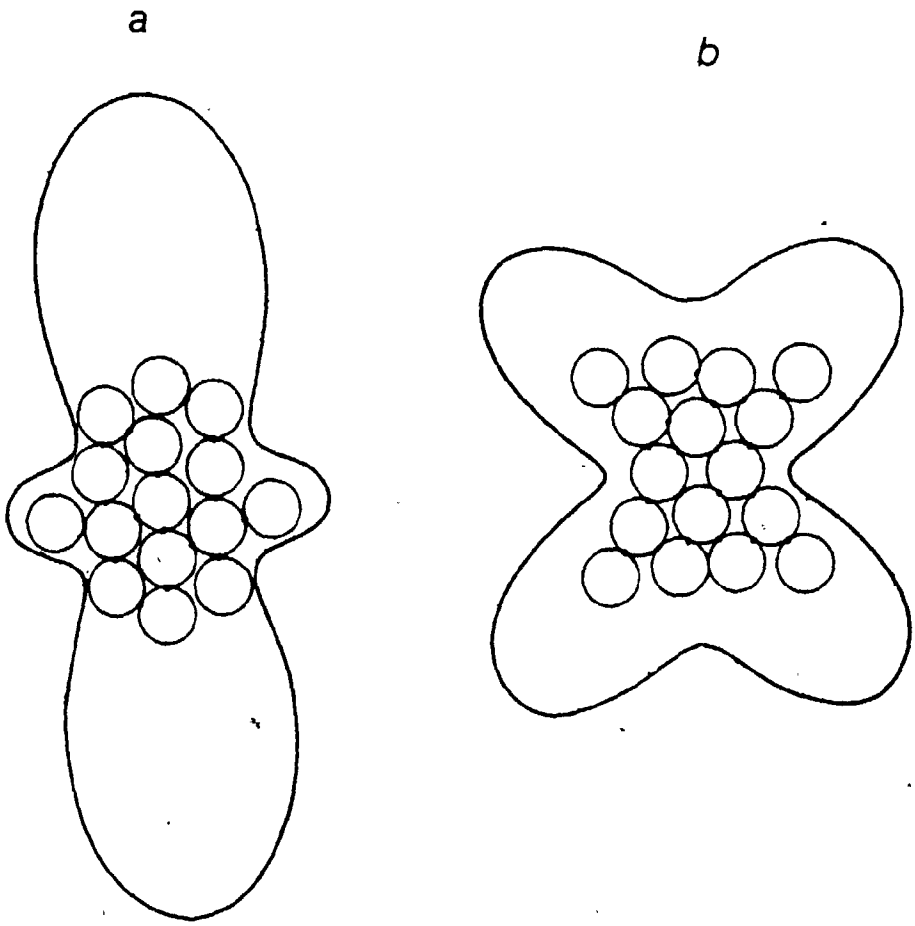

FIGURE 9.10

CONTACT ORIENTATION DISTRIBUTIONS FOR DENSE AND LOOSE ASSEMBLIES

parallelograms of segments in a corresponding network are isotropically distributed. In an anisotropic state the parallelograms are oriented and $S(\theta)$ shows maxima of contacts corresponding to this crystalline type of arrangement, scattered in an isotropic matrix as on Fig. 9.10[b].

This interpretation of structural characteristics of assemblies implies that the structure of the system under different densities corresponds to a combination of closely packed elements (triangles) and loose arrangements (parallelograms), both mixed to correspond to a system's density. In an anisotropic state, these geometrical figures, which form a corresponding network, are oriented.

It is interesting to note that a similar point of view does exist regarding the geometrical structure of three-dimensional systems [38]. This is only a crude examination of relationships in Fig. 9.9. They carry complete information on the contact orientation characteristics of granular assemblies.

9.9 Discussion and Conclusions

The analysis of the geometrical structure of plane assemblies focused on the contact orientation distribution $S(\theta)$ and a system of equations that this function must satisfy. The theory is based on transect analysis of granular assemblies that develops a distribution function of segments that runs parallel to the transect line.

For a transect line of arbitrary orientation the projections of chain segments on the line must add up to the length of the line and the total projection must be zero on perpendicular directions. This was the basis for setting equations referred to above as "equations of geo-

metrical compatibility". The developed distribution of segments in the chain is based on several approximations which proved accurate only for networks of equal size segments or segments with minor variation in length.

Equations of geometrical compatibility were applied to both regular and irregular structures with exact results obtained for regular networks and experimentally supported results for irregular systems. This fact indicates that the developed equations reflect the basic properties of geometrical compatibility and the equations are general in nature.

Inspite of the approximations made in the derivation of the compatibility equations, there is an indication that these equations are exact for a certain coordination number $\gamma^* = 2\pi/(\pi-2)$, interpreted as the coordination number corresponding to the densest state with irregular structure. At higher coordination numbers, a contact orientation distribution must be "gap-graded" to result in geometrical compatibility.

The developed equations were applied to analyze the contact orientation distribution $S(\theta)$. Considering the complexity of the developed non-linear integral equations with their unprecedented analytical structure, their analysis was approximate and based on an approximation of $S(\theta)$ in terms of second and fourth Fourier components. This approximation is analytically convenient, as all relationships containing $S(\theta)$ involve trigonometric integrals.

The analysis based on the noted approximation above is a typical perturbation type solution with perturbation parameter a, the parameter of anisotropy. The analysis showed, however, that perturbations with respect

the parameter of anisotropy are "singular" for coordination numbers close to γ^* (χ=0). The solution obtained is valid for small degrees of anisotropy and is applicable to the range $0 \leq a \leq 0.5$, as plotted on Fig. 9.7. This matter followed intuitively on the basis of extensive numerical analysis of terms neglected in perturbation analysis.

Solution (9.41) shows interesting numerical consistency when all curves for dense assemblies on Fig. 9.9 meet near the point a =0.5 b=0.25. Generally, the contact orientation distributions are different for different densities, although a highly anisotropic state with a=0.5, b=0.25 is the same for all densities.

A contact orientation distribution with these parameters was shown in Fig. 9.10. It has a minimum number of contacts in the direction $\frac{\pi}{4}$. to the direction of anisotropy. So far, the physical significance of this fact is not clear.

The theory also showed that the system's density is affected by the parameter of anisotropy a, as seen from (9.40). The relationship shows that the greater the anisotropy of the system, the higher the density. This is almost obvious: a unidirectional effort to compact a granular system is always associated with the creation of contacts in the direction of compaction.

In summary, the developed statistico-geometrical theory shows:

(1) exceptional significance of the average coordination number for the description of the geometrical structure of granular systems;

(2) that the density of anisotropic assemblies is influenced by the parameter of anisotropy a; the relationship is quadratic

with respect to a, so that the mentioned influence is not pronounced and the average coordination number can be assessed through the system's density only;

(3) that the average coordination number for an isotropic system is uniquely related to the system's density, a measureable parameter which can easily be assessed;

(4) that a contact orientation distribution is uniquely defined by specification of the average coordination number and anisotropy parameter a;

(5) that the parameter of anisotropy b is a function of the average coordination number and paramter a; this relationship is clearly qualitatively different for loose and dense assemblies and indicates that plane assemblies must be considered loose for $4 \leq \gamma \leq 4.5$ and dense for $4.5 \leq \gamma \leq 5.5$.

The above analysis of geometrical structure is adequate for plane granular assemblies under conditions when their phenomenological description is sufficient. The foregoing mechanical analysis showed that this is indeed the case for systems of bonded particles. It is felt that the developed relationship $b = b(a,\chi)$ is sufficient to explain the deformational features of cohesionless systems in all ranges of "plastic deformation", i.e. when the structure of the system varies, but geometrical compatibility requires observance of the above relationship.

Although certain approximations were involved in the derivation of the compatibility equations, it should be emphasized that one crucial assumption was made regarding the convexity of polygons in considered

networks of segments which geometrically reflects the concept of mechanical stability. Everything followed from this assumption.

CHAPTER X

LOAD TRANSMISSION IN ASSEMBLIES OF COHESIONLESS PARTICLES

10.1 Introduction

The theory outlined in chapter VII considered discrete assemblies of bonded particles. The rather lengthy analysis concluded that an ensemble of such systems can be described in continuum mechanics terms. Is this also true of assemblies of cohesionless particles?

The fact that a sample of sand can be placed in an apparatus with rectangular or cylindrical boundaries and be tested to obtain relationships between forces and relative displacements of loading plates does not imply that the medium can be described adequately in continuum terms, or what type of description is the most suitable.

It is therefore worth discussing again the specific conditions of the preceding analysis that led to a continuum-type description. The introduction of the phenomenological stress tensor was related only to equations of static equilibrium and can be done for any system of particles of any size, as long as it is known that the system is observed in static equilibrium. Mere knowledge of this fact does not make it possible to determine contact forces, since the systems of interest are highly statically indeterminate. Subsequent analysis resulted in expressions for average forces containing only one unspecified parameter which controls redistribution of contact forces between normal and tangential components.

To learn about the forces in the system, a deformation process must be considered. This process is related to considerations of connectivity within the

system. As soon as compatibility conditions are written, all forces can be determined. An energy principle follows which results in a set of all contact forces that assure geometrical compatibility.

The same principle resulted previously automatically in the strain tensor, also introduced from considerations of geometrical compatibility. The possibility of description with the strain tensor therefore hinges entirely on compatibility conditions describing connectivity of various blocks within the medium. In this case the system is *externally controlled* and cannot perform on its own. Relationships betweer the two quantities which can alternatively exercise an external control was obtained, i.e. *constitutive relationships*. The system behaves according to a certain minimum energy principle.

Dynamic systems do not behave in this way and the kind of external control that can be exercised over such systems is limited. Energy can be supplied to the system, but cannot be entirely extracted in the form of mechanical work. These are dynamic systems which perform according to the principle of maximum entropy. In such systems there is competition between chaos and order, competition between kinetic and potential energy, and a delicate balance is established between both forms of energy. This balance is of a probabilistic nature reflected in the entropy principle, i.e. a macroscopic observer observes the most probable response of a system with an overwhelming chance. *Equations of state* reflect the balance between both forms of energy (Appendix B).

Chapter X attempts an unbiased look at possible means of description of cohesionless assemblies. All computational aspects of the theory

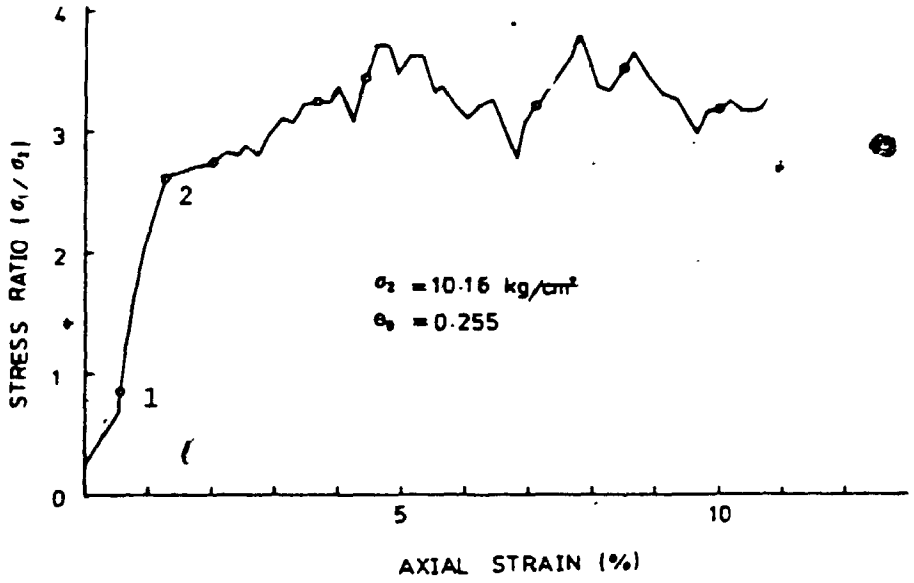

FIGURE 10.1

STRESS - STRAIN RELATIONSHIP IN PHOTO-ELASTICITY TESTS OF TWO-DIMENSIONAL GRANULAR MODEL
(after Kishino [21])

have already been developed in the preceding chapters. Presented here will be a discussion proposing a concept of "continuously unstable systems". Consequences of the introduced concept are employed to study the mechanisms of load transmission in cohesionless systems.

10.2 Concept of Continuously Unstable Systems

Fig. 10.1 presents the results of a biaxial test on an assembly of cylindrical rods. It can be seen that the deformation process proceeds in a series of jumps preceded by a nearly linear response. Observations show that during a spontaneous drop in load, the fabric of the assembly suffers drastic structural changes, so that any new load increase proceeds on an assembly with a different system of contacts. The whole deformation process proceeds in a series of micro-circles, where the load increases, hardening and drops, softening.

Such sharp fluctuations shown on Fig. 10.1 are due to the small size of the sample. If a large assembly be tested, there would be a misleading impression that the process proceeds smoothly and nothing drastic happens as on Fig. 10.1. In reality the same drastic structural changes occur in every element of volume of a large assembly, but are obscured.

Consider now how forces can be determined from the first principle, i.e. how can a precise mechanical problem be posed for cohesionless assemblies. Suppose the system is observed in static equilibrium under a certain load, and let the positions of all particles, discs for simplicity, be known. Even with this enormous information on the complete geometry of the system, contact forces can-

not be determined.

Normal components can be uniquely determined, as specification of relative particle positions immediately gives normal deformations in contacts. Tangential components, however, remain unspecified, since particle rotations from initial configurations are unknown. To determine tangential forces, the complete history of each and every contact in the assembly must be known.

The problem, therefore, cannot be solved as "static" and analysis of the complete history of jumps is necessary to determine contact forces. This is the reason that computer simulations of the deformation process in granular systems resort to dynamic analysis [7]. Strictly speaking, the considered problem simply cannot be posed as a static problem, even knowing for a fact that the system is observed in static equilibrium at the given instance.

We shall next pursue an attempt to trace the history of the system on the basis of static equilibrium. Suppose cohesionless particles are artificially bonded. Let loads be applied and the problem be solved as for bonded particles, so that all contact forces are determined for an infinitesimal load increment. From the analysis of the preceding chapters it is known that the distribution of contact forces is Gaussian, so that there will be contacts under tension and contacts on which tangential forces do exceed Coulomb's limit.

The situation can be corrected within the theory of static equilibrium. Fictitious loads can be applied at all contacts and the problem can be solved for the arbitrary fictitious forces. Than, a selection of these forces can be made to prevent the violation of tensile and Coulomb

restrictions. This program in fact is analytically manageable using the principle of minimum complementary work for systems under body forces. Unfortunately, such a solution will be of little practical value. The moment a load increment reaches a certain level, a drastic structural change (as observed in experiments)becomes inevitable and the system goes into a dynamic state due to internal instability. Without a dynamic analysis the meaning of the results is in doubt.

Experience with the buckling of columns shows that, although the process of buckling cannot be described completely in static terms, the initial and final configurations can be predicted using static analysis. An elastic system will release excessive potential energy which will somehow dissipate (it is usually irrelevant precisely how) and the system will be observed in a new static configuration.

There are therefore two options: either to pose a dynamic problem for large systems of conhesionless particles and attempt to solve it, or to adopt a simplified approach based on a physical hypothesis which will bypass intricate stages of a dynamic analysis.

Judging the state of the art of statistical mechanics of dynamic systems, the first approach is not feasible. Only recently has there been cognizance of the meaning of possible instabilities in dynamic systems [11] and there has not yet been developed proper analytical tools for their analysis. That is why chapter IX of the present work adopted an intuitive notion of mechanical stability and expressed it in geometrical form amenable for analysis.

A similar approach will be adopted here. What will follow now

is not a precise mechanical description based on precise laws of mechanics, but a modelling process that does not contradict them. A continuum mechanics type description will appear again, but not in the usually considered form. The governing idea which will be employed is an analogy with elastic buckling of columns. Configurations of a column can be obtained before bifurcations and after. The governing principle is the principle of minimum potential energy.

For granular systems the situation is not as straightforward. After local instability occurs, configurations are governed by intricate rules of local geometry. Once the geometrical requirements of stability are satisfied, the system of forces in the assembly can be internally adjusted according to the principle of minimum potential energy. Such processes of contact force adjustments are very fast, and relaxation time is determined by particle stiffnesses, so that the connectivity of the body after instability is restored after it was violated during the process of "softening".

A lack of connectivity within the body during gross load increments precludes the possibility of writing compatibility conditions even during an infinitesimal load increment. For a small system, as tested in experiments shown in Fig. 10.1, compatibility conditions can be written for the hardening part of the cycle when the system is externally controlled.

A transition to a "continuum" description requires consideration of either an ensemble of systems, or an infinite system. The moment the system becomes large, the frequency of local instabilities increases, but their effect on jumps in the gross sense is reduced. This, however,

does not imply that compatibility exists within the system.

For an infinite system, such local instabilities will be continuously present at some point of the medium at any time during deformation. This hypothesis prevents the stating of compatibility conditions for the *process of macro-deformations*. On the other hand, it is recognized that the system is also always in a state of static equilibrium. The history of this state of equilibrium, however, cannot be traced with the strain tensor alone.

The major hypothesis which will be put forward is the following: during the process of "continuously unstable deformations" the system establishes static equilibrium according to internal requirements and not under external mechanical control. This results in the state with minimum potential energy for any internally created system of contacts. The principle does not imply that the structure of the system is rearranged to result in minimum potential energy, but once the structure is formed, a rapid relaxation process restores equilibirum, i.e. there results a system of contact forces corresponding to minimum potential energy for a fixed structure.

This hypothesis reflects the continuing competition between the tendency to form internal stable structures and external actions which prevent them.

To a certain extent the introduced mechanism of establishing static equilibirum reflects the conditions in dynamic systems where there is a tendency to order due to potential interactions and chaos due to kinetic motions.

Statistical mechanics studies the conditions of this balance. In the present case, kinetic motions are small and result from local

instabilities. Dissipation of energy is fast and the problem of competition between kinetic and potential energies is solved unconditionally in the direction of forces created by minimum potential energy corresponding to a created stable structure. A stable structure is created according to internal requirements and is not controlled externally. This is why the strain tensor cannot be introduced in this problem.

Consider qualitatively how deformations of cohesionless systems proceed from the point of view of the above principle and the results of the geometrical analysis of Chapter IX based on the notion of stability expressed geometrically. Let the system be subject to deviatoric loads. Being continuously in static equilibrium in one part and in a state of rearranging structure in another part, the gross balance of forces requires relationship (4.17) to be satisfied, i.e.

$$a_\sigma = \frac{1}{2}(a + a_f + a_\mu) \qquad (10.1)$$

where the coefficients above describe anisotropy in contact orientation and components of normal and tangential forces.

An increase in deviatoric load (increase in a_σ) requires either an increase in structural anisotropy a or an increase in anisotropy of forces. The last tendency prevails in the parts of the system which currently are in equilibirum.

Fig. 2.1 showed a system of contact forces in an assembly of photoelastic discs under deviatoric load [8]. During the "hardening" part of a micro-cycle, directional variation of forces increases (a_f increases) and this creates a tendency towards instability. The load drops when structural rearrangement begins. When the load drops, a_f also drops locally; after a period of instability finally compensated by

increase in a, the cycle proceeds further.

The question remains as to how a structure of the system is formed. According to the above procedure, parameter a is controlled externally by a_σ, and distributions of forces (a_f, a_μ) are basically controlled by the principle of minimum potential energy for fixed a.

The results of geometrical analysis of chapter IX give an answer to this question. Parameter b was obtained there as a function of a and the average coordination number γ. It was obtained as a consequence of the assumption regarding convexity of polygons formed by the network. This resulted in $b = b(a,\chi) = b(a,\gamma)$.

As may be seen from (10.1), b is not related to gross loads, but is a reflection of the stability of the structure and condition $b = b(a,\gamma)$ can be viewed as the condition of geometrical stability of the structure.

Structural rearrangement discussed above results in gross deformations of the material. The type is sometimes called "plastic" and it is detected when cohesionless systems are subject to gross loads in a conventional testing apparatus.

No theory of load deformation response during such tests will be presented here. Only one feature of a typical response in a triaxial apparatus will now be considered. It is invariably observed that the volume of an assembly drops during the initial stages of such deformations. According to the above considerations, an increase in deviatoric load increases the anisotropy in the system. This is also confirmed experimentally [21]. According to the parameter of anisotropy - density relationship (9.40), an increase in anisotropy must be accompanied by increase in

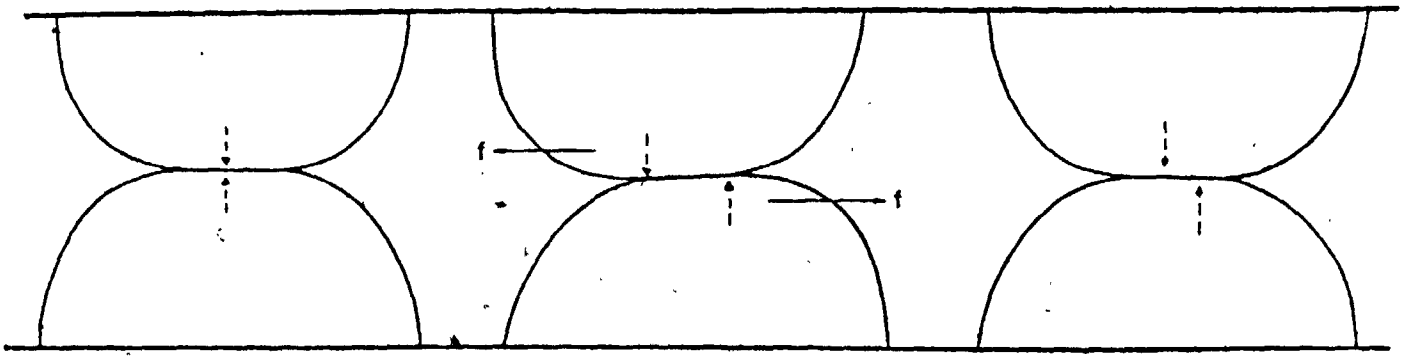

FIGURE 10.2

"LOCKED UP" TANGENTIAL FORCE

density, i.e. the drop in volume observed in experiments.

In future extensions of this theory, variations in the parameters of structural anisotropy a, b will be related to observed deformations. In the meantime, the theory will concentrate on means of studying contact forces and inhomogeneous stress distributions in systems where the loading process results in structures with known a, b, γ. It is natural to consider systems with inherent anisotropy in structure; that is, anisotropy which occurs during the process of the deformation of an assembly.

The principle of minimum potential energy, as formulated above for cohesionless systems, will be employed in further analysis to relate the coefficient of lateral pressure (at rest) to the parameter of structural anisotropy a. The following sections consider simplifications which will be introduced to subsequent analysis.

10.3 Tangential Contact Forces in Assemblies of Cohesionless Particles

The simplicity with which systems of bonded particles were analyzed is largely due to specification of a mechanical problem in terms of kinematic variables, positions of particle centers and their rotations. The linear contact model eliminated the necessity of studying stress distributions within the particles themselves, so that only two stiffnesses, k_n and k_t, represented the deformational properties of particles.

For cohesionless systems the situation is far less certain. There is no doubt that specification of particle positions (for spheres and discs) uniquely prescribes normal contact forces. The tangential force component can still be arbitrary. Fig. 10.2 shows how a contact can be

subject to an external load to produce slips. The load is released and a tangential force will be "locked up" in the contact. This force can be released spontaneously when the normal force is changed. Its release does not result in variations in interparticle positions, i,e, no strain is associated with such tangential forces. During a deformation process which goes through a series of dynamic states with drastic variations of contact forces [9], like the process shown in Fig. 10.1, such tangential forces cannot survive.

Tangential forces can also be related to relative interparticle displacements, as was the case of the linear contact model. During a single cycle of hardening (1-2 on Fig. 10.1), such tangential forces are induced due to relative tangential displacements between particles. The moment "softening starts" and forces decrease, this tangential force is released.

The point of view expressed here consists of the following: tangential forces are induced on the hardening part of a deformation micro-cycle and are released during micro-softening. If this approach is accepted, tangential forces will not accumulate during the deformation process. Moreover, since it is known that particles do slide with respect to each other, tangential forces on sliding contacts can be induced only during one cycle. This means that there must be a concentrated load transfer to these contacts. Since the increase in gross load is not very high in one micro-cycle and the gross balance of forces must be maintained, there must be very few sliding contacts in the assembly. This conclusion was drawn by J.Kishino [21] from observations of plane assemblies.

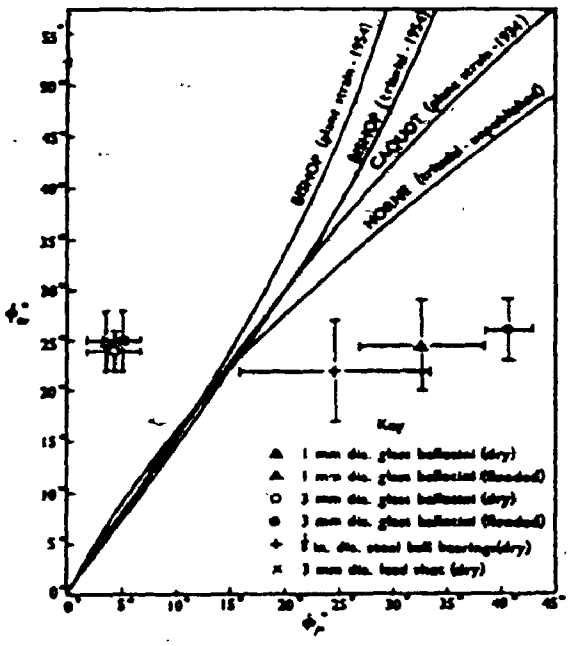

FIGURE 10.3

THEORETICAL AND EXPERIMENTAL RELATIONS BETWEEN ϕ_μ AND ϕ'_{cv}

(after Skinner [32])

This fact is attributed here to the impossibility of tangential force accumulation during deformations of cohesionless assemblies. This effect can only be combined with highly segregated local transmission in cohesionless assemblies. Observation of experiments with photo-elastic discs (Fig. 2.1) showed that this, indeed, is the case and it was observed that there are only a few contacts with significant force obliquity with respect to contacts. The possibility of sliding with solid friction is therefore limited. It is, however, a fact that sliding occurs, but the above considerations do not attribute it to mobilized Coulomb friction at contacts, as taken as a basic premise of many theories.

Fig. 10. 3 [32] shows a comparison of theoretical results which relate the coefficient of internal friction ϕ'_{cv} in the ultimate state to the angle of interparticle friction. According to theories based on friction, both quantities are nearly linearly related, but experiments conducted by Skinner [32] show the opposite. The above heuristic analysis of tangential forces in cohesionless systems results in the same conclusion. In existing literature there is no single approach to Skinner's results, but these experiments, which can point out to significant misconceptions in existing theories, cannot be dismissed.

A question therefore arises: if it is not solid friction that is responsible for strength of granular systems in the ultimate state, then, what is? The analysis of Chapter III sheds light on this matter. It was shown there that, if a system sustains a deviatoric load with $a_\sigma = \sigma_t/\sigma_n$, this load can be carried through structural anisotropy (a), and the anisotropy in the distribution of average normal and tangential

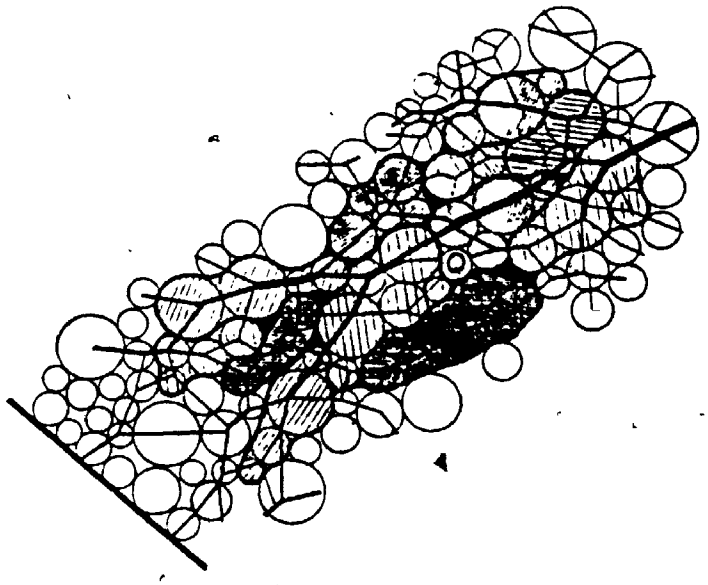

FIGURE 10.4

BLOCK-LIKE SUB-REGIONS

(after Dresher & DeJong [8])

forces (a_f, a_μ) so that (10.1) must be satisfied.

Even if the strength of granular systems is not associated with tangential forces, no contradiction appears and

$$\sin\phi_{cv} = a_\sigma = \frac{1}{2}(a + a_f)$$

Taking $\phi_{cv} = 25°$, as observed by Skinner, and assuming, for example, $a = a_f$, both parameters are about 0.42 which is a reasonable number for the parameter a, as shown by the geometrical analysis in chapter IX.

The above considerations show that elimination of the component of strength related to tangential forces does not result in any physical contradictions. Recall that (10.1) is based on static equilibrium and nothing else.

Theories of strength based on solid friction, the results of which are shown in Fig. 10.3 , are based on energy balance in a quasi-static process. The deformation process shown in Fig. 10.1 can hardly be viewed as quasi-static, so that there are significant dynamic losses of energy during contact exchange etc. These losses are the sharpest in the ultimate state when the frequency of jumps is the greatest (Fig. 10.1).

The above analysis cannot pronounce final judgement with regard to tangential forces, but it indicates physical reasons as to why tangential forces may not be developed and also shows that no contradiction appears if they are neglected, Moreover, Skinner's results then become understandable.

The mechanism of structural rearrangements, "plastic deformation", can also be explained without friction associated with sliding. Fig. 10.4 shows conglomerates of particles which slide in blocks, as observed in

[8]. It can be seen that contacts within the blocks are subject to fairly high forces which are clearly normal to particle contacts.

On the other hand, external contacts of these blocks are under much lower loads, with occassional obliquity. Sliding occurs along these stressed contacts, but the sliding is not a quasi-static process. It is viewed here as a result of structural breakdown at some conglomerates of nearby particles.

Observation of a general system of contact forces (Fig. 2.1) shows that there are paths of local transmission and high forces are normal to contacts. Some particles are not stressed at all. The existence of unstressed particles can be understood recalling the Gaussian character of the contact force distribution for bonded particles where there always are contacts under tension.

In cohesionless systems no tensile force can be transferred and such contacts will be unstressed as the load increases on the hardening part of the micro-cycle. The number of contacts released from contact forces increases with load increase. Finally, their number will increase up to a limit when structural stability is lost, so that micro-softening occurs until a new system of contacts is created.

In summary, contact forces in cohesionless materials will be viewed as normal and transmitted through networks of contacts, as in Fig. 2.1. Numerical consequences of this assumption will be discussed later.

10.4 The Coefficient of Lateral Pressure at Rest

Consider an infinite plane assembly deposited, for example, vertically under gravity. Particles will have a preferential tendency to create contacts in the vertical direction. The precise degree of anisotropy in contact orientations may depend on many factors that are not discussed here.

The problem considered in the present section is to determine the relationship between vertical and horizontal stress, assuming anisotropic structure of contact orientations; the systems is assumed homogeneous.

The above problem cannot be formally solved by making use of constitutive relationships, specification of zero lateral strain and calculation of corresponding horizontal stress,but is related to the process of deposition and the prior history of the deposit.

Regardless of the history of the deposit, conditions of equilibrium require (10.1) to be satisfied. Let vertical and horizontal stress components be principal components and therefore by definition

$$a_\sigma = \frac{\sigma_t}{\sigma_n} = \frac{\sigma_v - \sigma_h}{\sigma_v + \sigma_h} = \frac{1-K_o}{1+K_o} \qquad (10.2)$$

where $K_o = \sigma_h/\sigma_v$ is the coefficient of lateral (earth) pressure at rest. To calculate K_o it is necessary to make a decision with regard to parameters of force anisotropies a_f, a_μ in (10.1). With respect to a_μ the decision is simple. It was explained in section 10.3 that any disturbance or fluctuation of forces results in a release of tangential forces without affecting particle positions. Therefore $a_\mu = 0$ for an old deposit. Coefficient a_f defines directional variation of normal forces

and additional considerations are necessary to determine this parameter.

If a deformation process proceeds gradually, each particle will be disturbed at least several times after deposition before settling into a final position and being restricted in motion by its neighbours. The number of times the particle will be disturbed depends on the intensity of the process, particle shapes etc. This will also determine the number of contacts that will be formed and their orientations.

To simulate this process is difficult, but it can be assumed intuitively that the system will manage to find the most stable state under conditions with free adjustments of particle positions and contact forces. The fact that K_o is not very sensitive to overburden indicates that the position of a particle is unaltered after settling and adjusting.

Suppose that average contact forces have directional variation

$$\bar{f}_n(\theta) = \bar{f}_n^o(1+a_f \cos 2(\theta-\theta_o)).$$

If $a_f \neq 0$, there will be a sharp directional segregation of forces with increase in overburden when $\bar{f}_n^o$ increases. Two forces on contacts of the same particle can become very different and particle equilibrium becomes endangered. If $a_f = 0$, directional segregation does not occur and the influence of fluctuations is not as severe.

Even if a_f will not be zero locally, there must be structural adjustment with increase in overburden to eliminate local directional segregation of forces, i.e. $a_f = 0$, so that

$$a_\sigma = \frac{1}{2} a \tag{10.3}$$

and according to (10.2).

$$K_o = \frac{1 - \frac{a}{2}}{1 + \frac{a}{2}} . \tag{10.4}$$

To substantiate the above intuitive logic, consider Fig. 3.11 which gives levels of potential energy for different magnitudes of the parameter $R = 2a_\sigma/a$.

In the present case loads are in the direction of anisotropy ($\Delta_\sigma = 0$) and it can be seen that potential energy of an anisotropic system is minimum when a deviatoric load corresponds to $R = 1$, i.e. (10.3) is satisfied. The above mechanism of structural adjustments during deposition corresponds to minimum potential energy of the system of forces for a fixed level of compressive loads.

It can be seen from (10.4) that in isotropic case $a = 0$, $K_o = 1$. Note that relationship (10.4) is for plane systems only, although the logic leading to it is general. The same type of relationship should exist in the three-dimensional case.

The link between K_o and the parameter of anisotropy of a natural deposit opens a way to assess their anisotropy and calculate stress distributions. Note, however, that after a certain non-uniform load is imposed, the structure of the system is disturbed and the deposit becomes non-homogeneous with respect to anisotropic properties. Stress distributions presented below will, strictly speaking, be valid for an infinitesimal load increment.

10.5 Description of Contact Forces in Cohesionless Assemblies Subject to External Loads

The mechanism of force and structure adjustments presented in section 10.4 resulted in a state with minimum potential energy. The mechanism was related to the existence of disturbances in the system

which allowed an assembly to "act on its own", thus introducing a feature of dynamic systems. In the above example it was natural, since it is a feature of the process in which the system was created.

Consider now deformations of a system of cohesionless particles. Fig. 10.1 which describes such a process shows that the system also attempts to "act on its own" during short periods of softening. Therefore, there is an internal tendency to local instabilities. For a large system, this tendency may not be noticeable through a spontaneous drop in gross load, but such processes will occur locally and the system will have a local freedom to adjust its contact forces. The principle of minimum potential energy can be applied as stated in section 10.2, but under a restriction of specified external loads.

The stated principle of minimum potential energy will be applied for particles with linear contact interactions. In this case, potential energy coincides with complementary work of internal deformations (6.8), i.e.

$$w_f = \frac{r}{2}\gamma d_o n_v \int_0^{2\pi} \left[\frac{\overline{f_n^2}(\theta)}{2k_n} + \frac{\overline{f_t^2}(\theta)}{2k_t} \right] S(\theta) d\theta \qquad (10.5)$$

Complementary work is considered per unit volume and must be minimized subject to constraints related to external loads (3.29), i.e.

$$\sigma_{ij} = \frac{1}{2}\gamma d_o n_v \int_0^{2\pi} [\overline{f}_n(\theta) n_i n_j + \overline{f}_t(\theta) t_i n_j] \, S(\theta) d\theta \qquad (10.6)$$

Note that in final relationships tangential stiffnesses will be taken to be zero; that is, to result in a zero average of tangential forces. To perform minimization of complementary work it is necessary to relate averages of the square of forces to average forces.

The Gaussian distribution of contact forces developed for systems of bonded particles is not physically applicable, as well as a particular form of the principle on the basis of which it was obtained. It was assumed that any system of contact forces corresponds to a certain micro-structure which will develop this system of forces.

The amount of possible systems of contact forces associated with a certain set of distributions P_θ for different θ was related to the amount of missing information associated with P_θ. Missing information associated with the whole system of forces was the sum of missing information associated with P_θ for each group. This construction of missing information implied that, if a certain system has forces described by P_θ for a certain group of contacts θ, there was a variety of other systems which had the same distribution P_θ for this group of contacts and all possible combinations of distributions for other groups of contacts.

This assumption is not reasonable for cohesionless systems, when the structure of each system is the creation of the process of deformation. The variety of created structures must be strongly restricted. The restriction on tangential components of contact forces discussed above is viewed as resulting in concentrated load paths, such as were observed in Fig. 2.1. The direction of force θ now has a tendency to create contacts of this orientation.

It is intuitive that the higher the force on a chain of particles with given contact orientations, the greater will be the number of particles in the chain. The variety of produced structural arrangements will now be assumed to be associated with each group of forces. More-

over, due to the assumed lack of tangential forces, normal forces are uniquely controlled by gross load σ_{ij}, since the unknown parameter r defining average tangential forces (4.31) is zero.

With such a strong restriction on forces each group of forces with orientation θ must produce its own chain of contacts with orientation θ, regardless of conflicts with forces on other groups. This is viewed here as a major reason for observed instabilities.

The above point is illustrated in Fig. 10.5 where two overlapping concentrated load paths are shown. Each load path creates its own "column" and relieves forces on the sides of this "column". The other force of different orientation also tends to create its own "column", thus imposing a lateral load on the column associated with another group of created contacts leading to instability of the already existing chain of particles created by a concentrated force and the chain buckles.

The above mechanism is hypothetical. If accepted, it concludes that different fixed orientation groups compete independently and break the structure. To determine a distribution function of contact forces under these conditions presents no difficulty.

Average forces are fixed unconditionally, i.e.

$$\int_0^\infty f_n P_\theta(f)\, df = \bar{f}_n(\theta) \qquad (10.7)$$

A distribution function of contact forces must be such so as to correspond to the maximum possible options in giving the same average, i.e. missing information associated with this function

$$E = -\int_0^\infty P_\theta \log P_\theta \, df_n \qquad (10.8)$$

must be maximum. This function is the best for the process of competing in a "hostile" environment to create contacts in order to develop a load required by external constraints. If (10.8) is maximized subject to constraints (10.7), an exponential distribution function follows

$$P_\theta(f_n) = \frac{1}{\overline{f}_n(\theta)} \exp\left\{-\frac{f_n}{\overline{f}_n(\theta)}\right\}$$

This function automatically restricts normal forces to the same sign as the average of forces. Also, compared to the Gaussian distribution, it has a longer "tail", i.e. gives more chances to develop higher forces, as observed on local paths in Fig. 2.1 .

The dispersion of normal forces

$$\overline{f_n^2}(\theta) - \overline{f}_n^2(\theta) = \overline{f}_n^2(\theta)$$

is related to the average force of this group only. In the analysis of bonded particles, dispersion was related to the general level of potential energy in the system and was the same for all groups of contacts ("cooperative forces").

In the present case, dispersion in each group is individual ("competing forces"). Note that an exponential distribution of tangential forces will follow if the tangential forces are not neglected and the same logic is employed, i.e. all forces on contacts of the same orientation will have the same sign. This corresponds to "mobilization" of tangential forces. In the case of bonded particles, tangential forces were not mobilized and were symmetrically distributed over the average.

Knowing the relationship between averages, (10.5) can be minimized. The procedure is the same as in section 6.3 where the exponential distribution was employed as an illustration for minimization of comple-

mentary work. Average forces were obtained in terms of Lagrangian multipliers, i.e.

$$\overline{f}_n(\theta) = \xi k_n \lambda_{ij} n_j n_i$$
$$\overline{f}_t(\theta) = \xi k_t \lambda_{ij} t_j n_i$$

where $\xi = 0.5$ for the exponential distribution. Complementary work can now be given as follows:

$$w_f = \frac{1}{2} \sigma_{ij} \lambda_{ij} \tag{10.9}$$

Interpretations for λ_{ij} in this case must be viewed with caution. It was shown from the equations of compatibility for bonded particles that w_f must be of the form (10.9) with λ_{ij} being the strain tensor. This conclusion cannot be made now, so that λ_{ij} is just a set of Lagrangian multipliers which can be determined from constraints (10.6) to obtain

$$\sigma_{ij} = A_{ijkl} \lambda_{kl} \tag{10.10}$$

If (10.10) is inverted and complementary work was calculated in terms of σ_{ij}, one can obtain

$$w_f = \frac{1}{2} \tilde{A}_{ijkl} \sigma_{ij} \sigma_{kl} \tag{10.11}$$

where $\tilde{A}_{ijkl}$ is the inverse of the tensor in (10.10).

Complementary work was minimized so far with respect to average forces for a system subject to homogeneous loads. If the system is under "non-homogeneous" boundary loads, the ensemble logic of chapter III must be employed. Distribution P_θ is now position-dependent, i.e. $P_\theta = P_\theta(f, \underset{\sim}{r})$ and the minimization above must be done for each fixed $\underset{\sim}{r}$. Lagrangian multipliers then are position-dependent, i.e. $\lambda_{ij} = \lambda_{ij}(\underset{\sim}{r})$ and the total potential energy

$$W_f = \int_V w_f \, dV \tag{10.12}$$

must be once again minimized subject to constraints related to gross

boundary loads. The minimization is under conditions of static admissibility of σ_{ij}, i.e.

$$\frac{\partial \sigma_{ij}}{\partial r_j} = 0 \ . \tag{10.13}$$

The fact that σ_{ij} in the form (10.5) is statically admissible was proven in section 3.14.

The minimization problem for complementary work (10.12) subject to constraints (10.13) is presented in [33] for an isotropic elastic medium. It follows from the mentioned procedure (which uses the method of Lagrangian multipliers) that σ_{ij} satisfies the Beltram-Mitchel equations of isotropic elasticity [33]. The associated set of Lagrangian multipliers λ_{kl} is related to σ_{ij} according to (10.10) and position-dependent Lagrangian multipliers satisfy compatibility conditions for the strain tensor of continuum mechanics.

This procedure can be also applied to the present anisotropic situation with the only difference being that $\lambda_{ij}(r)$ will not be interpreted as strain tensor.

An interpretation of λ_{ij} is still desirable, and having the expression for potential energy (10. 9) it is clear that this tensor is related to elastic deformations of grains. It satisfies the equations of compatibility, but cannot be determined through a physical process. The moment the state of the system is changed, another system of contacts is created due to instabilities.

If it is assumed that structural changes are not as drastic on the unloading cycle of deformations, λ_{ij} can be approximately identified with elastic deformations on the unloading branch of the load-deformation

curve.

The logical scheme presented above and based on direct application of the postulate on minimum potential energy avoids the difficulties of obtaining elastic deformations under conditions when it is possible experimentally (only approximately) and it is theoretically recognized that elastic deformations cannot be separated from structural changes.

Relationships (10.10) relate the stress tensor directly to "elastic deformations".It is emphasized that the term can be used in quotes only. The scheme of obtaining stress distributions within a medium is as usually done using methods of continuum mechanics. The only difference is that the "elastic strain tensor" is simply a mathematical entity useful for computational purposes. A stress distribution is all that is necessary.

This approach recognizes that the medium can be in static equilibrium,but the moment a process on it is considered, compatibility is violated and two states of static equilibrium can not be connected through the elastic strain tensor.

The scheme of stress calculations proposed above does not contradict the usual concepts of a continuum description, but it also does not employ the so-called "plastic deformations" as an agent to calculate the stress tensor.

Plastic strains are not related to contact forces, in terms of which the stress tensor is defined and therefore cannot be used for its calculation. In formal continuum mechanics schemes, the stress tensor is an abstract entity and it is not always clear whether it can be calculated or related to strains which are not parameters of state.

The above scheme of stress calculations proposed on the basis of the concept of "continuously unstable medium" in fact is not new and is employed in soil mechanics engineering practice for calculating settlements of foundations in clay [39]. Stress distributions are computed using elastic solutions and settlement is calculated using an appropriate physical model for compressibility.

Qualitative features of stress distributions in granular systems will be studied in the next section.

10.6 Stress Distributions Under Point Load on a Granular Half-Plane

The title of this section emphasizes that the solution to the stated problem is for plane assemblies of discs and its direct applicability to the problem of a line load on half-space may have different quantitative features.

In the isotropic case, equations of linear elasticity were developed here for both assemblies of spheres and discs. Their direct comparison indicated that both constitutive relationships are similar in the case of zero tangential stiffnesses and must result in identical stress distributions.

An anisotropic case was investigated for plane systems only. Constitutive relationships (7.22) formally describe linearly elastic transversely isotropic material with a vertical direction of anisotropy. The same type of equations follows for three-dimensional assemblies of spheres if the anisotropic contact orientation distribution $S(\theta)$ is employed.

A prelimiary investigation, not reported here, indicated that

constants

$$c_1 = 3 - 2a + \frac{b}{2}$$
$$c_2 = 3 + 2a + \frac{b}{2}$$
$$c_3 = 1 - \frac{b}{2}$$

in (7.22) for plane assemblies will have different coefficients in front of parameters of anisotropy a, b. An attempt to develop relationships between parameters of anisotropy for three-dimensional assemblies has so far been unsuccessful.

According to the concept of a "continuously unstable system", the above equations also describe stress distributions in assemblies of cohesionless particles. Tensor ε_{ij} in this case is not interpreted as tensor of elastic deformations. The equations also describe a system of particles with linear contact interactions.

For homogeneous systems, a, b are constants, but for systems of cohesionless particles non-homogeneous stress distributions will alter the structure of the system, so that the system becomes non-homogeneous after the "first load increment".

The solution to the stated problem is presented in [24]. Present attention will concentrate on features of soultions. A set-up of the problem is shown on Fig. 10.6.

The distribution of stress is "radial", as in the case of an isotropic body. The solution is of the form

$$\sigma_r = -\frac{p}{\pi}(u_1+u_2)\sqrt{\beta_{11}\beta_{22}}\,\frac{\cos\theta}{r\,L(\theta)} \qquad (10.14)$$

$$\sigma_\theta = 0$$

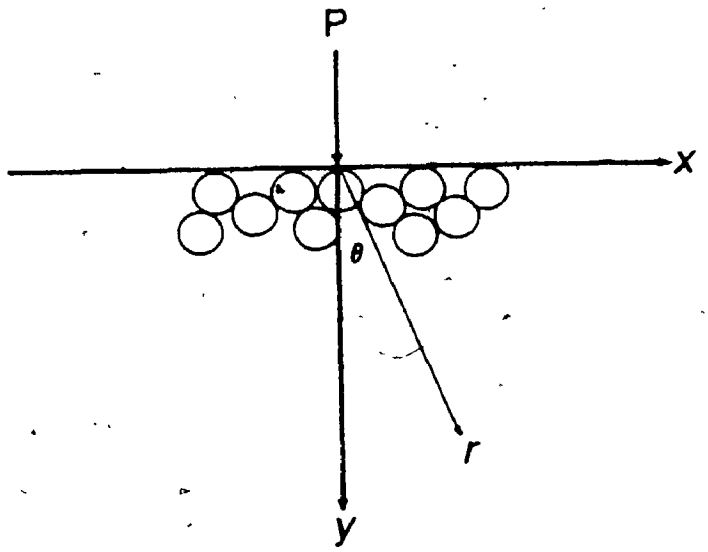

FIGURE 10.6

POINT LOAD ON GRANULAR HALF-PLANE

where

$$L(\theta) = \beta_{11}\sin^4\theta + (2\beta_{12}+\beta_{66})\sin^2\theta\cos^2\theta + \beta_{22}\cos^4\theta$$

and u_1, u_2 are roots of the equation

$$\beta_{11}u^4 - (2\beta_{12}+\beta_{66})u^2 + \beta_{22} = 0.$$

Constants β_{ij} are related to (10.) as follows:

$$\beta_{11} = \frac{c_2}{\Delta} \quad \beta_{12} = -\frac{c_o}{\Delta} \quad \beta_{22} = \frac{c_1}{\Delta} \quad \beta_{66} = \frac{1}{c_o}$$

where

$$\Delta = c_1c_2 - c_o^2.$$

Consider the shape of solutions (10.14). Fig. 10.7 shows the contours of equal radial stress for loose assemblies. Parameter a is uniquely related to K_o according to (10.4). Any fixed set a, b corresponds to a certain magnitude of parameter χ in (9.41) which is related to the average coordination number.

Considering that $\chi=0$ corresponds to the densest state and that $\chi=1$ corresponds to the loosest stable state, parameter χ can be expressed in terms of relative density of the assembly using relationship (9.33). Parameters K_o, D_r are given under corresponding stress distributions. Magnitudes of D_r for stress distributions on Fig. 10.7 indicate loose assemblies.

The physical reason for such a lateral spread of the load in this case is clear: loose assemblies are described by the contact orientation on Fig. 9.10[b] which shows predominance of "lateral" contacts. Fig. 7.1 also shows that lateral directions are the stiffest for the same reason. Contact forces are transmitted along a load path which corresponds to stiff directions.

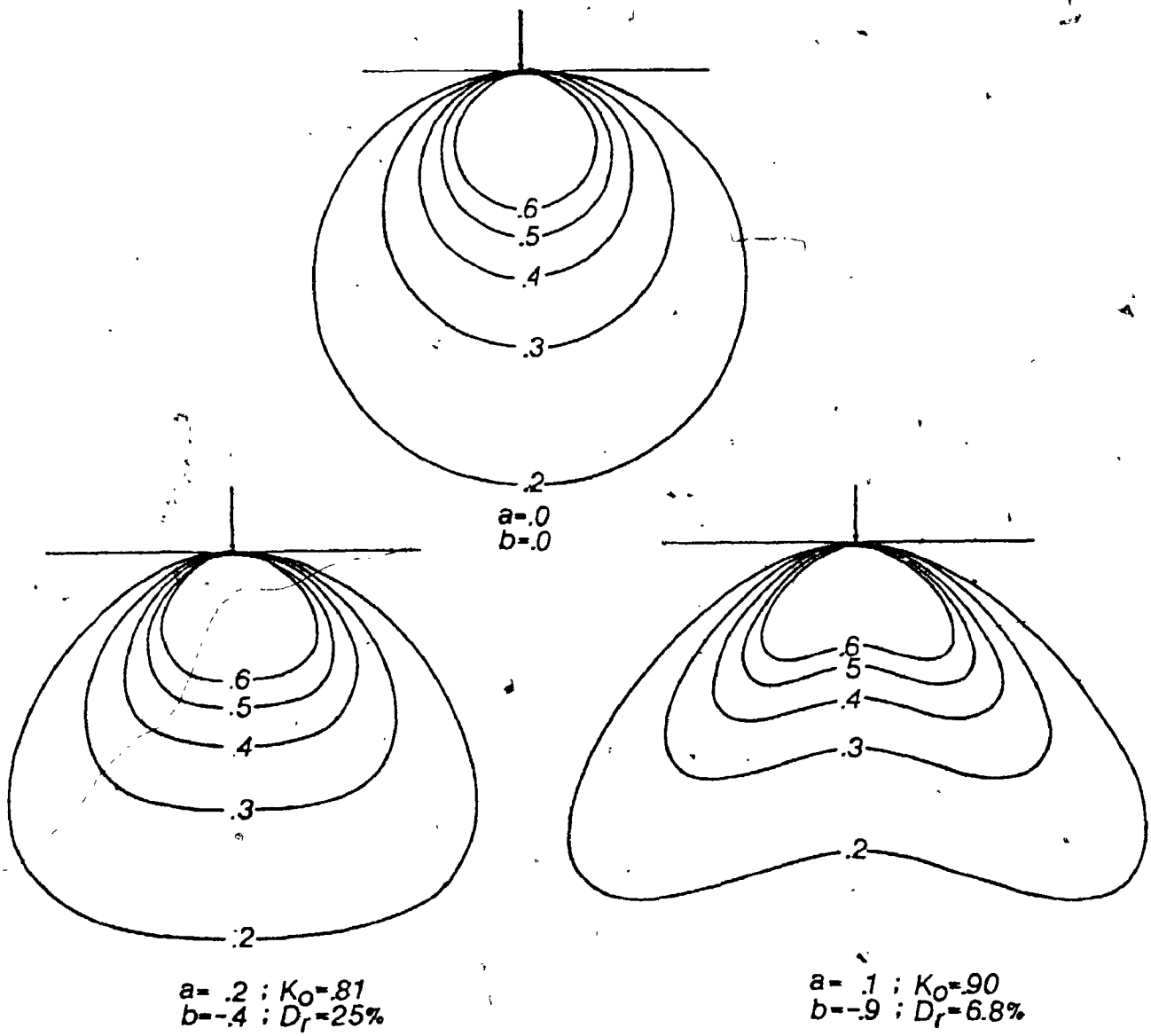

FIGURE 10.7

CONTOURS OF EQUAL RADIAL STRESS FROM A UNIT POINT LOAD ON A GRANULAR HALF-PLANE (loose assemblies)

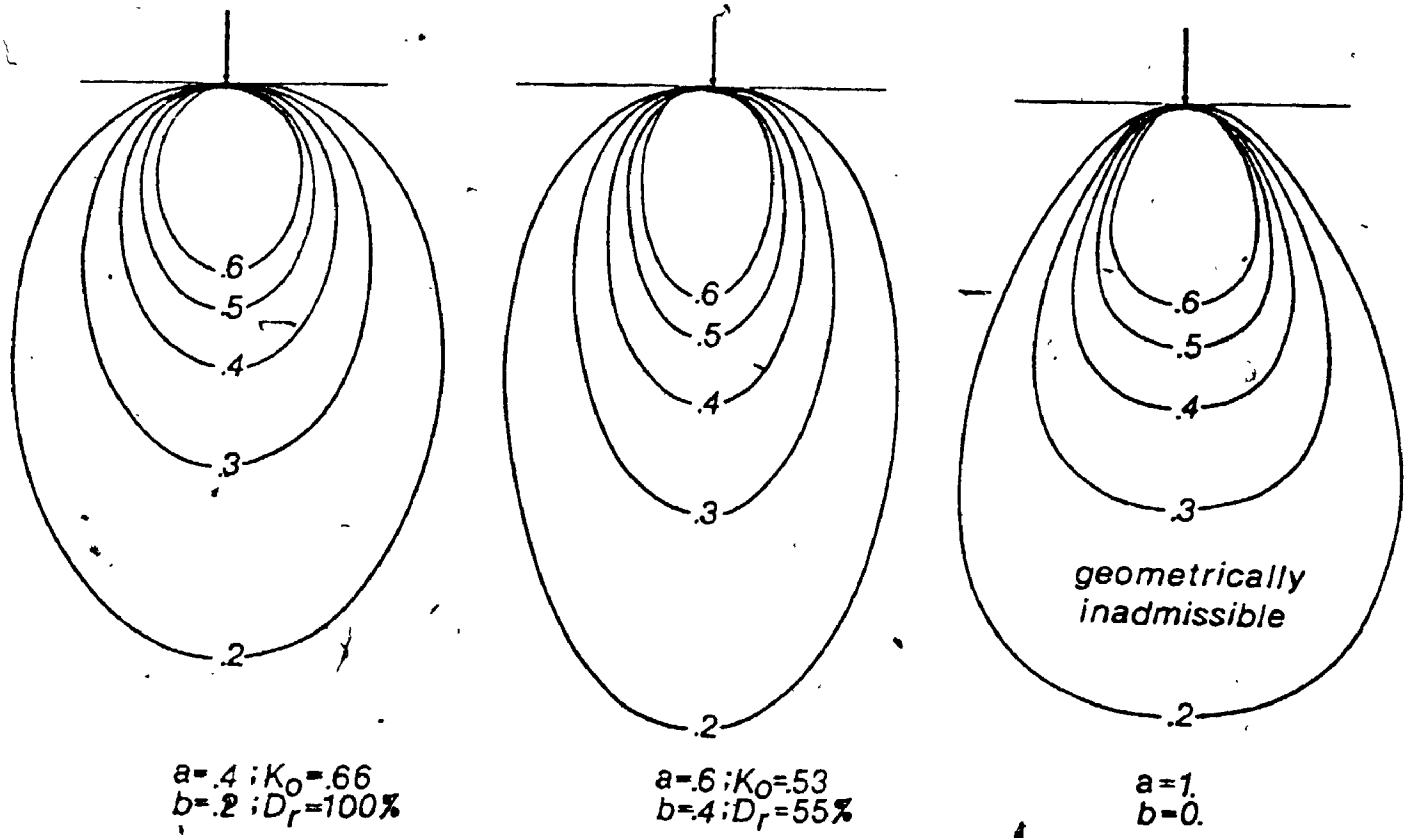

FIGURE 10. 8

CONTOURS OF EQUAL RADIAL STRESS FROM A
UNIT POINT LOAD ON A GRANULAR HALF-PLANE
(dense assemblies)

Fig. 10.8 shows contours of equal radial stress for dense assemblies as indicated by relative density. The load spreads predominately downward, along the stiffest direction (Fig. 7.1). For dense assemblies note that "the depth of penetration" of stress is mainly controlled by a, or, equivalently, by K_o.

The present solution reflects qualitative features of vertical stress distributions observed in plate loading tests conducted on sand (Fig. 10.9). Direct numerical comparison of theoretical and experimental results is not possible, since the above solution was developed for plane assemblies. Such comparisons must wait for adequate treatment of anisotropy of three-dimensional systems. However, the above solution clearly demonstrates how micro-features of contact forces result in the peculiar shapes of stress distributions. All experiments on photo-elastic discs (as on Fig. 2.1) clearly show "load paths" running in the direction of anisotropy, though statistically scattered. Such load paths of contact forces result in deep stress penetration, as indicated in Fig. 10.8 .

A discussion of the main theoretical concepts which lead to the solution presented in the preceding section will be given in the concluding chapter of the thesis. The present section discusses the above results towards which the developed theory was oriented.

The main physical reason for stress distributions so qualitatively different from solutions of isotropic elasticity is anisotropy in contact orientations. This inherent feature of natural granular deposits ultimately filtered through a series of theoretical constructions to result in a formal solution which qualitatively reflects results of plate loading tests shown in Fig. 10.9. The specific magnitudes of K_o and relative

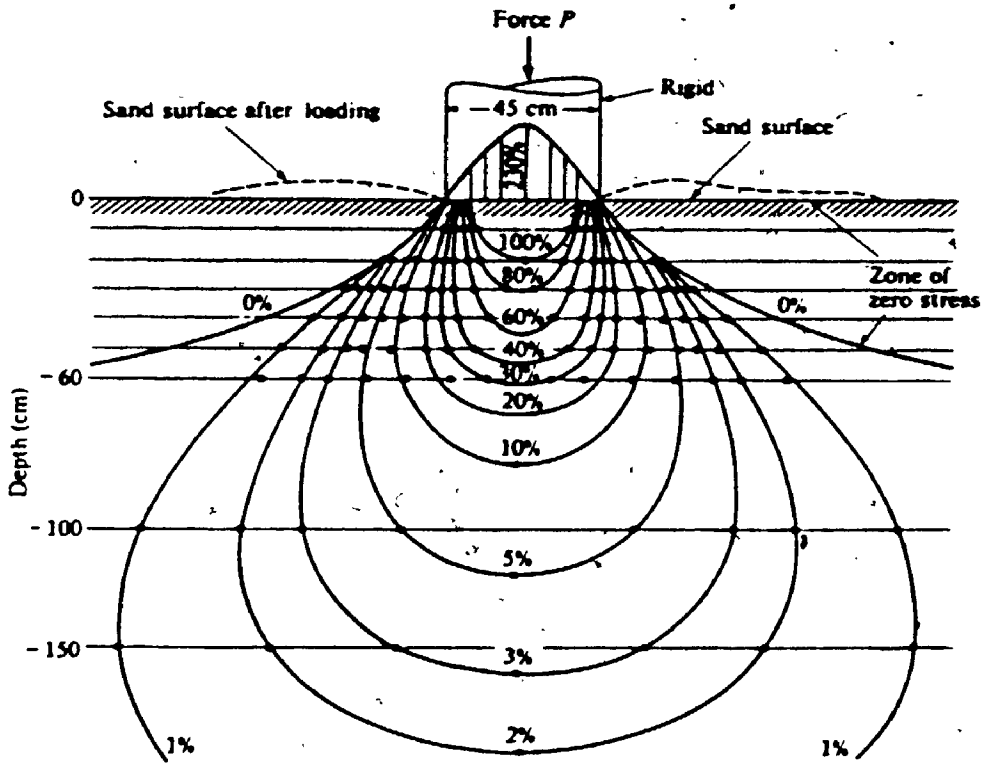

FIGURE 10.9

CONTOURS OF EQUAL VERTICAL STRESS IN PLATE LOADING TESTS ON A GRANULAR BASE (taken from [14])

density are for a plane assembly of equal size discs. Any plane assembly can, however, be described similiarly in terms of a, b.

The analysis of discs suggests that stress distributions in dense assemblies are controlled mainly by a which is related to K_0. This indicates practical means to apply the theory, once three-dimensional analysis of granular assemblies will be performed.

In essence the developed equations are equations of linear anisotropic elasticity derived strictly for systems of bonded particles and employed for cohesionless assemblies with justifications presented in this chapter. The idea of these arguments ultimately can be expressed in a few words: since stresses are related to contact forces and contact forces are a result of grain deformations, stress distributions must be determined from elastic type of relationships, but these need not necessarily be linear.

CHAPTER XI

DISCUSSION, CONCLUSIONS, RECOMENDATIONS

11.1 Discussion

Before discussing the main premises and results of the present theory, it is worth identifying its place in the context of theories concerned with phenomenological description.

A quote from Truesdell on modern natural philosophy [37] will put the relation between physical and continuum theories into historical perspective. "The history of physics shows that different, apparently almost contradictory hypotheses of structure and definition of gross variables based upon them lead to the same equations of continua. From incorrect molecular hypotheses the first correct theories of viscosity in fluids and elasticity in solids were derived. The main worth of a field theory is lost if the results are tied irrevocably to conjectures about particle structure. Molecular hypotheses have come and gone, but a sound continuum theory is a monument forever, except from fashion."

The theory presented in this work is a physical theory precisely of the type mentioned in the above quote. It is based partly on rigorous analysis of static equilibrium and compatibility, partly on mathematically expressed assumptions of physical nature. To a large extent it is based on physical intuition and hypothetical mechanisms. The final result is a continuum type description, but with parameters with physical meaning that can be explained. The parameters can be obtained not only by fitting equations to experimental data, as is frequently

the case of pure continuum modelling.

The theory was developed for highly idealized systems and its full strength can be felt only when sufficiently generalized, but not at the expense of losing relevance to the physical systems it describes.

This discussion attempts to evaluate the generality of the basic concepts developed in the present work and the general conclusions which follow from its concepts.

The definition of phenomenological parameters and their implications are the key point of the theory and they will be discussed in the following section.

11.1.1 Definition of Phenomenological Parameters

Although the terms "stress" and "strain" are used throughout the present work, the meaning attached to the quantities differs from those in continuum mechanics. Stress and strain tensors are viewed here as a means of external control over the system by specification of gross loads or displacements on assembly boundaries. Strictly speaking, stress and strain can be used in this capacity only for homogeneous loads. In the case of non-homogeneous loads, they indeed become field variables through the introduction of statistical elements of description and ensemble logic (section 3.14).

The essence of phenomenological description, however, does not lie in these technicalities. The basis for the whole theory are volume-additive identities (3.11) and (5.18)

$$\sigma_{ij}^{\beta} = \frac{1}{V} \sum_{c \in V} \frac{d^c}{2} f_i^c n_j^c$$
$$\varepsilon_{ij}^{\beta} = \frac{2}{M} \sum_{c \in V} n^c \delta_i^c n_j^c \qquad (11.1)$$

which follow directly from equations of static equilibrium and geometrical compatibility. These identities, which express the geometrical and the force connectivity of the system, basically indicate how phenomenological descriptions become possible: certain combinations of micro-parameters are fixed through external control by σ^{β}_{ij} or ε^{β}_{ij}. The volume-additive form of (11.1) immediately suggests that for homogeneous conditions such combinations of contact forces and relative displacements evaluated for sufficiently large volumes will be close to boundary tensors. These relationships can be written for any particulate system regardless of particle shape.

Applications of the developed relationships are still difficult due to the inherent uncertainties in statistico-geometrical analyses.

For linear systems there always will be equations of linear elasticity, but of a type not usually postulated from general considerations. It was shown that in anisotropic granular systems of bonded particles, components of displacement gradients must be constrained for systems with contacts that cannot transfer moments, otherwise Cosserat continuum would appear in its full generality. This development is not presented here and the topic of main concern in this work are assemblies of cohesionless particles, systems with no fixed geometry of contacts and no compatibility in contacts over a significant period of a deformation process.

For any finite system, there can, perhaps, be a small load increment when the system is compatible, i.e. externally controlled. Continuum description, however, corresponds to an infinite assembly subject to

loads on infinity. In this case it is doubtful that external control can be exercised even for an infinitesimal load increment. In any case the system will exhibit regular features and therefore can be described phenomenologically.

The difficulty is that the system becomes "quasi-dynamic" unlike the "quasi-static" systems for bonded particles. Its precise history cannot be traced with equations of static equilibrium only. In such quasi-dynamic processes there will be fast relaxations of contact forces, collisions and dissipation of energy.

To pose a mechanical problem precisely and solve it is extremely difficult. It becomes necessary to resort to hypotheses of physical nature.

In the case of bonded particles there were also assumptions involved with existence of certain limits for an infinite assembly and guesses about the form of distribution functions for contact forces. Right or wrong, the *type* of final result, the linear equations of elasticity, still follow. This is precisely the point made by Truesdell in his lecture. Guesses come and go, but a hypothesis about the mechanism of deformations for cohesionless systems will determine the type of continuum description for this system.

Rational mechanics cannot specify as to what type of description is adequate for "hard balls" and sufficient for practitioners. The scheme suggested can be analyzed, classified and generalized within the framework of continuum mechanics, as was the case of the Ossen-Frank physical theory of liquid crystals. Generalizations of the present theory were not intended here.

11.1.2. Compatibility in Cohesionless Systems

Observed deformational responses of cohesionless systems exhibit continuum type regularities. Up to the ultimate state a loading process can be stopped and the system be observed in static equilibrium. This immediately makes it possible to use volume-additive identities and justify the introduction of the stress tensor.

Taking the process to be quasi-dynamic with continuous structural changes raises serious questions as to how compatibility conditions can be written. For a plane assembly, such conditions can be written for any system of closed loops of segments connecting particle centers and it can be asusmed that contacts which are preserved during structural rearrangements always exist, so that compatibility conditions can be written on the basis of those contacts.

Observations of mechanisms of deformation show that particles move during the micro-softening state of the process in conglomerates. Due to the fact that forces on sliding contacts are not related to interparticle displacements, the system is not controlled externally during the process. Deformations related to sliding are the so-called "plastic deformations" for which a condition of compatibility can be written separately. This condition does not include contacts within blocks.

According to a hypothesis based on the concept of "continuously unstable systems", potential energy of the system related to deformation of contact points is always a minimum. The minimum potential energy related to contact forces is always associated with a second rank tensor that satisfies the equations of compatibility as a strain

tensor. This tensor was not identified with elastic strains, since it is impossible to separate "plastic" and "elastic" strains, as implied by the concept of continuously unstable systems.

If a formal continuum mechanics scheme is to constructed, there now are two strain tensors and both must satisfy conditions of compatibility, simultaneously. The stress tensor is related to elastic deformations; as in usual elasto-plastic models and plastic flow it is described separately. Plastic flow occurs in accordance with the requirements of geometrical compatibility. Therefore, there are two sets of equations linked through the structure of the system, i.e. parameters of anisotropy a, b. Flow rules based on these parameters have not been worked out yet due to the analytical complexity of relationship (9.41).

The simplicity of this scheme lies in a disjoint set of equations for any fixed a,b. They are position-dependent, but the stress tensor can be evaluated separately for any load increment and for fixed a, b at each point. Variations of a, b can be determined separately. This scheme assures that stress distributions will be "reasonable", as the example with constants a, b suggests. There is still a great deal of numerical work to be done in this direction.

The above scheme follows from micromechanical considerations of compatibility developed in the present work.

11.2 Conclusions

(1) Examination of idealized granular systems on the basis of equations of static equilibrium resulted in the introduction of

the phenomenological stress tensor as a fluctuating function of volume. Ensemble averages of the phenomenological stress tensor and its limit for an infinite assembly possess all formal properties of the continuum mechanics stress tensor which in described cases is related to average forces on contacts of the same orientation and contact orientation distribution. Considering that the mentioned development is based on conditions of static equilibrium only, granular systems cannot be studied without considerations of their internal structure.

(2) Introduction of the elastic strain tensor is possible, unconditionally, for systems of bonded particles due to micro-compatibility in contacts. The micromechanical analogue of the elastic strain tensor is expressed in terms of relative displacements between particle centers and contact orientation distribution. The mentioned expression was derived for plane assemblies only.

(3) Deformations of cohesionless materials related to structural rearrangement is viewed as a quasi-dynamic process and it is suggested that in continuum mechanics modelling schemes separate equations of compatibility should be written for "elastic" and "plastic" strain rates. The mechanism is believed to reflect compatibility in the system during local micro-cycles of "hardening" and "softening".

(4) The same view on the mechanism of deformations in cohesionless systems uses the equations of anisotropic elasti-

city to determine stress distributions in granular masses. Such equations were presented for plane granular assemblies and their use to describe plane strain conditions for three-dimensional systems is not recomended.

The above conclusions are related to the global objectives of the theory with respect to a phenomenological description of granular systems. Despite the specific formulae and derivations presented for idealized systems, the major conclusions regarding the nature of processes in granular systems are general. Conclusions of the present theory with regard to engineering problems of soil mechanics follow:

(1) Qualitative comparisons of stress distributions under point load on a plane assembly with the results of plate loading tests on granular masses indicate that the observed shapes of stress distributions are undoubtedly due to the inherent anisotropy of granular masses.

(2) Theoretical mechanisms of load transmission in granular assemblies presented here point to the use of the equations of anisotropic elasticity to determine stress distributions in granular masses.

(3) The statistico-geometrical analysis of plane assemblies of discs combined with the theory of lateral (earth) pressure at rest presented here indicate that parameters determining stress distributions in granular masses under a "first load increment" are related to K_o and relative density of the system.

(4) The link between K_o and the parameter of structural anisotropy

can potentially provide means for evaluating one parameter in terms of the other.

(5) Provided an efficient way of evaluating anisotropy parameters of granular deposits will be found, a routine procedure for evaluating settlements can be developed similar to that currently existing for settlement in clays.

The idealized granular systems studied here provide general guidance as to mechanisms of load transmission in such systems. Considering that patterns of stress distributions are sensitive to parameters a, b, their evaluation from experiments with plane assemblies should be approached with caution, if applications to three-dimensional systems are intended.

Conclusions of possible general interest are the following.

(1) The expression for Poisson's ratio in terms of normal and tangential contact stiffnesses can lead to the construction of an artificial material with negative Poisson's ratio.

(2) The presented statistico-geometrical analysis of plane assemblies resulted in a relationship between the average coordination number of the system and its density.

(3) The statistico-geometrical analysis also resulted in prediction of maximum random density for plane assemblies and instability in the structure of plane assemblies under anisotropic perturbations. Such instability occurs near the average coordination number 4 which corresponds to the point of "liquid-solid" phase transition for plane systems.

11.3 Recomendations

Recomendations for further research are presented in order of priority, as viewed by the author.

(1) To develop transversely isotropic stress-strain relationships for three-dimensional assemblies based on second and fourth Fourier components of contact orientation.

(2) To correlate theoretically the parameter of anisotropy a and K_o.

(3). To attempt to correlate nuclear densometer density readings with K_o in carefully controlled laboratory conditions, placing a nuclear probe in the vertical and horizontal directions.

APPENDIX A

KINEMATICS AND GENERAL THEOREM OF MECHANICS FOR ASSEMBLIES OF PARTICLES

A.1 Kinematics of Particles

The positions of particles in deformation processes can be described in terms of displacements of particle centers which uniquely define normal components of contact forces. Tangential components depend on relative tangential displacements of contact surfaces and are controlled both by interparticle displacements and rotations which must be considered simultaneously.

A set of displacement and rotation vectors define the motion of particles as rigid bodies, while contact forces are related to their deformations. For sufficiently rigid particles, however, a contact area is small, so that deformations in sufficiently separated contacts can be considered independent and contact deformations can be given in terms of kinematic parameters of rigid body motions.

Consider two particles, k and m, referred to a fixed Cartesian coordinate system. Let $\underset{\sim}{l}_o^k$, $\underset{\sim}{l}_o^m$ be displacements of particle centers and $\underset{\sim}{\omega}^k$, $\underset{\sim}{\omega}^m$ particle rotation vectors (Fig. A.1), assumed small along with relative translations. To be able to determine contact forces and moments it is convenient to describe the motion of particle m with respect to particle k, i.e. to consider the kinematics with respect to a coordinate system fixed at the center of particle k.

Let $\Delta'\underset{\sim}{l}^{km}, \Delta\underset{\sim}{\omega}^{km}$ be translation of the center and rotation of particle m with respect to the moving coordinate system. To determine $\Delta'\underset{\sim}{l}^{km}$, $\Delta\underset{\sim}{\omega}^{km}$ consider an arbitrary point A on particle m with position vector $\underset{\sim}{r}$ with

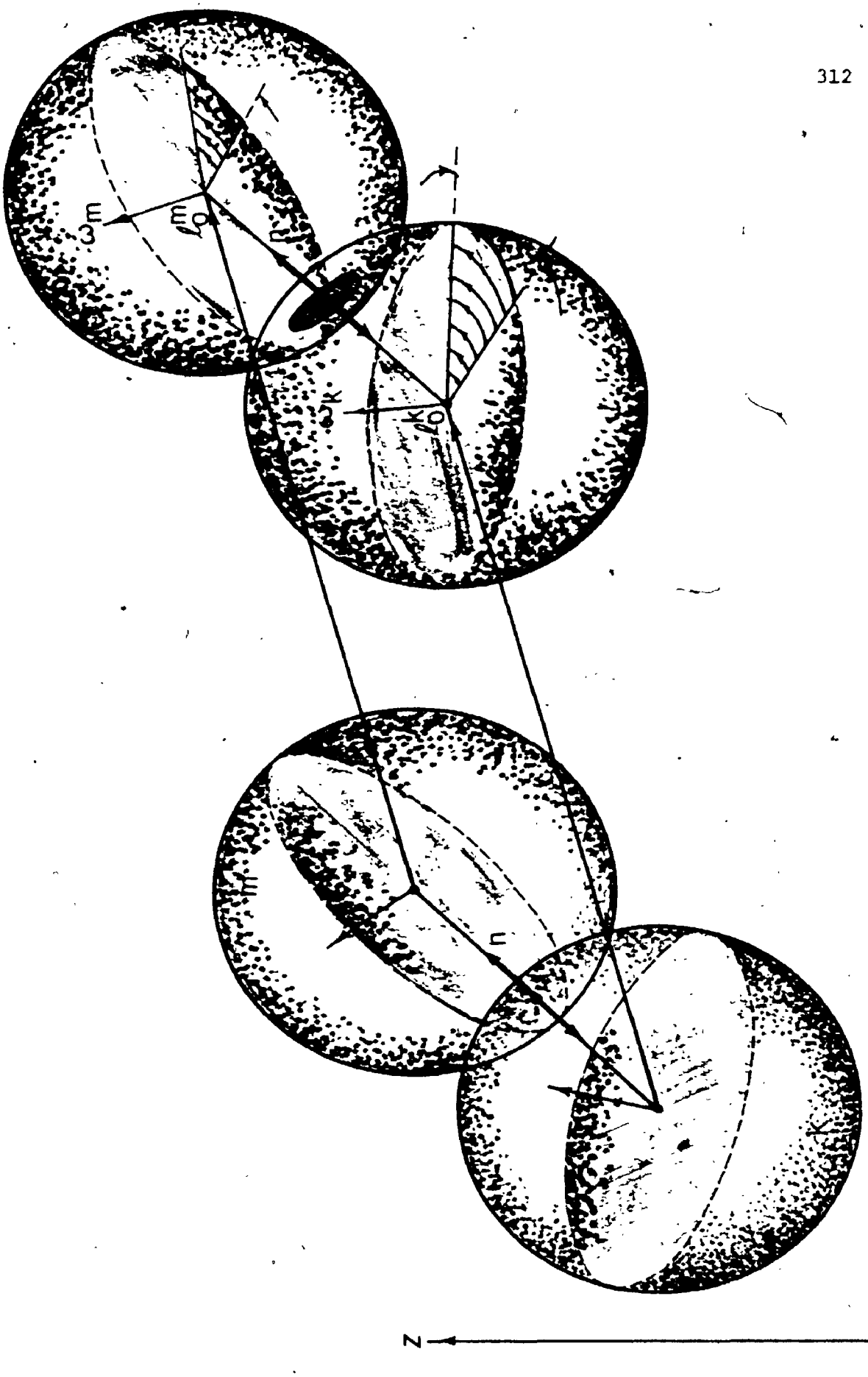

Fig A.1

respect to the center of the particle. By definition of particle rotations, this point will translate in space by the vector

$$\underset{\sim}{l}^m_r = \underset{\sim}{l}^m_o + [\omega^m \mathbf{x} \underset{\sim}{r}] \qquad \text{.....Eq.(A.1)}$$

where the brackets indicate a cross product of two vectors. On the other hand, the same translation of the selected point can be given as a sum of contributions from the motion of the coordinate system and the motion with respect to this coordinate system, i.e.

$$\underset{\sim}{l}^m_r = \underset{\sim}{l}^k + [\omega^k \mathbf{x} \underset{\sim}{r}'] + \Delta \underset{\sim}{l}^{km} + [\Delta\omega^{km} \mathbf{x} \underset{\sim}{r}] \qquad \text{.....Eq.(A.2)}$$

where r' is the position of the selected point in the moving coordinate system.

Both (A.1) and (A.2) must be identical as representing the same motion. If $\underset{\sim}{r}$ coincide with the center of particle m, $\underset{\sim}{r}' = d_o \underset{\sim}{n}^k$, where $\underset{\sim}{n}^k$ is the normal vector of the contact from the point of view of particle k, both (A.1-2) give

$$\Delta \underset{\sim}{l}^{km} = \underset{\sim}{l}^m - \underset{\sim}{l}^k - d_o[\omega^k \mathbf{x} \underset{\sim}{n}^k] \qquad \text{.....Eq.(A.3)}$$

If r coincide with the position of the contact (i.e. $\underset{\sim}{r} = \frac{d_o}{2}\underset{\sim}{n}^m$), (A.1-2) give

$$\Delta\omega^{km} = \omega_m - \omega_k \qquad \text{.....Eq.(A.4)}$$

Note that interparticle distance and orientations of contact points were taken in the above derivations as d_o and n^k, respectively i.e. as in an undeformed state. Observation of (A.3) shows that the mentioned quantities enter it as products with ω^k assumed small. Neglected quantities therefore contribute only terms of the order higher than the first and can be neglected for infinitesimal rotations and relative motions.

Assume for a moment that particle m is completely rigid and only

particle k deforms. The displacement of the contact point on m consists in translation Δl^{km} plus additional translation $[\Delta\omega^{km} \times \frac{d_o}{2} n^m]$ due to relative rotation $\Delta\omega^{km}$. Combination of both motions gives

$$\Delta l^{k,m} = l^m - l^k + \frac{d_o}{2}[\omega^m \times n^m] - \frac{d_o}{2}[\omega^k \times n^k] \qquad \text{.....Eq.(A.5)}$$

Since contact forces are related to deformations of particles, the latter can be expressed through relative displacements between particles centers as $\frac{1}{2} l^{k,m}$.

The term in (A.5) related to rotations is tangential to the surfact of the contact. Vector $l^{k,m}$ can be given as a sum of a vector in the direction of the contact normal n^k and a vector lying in the plane of the contact

$$\Delta \underset{\sim}{l}_n^{km} = [(\underset{\sim}{l}^m - \underset{\sim}{l}^k) \cdot \underset{\sim}{n}^k] \underset{\sim}{n}^k$$
$$\Delta \underset{\sim}{l}_t^{km} = \Delta \underset{\sim}{l}^{km} - \Delta \underset{\sim}{l}_n^{km} \qquad \text{.....Eq.(A.6)}$$

where the term in parenthesis is the scalar product of the two vectors.

Note that vectors of relative translation of the contact point change sign under permutations of superscripts, i.e. $\Delta l^{k,m} = - \Delta l^{mk}$.

The above kinematics is sufficient to describe contact interactions in terms of the introduced quantities.

A.2 Force Conditions in Contacts

Contact force - interparticle compliance relationships are generally non-linear, even for linearly elastic particles, due to change in the area of contact under varying normal forces. For the fixed level of normal loads, the response of the contact to tangential displacements in the area of contact is linear, if no slip occurs between particles.

In the last case, the tangential component of the contact force depends on the loading history . Such variability in the force-displacement response of an individual contact requires careful physical analysis of each particular problem.

In the case of bonded particles, the area of a contact can be considered fixed and linear force - compliance relationships reasonable approximations. If non-linearity occurs, deformational response can be considered in incremental form.

Linear analysis of bonded particles is also suitable for description of assemblies of cohesionless particles which behave as assemblies of bonded particles within extremely small ranges of external loads when all contacts are preserved and there is no particle rearrangement. After rearrangement of particles with resulting permanent deformations, the formation of contact forces is controlled again by elastic deformations of particles.

Although the magnitude of elastic deformations is insignificant compared to permanent deformations, their effect on contact forces is predominant. In such situations, interparticle contacts can be considered linear, with stiffnesses corresponding to the achieved level of external loads.

Consider two particles, k and m, and the relative motion of particle m with respect to k. The action of particle m on particle k can be specified in terms of forces and moments which are statically equivalent to the distributed load in the area of contact. The following linear relationships for an individual contact can be considered:

$$\underset{\sim}{f}_n^{km} = \tilde{k}_n \Delta \underset{\sim}{l}_n^{km}$$
$$\underset{\sim}{f}_t^{km} = \tilde{k}_t \Delta \underset{\sim}{l}_t^{km} \qquad \text{.....Eq.(A.7)}$$

$$\underset{\sim}{m}^{km} , \tilde{K}_n \Delta \underset{\sim}{\omega}_n^{km}$$
$$\underset{\sim}{m}_t^{km} = \tilde{K}_t \Delta \underset{\sim}{\omega}_t^{km} \qquad \text{.....Eq.(A.8)}$$

where $\underset{\sim}{f}_n^{km}$, $\underset{\sim}{f}_t^{km}$ are normal and tangential components of the force acting on particle k from m; $\underset{\sim}{m}_n^{km}$, $\underset{\sim}{m}_t^{km}$ are normal and tangential components of the moment transferred to k from m. Coefficients k_n, k_t are normal and tangential contact stiffnesses and K_n, K_t are torsional and rotational stiffnesses. The terminology and physical meaning of (A.7-8) will now be explained.

Since Δl_n^{km} and Δl_t^{km} are (twice) the normal and tangential components of the displacement of the contact point on k, equations (A.7) simply state that the resultants of distributed forces in the area of contact are in the directions of their respective

This is the alternative for a circular contact to two isotropic materials. Stiffnesses k_n, k_t are related to material properties (Young's modulus E and Poisson's ratio ν); for a circular contact of two spheres

$$k_n = \frac{E}{2(1-\nu^2)} d_c$$
$$k_t = \frac{E}{(1+\nu)(2-\nu)} d_c \qquad \text{.....Eq.(A.9)}$$

where d_c is the diameter of a Hertzian contact [22] related to the normal component of the force f_n^c as follows:

$$d_c = d_o \left[3 \frac{1-\nu^2}{E} \frac{f_n}{d_o^2} \right]^{1/3} \qquad \text{.....Eq.(A.10)}$$

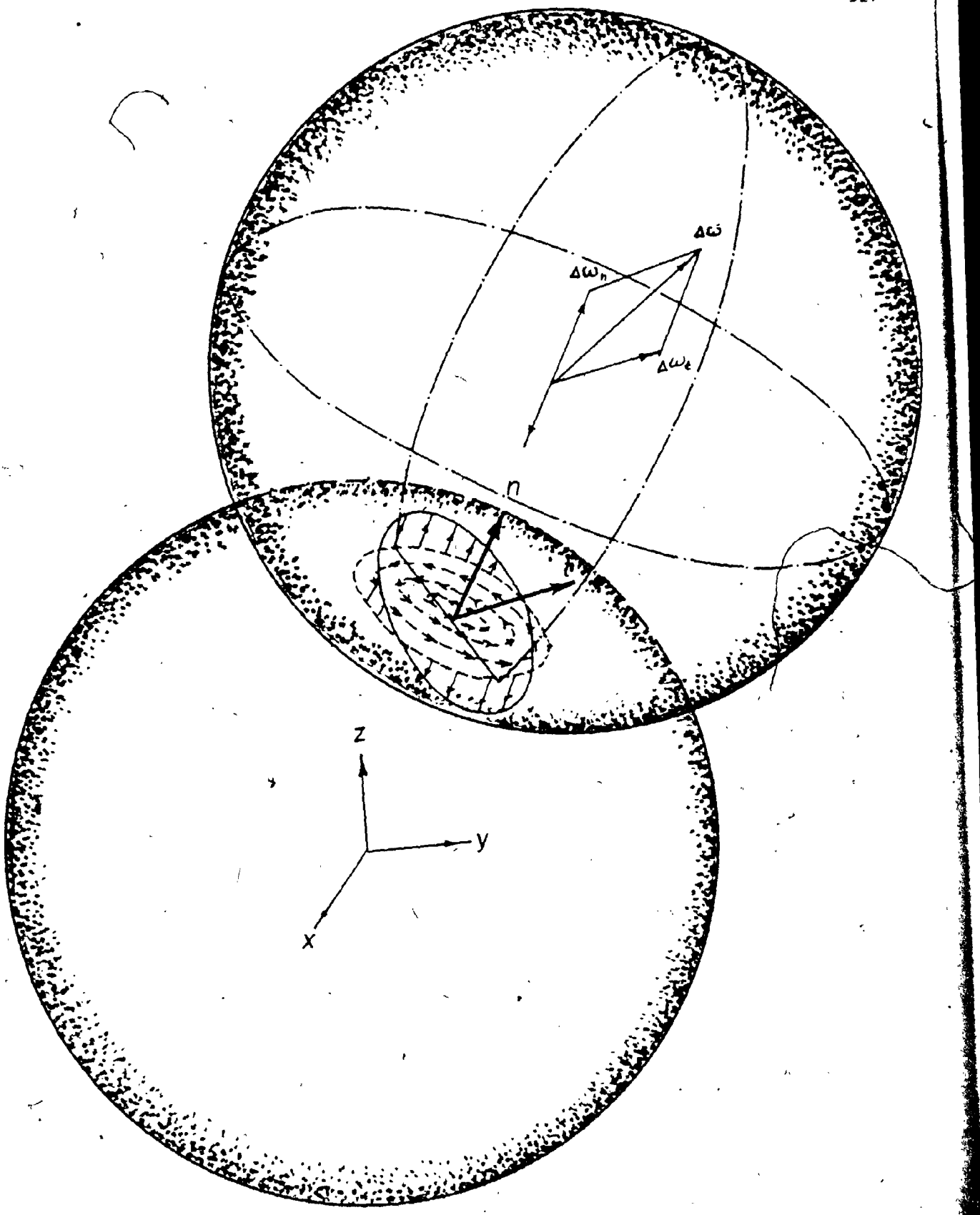

Fig. A.2

The theory is developed for arbitrary stiffnesses of the contact which allows flexibility in selecting the model of the contact.

Equations (A.8) require more elaborate discussion. Fig. A.2 shows that the relative rotation of particle m with respect to k can be decomposed into two rotations: $\Delta\omega_n^{km}$ subjects the plane of the contact to torsion and $\Delta\omega^{km}$, the tangential component of the relative rotation, tends to "lift" one part of the contact and "depress" the other, thus imposing linear variation of contact surface displacements in the normal direction. It is clear that such displacements result in a moment transferred to sphere k. The magnitude of the moment can be calculated by solving the corresponding density problem. Although to the knowledge of the author no solution to this problem is known, the moment transferred to m can be estimated using analogy with bending of a circular shaft.

The solution for the torsional stiffness belongs to Mindlin [39], and both constants $\tilde{K}_n$ and $\tilde{K}_t$ can be written in the form

$$\tilde{K}_n = \frac{E}{6(1+\nu)}\, d_c^{\,3}$$

$$\tilde{K}_t = E\, d_c^{\,3} \qquad \text{.....Eq.(A.11)}$$

The proportionality of K_t to the third power of the contact diameter can be established on the basis of dimensional analysis. Comparison of (A.10) and (A.11) shows that, for small areas of contact, rotational and torsional stiffnesses are negligible compared to normal and tangential stiffnesses of contacts. This fact enables to exclude contact moments from the theory of granular assemblies.

For example, an estimate shows that $d_c = 0.02\, d_o$ under hydrostatic stress 625 kPa on an assembly with void ratio 0.6. The following theo-

rems, however, are proven with contact moments included.

The applicability of such a contact model reaches far beyond the mechanics of granular systems and the developed methods are applicable to description of large random networks of straight elastic members, (for example, structural systems which are usually treated using the stiffness method).

A.3 Principle of Virtual Work

Further theoretical developments are based on the principle of virtual work derived here for general interactions in discrete systems of particles, including rotations.

Consider equations of equilibrium of particles in the form

$$\sum_{m=1}^{n_k} \underset{\sim}{f}^{k,m} + \underset{\sim}{X}^{k} = 0 \qquad \text{.....Eq.(A.12)}$$

$$\sum_{m=1}^{n_k} (\underset{\sim}{r}^{km} \times \underset{\sim}{f}^{km} + m^{km}) + (\underset{\sim}{r}_o^k \times \underset{\sim}{X}^k) + \underset{\sim}{M}^k = 0 \qquad \text{.....Eq.(A.13)}$$

where $\underset{\sim}{r}^{km}$ is the position of the contact point between particles k and m, $\underset{\sim}{r}_o^k$, position of the center of particle k; $\underset{\sim}{X}^k$, $\underset{\sim}{M}^k$, body foces and moments. Due to symmetry of particles, $\underset{\sim}{X}^k$ is applied at particle centers.

The second equation represents the balance of moments about the origin and can be rewritten in terms of moments of contact forces about particle centers. Making use of (A.12), (A.13) can be given in the form

$$\sum_{m=1}^{n_k} [(\underset{\sim}{r}^{km} - \underset{\sim}{r}_o^k) \times \underset{\sim}{f}^{km} + m^{km}] + \underset{\sim}{M}^k = 0 \qquad \text{.....Eq.(A.14)}$$

Suppose that positions of all particles and rotations vary with virtual rates $\dot{\underset{\sim}{l}}^k$, $\dot{\underset{\sim}{\omega}}^k$. Multiplication of (A.12) by $\dot{\underset{\sim}{l}}^k$, addition of all

equations and separation of terms corresponding to internal and boundary contacts gives

$$\sum_{(k,m)\in V} [(f^{km}\cdot \dot{l}^k) + (f^{mk}\cdot \dot{l}^m)] + \sum_{k\in V} (X^k\cdot \dot{l}^k) + \sum_{(k,m)\in B} (f^{km}\cdot \dot{l}^k) = 0 \quad \text{.....Eq.(A.15)}$$

Since $f^{km} = -f^{mk}$, the term in brackets can be rewritten in the form

$$-\frac{1}{2}\sum [f^{km}(\dot{l}^m - \dot{l}^k) + f^{mk}(\dot{l}^k - \dot{l}^m)]$$

Making use of (A.5) for $\dot{l}^m - \dot{l}^k$ and $\dot{l}^k - \dot{l}^m$, (A.14) can be transformed into

$$\frac{1}{2}\sum_{(k,m)\in V} f^{km}\Delta\dot{l}^{km} + \sum_{(k,m)\in V+B} f^{km}\frac{d_o}{2}[\dot{\omega}^k \times n^k] = \sum_{k\in V} (X^k\dot{l}^k) + \sum_{(k,m)\in B} f^{km}(\dot{l}^k + \frac{d_o}{2}[\dot{\omega}^k \times n^k]) \quad \text{(A.16)}$$

The summations in (A.15) are with respect to all pairs (k,m) corresponding to the contact of particles k and m. Note that terms (k,m) and (m,k) corresponding to the same contact are considered separately. Recalling that $\frac{1}{2}\Delta\dot{l}^{km}$ is the rate of displacement of the contact point when particle k is fixed, the first term in (A.16) is the rate of work of contact forces on internal deformations. The second term is the rate of work of contact forces on particle rotations. Since $\dot{l}^k + \dot{\omega}^k \times \frac{d_o}{2} n^{km}$ is the rate of translation of the contact point, the left-hand side of (A.16) is the rate of work of external forces on translations of boundary contacts.

The second term in the right-hand side of (A.16) is not related to the work of deformations and must be excluded on the basis of (A.14) for which scalar multiplication by $\dot{\omega}^k$ and further summation gives

$$\sum_{(k,m)\in V+B} f^{km}\cdot[\dot{\omega}^k \times \frac{d_o}{2} n^k] + \sum_{(k,m)\in(V+B)} m^{km}\cdot\dot{\omega}^k + \sum_{k\in V}[(M^k\cdot\dot{\omega}^k) + (r_o^k \times X^k)\cdot\dot{\omega}^k] = 0 \quad \text{(A.17)}$$

Note that the order of multiplication in triple products was interchanged. The second term in (A.17) can be represented in the form

$$\sum_{(k,m)\in(V+B)} m^{km}\,\dot{k} = -\frac{1}{2}\Big[\sum_{(k,m)\in V}(\underset{\sim}{m}^{km}\cdot\Delta\dot{\underset{\sim}{\omega}}^{km}) + \sum_{(k,m)\in B}(\underset{\sim}{m}^{mk}\cdot\Delta\dot{\underset{\sim}{\omega}}^{mk})\Big] + \sum_{(k,m)\in B}\underset{\sim}{m}^{km}\cdot\dot{\underset{\sim}{\omega}}^{k}$$

Combination of (A.16) and (A.17) finally gives

$$\dot{W}_{def} = \dot{W}_{ext} \qquad \text{.....Eq.(A.18)}$$

where

$$\dot{W}_{def} = \frac{1}{2}\Big[\sum_{(k,m)\in V}(f^{km}\cdot\Delta\dot{l}^{km}) + (f^{mk}\cdot\Delta\dot{l}^{mk})\Big] + \frac{1}{2}\Big[\sum_{(k,m)\in V}(m^{km}\Delta\dot{\omega}^{km} + m^{mk}\Delta\dot{\omega}^{mk})\Big] \qquad (A.19)$$

$$\dot{W}_{ext} = \sum_{(k,m)\in B} f^{km}\Big[\dot{l}^{k} + (\dot{\omega}^{k}\times\frac{d_o}{2}n^{km})\Big] + \sum_{(k,m)\in B}(m^{km}\cdot\dot{\omega}^{k}) + \sum_{k\in V} X^{k}\dot{l}^{k} + \sum_{k\in V}(M^{k}\cdot\dot{\omega}^{k}) \qquad (A.20)$$

All vectors entering (A.18) can be given in the form

$$\begin{aligned}
\underset{\sim}{f}^{km} &= f^{c}_{n}\underset{\sim}{n}^{km} + f^{c}_{t}\underset{\sim}{t}^{km}_{l}\\
\Delta\dot{\underset{\sim}{l}}^{km} &= \Delta\dot{l}^{c}_{n}\underset{\sim}{n}^{km} + \Delta\dot{l}^{c}_{t}\underset{\sim}{t}^{km}_{l}\\
\underset{\sim}{m}^{km} &= m^{c}_{n}\underset{\sim}{n}^{km} + m^{c}_{t}\underset{\sim}{t}^{km}_{\omega}\\
\Delta\dot{\omega}^{km} &= \Delta\dot{\omega}^{c}_{n}n^{km} + \Delta\dot{\omega}^{c}_{t}t^{km}
\end{aligned} \qquad \text{.....Eq.(A.21)}$$

The quantities f^{c}_{n}, f^{c}_{t}, Δl^{c}_{n}, m^{c}_{n}, m^{c}_{t}, $\Delta\dot{\omega}^{c}_{n}$, $\Delta\dot{\omega}^{c}_{t}$ are components of (A.21) in local coordinate systems. Being identical in both sides of the contact, these quantities completely describe the state of an individual contact.

Scalar products entering (A.19) can be explicitly evaluated on the basis of (A.21) and the work of internal deformations can be rewritten in the form

$$\dot{W}_{int} = \sum_{c\in V} f^{c}_{n}\Delta\dot{l}^{c}_{n} + f^{c}_{t}\Delta\dot{l} + m^{c}_{n}\Delta\dot{\omega}^{c}_{n} + m^{c}_{t}\Delta\dot{\omega}_{t} \qquad \text{.....Eq.(A.22)}$$

Deformational properties of particles given in vector form by (A.7-8) now can be rewritten in scalar form

$$\begin{aligned} f_n^c &= \tilde{k}_n \Delta l_n^c \\ f_t^c &= \tilde{k}_t \Delta l_t^c \\ m_n^c &= \tilde{K}_n \Delta\omega_n^c \\ m_t^c &= \tilde{K}_t \Delta\omega_t^c \end{aligned} \qquad \text{.....Eq.(A.23)}$$

where k_n, k_t are normal and tangential contact stiffnesses and Δl_n^c, Δl_t^c correspond to what is usually termed "normal" and "tangential particle compliances". K_n, K_t are torsional and rotational stiffnesses, and $\Delta\omega_n^c$, $\Delta\omega_t^c$ will be called "torsional" and "rotational compliances", respectively. Force characterstics of the contact f_n^c, f_t^c will be referred to as "normal" and "tangential contact forces"; m_n^c and m_t^c are called "contact torque" and "contact bending moments", respectively. The term "bending moment" for m_t^c originated in engineering mechanics where such a quantity is introduced as a characteristic of bending stress in the cross-section of a beam subject to in-plane loads. The introduction of m^c and m_t^c here using a local coordinate system at the contact corresponds to the selection of a specific "sign convention" for bending moments and shears in engineering mechanics.

A.4 Theorem on Minimum of Complementary Work of Internal Deformations

Consider the work of internal deformations in the process when all contact forces, moments and corresponding compliances are brought to their final value. Integration of the rate of work in terms of in-

crements of contact forces and moments substituted into (A.22) instead of increments of compliances according to (A.23) gives

$$W_f = \sum_{c \in V} \left| \frac{(f_n^c)^2}{2k_n} + \frac{(f_t^c)^2}{2k_t} + \frac{(m_n^c)^2}{2K_n} + \frac{(m_t^c)^2}{2K_t} \right| \qquad \text{.....Eq.(A.24)}$$

Let boundary and body forces and moments be fixed and the set of compliances $L(\Delta l_n^c,\ \Delta l_t^c,\ \Delta\omega_n^c,\ \Delta\omega_t^c)$ together with the set of contact forces, moments and orientations of tangential components of f_t^c and m_t^c $F(f_t^c,\ f_n^c,\ m_n^c,\ m_t^c,\ t_l^c,\ t_\omega^c)$ give the complete solution of the problem. Contact forces and moments then satisfy equations of equilibirium and compliances are related to particle displacements and rotations according to (A.21, A.22-3).

Consider another set of contact forces and moments $\overline{F}$ for which equilibrium equations are satisfied, but compliances calculated on the basis of relationships for contacts (A.23) do not result in a geometrically compatible set of particle displacements and rotations. It will be proven that

$$W_{\overline{f}} - W_f > 0 \qquad \text{.....Eq.(A.25)}$$

Consider positive expression

$$W_{\overline{f}-f} = \sum_{c \in V} \frac{(\overline{f}_n^c - f_n^c)^2}{2k_n} + \frac{(\overline{f}_t^c - f_t^c)^2}{2k_t} + \frac{(\overline{m}_n^c - m_n^c)^2}{2K_n} + \frac{(\overline{m}_t^c - m_t^c)^2}{2K_t} > 0$$

which immediately gives

$$W_{\overline{f}-f} = W_{\overline{f}} - W_f + \sum_{c \in V} (\overline{f}_n^c - f_n^c)\frac{f_n^c}{k_n} + (\overline{f}_t^c - f_t^c)\frac{f_t^c}{k_t} + (\overline{m}_n^c - m_n^c)\frac{m_n^c}{K_n} + (\overline{m}_t^c - m_t^c)\frac{m_t^c}{K_t} > 0$$

Substituting true compliances instead of f_n^c, f_t^c, m_n^c, m_t^c according to (A.23), one can obtian the following expression:

$$W_{\overline{f}-f} = W_{\overline{f}} - W_f + \sum [(\overline{f}_n^c - f_n^c)\Delta l_n^c + (\overline{f}_t^c - f_t^c)\Delta l_t^c + (\overline{m}_n^c - m_n^c)\Delta\omega_n^c + (\overline{m}_t^c - m_t^c)\Delta\omega_t^c] > 0 \qquad \text{(A.26)}$$

Contact forces and moments $\tilde{f}_n^c = \bar{f}_n^c - f_n^c$, $\tilde{f}_t^c = \bar{f}_t^c - f_t^c$, $\tilde{m}_n^c = \bar{m}_n^c - m_n^c$, $\tilde{m}_t^c = \bar{m}_t^c - m_t^c$ satisfy equations of equilibrium (A.12-13) with zero boundary and body forces and moments, since both sets $\bar{F}$ and F correspond to equilibrium with the same external actions. The sum (A.26) represents the work of internal deformations of forces $\tilde{F}$ on true displacements and rotations of the system. Due to the principle of virtual work, this sum must be equal to the work of external forces which is zero for set $\tilde{F}$.

The last statment completes the proof, since (A.25) follows immediately. Inequality (A.25) means that the set corresponding to geometrically compatible compliances among all statically admissible sets of contact forces and moments compatible with fixed and prescribed external actions, gives absolute minimum to W_f (A.24) which is called "complementary work of internal deformations".

The formulation of the theorem and the expression for complementary work is not the most general, since it covers the case when external forces and moments are prescribed on the entire boundary of the assembly. If displacements and particle rotations are prescribed on the part of the boundary, expression (A.24) must be slightly modified.

APPENDIX B

PRESSURE TENSOR

B.1 Pressure in dynamic assemblies

Although only systems of particles in static equilibrium are of major interest to the present work, it is instructive to consider well established ideas leading to phenomenological description of dynamic systems. The behavior of such systems is of interest to statistical thermodynamics where considered particles are material points with a certain mass and interpreted as molecules interacting with forces which can be derived from a potential function $U(\underset{\sim}{r}^1 \ldots \underset{\sim}{r}^N)$ as follows:

$$\underset{\sim}{f}^k = -\frac{\partial U}{\partial \underset{\sim}{r}^k}, \qquad \ldots\ldots \text{Eq.(B.1)}$$

where $\underset{\sim}{r}^1, \ldots \underset{\sim}{r}^N$ are positions of particles and $\underset{\sim}{f}^k$ is the force acting on the particle k from all other particles in the system. Note that interactions of ideally elastic frictionless spheres can be described in terms of a potential derivable from Hertz's solution of the contact problem [22] so that such assemblies can formally be studied using methods of statistical mechanics.

Motion of particles with interaction (B.1) can be described in terms of $3N$ equations of Newtonian mechanics for particles with masses m^k

$$m^k \ddot{r}_i^k = -\frac{\partial U}{\partial r_i^k} \qquad (k=1, \ldots, N;\ i=1, 2, 3) \qquad \text{(B.2)}$$

which can be solved if initial particle positions and velocities are known.

Consider an assembly of particles confined within a certain impermeable boundary B.

In order to calculate average forces acting on the boundary, consider a solution $r^k(t)$ of equations of motion for a certain set of initial conditions. Multiplication of (B.2) by r_j^k and further addition of all equations with the same combination of i,j result in 9 identities of the form

$$\sum_{k=1}^{N} m^k \ddot{r}_i^k r_j^k = -\sum_{k=1}^{N} \frac{\partial U}{\partial r_i^k} r_j^k \qquad i, j = 1, 3 \quad \text{.....Eq.(B.3)}$$

Note that interaction of particles with the boundary must be included in (B.3) and such interactions can be described in terms of an additional potential $W(r^1,\ldots r^N, R)$ which gives the force acting on a particle r^k due to interactions with a point R of the boundary as follows

$$F_i^k = -\frac{\partial W}{\partial r_i^k} \qquad \text{.....Eq.(B.4)}$$

Taking into account a trivial identity

$$m\ddot{r}_i r_j = \frac{d}{dt}(m\dot{r}_i r_j) - m\dot{r}_i \dot{r}_j$$

and boundary forces (B.4), equations (B.3) can be rewritten in the form

$$-\int_B \sum_{k=1}^{N} (F_i^k r_j^k)\, dS = \sum_{k=1}^{N} m^k (\dot{r}_i \dot{r}_j) + \sum_{k=1}^{N} \left(-\frac{\partial U}{\partial r_i^k} r_j^k\right) - \frac{d}{dt}\sum_{k=1}^{N} (m^k \dot{r}_i r_j) \quad \text{.....Eq.(B.5)}$$

Integration over the surface of the boundary indicates that, generally, all points of the boundary act on all particles in the system. This is the case of long range forces (molecular interactions, for example). The boundary can be viewed as an imaginary surface which separates two interacting parts of the system. The negative sign in the left-hand side of (B.5) indicates action of the system on the boundary. Due to motions in the system, the force acting on the boundary at each point will fluctuate in time and, if measured with a macroscopic device, only a certain time average will be detected.

Defining a time average of the fluctuating force as

$$\overline{f} = \lim_{t\to\infty} \frac{1}{t} \int_0^t f(t)dt ,$$

(B.5) can be averaged to obtain

$$-\int_B \sum_{k=1}^{N} \overline{(F_i^k r_j^k)} dS = \sum_{k=1}^{N} m^k \overline{\dot{r}_i^k \dot{r}_j} + \sum_{k=1}^{N} \overline{\left(-\frac{\partial U}{\partial r_i^k} r_j^k\right)} \qquad \text{.....Eq.(B.6)}$$

Note that the time average of a derivative with respect to time can be calculated immediately as follows:

$$\overline{\dot{\phi}} = \lim_{t\to\infty} \frac{1}{t} \int_0^t \frac{d\phi}{dt} dt = \lim_{t\to\infty} [\phi(t) - \phi(o)]/t = 0,$$

if $\phi(t)$ is bonded or increases slower than t. The average of the last term in (B.5) therefore disappears, since the considered particle motions have finite velocities within the bounded region.

Considering a large assembly and neglecting the influence of particles distant from the boundary on forces acting on it, the left-hand side of (B.6) can be represented in the form

$$-\int_B \overline{F}_i(R) R_j dS , \qquad \text{.....Eq.(B.7)}$$

where $-\overline{F}_i dS$ is the time average of the force with which the system acts on the element of boundary dS. Due to specific reasons discussed in greater detail in the next section, not all motions and states of static equilibrium will be of interest, but only such which result in macroscopically homogeneous phenomenological measurements. For such motions a time average of the force the system acts on its boundary depends only on orientation of the normal vector to the boundary and it can be shown that in this case the force acting on the element of the boundary can be represented in the form

$$-\overline{F}_i(R) dS = p_{ij} n_j dS, \qquad \text{.....Eq.(B.8)}$$

where p_{ij} is a certain second rank tensor which defines a force acting on the internal boundary of the system and is called "pressure tensor". Representation of the boundary force (B.8) enables to evaluate (B.7) as follows:

$$-\int_B F_i(R)R_j dS = \int_B p_{ik}n_k R_j dS = p_{ik}V \qquad \text{.....Eq.(B.9)}$$

where V is the volume of the system. The integral in (B.9) was evaluated using the Green-Gauss theorem*. The left-hand side of (B.6) is now finally evaluated and the introduced pressure tensor can be given in the form

$$Vp_{ij} = \sum_{k=1}^{N} m^k \overline{v_i^k v_j^k} + \sum_{k=1}^{N} \left(-\overline{\frac{\partial U}{\partial r_i^k} r_j^k}\right) \qquad \text{.....Eq.(B.10)}$$

where $\underset{\sim}{v}^k = \dot{\underset{\sim}{r}}^k$ is the velocity of the kth particle. The expression for pressure tensor (B.10) must be accepted as definition of this quantity [36] which is heuristically motivated by the analysis of equations of motion, pressure measurements and reasonable features of molecular interactions. The pressure tensor consists of two distinct components, the first of which depends on average particle velocities and is called "kinetic pressure"; the other component depends on particle positions and is called "configurational pressure". Due to the chaotic character of molecular motion, the time average of each velocity component is zero (if the system is at rest as a whole), and non-diagonal components of kinetic pressure disappear. Also, for systems with significant freedom in particle motions and isotropic potentials (fluids), components of particle displacements r_j and forces $-\partial U/\partial r_i$ are not correlated when $i \neq j$ so that only a hydrostatic component p of pressure tensor $p_{ij} = p\delta_{ij}$ remains and can be written in the form

$$pV = \frac{2}{3}\sum_{k=1}^{N} m^k \frac{\overline{(v^k \cdot v^k)}}{2} + \sum_{k=1}^{N} \overline{r_i^k \frac{\partial U}{\partial r_i^k}} \qquad \text{.....Eq.(B.11)}$$

Note that the first term in (B.11) is the average kinetic energy of the system. For rarified systems, particle interactions can be neglected and (B.11) gives

$$pV = \frac{2}{3} N\bar{E} \qquad \text{.....Eq. (B.12)}$$

where $\bar{E}$ is the average kinetic energy per particle. The above equation can be written in the form of the equation of state for an ideal gas if a measure of kinetic energy of a system (temperature T) is introduced in the usual manner ($\bar{E} = \frac{3}{2} kT$)

$$pV = NkT,$$

where k is Boltzmann's constant.

For dense systems, particle interactions cannot be neglected and an equation of state for dense systems cannot be easily established directly without integration of equations of motion. It is the specific function of statistical mechanics to establish reasonable methods for calculating time averages (B.11) without integration of equations of motion.

REFERENCES

(1) Archard, J.F. (1958): "Elastic Deformation and the Laws of Friction", Proc. R. Soc., ser. A, vol. 243, pp. 191-205.

(2) Axelrad, D.R. (1978): Micromechanics of Solids, Elsevier/North-Holland, Inc., New York.

(3) Bishop, A.W. (1972):"Shear Strength Parameters for Undisturbed and Remoulded Soil Specimens." Proc. Roscoe Memorial Symposium, Cambridge University, pp. 3-58.

(4) Brillouin, L. (1962): Science and Information Theory, Academic Press, New York.

(5) Chen, J.Y. and Vetelino, J.F. (1976): "Vibrational Properties of a Three-Fold Coordinated Two-Dimensional Random Lattice." In: Structures and Excitations of Amorphous Solids, Editors Lucovsky, G. and Galeener, F.L., American Institute of Physics, New York.

(6) Cowin, S.C., Editor, (1978): Proc. U.S.-Japan Seminar on Continuum Mechanical and Statistical Approaches in the Mechanics of Granular Materials, Tokyo, published by Gakujutsu Bunken Fukyukai, Tokyo, 1978.

(7) Cundall, P.A. and Strack, O.D.C. (1979): "A Discrete Numerical Model for Granular Assemblies." Geotechnique, vol. XXIX, No. 1, pp. 47-65.

(8) De Jong, J. and Verruijt, A. (1969): "Etude Photo-Elastique d'un Emilement de Disques." Can. Grpe. fr. Etud. Rheol., 2, pp. 73-86.

(9) Dresher, A. and De Jong, J. (1972): "Photo-Elastic Verification of a Mechanical Model for the Flow of Granular Material." J. Mech. Phys. Solids, 20, pp. 337-351.

(10) El-Sohby, A.A.K. (1969): "Deformation of Sands Under Constant Stress Ratio." Proc. 7th Int. Conf. Soil Mech., Mexico, vol. 1, pp. 111-119.

(11) Erber, T. and Sklar, A. (1974): "Macroscopic Irreversibility as a Manifestation of Micro-Instabilities." In: Modern Developments in Thermodynamics, John Wiley & Sons, Inc., New York.

(12) Frechette, V.D., Editor (1958): Conf. on Non-Crystalline Solids, Alfred, New York, Sept.,1958, John Wiley & Sons, New York.

(13) Gibbs, J.W. (1960): Elementary Principles in Statistical Mechanics, Dover Publications, Inc., New York.

(14) Harr, M.E., (1977): Mechanics of Particulate Media, McGraw-Hill Book Inc., New York.

(15) Horne, M.R. (1969): "The Behavior of an Assembly of Rotund, Rigid, Cohesionless Particles", III, Proc. Roy. Soc., A310, pp. 21-34.

(16) Katz, A. (1967): Principles of Statistical Mechanics, W.H. Freemen and Company, San Francisco.

(17) Kaye, G.W.C., Laby, T.H. (1966): Tables of Physical and Chemical Constants, Longmans.

(18) Kendall, D.G., Moran, D.A.P. (1963): Geometrical Probability, Charles Griffin & Co., London.

(19) Kestin, J. and Rice, J. (1970): "Paradoxes in the Application of Thermodynamics to Strained Solids." In: Critical Review of the Foundations of Relativistic and Classical Thermodynamics, distributed by Mono Book Corp., Baltimore.

(20) Kirkwood, J.G. (1976): Selected Topics in Statistical Mechanics, Gordon and Breach, New York.

(21) Konishi, J. (1978): "Microscopic Model Studies on the Mechanical Behavior of Granular Materials." Proc. U.S.-Japan Seminar on Continuum Mechanical and Statistical Approaches in the Mechanics of Granular Materials, Tokyo, 1978, published by Gakujutsu Bunken Fukyukai, Tokyo.

(22) Landau, L.D., Lifshitz, E.M. (1959): Theory of Elasticity, Pergamon Press, London.

(23) Landau, L.D., Lifshitz, E.M. (1958): Statistical Physics, Pergamon Press, London.

(24) Lekhnitskii, S.G. (1963): Theory of Elasticity of an Anisotropic Elastic Body, Holden-Day Inc., San Francisco.

(25) Litwiniszyn, J. (1964): "An Application of the Random Walk Argument to the Mechanics of Granular Media." International Union of Theoretical and Applied Mechanics Symposium, Grenoble.

(26) Loeve, M. (1963): Probability Theory, D. Van Nostrand Co., Princeton, New Jersey.

(27) Love, A.E.H. (1944): A Treatise on the Mathematical Theory of Elasticity, Dover Publications, Inc., New York.

(28) Miles, R.E. (1974): "A Synopsis of Poisson Flats in Euclidian Spaces." In: Stochastic Geometry, Editors Harding, E.F. and Kendall, D.G., John Wiley & Sons, Inc., New York.

(29) Quickenden, T.I. and Tan, G.K. (1974): "Random Packing in 2D and Monolayers." Journal of Colloid and Interface Science, vol. 48, 382.

(30) Rowe, P.W. (1972): "Theoretical Meaning and Observed Values of Deformation Parameters for Soil." Proc. Roscoe Memorial Symposium, Cambridge University, pp. 143-192.

(31) Santalo,L.A. (1976): Integral Geometry and Geometric Probability, Addison-Wesley Publishing Company, Reading, Mass.

(32) Skinner, A.E. (1969): "A Note on the Influence of Inter-Particle Friction on the Shearing Strength of a Random Assembly of Spherical Particles." Geotechnique, vol. XIX, pp. 150-157.

(33) Sokolnikoff, I.S. (1956): Mathematical Theory of Elasticity, McGraw-Hill Book Company, New York.

(34) Sutherland, D.N. (1977): "Random Packing of Circles in Plane." Journal of Colloid and Interface Science, vol. 60, No.1.

(35) Tolman, R.C. (1962): The Principles of Statistical Mechanics, Oxford University Press, Oxford.

(36) Truesdell, C. and Muncaster, R.G. (1980): Fundamentals of Maxwell's Kinetic Theory of a Simple Monoatomic Gas, Academic Press, Inc., New York.

(37) Truesdell, C. (1966): Six Lectures on Modern Natural Philosophy, Springer-Verlang, Berlin.

(38) Smith, W.O., Foote, P.D. and Budang, P.F. (1929): "Packing of Homogeneous Spheres." Phys. Rev., vol. 34, 1271-1274.

(39) Perloff, W.H. and Baron, W. (1976): Soil Mechanics, Ronald Publishing Company, New York.

(40) Washizu, K. (1968): Variational Methods in Elasticity and Plasticity, Pergamon Press, Oxford.

END

03H09H82

FIN